VNIVERSITAT DE VALÈNCIA

DEPARTAMENTO DE FÍSICA TEÓRICA

Neutrinos in GUT's and left-right symmetry

TESIS DOCTORAL

Carolina Arbeláez Rodríguez

Directores:
Martin Hirsch
José Wagner Furtado Valle

Valencia, 2014

Dr. Martin Hirsch, Investigador Científico del Consejo Superior de Investigaciones Científicas (CSIC),
Dr. José Wagner Furtado Valle, Profesor de Investigación del CSIC.

CERTIFICAN:

Que la presente memoria *Neutrinos in GUTs and left-right symmetry*, ha sido realizada bajo su dirección en el Departamento de Física Teórica de la Universidad de Valencia por Carolina Arbélaez Rodríguez y constituye su tesis doctoral para optar al grado de Doctora en física.

Y para que así conste, en cumplimiento con la legislación vigente, presentan ante el Departamento de Física Teórica, la referida memoria, firmando el presente certificado en Burjassot (Valencia) a 17 de Septiembre de 2014.

Martin Hirsch **José Wagner Furtado Valle**

Agradecimientos

Mi familia, a quien dedico esta tesis, ha sido y será la base, el pilar de mi vida. A ellos, siempre gracias.
Con mis amigos, he aprendido a vivir: v, Boris, gracias por su incondicionalidad. Con mis maestros, la duda he encaminado. Gracias a Martin por ser el valioso profesor y excepcional ser humano.

El inicio y realización de este proyecto se ha dado gracias al apoyo de diferentes personas y entidades, en particular el grupo AHEP. Gracias en especial a José, Martin, Sergio y Mariam por ofrecerme la oportunidad de estar aquí. Al resto del grupo por las horas de café, discusiones y buen ambiente de trabajo. Agradezco también al profesor Jorge Romão y a Michal Malinsky por abrirme un espacio en su grupo (IST, IPNP) y haberme acogido de tal forma. A Laslo Reichert, Renato Fonseca, Helena Kolešová por la valiosa colaboración en los diferentes proyectos. A las entidades y programas: Beca Santiago Grisolía, Septimo Programa Marie Curie Initial Training Network y grant Prometeo por la financiación. Y también, por qué no?, agradezco a las entidades de gobierno Españo-Portuguesas por permitirme la permanencia en el respectivo país y obsequiarme además, como bonus, una intensiva (...y un tanto dura) "terapia" a mi paciencia y persistencia.

Finalmente, gracias a los amigos y demás personas que aquí conocí y con quien pude compartír valiosos momentos: Joaquín, Paula, Angie, Ebhe, muchas gracias. También a David, Sofiane, Daniel, Alma, Valentina, Agustín, Marcela, etc... Me quedo corta en palabras.

This doctoral thesis is based on the following publications:

[1] C. Arbeláez, M. Hirsch and L. Reichert,
"Supersymmetric mass spectra and the seesaw type-I scale,"
JHEP **1202**, 112 (2012)
[arXiv:1112.4771 [hep-ph]].

[2] C. Arbeláez, R. M. Fonseca, M. Hirsch and J. C. Romão,
"Supersymmetric $SO(10)-$inspired GUTs with sliding scales,"
Phys. Rev. D **87**, 075010 (2013)
[arXiv:1301.6085 [hep-ph]].

[3] C. Arbeláez, M. Hirsch, M. Malinský and J. C. Romão,
"LHC-scale left-right symmetry and unification,"
Phys. Rev. D **89**, 035002 (2014)
[arXiv:1311.3228 [hep-ph]].

[4] C. Arbeláez, H. Kolešová and M. Malinský,
" Witten's mechanism in the flipped $SU(5)$ unification,"
Phys. Rev. D **89**, 055003 (2014)
[arXiv:1309.6743 [hep-ph]].

***PROCEEDINGS*:**

[5] C. Arbeláez R.,
"Supersymmetric $SO(10)$ with sliding scales,"
J. Phys. Conf. Ser. **447**, 012036 (2013).
Contribution to the proceedings "*Discrete 2012*". 3 December-7 December 2012. Lisbon-Portugal.
[6] M. Malinský, C. Arbeláez and H. Kolešová,
"Witten's loop in the flipped SU(5) unification,"
arXiv:1310.0914 [hep-ph].
Contribution to the proceedings "*CETUP 2013*". 15 July-26 July 2013. South Dakota-U.S.

Abstract

First indications for physics beyond the SM, such as neutrino masses and dark matter, have attracted considerable attention. This thesis focuses on neutrinos in models derived from Grand Unified Theories (GUTs). Supersymmetric and nonSupersymmetric realizations are studied. In [1] a numerical and analytical analysis of possible ILC-LHC experimental data was done, identifying the parameter region in which pure CMSSM and CMSSM plus Seesaw Type-I might be distinguishable.
Considering that neutrino masses could successfully be explained in GUTs, in particular $SO(10)$, in [2] supersymmetric models with extended gauge groups at intermediate LR scales where constructed, all of which are inspired by $SO(10)$ unification. Analyzing some special combinations of the SUSY soft terms, it was shown that future LHC data could contain information about the LR scale. Reconsidering the possibility to explain unification in non-SUSY theories, in [3] a list of non-SUSY models which unify equally well or better than the MSSM was found. These models are interesting from the phenomenological point of view: they can explain CKM and also obey proton decay limits while giving testable phenomenology at the LHC. Finally, we briefly explored the DM problem, searching for a consistent explanation of the DM candidate in the framework of LR nonSUSY $SO(10)$ GUT models
Considering the possible information that future Baryon Number Violation experiments might give for proton decay and GUTs, in [4] an analysis of Witten's mechanism within flipped $SU(5)$ was done. Interesting relations between neutrino parameters and proton decay partial widths were found.

Contents

Chapter 1

INTRODUCTION

The Standard Model (SM) is known currently as the best theory of the fundamental particles and interactions. This theory has been confirmed with ever increasing precision by improved experimental tests. The recent discovery of the Higgs boson at the ATLAS [5] and CMS [6] detectors has found its last missing piece. It seems that the idea of spontaneous symmetry breaking as origin of mass has been confirmed. However, some remaining puzzles can only be explained by physics beyond the standard model (PBSM). In order to address these subjects, different searches like neutrino oscillations, neutrinoless double beta decay, lepton number and baryon number violation process (LNV+BNV), etc, will be made in the coming years. Furthermore, the next run at the LHC may help to solve some exciting questions. The upgrade to 13 or 14 TeV, expected for 2015, will renew the possibility to discover new particles and understand better the physics behind the electroweak symmetry breaking. On the other hand, proton instability, if observed, would provide a signal of Grand Unification. Up to now Water Cherenkov detectors, such as Super-K [7], have provided the most stringent limits on proton decay. It is likely that in the future this "classical" experiment will be complemented by liquid argon detectors which could improve substantially the existing limits (for certain decay modes).

Theories like Supersymmetry (SUSY) address successfully some the SM shortcomings. SUSY as a *well-behaved* theory at high energies can explain not only the Higgs mass stabilization but also Gauge Coupling Unification (GCU). On the other hand, experimental evidence also confirm the presence of PBSM. As an example, there is a clear evidence for Dark Matter (DM) in the universe. This has led to a

rich field of investigation in which many different models have been explored. For example, SUSY DM (with the neutralino as a realistic candidate) but also non-SUSY DM candidates such as generic WIMPS. A short review of the main SM shortcomings and also some general features of BSM are presented in **chapter 2**. Below, the outline, motivations and main results of this thesis are briefly discussed.

Neutrinos are the oddest of the fundamental particles. Oscillation experiments [7, 8, 9, 10, 11, 12, 13] have shown these particles have mass, the first laboratory measurement demonstrating the existence of physics beyond the standard model (PBSM). At the same time, while many possible theoretical models have been put forward to explain neutrino data, progress in theory has been rather limited, for example: a) we do not know the scale of neutrino mass generation, b) we do not know if neutrinos are Dirac or Majorana particles, among some other so far not explained puzzles. The smallness of the neutrino masses can be successfully explained by, for example, the well-known seesaw [14, 15, 16, 17, 18]. However, the SM implementation of this mechanism leaves only unmeasurable small changes in a very few observables, such as $\mu \to e\gamma$. This motivates to explore additional BSM models to explain neutrino mass. A supersymmetric extension of the seesaw is studied in **chapter 3**. In SUSY seesaw models, the soft mass terms contain indirect information on the seesaw parameters through the RGE runnings. Imposing CMSSM boundary conditions and considering the possible experimental information that LHC and ILC could give of the SUSY spectra, indirect hints of seesaw type-I coming from the LHC-ILC SUSY mass spectra is explored [1].

The upcoming generation of large-scale experiments dedicated to the search of Baryon Number Violation (BNV) [19, 20], will hopefully allow to study and test with better sensitivity proton decay processes in $SO(10)$ and $SU(5)$ theories. Nowadays, new multipurpose experiments which could improve about one order of magnitude existing proton decay limits from Super-Kamiokande have been proposed. These projects will function also as astrophysical neutrino observatories. Taking up this motivation, in **chapter 4** we investigate the possibility to generate neutrino masses in the Flipped $SU(5)$ model [4]. Despite the fact that the standard seesaw in unified models has been in part successful for explaining neutrino masses, the hierarchy between the masses $m_R \leq 10^{15}$ GeV and $m_G \geq 10^{16}$ GeV is a potential problem in GUTs. A mechanism that generates two-loop masses for the

right handed neutrinos as first proposed by Witten in 1980 [21] could explain this mild hierarchy. In this model the partial *proton decay* widths to neutral mesons are governed in part by the neutrino parameters related via the Witten loop.

From the theoretical point of view, GUT models based on $SO(10)$ offer a number of advantages compared to the simplest models based on $SU(5)$. For example, there are several chains through which $SO(10)$ can be broken to the SM using left-right intermediate symmetry, thus potentially explaining the V-A structure of the SM. Probably one of the most interesting aspects of SO(10) is that it automatically contains the necessary ingredients to generate the seesaw mechanism since (a) the right handed neutrinos are included in the irreducible 16 representation (rep) and (b) B-L is one of the generators $SO(10)$. In addition, this kind of models, apart from offering experimental signals, e.g proton decay, give also rise to non-trivial correlations among observables in the theory. Gauge coupling unification (GCU) in SUSY [22, 23, 24, 25, 26, 27, 28] and nonSUSY [29, 30, 31] GUT models have been widely studied in the literature. After the discovery (more than 20 years ago) that the MSSM leads to almost perfect unification, LR models fell from favour because the minimal non-SUSY LR models can give gauge coupling unification only if the intermediate scale lives in the ballpark range of $[10^9, 10^{11}]$ GeV, which is completely untestable. However, in Supersymmetric extensions of $SO(10)$, like [32], the authors have demonstrated that a low LR scale becomes allowed, once certain conditions are fulfilled. These models are *non-minimal*: more fields than the minimal LR (mLR) are needed but not many more. A particular interesting extension correspond to models in which the independence between the unification scale m_G and the LR intermediate scale m_{LR} is imposed. This mechanism is called in the literature *sliding mechanism*, and has been studied in [33]. Following this idea, in [2] we constructed supersymmetric models with extended gauge groups at intermediate steps, all of which are based on SO(10) unification. Three different constructions based on different $SO(10)$ breaking channels were considered: left-right group $SU(3)_c \times SU(2)_L \times SU(2)_R \times U(1)_{B-L}$, the Pati Salam group $SU(4) \times SU(2)_R \times SU(2)_L$ group and $SU(3)_c \times SU(2)_L \times U(1)_R \times U(1)_{B-L}$ group. A large number of models and configurations that unify and follow also sliding conditions were found. These configurations predict different additional particle content and some of them (being colored) could give rise to particularly large cross sections at the LHC. Moreover, assuming mSugra boundary conditions, we calculated cer-

tain combinations of the soft terms, called invariants, which allow, if measured, to obtain information on the scale of beyond MSSM physics. These topics are studied in **chapter 5, section 5.1**. Considering that actually no signals of supersymmetry in the sub-TeV domain have been seen by accelerator experiments at the LHC, ATLAS/CMS, we decided to reconsider the question whether: a) SUSY is needed for obtaining GCU and b) whether low-scale LR model can have good GCU. In [3] we studied in detail intermediate scale models and identified potentially viable (and yet very simple) non-SUSY scenarios where unification could be perfect. We constructed a list of models with a LR symmetric intermediate stage at or close to the electroweak scale, where GCU is achieved by adding to the SM a very simple phenomenological realistic particle content that explains successfully CKM (and neutrino) angles and obey limits from *proton decay* searches. This is explored in **chapter 5, section 5.2**.

Nowadays, there exists clear evidence that there is DM in the universe and, as is known, the SM fails to provide a DM candidate. One of the most interesting questions is to understand its nature, i.e, which particle DM is made of. Grand unified theories provide a successful explanation of DM. In **chapter 5, section 5.3** we explore the possibility to connect nonSUSY $SO(10)$ models with DM. Unlike the typical DM models, in these scenarios, matter parity $Z_2 = (-1)^{3(B-L)}$ (which stabilize DM) is not an *ad hoc* symmetry. This symmetry is a remnant symmetry after the breaking $SO(10) \to SU(3) \times SU(2)_R \times SU(2)_L \times U(1)_{B-L}$. There exist few papers in the literature which deal with DM unified scenarios in the framework of a gauged $U(1)_{B-L}$ symmetry, using SUSY R-parity [34] or using matter parity in nonSUSY models [35, 36]. Therefore there are still many questions left unexplored to investigate. In this section of the thesis, simple configurations which contain at least a DM candidate and follow some phenomenological constraints are presented.

In summary, this thesis is organized as follows. The motivation and some topics in PBSM, such as supersymmetry, neutrino physics, grand unified theories and dark matter are discussed in chapter 2. In chapters 3,4,5 we present the results of the papers [1],[2],[3],[4]. A possible connection between our nonSUSY $SO(10)$ models and DM is explored in chapter 5, section 5.3. General conclusions are given in chapter 6. Some additional remarks are presented in the appendix.

Chapter 2

RESUMEN

Actualmente, el Modelo Estandar es conocido como la teoría que mejor explica las interacciones fundamentales entre las partículas en el universo. Descubrimientos recientes del boson de Higgs en ATLAS [5] y CMS [6] han encontrado la pieza perdida de esta teoría, además de representar una relevante evidencia experimental. Parece entonces que la idea de la ruptura espontánea de la simetría como la teoría que mejor explica el origen de las masas ha sido confirmada. Sin embargo, otros interrogantes sólo pueden ser explicados por la física mas allá del Modelo Estandar. En torno a esto, diferentes búsquedas como las oscilaciones de neutrinos, violación del número leptónico y violación del número bariónico (LNV+BNV), entre otras, se harán en los próximos años. Adicionalmente, la próxima puesta en marcha del LHC ayudará a resolver otros interrogantes. El incremento en la energía de este colisionador, de 8 a 14 TeV, esperada para el 2015, abrirá las posibilidades de descubrir nuevas partículas y entender mejor la física detrás del rompimiento espontáneo de la simetría. Por otro lado, el decaimiento del protón, si es observado, podría ser una señal relevante de las teorías de Gran Unificación. Hasta ahora, los detectores Cherenkov, tal como el Super-K [7], han establecido límites en la vida media del protón. Es posible que en el futuro, estos experimentos sean complementados por detectores del Argon líquido, los cuales puede mejorar sustancialmente los límites actuales.

Algunas teorías, tales como Supersimetría, explican satisfactoriamente algunos del los interrogantes no resueltos en el Modelo Estandar. Supersimetría, como un teoría consistente a altas energías, puede explicar no sólo la estabilización de la masa del Higgs sino también la unificación de los acoplamientos gauge. Por otro

lado, diferentes experimentos confirman también la presencia de física más allá del Modelo Estandar. Un ejemplo claro de esto es la evidencia de la materia oscura en el universo, lo cual ha abierto el camino para que otros diferentes modelos sean explorados. Un pequeño resumen de los principales interrogantes del modelo estandar será estudiado en el capítulo 2. Un resumen general, las motivaciones y los resultados relevantes de esta tesis serán discutidos brevemente en lo que sigue.

Experimentos de oscilaciones de neutrinos [7, 8, 9, 10, 11, 12, 13] han mostrado que estas partículas tienen masa, lo cual constituye la primera evidencia experimental de física más allá del Modelo Estandar. A pesar de los avances en la física de neutrinos, algunos otros aspectos e interrogantes surgen, como por ejemplo: a) hasta ahora no se sabe la escala de la masa de los neutrinos y b). no sabemos si los neutrinos son particulas de Dirac ó de Majorana, entre otros. Varios intentos para resolver estos interrogantes se han hecho en los ultimos 30 años. La masa pequeña de los neutrinos puede ser satisfactoriamente explicada por el mecanismo seesaw [14, 15, 16, 17, 18]. Sin embargo, en el Modelo Estandar, este mecanismo deja inconmensurables cambios en los observables, tal como $\mu \to e\gamma$. Esto, entre otros aspectos, es una de las motivaciones para ir mas allá del Modelo Estandar. Una extensión supersimétrica del mecanismo seesaw es estudiada en el capítulo 3. En los modelos seesaw supersimétricos, los términos soft contienen información indirecta de los parámetros seesaw a traves de los acoplamientos gauge. Imponiendo ciertas condiciones de frontera, y considerando los resultados experimentales que el LHC y el ILC pueden dar del espectro SUSY, las señales del seesaw type-I que vienen del espectro SUSY son estudiadas [1].

La próxima generación de experimentos dedicados a la busqueda de la violación del número bariónico (BNV) [19, 20] dará límites del decaimiento del proton más precisos, en teorías de unificación tales como $SO(10)$ y $SU(5)$. Recientemente, nuevos experimentos tales como Super-Kamiokande, los cuales contribuirán en un orden de magnitud a los límites del decaimiento del proton, serán puestos en marcha en los próximos años. Estos experimentos funcionarán también como observatorios de astropartículas. Teniendo en cuenta esta motivación, en el capítulo 4 investigamos la posibilidad de generar la masa de los neutrinos en un modelo basado en la teoría Flipped $SU(5)$ [4]. A pesar de que la implementación estandar del mecanismo seesaw en modelos de unificación ha sido en parte satisfactorio, la

jerarquía entre la masa de los neutrinos y la escala de unificación es aún uno del los principales interrogantes de las teorías de unificación. El mecanismo que genera la masa de los neutrinos a 2 loop en $SO(10)$ fue propuesto por primera vez por Edward Witten en los años 1980's [21]. En este modelo, basado en $SU(5) \times U(1)$ las amplitudes de decaimiento del proton a mesones neutros son gobernados en parte por los parámetros de los neutrinos explicados a travéz del Witten loop.

Desde el punto de vista teórico, los modelos de gran unificación basados en $SO(10)$ ofrecen un numero de ventajas comparados con los modelos simples en $SU(5)$. Por ejemplo, hay muchos canales a través de los cuales $SO(10)$ puede ir al Modelo Estandar usando simetrías intermedias LR, y así explicar por ejemplo la estructura V-A del modelo estandar. Probablemente, uno de los aspectos más interesantes de $SO(10)$ es que automaticamente contiene los ingredientes necesarios para explicar la masa de los neutrinos a través del mecanismo seesaw: a) los neutrinos derechos son incluidos en la representación irreducible 16, b) $B-L$ es uno de los generadores de $SO(10)$. Adicionalmente, este tipo de modelos, aparte de ofrecer señales experimentales, como por ejemplo el decaimiento del protón, dan lugar también a correlaciones no triviales entre los observables en la teoría. Teorías de unificación en modelos supersimétricos [22, 23, 24, 25, 26, 27, 28] y no supersimétricos [29, 30, 31] han sido ampliamente estudiados en la literatura. Después del descubrimiento de que el modelo mínimo supersimétrico (MSSM) deja como consecuencia la unificación casi perfecta de los acoplamientos gauge, los modelos de unificación LR no supersimétricos perdieron interés debido a que su escala de unificación era del orden de los $[10^9, 10^{11}]$ GeV, lo cual no puede ser testeado experimentalmente. Sin embargo, en extensiones supersimétricas de $SO(10)$, tal como las explicadas en [32], los autores han demostrado que es posible tener bajas escalas intermedias, una vez se impongan ciertas condiciones. Esos modelos son no-mínimos: se necesitan más campos que en el modelo mínimo LR (mLR) pero no muchos más. Algunas extensiones interesantes corresponden a modelos en los cuales se impone la independencia entre la escala de unificación m_G y la escala intermedia m_{LR}. Este mecanismo es conocido en la literatura como el "sliding mechanism", y ha sido estudiado en [33]. Siguiendo esta idea, en [2] construimos modelos supersimétricos con grupos gauge extra a escalas intermedias, todos ellos basados en $SO(10)$. Tres construcciones diferentes basadas en diferentes formas de romper la simetría fueron estudiados: el grupo LR $SO(10) \to SU(3)_c \times SU(2)_R \times SU(2)_L \times U(1)_{B-L}$, el grupo Pati Salam

$SU(4) \times SU(2)_R \times SU(2)_L$ y finalmente $SU(3)_c \times SU(2)_L \times U(1)_R \times U(1)_{B-L}$. Un gran número de modelos y configuraciones que unifican y siguen ciertas condiciones fueron encontrados. Esas configuraciones predicen diferentes contenidos de partículas y algunos de estos (siendo coloridos), pueden dar lugar a secciones eficaces que pueden ser medidas en el LHC. Además, asumiendo las condiciones de frontera de mSUGRA, fueron calculadas ciertas combinaciones de los términos SOFT, llamados invariantes, los cuales, si son medidos, permiten obtener información de la escala de la nueva física mas allá del modelo minimo supersimétrico (MSSM). Estos temas son estudiados en el capítulo 5, sección 5.1. Considerando que actualmente no hay señales de supersimetria a la escala sub-TeV, hemos decidido reconsiderar la pregunta: a) se necesitan teorias supersimetricas para obtener GCU? y b) models con baja escala LR podrían tener una buena unificación?. En [3] estudiamos en detalle modelos con simetrías LR intermedias identificando escenarios no supersimetricos donde la unificación puede ser aún perfecta. Una lista de modelos donde la escala intermedia es cerca de la escala m_Z fue construida. En estos, se logra unificación añadiendo al modelo estandar un contenido simple de partículas que explican fenomenología tal como CKM y los actuales límites del decaimiento del proton. Estos aspectos son estudiados en el capítulo 5, sección 5.2.

Actualmente, la presencia de materia oscura en el universo es una clara evidencia y, como es sabido, el modelo estandar no explica este hecho satisfactoriamente. Una de los aspectos más interesantes es entender su naturaleza, es decir, que partícula es el posible candidato a la materia oscura. Teorías de unificación ofrecen una explicación satisfactoria de DM. En el capítulo 5, sección 5.3 exploramos brevemente la posibilidad de conectar modelos no supersimétricos basados en $SO(10)$ y materia oscura. Diferente a los modelos típicos que explican materia oscura, en estos escenarios la simetría de paridad $Z_2 = (-1)^{3(B-L)}$ no es una simetría impuesta. Esta es una simetría remanente después de la ruptura espontánea de $SO(10)$ al modelo estandar $SO(10) \to SU(3) \times SU(2)_R \times SU(2)_L \times U(1)_{B-L}$. Existen pocos trabajos en la literatura donde se estudien los modelos con materia oscura en un marco de simetrías gauge $U(1)_{B-L}$ [34, 35, 36]. Por lo tanto, hay aún muchas preguntas para ahondar. En esta sección, configuraciones simples que contienen como mínimo un candidato a la materia oscura y siguen ciertas condiciones fenomenológicas son presentados.

En resumen, esta tesis se organiza como sigue: la motivación y algunos temas relacionados con la física más allá del modelo estandar, tales como supersimetría, fisica de neutrinos, teorías de unificación y materia oscura son discutidos en el capítulo 2. En los capítulos 3,4,5 presentamos los resultados de los artículos [1],[2],[3],[4]. En breves palabras, una posible conección entre modelos nos supersimetricos $SO(10)$ y la materia oscura es discutida en el capítulo 5, sección 5.3. Conclusiones generales son dadas en el capítulo 6. Algunas extensiones a los modelos previamente analizados se presentan en el apéndice.

Chapter 3

PHYSICS BEYOND THE STANDARD MODEL

3.1 WHY TO GO BSM?

The Standard Model (SM) of elementary particles represents one of the greatest achievements of physics in the last century, describing the universe in terms of matter and forces. Particle interactions are derived from local symmetries and explained at a fundamental level by the gauge principle. This theory has been successfully tested by many experiments and one of the most important ones is the Large Hadron Collider (LHC). The hunt for the Higgs boson has become the major goal of these experiments and a measurement of its mass, to be around 125 GeV [5, 6], seems to confirm successfully the SM predictions from the fit of electroweak precision data [37, 38]. But, although experiments show the extraordinary power of the SM, it is considered only an *effective theory* which doesn't provide a real explanation for some other elementary particle properties, for example the fermion masses and mixing angles [1]. This theory is also not able to explain physics at energies near the Plank scale where quantum gravitational effects become important. Below, some motivations to study PBSM are briefly discussed.

[1] It is important to note here that these quantities can not be predicted but are actually input parameters in the SM.

I. Gauge coupling unification

Although the SM is a successful theory of both the charged and neutral weak processes, it doesn't truly unify the three $SU(3)_c \times SU(2)_L \times U(1)_Y$ gauge couplings. The idea of unification is not new to physics [2]. One of the most important contributions was made in the 1960′s by Glashow who proposed to unify the electromagnetic and the weak interactions into the electroweak theory $SU(2)_L \times U(1)_Y$ [39]. The Glashow theory was later revisted by Weinberg who introduced the masses for the W and Z particles through the spontaneous symmetry breaking [40], completing the basic setup of the electroweak theory. The hypothesis of *Grand Unification* was introduced first by Pati and Salam [41], who describe a model based on $SU(4) \times SU(2)_L \times SU(2)_R$ and later by Georgi and Glashow [42] who proposed the rank-4 simple group $SU(5)$ as the GUT group. Since then $SO(10)$ models [44, 45] have been widely studied too. These models have the remarkable feature of accommodating a complete family of fermions in a single representation, including the right handed neutrinos. Therefore, this theory generically provides some interesting and testable relations between the charged fermions and the Higgs sector [46, 47, 48]. Furthermore, $SO(10)$ contains a Left-Right (LR) subgroup (one of the beaking chains to the SM is $SO(10) \to SU(3)_c \times SU(2)_L \times SU(2)_R \times U(1)_{B-L}$) so the implementation of the seesaw mechanism arises naturally.
GUTs make some interesting predictions and can potentially explain some of the open questions of the SM. Here, some of these are briefly discussed:

a. Charge Quantization
One of the consequences of grand unified models, for example $SU(5)$, is the explanation of the experimentally observed charge quantization. This follows because the eigenvalues of the generators of a simple non-abelian group are discrete, while those corresponding to an Abelian group, like $U(1)$ are continuous. Hence, in $SU(5)$, since the charge matrix Q is one of the group generators, its eigenvalues are discrete and then quantized.

[2] In the 7th century B.C Anaximenes identifies the air as the fundamental component of everything. Many years later Democrito and Leucipo affirmed that the matter is composed by invisible particles called Atomos (*Mechanistic Atomims*). Centuries later Newton showed that celestial moving and falling bodies can be described by an universal gravitational theory and two hundred years later Maxwell proposed the Electromagnetism, unifying the electric and magnetic forces.

b. Proton decay

Symmetries like $SU(5)$ transform quarks into leptons (they put quarks and leptons in a common multiplet) which means that gauge interactions violate baryon and lepton number. With the exchange of heavy vector bosons ($M_{X,Y}$), called leptoquarks, dimension-6 operators arise, predicting a proton life-time of roughly $\tau(p \to e^+\pi^0) \simeq \alpha_G^2 m_p^5/M_X^4$ [49, 44]. Here α_G is the common coupling constant at the unification scale m_G, m_p is the proton mass and $m_{X,Y}$ is the leptoquark mass. Recent experiments, like Super-Kamiokande, set stringent limits on the proton decay life time. In SUSY models, unification occurs at a high scale $M_G \simeq 10^{16}$ GeV, so predicted proton decay half-lifes are about 10^{34-38} years [50].

c. Baryon number asymmetry in the universe

The origin of the baryon asymmetry in the universe has become a fundamental question for cosmology today. Standard cosmology tells us that the early universe was extremely hot and energetic and it is expected that an equal number of baryons and antibaryons in the universe existed. However, this hypothesis is in contrast with what is observed by experiments. Direct observations show that the universe contains no appreciable primordial antimatter. The ratio $\eta = \frac{n_b - n_{\bar{b}}}{s}$, coming from measurements of the cosmic microwave background (CMB) by the WMAP satellite [51], is $\eta = 6.1 \times 10^{-10}$. However, the standard cosmological model cannot explain this observed value. The *Sakharov Criteria* define a set of three necessary conditions that a baryon-generating mechanism must satisfy to produce this matter and antimatter difference. The three conditions are : i) baryon number violation, ii) violation of C (charge conjugation) and CP (the composition of parity and C) and iii) departure of termal equilibrium [52].

Since the linear combination $B - L$ is left unchanged by SM sphaleron transition, in the SM the baryon asymmetry may be generated from a lepton asymmetry (*Baryogenesis via leptogenesis* [53, 54, 55]). It is possible to generate a net $B - L$ dynamically in the early universe adding right handed Majorana neutrinos to the theory. In this case the primordial lepton asymmetry can be generated by the out-of-equilibrium decay of the heavy right-handed Majorana neutrinos N_L^c. This lepton number will then be partially converted into baryon number via electroweak sphaleron processes. These kind of scenarios can be realized in GUT theories like

$SO(10)$ which contains the right handed neutrinos in a non-trivial representation and breaks to the SM through $SO(10) \rightarrow SU(3)_c \times SU(2)_L \times SU(2)_L \times U(1)_{B-L}$.

d. Inflation and unification

The inflationary theory proposes that the universe expanded extremely quickly in the first fraction of a nanosecond after it was born. This theory is considered now a key in our understanding of the early universe. Data coming from WMAP satellite and recently from Plank [56] indicate an almost scale-free spectrum of Gaussian adiabatic density fluctuations just as predicted by simple models of inflation. Recently, the BICEP2 [57, 58] claimed to have measured signatures of inflation by detecting the CGB (cosmic gravitational background) via its imprint as the unique B-mode polarization signature of the CMB. This fact, if confirmed, is also an indirect proof of the inflationary theory.

The measurement of $r = 0.2 \pm 0.05$ (ratio of the tensor to scalar modes) by BICEP2 suggests that the energy scale of the universe during inflation was similar to the energy scale at which all the forces of the nature, except gravity, are unified into a single force [58]. Some GUT-inflation models, like [59],[60], propose that the inflaton might be the Higgs associated with the spontaneous breaking of the GUT model like $SU(5)$ and $SO(10)$. Supersymmetric and nonSupersymmetric GUT-inflation schemes in this direction have been widely discussed in the last years (for example see the GUT Coleman-Weinberg inflation model described in [61]).

II. Neutrino mass

Neutrino oscillation experiments show that at least two neutrinos have non-zero mass. One of the best studied mechanism to give mass to the neutrinos arises in grand unified theories where the large mass of the right handed neutrinos is explained through the seesaw mechanism. Here new entities called right handed neutrinos are added to the SM.

Actual measurements of fluxes of solar, atmospheric and reactor neutrinos show that at least two of the observed, weakly interacting neutrinos have a very small but non-zero mass: $\Delta m^2_{sol} = 7.67 \times 10^{-5} eV^2$ and $\Delta m^2_{atm} = 2.46 \times 10^{-3} eV^2$ [8, 7, 9, 10]. However, the overall scale of the neutrino masses is not known, except an upper limit of the order of 1 eV coming from direct experiments (double beta decay exper-

iments [62, 63, 64]) and cosmology [65]. Current data, including the measurement of reactor antineutrino reported by Daya Bay and RENO, and also the latest T2K and MINOS fit the values of the mixing angles as: $sin^2\theta_{12}/10^{-1} = 2.78 - 3.75$, $sin^2\theta_{23}/10^{-1} = 3.92 - 6.43$, $sin^2\theta_{13}/10^{-2} = 1.77 - 2.94$ at 3σ of C.L [8, 7, 9, 10].

III. Dark matter

Nearly 95% of the total matter-energy content of the Universe has to be explained by some physics beyond the SM [66]. Dark matter (DM) makes up the bulk of the mass of galaxies and is fundamental in the formation of galaxies and stars. Thus its study is essential for our understanding of the origin of the universe. The present energy density in the universe is dominated by non-relativistic matter (roughly 30% of the total) in the form of baryons and cold dark matter (CDM) and dark energy (the remaining 70%). The density of the baryons can be inferred through the knowledge of light element abundances. On the other hand, the total density of the matter affects, through gravity, the evolution of perturbations and then can be constrained by measuring the clustering properties of galaxies or the by CMB observations [56].

Evidence for DM has grown over the years, and although no solid direct signal of DM has been detected, several possible candidates have been proposed to explain its properties [3]. DM is widely thought to be a kind of massive elementary particle originated from the big-bang with no electric charge nor color with low velocities, that interacts weakly with the ordinary matter so-called *WIMPs* [67, 68]. Some of the best known WIMP candidates are the neutralino and the lightest Kaluza-Klein particles. Another widely studied DM candidate is the *Axion* introduced as a possible solution to the strong CP problem. Axions are stable but much lighter than the WIMPs.

In the next subsections, some topics of PBSM will be discussed, in particular, supersymmetry, neutrino physics and grand unified theories.

[3] DM can not be seen directly, but it is possible to study its effects, for example the light bent from the gravity of invisible objects (called gravitational lensing). Astronomers can also measure that stars are orbiting around in their galaxies faster than they should be.

3.2 SUPERSYMMETRY

3.2.1 Motivation

Supersymmetry (SUSY) is a global symmetry between fermions and bosons which solves some of the shortcomings present in the SM [69, 70]. In the second half of the 1970′s relevant progress in the study of supersymmetric theories was made: The idea of supersymmetry was first explored by Golfand and Likhtman in 1971 [71]. Later Akulov and Volkov proposed the first model that connected SUSY and particle physics [72]. In 1974, Wess and Zumino as well as Salam and Strathdee combined SUSY with quantum field theories in the context of abelian and non-abelian gauge theories respectively [73, 74]. In the early 1980′s gauge coupling unification in SUSY models was studied [22, 23, 24].

SUSY is considered as a *"well-behaved"* theory at high energies and offers some interesting features from the theoretical and phenomenological point of view solving at the same time some of the problems present in the SM:

- How can the electroweak scalars remain massless far below the GUT scale (at least 10^{15} GeV) when it is not protected by any symmetry which guarantees this? This problem, known as the *hierarchy problem*, is solved in Supersymmetry which automatically cancels the quadratic divergences in all orders of perturbation theory [75]. If there is a symmetry that relates fermions (constituents of matter) and bosons (mediators of interaction) there is a cancellation because of the negative sign associated to the closed fermion loops as compared to the bosonic loops. This cancellation is maintained up to logarithmic corrections after the soft SUSY breaking parameters are added. However this cancellation solves the hierarchy problem only in part. The logarithmic divergences still remain in the theory. The larger m_{SUSY}, the larger the log divergences. Also (in the MSSM) the supersymmetric μ term contains quadratic divergences.

- In the MSSM (Minimal Supersymmetric extension of the Standard Model) the gauge couplings unify at an scale of about $m_G = 2 \times 10^{16}$GeV [75, 76]. In general this property is achieved in supersymmetric theories where the SUSY scale m_S is close to the electroweak scale. Significant progress in supersymmetric $SO(10)$ GUTs has been made over the years. These models are particularly interesting

and offer an number of advantages which will be discussed in the next chapters.

• Supersymmetry predicts a stable and neutral particle (the lightest supersymmetric particle, LSP) which is usually a viable candidate to explain DM if R-parity is conserved [77]. In supersymmetric theories, with Baryon and Lepton number conservation, R-parity (R_p) can be expressed as $(-1)^{3B+L+2S}$ and the assumptions of an exact R_p conservation guarantees that the lighest supersymmetric particle (LSP) is stable [4]. In the MSSM, the neutralino $\widetilde{\chi}_1^0$ is considered as the most viable LSP candidate [5]. This candidate interacts weakly with the ordinary particles, so is considered a good WIMP (weakly interacting massive particle) DM candidate. The Gravitino $\widetilde{G}$ (supersymmetric particle of the Graviton) is considered also as a possible DM candidate[6] which can be produced by WIMP decays or thermal production.

• Any anticommutator of two SUSY transformations:

$$\{Q_r, \overline{Q_s}\} = 2\gamma^{\mu}_{rs} P_{\mu},$$

is a local coordinate translation then the group parameters should be allowed to be functions of the space-time point [79]. Supersymmetry is then expected to be a theory of general coordinate transformations of space time, it means, a theory of gravity, referred to here as *supergravity*.

Although SUSY remains attractive from the theoretical and phenomenological point of view, no supersymmetric partners of any known particle has been discovered yet. Thus SUSY must be broken at a scale beyond the electroweak scale. As will be discussed in the next subsections, there are two ways to break supersymmetry: i) SUSY is broken explicitly and ii) SUSY is broken spontaneously. In both methods, new SUSY breaking terms so-called soft SUSY breaking terms are added to the Lagrangian. In the following we review some of the main features of the Minimal Supersymmetric Standard Model (MSSM) and the mechanisms of SUSY breaking, in particular the CMSSM (constrained MSSM).

[4] As a DM candidate, the LSP particle needs also be neutral and non-coloured.

[5] Also the sneutrino $\widetilde{\nu}$ was considered as a viable LSP, but now this is ruled out [78].

[6] The Gravitino is a fermion which mediate the supergravity interactions. This LSP is produced relativistically and form warm DM which can affect structure formation on small scales.

3.2.2 Setup and mathematics

A supersymmetric theory implies that all particles possess supersymmetric partners having opposite statistics. This is because supersymmetric multiplets consist of equal mass particles whose spins differ by (1/2). One of the first requirements of supersymmetry is an equal number of fermionic and bosonic degree of freedom. This means, SUSY is a symmetry between fermions and bosons:

$$\begin{aligned} Q_a \left| fermion \right\rangle &\propto \left| boson \right\rangle , \\ Q_a \left| boson \right\rangle &\propto \left| fermion \right\rangle . \end{aligned} \tag{3.1}$$

In order to write down the supersymmetric Lagrangian in the minimal supersymmetric extension of the standard model (MSSM), it is necessary to introduce the notation of the superfields that involves a spinor generator, i.e: a two-component Weyl spinor generator Q_α [7],[8]. The transformation properties with respect to the Poincare group are [79][9]:

$$\begin{aligned} [P^\mu, Q_{\alpha i}] &= 0, \\ [Q_{\alpha i}, M^{\mu\nu}] &= \frac{1}{2}(\sigma^{\mu\nu})^\beta_\alpha Q_{\beta i}, \\ \{Q_{\alpha i}, Q^j_\beta\} &= 0, \\ \{\overline{Q}_{\dot{\alpha} i}, \overline{Q}^j_{\dot{\beta}}\} &= 0. \end{aligned} \tag{3.2}$$

These equations, joined with the relations satisfied by the hermitian generators P_μ and $M_{\mu\nu}$, comprise the super-Poincare algebra. In this theory the number of bosons is equal to the number of fermions ($n_B = n_F$) [69].

[7] The generators of such a symmetry must carry a spinorial index, since they correspond to the transformation of an integer spin field into a spinor field. They are thus not commuting with Lorentz transformations. In this sense, supersymmetry is necessarily a spacetime symmetry [80, 70].

[8] The last commutation relation is for the case of $N = 1$ supersymmetry. For the particular case of $N = 2$ it follows $\{Q_{\alpha i}, \overline{Q}^j_{\dot{\beta}}\} = 2\delta^j_i \sigma^\mu_{\alpha\dot{\beta}} P_\mu$.

[9] More details in of the supersymmetry algebra is given in the Appendix A

The supermultiplets are the irreducible representations of the supersymmetry algebra. Each one contains bosonic and fermionic states and their degree of freedom must be the same. The supermultiplets used for the MSSM are:
*(ϕ, ψ) chiral superfield: 1 Weyl fermion ($n_F = 2$) and 2 real scalars ($n_B = 2$).
*(V^μ, λ) vectorial superfield: 1 spin mass zero boson ($n_B = 2$) and 1 Weyl fermion ($n_F = 2$).

3.2.3 Minimal Supersymmetric Standard Model

The *Minimal Supersymmetric Standard Model* MSSM is the most general renormalizable SUSY model respecting the gauge symmetries of the SM with the minimal number of fields, including R-parity [10] and the most general couplings under the gauge group which satisfy several phenomenologycal constraints [75].

As mentioned before, a supersymmetry transformation does not change the $SU(3)_c \times SU(2)_L \times U(1)_Y$ quantum numbers: that is to say, each SM field and its partner in a SUSY supermultiplet must have the same $SU(3)_c \times SU(2)_L \times U(1)_Y$ numbers. The fields of the SM, which comprise $spin - 0$ Higgs, $spin - \frac{1}{2}$ quark and lepton fields, and $spin - 1$ gauge fields, can be assigned to chiral and gauge supermultiplets. Therefore, for every particle a superpartner is introduced: for matter fermions, the superpartners are taken to be spin zero scalars and are described, along with the latter, by chiral superfieds. These scalars are called sfermions and they can be classified into scalar leptons or sleptons and scalar quarks or squarks. The superpartner fields of the SM gauge bosons are chosen to have $spin - \frac{1}{2}$ and are called gauginos. These and the bosons are described by vector superfields and can be classified as zino (corresponding to the Z boson) and winos (corresponding to W bosons). Spin zero Higgs bosons have $spin - \frac{1}{2}$ superpartners called higgsinos. Different from the SM, in the MSSM one Higgs doublet is no longer enough. This theory contains two Higgses: H_u and H_d with different hypercharges. H_d is in the same representation of the gauge group as left-handed leptons.

The MSSM spectrum is shown in Table 2.1, where the hypercharge has been

[10] In the MSSM the terms which include R-parity violation are not considered in the superpotential.

Sup.	**Bos**	**Fer.**	$SU(3)_c$	$SU(2)_L$	$U(1)_Y$	**Q**
$\hat{G}$	g	$\widetilde{g}$	8	1	0	0
$\hat{V}$	W^a	$\widetilde{W}^a$	1	3	0	$(1, 0, -1)$
$\hat{V}'$	B	$\widetilde{B}$	1	1	0	0
$\hat{L}$	$\widetilde{L}_i = (\widetilde{\nu}_i, \widetilde{e_i^-})$	$(\nu_i, e_i^-)_L$	1	2	-1	(0,-1)
$\hat{E}^c$	$\widetilde{E}_i = (\widetilde{e}_i)^*_R$	$(e_i)^c_L$	1	1	2	1
$\hat{Q}$	$\widetilde{Q}_i = (\widetilde{u}_i, \widetilde{d}_i)_L$	$(u_i, d_i)_L$	3	2	$\frac{1}{3}$	$(\frac{2}{3}, -\frac{1}{3})$
$\hat{U}^c$	$\widetilde{U}_i = (\widetilde{u}_i)^*_R$	$(u_i)^c_L$	3^*	1	$-\frac{4}{3}$	$-\frac{2}{3}$
$\hat{D}^c$	$\widetilde{D}_i = (\widetilde{d}_i)^*_R$	$(d_i)^c_L$	3^*	1	$\frac{2}{3}$	$\frac{1}{3}$
$\hat{H}_d$	(H_d^0, H_d^-)	$(\widetilde{H}_d^0, \widetilde{H}_d^-)_L$	1	2	-1	$(0, -1)$
$\hat{H}_u$	(H_u^+, H_u^0)	$(\widetilde{H}_u^+, \widetilde{H}_u^0)_L$	1	2	1	$(0, 1)$

Table 3.1: MSSM particle content

normalized such that:

$$Q_f \;\; = \;\; T_{3L}^f + \frac{Y_f}{2}. \tag{3.3}$$

Although this model is a minimal version, there are yet a lot of parameters in the theory. Besides the 19 parameters of the SM, there are 105 new ones: five real parameters and three CP-violating phases in the gaugino-Higgsino sector, 21 masses, 36 real mixing angles and 40 CP-violating phases in the squark and slepton sector. Overall, this makes 124 parameters [80]. More fundamental theories (grand unification, family symmetries, string theory, etc.) usually provide additional relations between these parameters. In models such as minimal CMSSM we will be left with only five extra parameters besides those of the SM.

Assuming R-parity, the MSSM superpotential is:

$$W^{MSSM} = \epsilon_{ab}[Y_u^{ij}\hat{Q}_i^a\hat{U}_j^c\hat{H}_u^b + Y_d^{ij}\hat{Q}_i^b\hat{D}_j^c\hat{H}_d^a + Y_e^{ij}\hat{L}_i^b\hat{E}_j^c\hat{H}_d^a - \mu\hat{H}_d^a\hat{H}_u^b], \tag{3.4}$$

where i, j are the family indices, $a, b = 1, 2$ are the $SU(2)$ indices and ϵ_{ab} is the totally antisymmetric Levi-Civita tensor. The matrices Y_u, Y_d and Y_e are the usual

Yukawa couplings while μ is a parameter with dimensions of mass.

The Lagrangian density of the theory associated to W can be written as [11]:

$$\begin{aligned} L_{SUSY} = & - D^{\mu}\phi^{i*}D_{\mu}\phi_i + i\psi^{i\dagger}\overline{\sigma}^{\mu}D_{\mu}\psi_i - \frac{1}{2}(\frac{\partial^2 W}{\partial\phi_i\partial\phi_j}\psi_i\psi_j + h.c) - \frac{\partial W}{\partial\phi_i}(\frac{\partial W}{\partial\phi})^* \\ & - \frac{1}{4}F^a_{\mu\nu}F^{a\nu\mu} + i\lambda^{\dagger}_a\overline{\sigma}^{\mu}D_{\mu}\lambda_a - \frac{1}{2}g^2[(T^a)_{ij}\phi^{i*}\phi_j]^2 - gk^a(T^a)_{ij}\phi^{i*}\phi_j \\ & - [\sqrt{2}g(T^a)_{ij}\phi^{i*}\psi_j\lambda^a + h.c]. \end{aligned} \tag{3.5}$$

Due to the large number of parameters in this theory, its phenomenological analysis is not an easy task, unless, there is a theory at high energy which reduces the number of parameters. This problem is also addressed by choosing the proper mechanism to break the symmetry. Below we discuss mSUGRA or gravity mediated supersymmetry breaking in which the SUSY breaking is mediated by gravity in a hidden sector.

3.2.4 Supersymmetry breaking

In supersymmetric models, sparticles would be degenerated in mass with particles. Since no sparticle has yet been observed at experiment, if SUSY is a symmetry of Nature, it must be broken at low energies.

a. Spontaneous supersymmetry breaking

The criterion for spontaneous symmetry breaking is that the physical vacuum state $|0>$ should not be invariant under a general supersymmetric transformation. This means, $|\Omega>$ should not be annihilated by all the supersymmetry generators Q_α, i.e [79]:

$$\begin{aligned} Q_\alpha|0> &\neq |0>, \\ <0|H|0> &\neq 0. \end{aligned} \tag{3.6}$$

[11] Here, g is the gauge coupling constant, f^{abc} the group structure constants, T^a the representation matrices for each chiral supermultiplet and the k parameter is only allowed for $U(1)$ gauge factors (Fayet-Iliopoulos term). More details in the Appendix A.2

Such violation occurs if and only if the global minimum has a positive value [12]. This supersymmetry breaking must arise from some fields in the theory which VEV is not invariant under supersymmetric transformations. These fields are namely known as the chiral F_i superfields, where $< 0|H|0 > \neq 0$.
There are some shortcomings regarding to the spontaneous symmetry breaking schemes: These always extend the MSSM to include new particles and interactions at very high mass scales (D-terms and F-term).

b. SOFT supersymmetry breaking

From a practical point of view, it is useful, instead of breaking SUSY spontaneously, just to introduce extra terms that break supersymmetry explicitly in the effective MSSM Lagrangian.
For realistic SUSY models, certain soft supersymmetry breaking operators which involve new fields beyond those of the MSSM are explicitly added to the Lagrangian density to make sparticles much heavier than particles. The coefficients of these operators are treated as unknown parameters in the MSSM. [13]. The symmetry breaking in this case needs to be generated in a *hidden sector*, where the new fields are singlets with respect to the SM gauge group. The symmetry breaking is then transmitted to the *observable sector* by a messenger sector associated with a messenger scale M_M that needs to be at least two orders of magnitude above the mass of the MSSM fields. When these fields are integrated out at lower energies, the residual theory is described by the standard supersymmetric Lagrangian density L_{SUSY} plus some soft explicit supersymmetric breaking terms, described in L_{soft}.

Possible terms that can be added to the Lagrangian of a supersymmetric gauge theory without perturbing cancellation of quadratic divergences are:
- Scalar mass terms: $\phi_i^* \phi_j$, $b^{ij}\phi_i\phi_j$.
- Trilinear scalar terms: $a^{ijk}\phi_i\phi_j\phi_k + h.c.$
- Gaugino mass terms: $\frac{1}{2}M_a\lambda^a\lambda^a$.

[12] Whenever a supersymmetric vacuum state exist as a local minimum of the effective potential it is the global minimum. If there is more than one supersymmetric vacuum, they are all degenerate in energy with zero energy.

[13] In order to keep the properties of SUSY, for example, the cancellation of quadratic divergences, the breaking terms must be of dimension lower than 4, i.e, SUSY breaking parameters must be dimensionful.

These are known as soft SUSY breaking terms and the Lagrangian that contains these is called L_{soft}:

$$L_{soft} = -(\frac{1}{2}M_a\lambda^a\lambda^a + \frac{1}{6}a^{ijk}\phi_i\phi_j\phi_k + \frac{1}{2}b^{ij}\phi_i\phi_j + c^i\phi_i) + c.c - (m^2)^i_j\phi^{j*}\phi_i. \tag{3.7}$$

Considering all the fields, the Lagrangian which describes the soft SUSY terms in the MSSM is:

$$\begin{aligned} L_{soft} = -[&\frac{1}{2}M_1\widetilde{B}\widetilde{B} + \frac{1}{2}M_2\widetilde{W}^a\widetilde{W}^a + \frac{1}{2}M_3\widetilde{g}^b\widetilde{g}^b + h^u_{ij}\widetilde{u}^*_{Ri}\widetilde{Q}_j.H_u \\ &+ h^d_{ij}\widetilde{d}^*_{Ri}\widetilde{Q}_j.H_d + h^l_{ij}\widetilde{e}^*_{Ri}\widetilde{L}_j.H_d + B_\mu H_u.H_d + h.c] \\ &+ (m^2_{\widetilde{Q}})_{ij}\widetilde{Q}^*_i\widetilde{Q}_j + (m^2_{\widetilde{u}})_{ij}\widetilde{u}^*_{Ri}\widetilde{u}_{Rj} + (m^2_{\widetilde{d}})_{ij}\widetilde{d}^*_{Ri}\widetilde{d}_{Rj} \\ &+ (m^2_{\widetilde{L}})_{ij}\widetilde{L}^*_i\widetilde{L}_j + (m^2_{\widetilde{e}})_{ij}\widetilde{e}^*_{Ri}\widetilde{e}_{Rj} + (m^2_{H_u})H^*_uH_u + (m^2_{H_d})H^*_dH_d, \end{aligned} \tag{3.8}$$

where $a = 1, 2, 3$ and $b = 1, ..., 8$. This is the most general soft supersymmetry-breaking Lagrangian that is compatible with gauge invariance and matter parity conservation in the MSSM. This Lagrangian breaks SUSY, since it introduces mass terms for some fields but not for their superpartners.

As noted L_{soft} involves only scalars and gauginos and not their respective superpartners. The soft terms in L_{soft} are able to give masses to all of the scalars and gauginos in a theory, even if the gauge bosons and fermions in chiral supermultiplets are massless. The gaugino masses M_a are always allowed by gauge symmetry. The $(m^2)_{ij}$ terms are allowed for i; j such that ϕ_i, ϕ^{j*} transform in complex conjugate representations of each other under all gauge symmetries. The Feynman diagrams corresponding to the allowed soft terms are shown in Figure 2.1. For each of the mass graphs (a),(c),(d) there is another with all arrows reversed, corresponding to the complex conjugate term in the Lagrangian.

Now, we will turn to the transmission of supersymmetry breaking from the *hidden sector*. The most popular scenarios are [75, 79]:

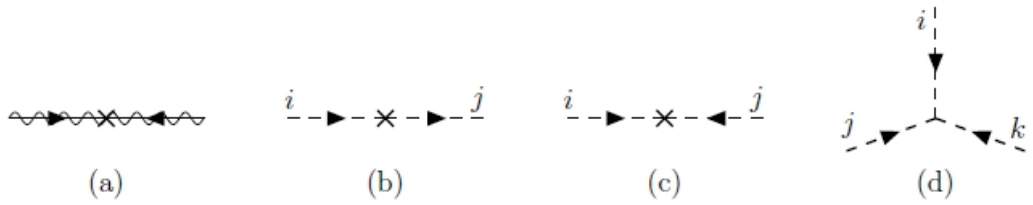

Figure 3.1: Soft supersymmetric breaking terms: (a) Gaugino mass M_a; (b) scalar squared mass $(m^2)^i_j$; (c) scalar squared mass b^{ij} and scalar cubic coupling a^{ijk}.

* GMSB: Gauge mediation of symmetry breaking in which the messenger interaction is the same as the SM gauge interaction.
* SUGRA: Gravitational mediation of symmetry breaking in which gravity is the messenger of this breaking. When we turn to local supersymmetry, gravity becomes part of the theory and strongly modifies the description of SUSY breaking. Indeed, the anticommutation relation: $\{Q_r, \overline{Q_s}\} = 2\gamma^\mu_{rs} P_\mu$ impose to include *local* translations. A local version of supersymmetry is called supergravity (the inclusion of gravity modifies the criterion of spontaneous supersymmetry breaking) [80] [14].

mSUGRA parameters

CMSSM (or the "so-called" mSUGRA) is defined at the GUT-scale by the following soft supersymmetry breaking parameters: a common scalar mass m_0 (squarks, sleptons, Higgs bosons), a common gaugino mass $M_{1/2}$, a common trilinear coupling A_0, $tan\beta = v_u/v_d$: the ratio of the Higgs (H_d, H_u) vacuum expectation values and $sign(\mu)$: SUSY conserving Higgsino mass parameter. Considering an idealized limit in which the squark and slepton mass matrices are flavour-blind, this means these parameters are assumed to take a simple structure at the GUT scale[15]:

[14] In this theory, an invariance under local transformations implies an invariance under local coordinate shifts, generated by the four momentum operator P_μ and then an invariance under the full Poincare Algebra.

[15] All the potentially dangerous flavour-changing and CP-violating effects in the MSSM can be evaded if one assumes that SUSY breaking is suitably "universal" [81].

•Universality: all scalar masses are equal and generation diagonal

$$M_Q^2 = M_D^2 = M_U^2 = M_L^2 = M_R^2 = m_0^2 I, \tag{3.9}$$

(in this case, all the squark and slepton mixing angles are rendered trivial, because squarks and sleptons with the same electroweak quantum numbers will be degenerate in mass and can be rotated into each other at will) [16]

•All Gaugino masses are equal:

$$M_1 = M_2 = M_3 = M_{1/2}. \tag{3.10}$$

Making the further assumption that the scalar couplings are each proportional to the corresponding Yukawas in the superpotential:

$$h_u = t_u A_{u0}, h_d = t_d A_{d0}, h_e = t_e A_{e0}. \tag{3.11}$$

will ensure that only the squarks and sleptons of the third family can have large couplings (where A_0 is a common parameter).

All of these universality relations are assumed to be the result of some specific model for the origin of supersymmetry breaking. This means, these relations are indicative of an assumed underlying simplicity or symmetry of the Lagrangian at some very high scale. These conditions are boundary conditions on the runnung soft parameters at the high scale.
It is usual to define the mSUGRA parameter space as: $(sign\mu, m_0, M_{1/2}, A_0, tan\beta)$. Searches for SUSY by CMS and ATLAS define an excluded range in the mSUGRA parameters space, ruling out certain regions in the parameter space. Figure 2.2 shows some of the LHC excluded regions for m_0 and $M_{1/2}$ parameters and the dependence with different SUSY observables. This plot shows the exclusion limits at 95% C.L for 8 TeV analyses in the (m_0 and $m_{1/2}$) parameter space for the CMSSM model with the remaining parameters set $tan\beta = 30$, $A_0 = -2m_0$, $\mu > 0$. Part of the model plane accommodates the lightest neutral scalar Higgs boson mass of 125 GeV. The theoretical signal cross section uncertainties are not included in the

[16] This is true only at the GUT scale. This is not invariant under RGE.

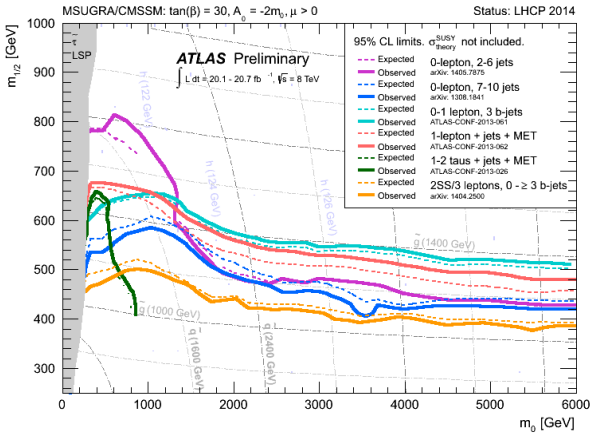

Figure 3.2: Region in CMSSM parameter space excluded by ATLAS [82].

limits shown [82].

It is known that the LHC collider should be able to detect signals of supersymmetry. However, actual data don't reveal considerable deviations from the SM. It means, until now the world appears even more SM-like. Using the combined 7 TeV and 8 TeV data, the ATLAS and CMS collaboration find a signal for a Higgs like boson at a mass of $\simeq$ 126 GeV. In supersymmetric theories the Higgs boson mass is predicted to be less than M_Z and loop corrections are needed to fit the mass above M_Z. This mass value ($m_h \simeq 126$ GeV) implies for instance that the squark masses are likely of the order of several TeV.

3.3 NEUTRINO PHYSICS

3.3.1 Introduction

Neutrinos have played a key role in the development of particle physics [16, 17]. In the 1980′s a lot of activity in neutrino physics has devoted mainly to the gauge theoretic formulation of neutrino mass and oscillations [17]. Some experiments and solar

[17] In the 1950′s it was believed that neutrinos only existed as a left handed neutrinos or right handed antineutrinos.

neutrino astronomy confirmed the idea of massive neutrinos and non-trivial mixing. Ultimate confirmation of neutrino mass only came with the results of atmospheric, solar and reactor neutrino experiments [8, 7, 9, 10]. The actual data of the masses and mixings are: $\Delta m^2_{21}[10^{-5}eV^2] = 7.11 - 8.18$, $\Delta m^2_{31}[10^{-3}eV^2] = 2.30 - 2.65$, $sin^2\theta_{12}/10^{-1} = 2.78 - 3.75$, $sin^2\theta_{23}/10^{-1} = 3.92 - 6.43$, $sin^2\theta_{13}/10^{-2} = 1.77 - 2.94$ for the normal hierarchy and 3σ of c.l [83, 84, 85, 86, 87, 88, 89].

Despite the success of the experiments, some important questions are still open. For instance, what is the nature of the neutrinos?. Most physicists expect the neutrino to be a Majorana particle. The smallness of its mass with respect to the charged fermions can be naturally explained by the seesaw mechanism, in which singlet fermions N_i (assumed to have large Majorana masses) are added to the SM. These can couple with the left handed neutrinos and the (up-type) Higgs doublet. The dimension five operator $m_\nu = \frac{F}{\Gamma}(HL)(HL)$ induces Majorana masses also for left handed neutrinos once the electroweak symmetry is broken. Current neutrino data point to a seesaw scale of $M_R \simeq 10^{10} - 10^{15}$ GeV [18].

Although the seesaw mechanism describes qualitatively well the observations, it lacks predictive power: the leptonic Lagrangian is defined at high energy by 21 parameters, whereas experimentally we can only measure at most 12 observables. The remain 9 parameters, which are undetermined, are lost in the decoupling process and can be arbitrarily chosen [90]. It may be possible to gain some indirect information of these parameters in the supersymmetric version of the seesaw, where the neutrino Yukawa couplings affect the renormalization group evolution of the slepton parameters above the decoupling scale and thus can leave an imprint, that in principle, could be disentangled using low energy experiments. Therefore, the SUSY softs at the electro-weak scale contain indirect information about all particles, intermediate scales and the seesaw scale. These aspects will be analyzed in detail in Chapter 3.

[18] With such high scale, the effects of lepton flavor violation in processes other than neutrino oscillations themselves become extremely small.

3.3.2 Seesaw Models

The most widely accepted mechanism to generate the small neutrino masses is the canonical see-saw mechanism, where the neutrinos are assumed to be Majorana particles. Here three (at least two) very heavy gauge singlets, called right handed neutrinos, are added to the spectrum of the Standard Model.
If neutrinos are Majorana particles, their masses below the scale Λ are described by a unique dimension-5 operator [91]:

$$m_\nu = \frac{F}{\Lambda}(L_i H)^T (L_j H), \tag{3.12}$$

where L_i denotes an electroweak doublet $(i, j = e, \mu, \tau)$ and H is the SM higgs doublet. This operator violates lepton number by two units and generates the neutrino mass $m_\nu \propto v^2$ once the electroweak symmetry is broken and the Higgs acquires a vacuum expectation value $v =< H >$ [91].

In seesaw models, and with renormalizable interactions only, the effective operator (2.12) is generated at tree level by the exchange of heavy particles and this can be achieved in different ways [92] [19]:
• Seesaw type I: exchanges a heavy $SU(3)_c \times SU(2)_L \times U(1)_Y$ fermionic singlet [17, 45, 95]. Here, if the Majorana mass M_R is much larger than the Dirac mass m_D, then the mass eigenvalues are approximately M_R and $m_D^2/M_R << M_R$.
• Seesaw type II: a $SU(2)$ scalar triplet Δ is added to the theory [17, 45]. This field couples to the ordinary neutrinos through: $L_2 = Y_2 L^T \Delta L + h.c.$ Once the triplet acquires a vacuum expectation value $v =< \Delta >$, it gives a neutrino mass term proportional to: $Y_2\Delta$ and to the Higgs field itself. This triplet vev induces a change in the electroweak ρ parameter. This vev is experimentally constrained to be below a few $GeVs$.
• Seesaw type III: exchanges of at least two $SU(2)_L$ fermionic triplets Σ^a with zero hypercharge [92, 96].

In this thesis, we will describe in detail the type-I seesaw and its supersymmetric implementation.

[19] This operator can be generated also at loop level. Two classical examples are the Zee model (1-loop) [93] and the Babu-Zee model (2-loop)[94].

Supersymmetric seesaw type I

In the case of seesaw type-I one postulates very heavy right-handed neutrinos with the following superpotential below the GUT scale, M_G:

$$W_I \;=\; W_{MSSM} + W_\nu. \tag{3.13}$$

Here W_{MSSM} is the usual MSSM part and

$$W_\nu \;=\; \widehat{N}_i^c Y_{ij}^\nu \widehat{L}_j \cdot \widehat{H}_u + \frac{1}{2}\widehat{N}_i^c M_{R,ii} \widehat{N}_i^c \; . \tag{3.14}$$

We have written eq. (3.13) in the basis where M_R and the charged lepton Yukawas are diagonal. In the seesaw one can always choose this basis without loss of generality. For the neutrino mass matrix, upon integrating out the heavy Majorana fields, one obtains the well-known *seesaw* formula

$$m_\nu = -\frac{v_u^2}{2} Y^{\nu,T} M_R^{-1} Y^\nu, \tag{3.15}$$

valid up to order $\mathcal{O}(m_D/M_R)$, $m_D = \frac{v_u}{\sqrt{2}} Y^\nu$. Being complex symmetric, the light Majorana neutrino mass matrix in eq. (3.15), is diagonalized by a unitary 3×3 matrix U [17]

$$\hat{m}_\nu = U^T \cdot m_\nu \cdot U \; . \tag{3.16}$$

Inverting the seesaw equation, eq. (3.15), allows to express Y^ν as [97]

$$Y^\nu = \sqrt{2}\frac{i}{v_u}\sqrt{\hat{M}_R} \cdot R \cdot \sqrt{\hat{m}_\nu} \cdot U^\dagger, \tag{3.17}$$

where $\hat{m}_\nu$ and $\hat{M}_R$ are diagonal matrices containing the corresponding eigenvalues. R is in general a complex orthogonal matrix. Note that, in the special case $R = \mathbf{1}$, Y^ν contains only "diagonal" products $\sqrt{M_i m_i}$. For U we will use the standard form

$$U = \begin{pmatrix} c_{12}c_{13} & s_{12}c_{13} & s_{13}e^{-i\delta} \\ -s_{12}c_{23} - c_{12}s_{23}s_{13}e^{i\delta} & c_{12}c_{23} - s_{12}s_{23}s_{13}e^{i\delta} & s_{23}c_{13} \\ s_{12}s_{23} - c_{12}c_{23}s_{13}e^{i\delta} & -c_{12}s_{23} - s_{12}c_{23}s_{13}e^{i\delta} & c_{23}c_{13} \end{pmatrix} \times \begin{pmatrix} e^{i\alpha_1/2} & 0 & 0 \\ 0 & e^{i\alpha_2/2} & 0 \\ 0 & 0 & 1 \end{pmatrix}$$

with $c_{ij} = \cos\theta_{ij}$ and $s_{ij} = \sin\theta_{ij}$. The angles θ_{12}, θ_{13} and θ_{23} are the solar neutrino angle, the reactor angle and the atmospheric neutrino mixing angle, respectively. δ is the Dirac phase and α_i are Majorana phases. Since U can be determined experimentally only up to an irrelevant overall phase, one can find different parameterizations of the Majorana phases in the literature.
Eq. (3.15) contains 9 a priori unknown parameters, eq. (3.17) contains 18. The additional 9 unknowns encode the information about the high scale parameters, the three eigenvalues of M_R and the 3 moduli and 3 phases of R.

3.3.3 $\nu^{'}$s and GUTs

Left-right intermediate scale

The left-right symmetric treatment of the weak interactions requires the existence of the right handed neutrinos and the smallest group that implement this hypothesis is $SU(2)_L \times SU(2)_R \times U(1)_{B-L}$. Unlike $SU(5)$, GUT's models based on $SO(10)$ contain a left-right symmetry [20] and also the necessary ingredients to generate automatically the seesaw mechanism: (i) the right handed neutrino is included in the 16 which forms a fermion family; and (ii) is the minimal LR symmetric GUT model that gauges the $(B-L)$ symmetry. When the symmetry $B-L$ is broken the RH neutrinos acquire mass. The LR symmetry can be broken either by the field $\Phi_{1,1,3,-2}$ or $\Phi_{1,1,2,-1}$. Thus, models where $\Phi_{1,1,2,-1}$ and $\Phi_{1,3,1,0}$ are present can break the LR symmetry and also explain the CKM matrix. An additional singlet $\Phi_{1,1,1,0}$ can explain an inverse seesaw, while an additional $\Phi_{1,1,3,-2}$ generates a seesaw type-I [21].

$SO(10)$ SUSY models usually break the LR symmetry at a rather large energy scale, m_R. If LR is broken by the vev of $(B-L)=2$ triplets or by a combination of $(B-L)=2$ and $(B-L)=0$ triplets, $m_R = 10^{15}$ GeV is the typical scale consistent with the gauge coupling unification. This kind of high LR scale models will never be probed experimentally and this explains, perhaps, why LR models have not been studied very much in literature in the context of GCU. However, it is quite straightforward to construct nonSUSY LR models where the LR scale is

[20] $SO(10)$ breaks to the SM like $SO(10) \to SU(3)_c \times SU(2)_L \times SU(2)_R \times U(1)_{B-L} \to SM$

[21] The indices are the transformation properties under the LR group, see Chapter 5 and the appendix for notation.

close to the EW scale. In Chapter 5 we will analyze in detail SUSY and nonSUSY $SO(10)$ GUT models with LR intermediate scales and simple configurations that explain neutrino masses through different realizations of the seesaws mechanism.

Loop induced neutrino mass

$SO(10)$ loop induced neutrino mass was first introduced by Edward Witten [98]. In this model a pair of lepton-number violating vacuum expectation values (VEV's) is tied to the leptonic sector at two loop. Here, the RH neutrinos masses are generated at the renormalizable level with just the minimal scalar content sufficient for the desired spontaneous symmetry breaking (i.e., $10 \oplus 16 \oplus 45$). The absolute size of the Witten loop is governed by the position of the $B-L$ breaking scale M_{B-L} which is required to be around the GUT-scale (M_G) in order to yield the correct seesaw scale $M_R \simeq (\alpha/\pi)^2 M_{B-L}^2/M_G$ in the 10^{13} GeV ballpark. The realization of this mechanism in a flipped $SU(5)$ theory will be studied in detail in Chapter 4.

3.4 GRAND UNIFIED MODELS

Particle interactions down to distances as small as 10^{-16} cm are perfectly described by the SM gauge theory. However many attempts have been made to explain nature with a unified theory that combines all the three fundamental interactions as a component of a single force. Georgi and Glashow $SU(5)$ unification [42], Pati and Salam $SU(4)_c \times SU(2)_L \times SU(2)_R$ unification [41] and models based in $SO(10)$ [99] have been the three GUT groups studied most estensively in the literature.

Apart from reducing all gauge interactions to one single gauge group, GUTs have some other advantages with respect to the SM, as described in the last section. These features are realized for both supersymmetric and non-supersymmetric scenarios. SUSY GUTs appear as an extension of nonSUSY GUTs. However, they lead to different low energy effective theories. For SUSY, the low energy spectrum includes the SM states plus their supersymmetric partners and a pair of higgs doublets. Figure 2.3 shows the running of the three $SU(3)_c \times SU(2)_L \times U(1)_Y$ gauge couplings for the SM, MSSM, a simple nonSUSY GUT model based on the LR group and a simple SUSY model based in the Pati-Salam group [2, 3]. As is known, the three gauge couplings do not unify in a single point at any energy

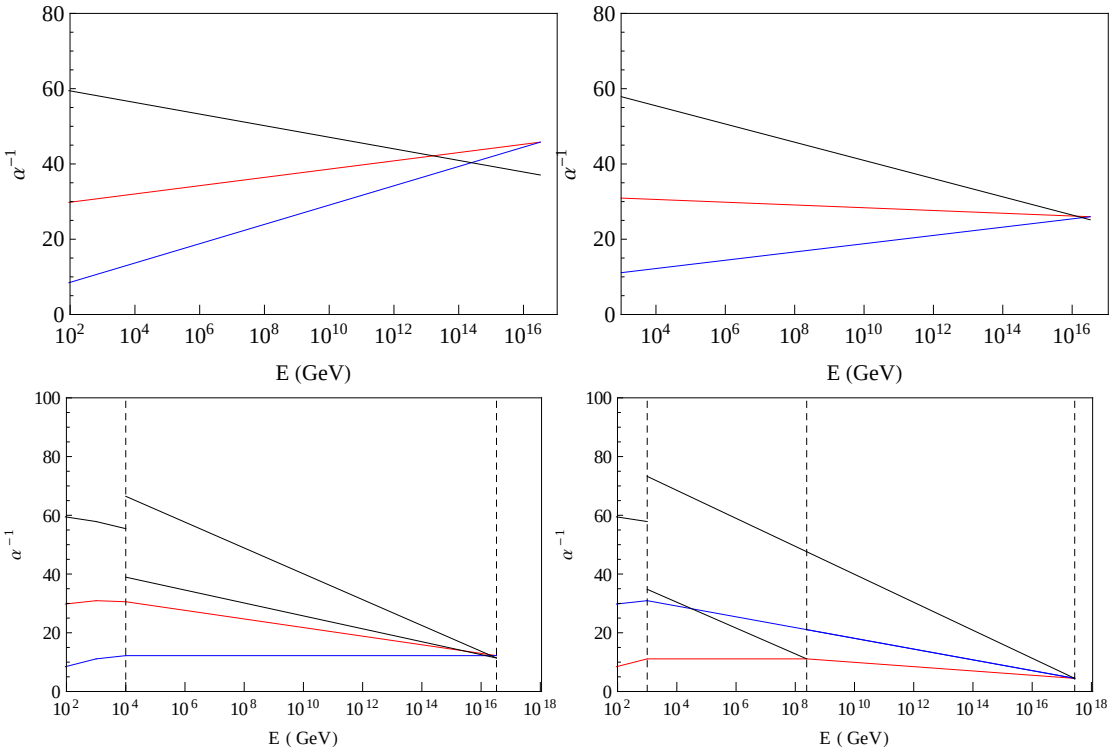

Figure 3.3: 1-loop evolution of the three gauge coupling constants with the energy scale for four cases: SM (up-left), MSSM (up-right) a simple left-right nonSUSY model (bottom-left) and a simple left-right Pati-Salam SUSY model (bottom-right). [2, 3]

in the SM. In the MSSM there is unification (although not perfect [22]) at a scale of about $m_G = 10^{16}$ GeV. Simple Left-Right (LR) symmetric models (SUSY or nonSUSY), where some additional particles need to be added, can unify equally well or even better than the MSSM.

There are many ways to construct such unified models. However, more restrictive requirements, such as a theory to provide a natural understanding of the small neutrino masses and correct explanation of the CKM angles narrow down the possibilities. In this thesis, $SO(10)$ and $SU(5)$ unified theories will be studied, for both, supersymmetric and non-supersymmetric realizations. Special field con-

[22] Perfect unification for nonSUSY GUTs models can be realized if two loop contributions for the gauge couplings is considered, already shown in [3].

figurations that obey phenomenological requirements such as neutrino masses, a candidate for DM, correct CKM angles and proton decay constraints will be constructed. Before entering in the detailed analysis (next chapters), some general features of $SU(5)$, flipped $SU(5)$, $SO(10)$ and LR gauge groups will be discussed in this chapter. Proton decay processes and how these arise in GUT theories will be discussed in some detail.

3.4.1 $SU(5)$ Unification

To construct a GUT theory which describes the weak, electromagnetic and strong interactions with only one gauge coupling, a simple gauge group is needed. This group must be large enough to contain the 4 non-diagonal SM generators, thus must be at least rank-4. Among all the possible simple Lie rank-4 groups [42], the only ones with complex representations [23] are $SU(5)$ and $SU(3) \times SU(3)$. Since $SU(3) \times SU(3)$ can not accommodate fractionally charged particles, then $SU(5)$ remains as the simplest gauge group which can describe the SM without introducing new fermions.

Preliminaries

1. Particle content

The fundamental 5 (Ψ^p) and the antisymmetric 10 ($5 \times 5 \chi^{pq} = -\chi^{pq}$) $SU(5)$ representations decompose under $SU(3)_c \times SU(2)_L$ as [24]:

$$\begin{aligned} \overline{5} &: \Psi^p_L \to (3^*, 1)_{2/3} + (1, 2^*)_{-1}, \\ 10 &: \chi^{pq}_L \to (3, 2)_{1/3} + (3^*, 1)_{-4/3} + (1, 1)_2. \end{aligned} \tag{3.18}$$

Given the quantum numbers of the fermions in the SM, it follows that the 15 helicity states of a generation are contained in the $SU(5)$ irreducible representation $\overline{5} + 10$:

[23] The SM fermions, with the following $SU(3) \times SU(2)$ quantum numbers: $(\nu_e, e^-)_L = (1, 2), e_L = (1, 1), (u_\alpha, d_\alpha)_L = (3, 2), u^{c\alpha}_L = (3^*, 1), d^{c\alpha}_L = (3^*, 1)$ must be described by complex representations.

[24] The right handed fields are described in terms to the left handed fields like $\Psi^c = C\overline{\Psi}^T$ and $\Psi^c_L = (\Psi_R)^c$, with $C = i\gamma^2\gamma^0$.

$$(\Psi^p)_L = \begin{pmatrix} d_1^c \\ d_2^c \\ d_3^c \\ e \\ -\nu_e \end{pmatrix}_L , \ \chi_L^{pq} = \frac{1}{\sqrt{2}} \begin{pmatrix} 0 & u_3^c & -u_2^c & -u_1 & -d_1 \\ -u_3^c & 0 & u_1^c & -u_2 & -d_2 \\ u_2^c & -u_1^c & 0 & -u_3 & -d_3 \\ u_1 & u_2 & u_3 & 0 & -e^c \\ d_1 & d_2 & d_3 & e^c & 0 \end{pmatrix}_L . \quad (3.19)$$

The 24 gauge fields are accommodated in the adjoint A_j^i 24 dimensional representation, decomposed under $SU(3)_c \times SU(2)_L$ as:

$$24 = (8,1)_0 + (1,3)_0 + (1,1)_0 + (3,2)_{-5/3} + (3^*,2)_{5/3}. \quad (3.20)$$

This decomposition corresponds to the following gauge bosons: $(8,1)_0$: $SU(3)$-Gluons, $(1,3)_0$: W_u^+, W_u^-, W_u^3-$SU(2)$ gauge fields, $(1,1)_0$: B_μ, $(3,2)_{-5/3}$: X_μ Leptoquarks and $(3^*,2)_{5/3}$: Y_μ Leptoquarks[25], [26]. The 12 *Leptoquarks* mediate nucleon decay processes, discussed in more detail in the next subsections.

2. $SU(5)$ symmetry breaking

The breaking of the $SU(5)$ gauge symmetry down to $SU(3)_c \times U(1)_Q$ is achieved in two steps:

$$SU(5) \to SU(3)_c \times SU(2)_L \times U(1)_Y \to SU(3)_c \times U(1)_Q, \quad (3.21)$$

at the scales M_X and M_W respectively. The two Higgs which mediate the breaking are:

$$H = \{\bar{5}\}, \ \Phi = \{24\}. \quad (3.22)$$

Φ with vacuum expectation value $\langle\Phi\rangle = \text{diag}\, V(1,1,1,-3/2,-3/2)$ mediates the first symmetry breaking step and gives masses to the Leptoquarks: $M_X^2 = M_Y^2 = \frac{25}{8} g^2 m_G^2$ (m_G is the unification scale). In order to break the electroweak symmetry at the weak scale M_W and give mass to the quarks and leptons, the Higgs doublet is needed in the $\bar{5}$-rep and gets vev: $\langle H\rangle = (0,0,0,0,\frac{v}{\sqrt{2}})$ [27]. The additional states

[25] The Leptoquarks carry fractional charges: $Q_X = -4/3$ and $Q_Y = -1/3$.

[26] The gauge bosons in $SU(5)$ are described by the matrix A_μ in the appendix.

[27] H gives also mass to the W and Z bosons, where $M_W = \frac{1}{2} g v$, $M_Z = \frac{gv}{2cos\theta_W}$ and θ_W the Weinberg angle.

are the coloured Higgs scalars. The couplings of these coloured triplets violate also baryon and lepton number, thus nucleon decay processes via the exchange of a single Higgs scalar arise. This implies that the coloured triples must be very heavy. The lightness of the doublet versus the heaviness of the triplet is known as the doublet-triplet splitting problem.

Important features of $SU(5)$

1. Anomaly free

In general the anomaly of any fermion-representation is proportional to the trace of its generators: $Tr(T^a(R), T^b(R)T^c(R)) = \frac{1}{2}A(R)d^{abc}$ ($T^a(R)$ is the representation of the group and d^{abc} is the totally symmetric coefficient appearing in the commutation relation $\{\lambda^a, \lambda^b\} = 2d^{abc}\lambda^c$) [100]. Using some simple $SU(5)$ generator to calculate $A(R)$ and the property $T^a = T^b = T^c = Q$ it follows:

$$\frac{A(5^*)}{A(10)} = \frac{trQ^3(\Phi^i)}{trQ^3(\Phi_{ij})} = -1, \tag{3.23}$$

$$A(5^*) + A(10) = 0. \tag{3.24}$$

Thus, the combination of 5^* and 10 of the fermion-representation is anomaly free in the $SU(5)$ theory.

2. Charge quantization

$SU(5)$ explains the experimentally observed charge quantization. The eigenvalues of the generators of a simple non-Abelian group are discrete while those corresponding to the Abelian $U(1)$ group are continuous. Thus, in $SU(5)$, since the electric charge Q is one of the generators, its eigenvalues are discrete and hence quantized. The traceless condition of the charged fermion matrix $Q = diag\{1/3, 1/3, 1/3, -1, 0\}$ (Q is one of the $SU(5)$ generators) requires $Tr(Q) = 3Q_q + Q_e + Q_\nu = 0$. It follows that $Q_q = -\frac{1}{3}Q_e$ (quarks carry 1/3 of the electron charge because they have three colours). $SU(5)$ thus provides a rational basis to understand the particle charges and electroweak hypercharge assignments.

3. Proton decay

A special feature of GUTs is the nonconservation of baryon and lepton number. The X and Y bosons that mediate proton decay couple two fermions with different baryon and lepton number. In one case they couple to quarks and leptons ($B_1 = 1/3$), in the other case they transform quarks to antiquarks ($B_2 = 2/3$). Therefore, through the mediation of a X boson, a ($B = -1/3$) channel can be converted into a ($B = 2/3$) one, changing the baryon number one unit ($\Delta B = 1$). However, baryon minus lepton number is conserved ($\Delta(B - L) = 0$) and $SU(3) \times SU(2) \times U(1)$ is invariant in these kind of processes. In section 2.4.3 more details of proton decay are discussed.

3.4.2 Flipped $SU(5)$

Another possibility to unify the SM matter into a $SU(5)$-based framework is the so-called flipped $SU(5)$ scenario: $SU(5) \times U(1)_X$, which is a maximal subgroup of $SO(10)$. In this model, the generator of the electric charge is given as a linear combination of the $U(1)$ generator that resides in $SU(5)$ and an extra $U(1)$ generator, as if both of these originate from a $SO(10) \to SU(5) \times U(1)$ decomposition. This guarantees anomaly cancellation at the price of introducing one extra state per family, i.e, the right handed neutrino ν^c. The quantum numbers of the matter multiplets in the $SU(5) \otimes U(1)_X$ extensions of the canonical $SU(5)$ framework are dictated (up to an overall normalization factor) by the requirement of gauge anomaly cancellation: $\overline{5}_M \equiv (\overline{5}, -3)$, $10_M \equiv (10, +1)$, $1_M \equiv (1, +5)$. Besides the "standard" $SU(5)$ assignment there is a second "flipped" embedding of the Standard Model (SM) hypercharge into the correspondin g algebra, namely

$$Y = \tfrac{1}{5}(X - T_{24}), \tag{3.25}$$

where the T_{24}

$$T_{24} = \sqrt{\frac{3}{5}} \begin{pmatrix} 1/3 & 0 & 0 & 0 & 0 \\ 0 & 1/3 & 0 & 0 & 0 \\ 0 & 0 & 1/3 & 0 & 0 \\ 0 & 0 & 0 & -1/2 & 0 \\ 0 & 0 & 0 & 0 & -1/2 \end{pmatrix}, \tag{3.26}$$

generator of $SU(5)$ above is understood to conform the SM normalization (i.e., $Y = T_{24}$ and $Q = T_L^3 + Y$ in the standard case). This swaps $u^c \leftrightarrow d^c$, $\nu^c \leftrightarrow e^c$, $u \leftrightarrow d$ and $\nu \leftrightarrow e$ with respect to the standard $SU(5)$ field identification and, hence, the RH neutrinos fall into 10_M rather than[28] 1_M. This also means that a vacuum expectation value (VEV) of a scalar version of $(10, +1)$ (to be denoted by 10_H) can spontaneously break the $SU(5) \otimes U(1)_X$ gauge symmetry down to the SM[29].

Besides that, the scheme benefits from several interesting features not entertained by the "standard" $SU(5)$ scenario, namely: i) The Yukawa Lagrangian

$$\mathcal{L} \ni Y_{10} 10_M 10_M 5_H + Y_{\bar{5}} 10_M \bar{5}_M 5_H^* + Y_1 \bar{5}_M 1_M 5_H + h.c, \tag{3.27}$$

including the 5-dimensional scalar $5_H = (5, -2)$ hosting the SM Higgs doublet, yields $M_d = M_d^T$, M_e arbitrary and, in particular, $M_\nu^D = M_u^T$, none of which is in a flagrant conflict with the observed quark and lepton flavour structure, as is the case for $M_d = M_e^T$ in the "standard" $SU(5)$. ii) The gauge unification is in a better shape than in the "standard" $SU(5)$ case because only the two non-abelian SM couplings are required to unify (which, indeed, they do at around 10^{16} GeV). Note that the SM hypercharge is a "mixture" of the T_{24} and X charges and, thus, the SM coupling g' obeys a nontrivial matching condition including an unknown coupling g_X associated to the extra $U(1)_X$ gauge sector. Hence, there is no need to invoke TeV-scale supersymmetry for the sake of gauge unification here as in the case of "standard" $SU(5)$. iii) Remarkably, the issue with the out-of-control Planck-scale induced shifts of the effective gauge couplings (and thus induced large

[28] Recall that in the standard $SU(5)$ Q, u^c and e^c are in 10_M, d^c and L in $\bar{5}_M$ and ν^c in 1_M.

[29] This observation is the core of the "missing partner" doublet-triplet splitting mechanism that brought a lot of interest to the flipped $SU(5)$ scenario in 1980's [102].

uncertainties in the M_G determination [103, 104, 105, 106]) is absent at leading order because there is no way to couple the 10_H, as the carrier of the large-scale VEV to a pair of the gauge field tensors $F_{\mu\nu}$. Thus, the prospects of getting a reasonable good grip on the proton lifetime in the flipped $SU(5)$ are much better than in the ordinary $SU(5)$ model.

The main drawback of such a scenario is the fact that the simplest "conservative" mechanism for generating a Majorana mass term for the RH neutrinos at the tree level requires an extra 50-dimensional scalar field $50_H \equiv (50, -2)$ whose large VEV in the $10_M 10_M 50_H$ contraction picks up just the desired components[30].

3.4.3 Proton Decay in $SU(5)$ GUTs

Proton decay, as a probe of fundamental interactions at extremely short distances, is an instrument for the exploration of grand unified theories. Thus it is crucial to have new experiments to search for these kind of processes and improve the current bounds. In this subsection, some theoretical and experimental aspects of proton decay will be described. In particular, the actual and future proposed experiments will be discussed.

Gauge $D = 6$ operators

In $SU(5)$, the effective Lagrangian, [31] which gives rise to processes that violate baryon and lepton number (such as $p \to e^+\pi^0$) is described by:

$$\begin{aligned} L_{XY} =& \frac{ig_G}{\sqrt{2}} X_{\mu,i}(\epsilon_{ijk}\overline{u}^c_k\gamma^\mu u_{jL} + \overline{d}_i\gamma^\mu e^+) + \\ &+ \frac{ig_G}{\sqrt{2}} Y_{\mu,i}(\epsilon_{ijk}\overline{u}^c_{kL}\gamma^\mu d_{jL} - \overline{u}_{iL}\gamma^\mu e^+_L + \overline{d}_{iR}\gamma^\mu \nu^c_R) + h.c. \end{aligned} \tag{3.28}$$

The most important proton decay operators are in general those of minimal dimension with the appropriate quantum numbers. Operators with non-zero baryon

[30] as does $\langle \overline{126}_H \rangle$ coupled to $16_M 16_M$ in $SO(10)$.

[31] This Lagrangian is derived writing down the couplings of the components 5 and 10 with the Leptoquarks in the kinetic Lagrangian: $L = i(\overline{\psi}_p)_L\gamma^\mu(D_\mu\psi_p)_L + i\overline{X}^{pq}_L\gamma^\mu(D_\mu X^{pq}_L)$

number must have at least three quarks fields to be colour singlets, and then at least four fermion fields to form a Lorentz scalar. So, their dimension is at least six, with $\Delta B \neq 0$, $\Delta L \neq 0$ and $SU(3)_c \times SU(2)_L \times U(1)$ singlets [50, 107]. The possible non-supersymmetric operators which conserve $B-L$ (i.e, the proton always decay into an antilepton) mediated by vector-like leptoquarks are [50]:

$$\begin{aligned} O_I^{B-L} &= k_1^2 \epsilon_{ijk}\epsilon_{\alpha\beta}\overline{u_{iaL}^c}\gamma^\mu Q_{j\alpha aL}\overline{e_{bL}^C}\gamma_\mu Q_{k\beta bL}, \\ O_{II}^{B-L} &= k_1^2 \epsilon_{ijk}\epsilon_{\alpha\beta}\overline{u_{iaL}^c}\gamma^\mu Q_{j\alpha aL}\overline{d_{kbL}^C}\gamma_\mu L_{\beta bL}, \\ O_{III}^{B-L} &= k_2^2 \epsilon_{ijk}\epsilon_{\alpha\beta}\overline{d_{iaL}^c}\gamma^\mu Q_{j\beta aL}\overline{u_{kbL}^C}\gamma_\mu L_{\alpha bL}, \\ O_{IV}^{B-L} &= k_2^2 \epsilon_{ijk}\epsilon_{\alpha\beta}\overline{d_{iaL}^c}\gamma^\mu Q_{j\beta aL}\overline{\nu_{bL}^C}\gamma_\mu Q_{k\alpha bL}, \end{aligned} \tag{3.29}$$

where $k_1 = g_{GUT}/\sqrt{2}M_{(X,Y)}$, $k_2 = g_{GUT}/\sqrt{2}M_{(X',Y')}$, $M_{(X,Y)}, M_{(X',Y')} \simeq M_G$ are the masses of the superheavy gauge bosons, and g_{GUT} the coupling at the GUT scale. The indices i, j and k are the colour indices, a, b the family indices and $\alpha, \beta = 1, 2$. The effective operators O_I^{B-L} and O_{II}^{B-L} appear when the superheavy gauge fields $(X, Y) = (3, 2, 5/3)$ are integrated out (X, Y have electric charge $4/3$ and $1/3$ respectively). This is the case of theories based on minimal $SU(5)$. Integrating out $(X', Y') = (3, 2, -1/3)$ the operators O_{III}^{B-L} and O_{IV}^{B-L} are obtained, corresponding to the case of flipped SU(5) scenarios [50].

The mass of the superheavy gauge bosons that mediate the decays is estimated using the experimental lower bound of the proton decay $\tau(p \to \pi^0 e^+) > 1.6 \times 10^{34}$ ys and:

$$\Gamma_p \sim \alpha_G^2 \frac{m_p^5}{M_V^4}. \tag{3.30}$$

A general lower bound on the heavy gauge boson masses is:$M_V > (2.6 - 3.2) \times 10^{15}$ GeV for $\alpha_G = 1/40 - 1/25$. Note that, in order to satisfy experimental bounds, the unification scale has to be very large.

The second contribution to proton decay is the scalar-like $d = 6$ operator, mediated in this case by the scalar leptoquarks $T = (3, 1, -2/3)$. For the $SU(5)$ case, this scalar lives in the 5_H representation together with the SM Higgs, and the relevant operators for proton decay are shown in the appendix. All the cases are mediated by the Higgs triplet. Although these contribution are quite model dependent, it is possible to give a naive estimation of the heavy scalar mass, using:

Theory	Decay Mode	τ_p limit
Minimal $SU(5)$	$p \to e^+\pi^0$	$10^{28.5} - 10^{31.5}$
Minimal SUSY $SU(5)$	$p \to \overline{\nu}k^+$	$< 10^{30}$
SUGRA $SU(5)$	$p \to \overline{\nu}k^+$	$10^{32} - 10^{34}$
Fipped $SU(5)$	$p \to \pi^+\overline{\nu}$	$>10^{38.5}$
Minimal $SO(10)$	$p \to e^+\pi^0$	$10^{30} - 10^{40}$
Minimal SUSY $SO(10)$	$p \to \overline{\nu}k^+$	$10^{32} - 10^{34}$
	$p \to e^+\pi^0$	$< 5.3 \times 10^{34}$

Table 3.2: Theoretical proton life time predictions

$$\Gamma_p \sim |Y_u|^2 |Y_d|^2 \frac{m_p^5}{M_T^4}, \tag{3.31}$$

and $\tau(p \to \pi^0 e^+) > 1.6 \times 10^{34}$ years.

Minimal $SU(5)$ predicts a proton decay lifetime of about $\tau_p \sim 10^{28.5} - 10^{31.5}$ years [108]. However, current limits ($\tau_p \sim 10^{34}$) years [108] impose stringent bounds on the mass of the X, Y bosons ($O(10^{15})$ GeV) and thus exclude the minimal-$SU(5)$ predictions. Extended models, like flipped SU(5) [108] improve the proton decay predictions. Table 2.2 shows the theoretical proton life time predictions in the most relevant channels for different GUT theories [50, 108, 109, 110].

Some experiments for proton decay

From the theoretical point of view, the idea that the proton may be unstable arose in the work of Sakharov in 1967, who postulated that an explanation of the baryon asymmetry in the universe requires CP violation and baryon-number non conservation [111, 112]. Further impetus for proton decay searches came from the work of Pati and Salam in 1973 and latter with non-supersymmetric [42] , supersymmetric and grand unification [50] in the framework of $SU(5)$ and $SO(10)$ theories. On the other hand, several experimental attempts to test nucleon decay processes have been done. Actual experiments are based on water Cherenkov detectors with a good capability to observe the different proton decay modes. Two of the most dominant channels tested in these experiments are $p \to e^+\pi^0$ and $p \to K^+\overline{\nu}$. This kind of detectors use water as the source of protons which decay into a positron

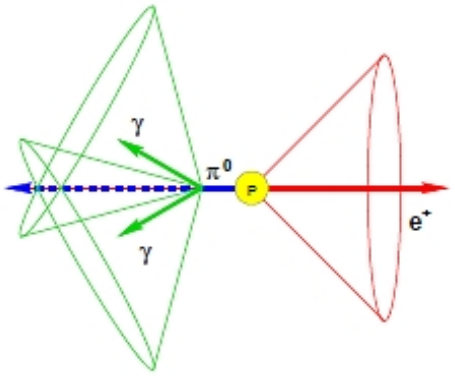

Figure 3.4: Main proton decay chanel $p \to e^+\pi^0$

e^+ and a pion π^0 (first mode). The positron produces an electromagnetic shower which is balanced by two electromagnetic showers from the decays of the pion to two photons ($\pi^0 \to \gamma\gamma$) [32]. Figure 2.4 shows a schematic presentation of an ideal $p \to e^+\pi^0$, $\pi^0 \to \gamma\gamma$ decay.

Super-Kamiokande (*Kamioka nucleon decay experiment*) [33] is the biggest (by far at the moment) experiment to test neutrino properties and, on the other hand, test grand unified theories. This experiment consists in a large water Cherenkov detector filled with 50,000 tons of ultra pure water to test the most important decay channels. Recent limits set by this experiment are [7]:

$$\begin{aligned}
\tau(p \to e^+\pi^0) &\geq 1.6 \times 10^{34} ys., \\
\tau(p \to \mu^+\pi^0) &\geq 4.7 \times 10^{32} ys., \\
\tau(p \to K^+\overline{\nu}) &\geq 2.3 \times 10^{33} ys., \\
\tau(p \to K^0\mu^+) &\geq 1.3 \times 10^{33} ys., \\
\tau(p \to K^0 e^+) &\geq 1.0 \times 10^{33} ys.
\end{aligned} \tag{3.32}$$

Nowadays, new multipurpose experiments which could improve about one order of magnitude existing proton decay limits from Super-Kamiokande (i.e could extend

[32] For the other typical decay mode $p \to K^+\overline{\nu}$, the detector in this case search for the two primary branches of the K^+ decay.

[33] *Kami: "Spirit" - oka: "hill" - nde: "nucleon decay experimente"* is located underground in the Mozumi Mine of the Kamioka Mining and Smelting Co. near the Kamioka section of the city of Hida in Gifu Prefecture, Japan.

Experiment	Features	Decay Mode	τ_p limit
HYPER-K	Water Cherenkov Detector (Japan)	$p \to e^+\pi^0$	1.3×10^{35}, 90 CL
			5.7×10^{34}, 3σ CL
		$p \to K^+\overline{\nu}$	2.5×10^{34}, 90 CL
			1.0×10^{34}, 3σ CL
MEMPHYS	Megaton Mass Physics (EU) Water Cherenkov like detector with a fiducial mass of about 500 kt.	$p \to \pi^0 e^+$	$> 10^{35}$
GLACIAR	Giant Liquid Argon Charge Imaging (EU) Experiment. Mass of about 100 kt.	$p \to K^+\nu$	$> 10^{35}$
LENA	Low Energy Neutrino Astronomy (EU) Liquid Scintillator like detector 51 kt.	$p \to K^+\overline{\nu}$	$> 2 \times 10^{34}$

Table 3.3: Some experiments for future proton decay measurements

proton life time searches sensitivities up to 10^{35} years) have been proposed. Three detection techniques are being studied for such large detectors: Water-Cherenkov, liquid scintillator and Liquid Argon. LAGUNA (Large Apparatus Studying Grand Unification and Neutrino Astrophysics)[19] is a project with the purpose to explore GUTs and neutrino physics in Europe. In North America, DUSEL (Deep Underground Science and Engineering Laboratory) [20] located at South Dakota, is envisioned for long baseline neutrino oscillation and GUT experiments. In Japan, Hyper-K [113]will increase the sensitivity of the nucleon decays far beyond of Super-K, mainly in the decay modes $p \to e^+\pi^0$ and $p \to \overline{\nu}K^+$. This experiment will function also as an astrophysical neutrino observatory. The main properties of these experiments are described in Table 2.3 [114, 115, 116]. [34] Figure 2.5 show the status of the past, recent and future proton decay experiments, together with the prediction of different theoretical models.

As the figure shows, next generation of experiments is needed to gain an order of magnitude in nucleon decay sensitivity . In 10 years, proton decay half life times would improve for the different decay channels by the different experiments.

[34]Future LBNE (17 kt-US) and DEAδALUS experiments will measure the chain $p \to K^+\overline{\nu}$. The expected limit on proton decay is $\tau_p > (2 \times 10^{34})$ ys.

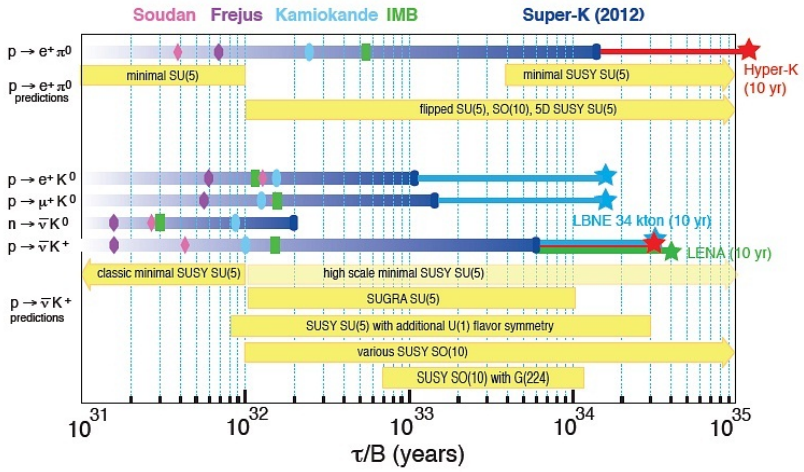

Figure 3.5: Theoretical predictions and experimental bounds for proton decay [117].

3.4.4 $SO(10)$ unification

Nowadays, prospects for $SO(10)$ being the minimal grand unified model have improved, not only for SUSY models but also for non-SUSY ones. This gauge group has some special advantages compared with the minimal $SU(5)$ from both the theoretical and the phenomenological point of view. For example: neutrino mass and dark matter explication, all fit rather naturally in grand unified $SO(10)$ models.

Preliminaries

The smallest of the orthogonal $SO(2n)$ gauge groups which can accommodate complex representations and have rank ≥ 4 is $SO(10)$ (with rank-5). Its two maximal continuous subgroups are:

$$\begin{aligned} G_{224} &= SU(4)_c \times SU(2)_L \times SU(2)_R, \\ G_5 &= SU(5) \times U(1). \end{aligned} \tag{3.33}$$

As is known, only complex representations are suitable for building a GUT theory with the minimal particle content. $SO(10)$ contains the 16 spinorial representation which decomposes under G_{224} and G_5 as follow.

$$G_{224} : 16 : (2,1,4) + (1,2,\overline{4}),$$
$$G_5 : 16 : (10)_1 + (\overline{5})_{-3} + (1)_5. \tag{3.34}$$

Symmetry breaking

Considering that $SO(10)$ has rank-5 and the SM has rank-4, there are several ways through which this group can break to the SM. Some of these channels involve different intermediate symmetries and scales:

In chain-I, $SO(10)$ is broken in exactly one intermediate (LR symmetric) step to the standard model group [35]:

$$SO(10) \to SU(3)_c \times SU(2)_L \times SU(2)_R \times U(1)_{B-L}.$$

In chain-II, $SO(10)$ is broken first to the Pati-Salam group:

$$\begin{aligned} SO(10) &\to SU(4) \times SU(2)_L \times SU(2)_R \\ &\to SU(3)_c \times SU(2)_L \times SU(2)_R \times U(1)_{B-L}, \end{aligned}$$

and finally, in chain-III:

$$\begin{aligned} SO(10) &\to SU(3)_c \times SU(2)_L \times SU(2)_R \times U(1)_{B-L} \\ &\to SU(3)_c \times SU(2)_L \times U(1)_R \times U(1)_{B-L}. \end{aligned}$$

In order for a group G to break into a subgroup $H \supset G$, there must be a field transforming non-trivially under G which contains a singlet scalar of H that gets a vacuum expectation value. From this observation alone we know that certain fields must be present in the fundamental model if we are to achieve a given breaking sequence (here we note as LR: $SU(3)_c \times SU(2)_L \times SU(2)_R \times U(1)_{B-L}$, PS: $SU(4) \times SU(2)_L \times SU(2)_R$, (3211): $SU(3)_c \times SU(2)_L \times U(1)_R \times U(1)_{B-L}$ and (321): SM):

[35] In the first stage, $SO(10)$ is broken to the LR group at the m_G scale of the order 2×10^{16} GeV. For the chain-I, for example, the breaking is given via the interplay of the vev 54. The second symmetry breaking $SU(3)_c \times SU(2)_L \times SU(2)_R \times U(1)_{B-L} \to SM$ occurs at the scale m_R, by means of the fields $\Phi_{1,1,3,-2}$ or $\Phi_{1,1,2,-1}$.

1. The breaking of $PS \to LR$ is possible only with the $\Psi_{15,1,1}$ while $PS \to 3211$ requires the combination $\Psi_{15,1,1} + \Psi_{1,1,3}$. For the direct breaking $PS \to 321$ there are two choices $\Psi_{4,1,2}$, $\Psi_{10,1,3}$ or their conjugates.
2. The breaking of $LR \to 3211$ requires the $\Phi_{1,1,3,0}$ representation while the direct route $LR \to 321$ is possible with the presence of $\Phi_{1,1,2,-1}$, $\Phi_{1,1,3,-2}$ or their conjugates.
3. The group 3211 can be broken down to 321 with the representation $\Phi'_{1,1,\frac{1}{2},-1}$, $\Phi'_{1,1,1,-2}$ or their conjugates [36].

Some $SO(10)$ properties

The Higgs Boson that gives mass to the quarks and leptons must belong to $10, 120$, or 126 dimensional $SO(10)$ representations. The fermion masses arise when any of 10_H, 120_H or 126_H acquire nonzero vev's in L_Y. This Lagrangian give rise to the potential:

$$W_Y = Y_{10}^{ij} 16_i 10_H 16_j + Y_{120}^{ij} 16_i 120_H 16_j + Y_{126}^{ij} 16_i \overline{126}_H 16_j. \tag{3.35}$$

Note that $\overline{126}_H$ plays a double role, contributing to the symmetry breaking and generating mass for the matter fermions [37]. Once decomposed into its components under the next step gauge symmetry, the component which gets a vev capable of breaking the left right symmetry, being a $SU(2)_L$ singlet, can also generate a Majorana mass for the neutrino through the Yukawa coupling of the $\overline{126}_H$ with the matter multiplete 16_f.
Some of the advantages of $SO(10)$ compared with $SU(5)$ are:

- All the fermions of one family are accommodated in only one 16-dimensional spinor representation of $SO(10)$, therefore, both the particle and the antiparticle are assigned the same irreducible representation.
- Since $SU(5)$ is a subgroup of $SO(10)$, charge quantization works in the same way as in $SU(5)$. However, $SO(10)$ is the smallest Lie group with a single anomaly free representation. This implies, for the $SU(5)$ anomalies, a cancellation of the $\overline{5}$

[36] The indices are the transformation properties under the LR, PS and (3211) groups, see Chapter 5 and appendix for notation.
[37] $\overline{126}_H$ generates $m_M \nu_c \nu_c$.

and 10 contributions.

- $SO(10)$ is the minimal grand unified model that gauges the $B-L$ symmmetry and doesn't need mirror fermions. The model does not have global symmetries.
- It gives naturally $M_N >> M_W$ and therefore, neutrinos get a tiny mass through the seesaw mechanism. So, unlike the $SU(5)$ models, in $SO(10)$ massive neutrinos arise naturally.
- As $B-L$ is a subgroup of $SO(10)$, a natural dark matter candidate can emerge.

However, although it seems that $SO(10)$ is more realistic than $SU(5)$, we find enormous freedom in the ways to break this group to the SM. In this thesis, we will work with some $SO(10)$ models with intermediate scales, analyzing in detail the additional scales and the phenomenology associated with.

Chapter 4

SUSY SPECTRA AND THE SEESAW TYPE-I SCALE

4.1 Introduction

The seesaw mechanism [14, 15, 16, 17, 18] provides a rationale for the observed smallness of neutrino masses [7, 8, 9, 10, 11, 12, 13]. However, due to the large mass scales involved, no direct experimental test of "the seesaw" will ever be possible. Extending the standard model (SM) only by a seesaw mechanism does not even allow for indirect tests, since all possible new observables are suppressed by (some power of) the small neutrino masses. [1]

The situation looks less bleak in the supersymmetric version of the seesaw. This is essentially so, because soft SUSY breaking parameters are susceptible to all particles and couplings which appear in the renormalization group equation (RGE) running. Thus, assuming some simplified boundary conditions at an high energy scale, the SUSY softs at the electro-weak scale contain indirect information about all particles and intermediate scales. Perhaps the best known application of this idea is the example of lepton flavour violation (LFV) in seesaw type-I with CMSSM [2] boundary conditions, discussed already in [120]. A plethora of papers on LFV,

[1] "Low-energy" versions of the seesaw, such as inverse seesaw [223] or linear seesaw [119], might allow for larger indirect effects. In this chapter we will focus exclusively on the "classical" seesaw with a high (B-L) breaking scale.

[2] "constrained" Minimal Supersymmetric extension of the Standard Model, also sometimes called mSugra in the literature.

both for low-energy and for accelerator experiments, have been published since then (for an incomplete list see, for example, [121, 122, 123, 124, 125, 126, 127, 128, 129, 130, 131, 132, 133]), most of them concentrating on seesaw type-I.

Seesaw type-I is defined as the exchange of fermionic singlets. At tree-level there is also the possibility to exchange (Y=2) scalar triplets [17, 18], seesaw type-II, or exchange (Y=0) fermionic triplets, the so-called seesaw type-III [92, 134]. Common to all three seesaws is that for $m_\nu \sim \sqrt{\Delta m^2_{\rm A}} \sim 0.05$ eV, where $\Delta m^2_{\rm A}$ is the atmospheric neutrino mass splitting, and couplings of order $\mathcal{O}(1)$ the scale of the seesaw is estimated to be very roughly $m_{SS} \sim 10^{15}$ GeV. Much less work on SUSY seesaw type-II and type-III has been done than for type-I. For studies of LFV in SUSY seesaw type-II, see for example [135, 136], for type-III [137, 138].

Apart from the appearance of LFV, adding a seesaw to the SM particle content also leads to changes in the absolute values of SUSY masses with respect to cMSSM expectations, at least in principle. Type-II and type-III seesaw add superfields, which are charged under the SM group. Thus, the running of the gauge couplings is affected, leading to potentially large changes in SUSY spectra at the EW scale. In [139] it was pointed out, that for type-II and type-III seesaw certain combinations of soft SUSY breaking parameters are at 1-loop order nearly constant over large parts of CMSSM parameters space, but show a logarithmic dependence on m_{SS}. [3] This was studied in more detail, including 2-loop effects in the RGEs, for type-II in [136] and for type-III in [137]. Using forecasted errors on SUSY masses, obtained from full simulations [141, 142], the work [143] calculated the error with which the seesaw (type-II and -III) scale might be determined from LHC and future ILC [144] measurements. Interestingly, [143] concluded that, assuming CMSSM boundary conditions, ILC accuracies on SUSY masses should be sufficient to find at least some hints for a type-II/type-III seesaw, for practically all relevant values of the seesaw scale.

Seesaw type-I, on the other hand, adds only singlets. Changes in SUSY spectra are expected to be much smaller and, therefore, much harder to detect. Certainly because of this simple reasoning much fewer papers have studied this facet of the

[3] These so-called invariants can be useful also in more complicated models in which an inverse seesaw is embedded into an extended gauge group [140].

type-I SUSY seesaw so far. Running slepton masses with a type-I seesaw have been discussed qualitatively in [129, 130, 145, 146]. In [147] it was discussed that in cMSSM extended by a type-I seesaw, splitting in the slepton sector can be considerably larger than in the pure CMSSM. This is interesting, since very small mass splittings in the smuon/selectron sector might be measurable at the LHC, if sleptons are on-shell in the decay chain $\chi_2^0 \to l^\pm \tilde{l}^\mp \to l^\pm l^\mp \chi_1^0$ [148].

In this chapter, we calculate SUSY spectra with cMSSM boundary conditions and a seesaw type-I. We add three generations of right-handed neutrinos and take special care that observed neutrino masses and mixing angles are always correctly fitted. We then follow the procedure of [143]. Using predicted error bars on SUSY mass measurements for a combined LHC+ILC analysis, we construct fake "experimental" observables and use a χ^2-analysis to estimate errors on the parameters of our model, most notably the seesaw scale. We identify regions in parameter space, where hints for a type-I seesaw might show up at the ILC/LHC and discuss *quantitatively* the accuracy which need to be achieved, before a realistic analysis searching for signs of type-I seesaw in SUSY spectra can be carried out.

The rest of this chapter is organized as follows. In the next section we define the supersymetric seesaw type-I model, fix the notation and define the CMSSM. In section 4.3 we present our results. After a short discussion of the procedures and observables in section 4.3.1, we show a simplified analysis, which allows to identify the most important observables and discuss their relevant errors in section 4.3.2. Section 4.3.2 then shows our full numerical results. We then close with a short summary and discussion in section 4.4.

4.2 Setup

4.2.1 CMSSM, type-I seesaw and RGEs

The CMSSM is defined at the GUT-scale by: a common gaugino mass $M_{1/2}$, a common scalar mass m_0 and the trilinear coupling A_0, which gets multiplied by the corresponding Yukawa couplings to obtain the trilinear couplings in the soft SUSY breaking Lagrangian. In addition, at the electro-weak scale, $\tan\beta = v_u/v_d$

is fixed. Here, as usual, v_d and v_u are the vacuum expectation values (vevs) of the neutral component of H_d and H_u, respectively. Finally, the sign of the μ parameter has to be chosen.

Two-loop RGEs for general supersymmetric models have been given in [149]. [4] In our numerical calculations we use `SPheno3.1.5` [151, 152], which solves the RGEs at 2-loop, including right-handed neutrinos. It is, however, useful for a qualitative understanding, to consider first the simple solutions to the RGE for the slepton mass parameters found in the leading log approximation [122, 128], given by

$$\begin{aligned}(\Delta M^2_{\tilde{L}})_{ij} &= -\frac{1}{8\pi^2}(3m_0^2 + A_0^2)(Y^{\nu\dagger}LY^{\nu})_{ij} \\ (\Delta A_l)_{ij} &= -\frac{3}{8\pi^2}A_0 Y_{l_i}(Y^{\nu\dagger}LY^{\nu})_{ij} \\ (\Delta M^2_{\tilde{E}})_{ij} &= 0,\end{aligned} \tag{4.1}$$

where only the parts proportional to the neutrino Yukawa couplings have been written. The factor L is defined as

$$L_{kl} = \log\left(\frac{M_G}{M_k}\right)\delta_{kl}. \tag{4.2}$$

Eq. (4.1) shows that, within the type-I seesaw mechanism, the right slepton parameters do not run in the leading-log approximation. Thus, LFV is restricted to the sector of left-sleptons in practice, apart from left-right mixing effects which could show up in the scalar tau sector. Also note that for the trilinear parameters running is suppressed by charged lepton masses.

It is important that the slepton mass-squareds involve a different combination of neutrino Yukawas and right-handed neutrino masses than the left-handed neutrino masses of eq. (3.15). In fact, since $(Y^{\nu\dagger}LY^{\nu})$ is a hermitian matrix, it obviously contains only nine free parameters [123], the same number of unknowns as on the right-hand side of eq. (3.17), given that in principle all 3 light neutrino masses, 3 mixing angles and 3 CP phases are potentially measurable.

Apart from the slepton mass matrices, Y^{ν} also enters the RGEs for $m^2_{H_u}$ at 1-loop level. However, we have found that the masses of the Higgs bosons are not very

[4] The only case not covered in [149] is models with more than one $U(1)$ gauge group. This case has been discussed recently in [150].

sensitive to the values of Y^ν, see also next section. We thus do not give approximate expressions for $m^2_{H_u}$. For all other soft SUSY parameters, Y^ν enters only at the 2-loop level. Thus, the largest effects of the SUSY type-I seesaw are expected to be found in the left slepton sector.

4.3 Numerical resuts

4.3.1 Preliminaries

We use `SPheno3.1.5` [151, 152] to calculate all SUSY spectra and fit the neutrino data. Unless noted otherwise the fit to neutrino data is done for strict normal hierarchy (i.e. $m_{\nu_1} = 0$), best-fit values for the atmospheric and solar mass squared splitting [12] and tri-bimaximal mixing angles [153]. To reduce the number of free parameters in our fits, we assume right-handed neutrinos to be degenerate and R to be the identity. The seesaw scale, called m_{SS} below, is equal to the degenerate right-handed neutrino masses. We will comment on expected changes of our results, when any of these assumptions is dropped in the next subsections. Especially, recently there have been some indications for a non-zero reactor angle, both from the long-baseline experiment T2K [154] as well as from the first data in Double CHOOZ [155]. We will therefore comment also on non-zero values of $\theta_{13} = \theta_R$ [5].

SPheno solves the RGEs at 2-loop level and calculates the SUSY masses at 1-loop order, except for the Higgs mass, where the most important 2-loop corrections have been implemented too. Theoretical errors in the calculation of the SUSY spectrum are thus expected to be much smaller than experimental errors at the LHC. However, since for the ILC one expects much smaller error bars, theory errors will become important at some point. We comment on theory errors in the discussion section.

Observables and their theoretically forecasted errors are taken from the tables (5.13) and (5.14) of [141] and from [142]. For the LHC we take into account the "edge variables": $(m_{ll})^{edge}$, $(m_{lq})^{\rm edge}_{\rm low}$, $(m_{lq})^{\rm edge}_{\rm high}$, $(m_{llq})_{\rm edge}$ and $(m_{llq})_{\rm thresh}$ from the decay chain $\tilde{q}_L \to \chi^0_2 q$ and $\chi^0_2 \to l\tilde{l} \to ll\chi^0_1$ [156, 157, 158]. In addition,

[5] θ_R was not yet measured at the time this work was done.

we consider $(m_{llb})_{thresh}$, $(m_{\tau^+\tau^-})$ (from decays involving the lighter stau) and the mass differences $\Delta_{\tilde{g}\tilde{b}_i} = m_{\tilde{g}} - m_{\tilde{b}_i}$, with $i = 1, 2$, $\Delta_{\tilde{q}_R\chi_1^0} = m_{\tilde{q}_R} - m_{\chi_1^0}$ and $\Delta_{\tilde{l}_L\chi_1^0} = m_{\tilde{l}_L} - m_{\chi_1^0}$. Since $m_{\tilde{u}_R} \simeq m_{\tilde{d}_R} \simeq m_{\tilde{c}_R} \simeq m_{\tilde{s}_R}$ applies for a large range of the parameter space LHC measurements will not be able to distinguish between the first two generation squarks. The combined errors for an LHC+ILC analysis, tables (5.14) of [141], are dominated by the ILC for all non-coloured sparticles, except the stau. For us it is essential that both, left and right sleptons are within reach of the ILC. Also the two lightest neutralinos and the lighter chargino measured at ILC are important. The errors in [141] were calculated for relatively light SUSY spectra, thus we extrapolate them to our study points, see below, assuming constant relative errors on mass measurements. We will comment in some detail on the importance of this assumption below. Finally, we use the splitting in the selectron/smuon sector [148] as an observable:

$$\Delta(m_{\tilde{e}\tilde{\mu}}) = \frac{m_{\tilde{e}} - m_{\tilde{\mu}}}{m_{\tilde{l}}^{mean}}. \tag{4.3}$$

Here, $m_{\tilde{l}}^{mean} = \frac{1}{2}(m_{\tilde{e}} + m_{\tilde{\mu}})$. The LHC can, in principle, measure this splitting from the edge variables for both, left and right sleptons, if the corresponding scalars are on-shell. In CMSSM type-I seesaw only the left sector has a significant splitting, we therefore suppress the index "L" for brevity. For this splitting [148] quote a "one sigma observability" of $\Delta(m_{\tilde{e}\tilde{\mu}}) \sim 2.8$ ‰ for SPS1a. [6] For comparison, the errors on the left selectron and smuon mass at the ILC for this point are quoted as $\Delta(m_{\tilde{e}}) \simeq 1$ ‰ and $\Delta(m_{\tilde{\mu}}) \simeq 2.5$ ‰, respectively [141].

The negative searches for SUSY by CMS [159] and ATLAS [160] define an excluded range in CMSSM parameter space, ruling out the lightest SPS study points, such as SPS1a' [142] or SPS3 [161]. For our numerical study, we define a set of five points, all of which are chosen to lie outside the LHC excluded region, but have the lightest non-coloured SUSY particles within reach of a 1 TeV linear collider.

[6] SPS1a has only the edge in the right-slepton sector on-shell, see discussion fig. (4.3).

The points are defined as follows:

$$\begin{aligned}
\mathrm{P}_1 &\rightarrow (m_0 = 120, M_{1/2} = 600, A_0 = 0, \tan\beta = 10),\\
\mathrm{P}_2 &\rightarrow (m_0 = 120, M_{1/2} = 600, A_0 = 300, \tan\beta = 10),\\
\mathrm{P}_3 &\rightarrow (m_0 = 120, M_{1/2} = 600, A_0 = -300, \tan\beta = 10),\\
\mathrm{P}_4 &\rightarrow (m_0 = 180, M_{1/2} = 550, A_0 = 0, \tan\beta = 10),\\
\mathrm{P}_5 &\rightarrow (m_0 = 180, M_{1/2} = 550, A_0 = 300, \tan\beta = 10).
\end{aligned} \tag{4.4}$$

All points have $sgn(\mu) > 0$, masses are in units of GeV. Points P_1-P_3 lie very close to the stau-coannihilation line. We have checked by an explicit calculation with MicrOmegas [162, 163, 164, 165] that the relic density of the neutralino agrees with the current best fit value of $\Omega_{CDM}h^2$ within the quoted error bars [13] for P_1. P_4 and P_5 have been chosen such that deviations from the pure cMSSM case are larger than in P_1-P_3, see eq.(4.1), i.e. to maximize the impact of the seesaw type-I on the spectra, see below.

At the date this work was done, all points described in (3.4) lie outside of the LHC excluded region. However, now, negative searches for SUSY given by CMS [55] and ATLAS [56] define an excluded range in the CMSSM parameter space, ruling out all the SPS points studied in this work. Future LHC data, if there are signals of supersymmetry, would reopen the window in the searches for signs of type-I seesaw in the SUSY spectra.

4.3.2 Observables and seesaw scale

In this subsection we will first keep all parameters at some fixed values, varying only the seesaw scale. These calculations are certainly simple-minded, but also very fast compared to the full Monte Carlo parameter scans, discussed later. However, as will be shown in the in the next subsection, there is nearly no correlation between different input parameters. Thus, the simple calculation discussed here already gives a quite accurate description of the results of the more complicated minimization procedures of the "full" calculation. Especially, this calculation allows us to identify the most important observables and discuss their maximally acceptable errors for our analysis.

In fig. (4.1) we show

$$\sigma_i = \frac{m_i^{m_{SS}} - m_i^{cMSSM}}{m_i^{cMSSM}} \Big/ \Delta(m_i), \tag{4.5}$$

where $\Delta(m_i)$ is the expected relative experimental error for the mass of sparticle i at the ILC, as a function of m_{SS}. We remind the reader that we assume that $\Delta(m_i)$ can be extrapolated to our study points. To the left results for P_1 and to the right for P_5. m_i^{cMSSM} is the value of the mass calculated in the CMSSM limit and $m_i^{m_{SS}}$ the corresponding mass for a seesaw scale of m_{SS}. These latter values have always been calculated fitting the Yukawa matrix of the neutrinos at m_{SS}, such that the best fit values of solar and atmospheric neutrino mass differences are obtained and $m_{\nu_1} \equiv 0$ is maintained. As expected the departures from the CMSSM values then increase with increasing seesaw scale. Note that the lines stop at values of $m_{SS} \sim (2-3) \times 10^{15}$ GeV, since for larger values neutrino Yukawas, which are required to fit the neutrino data, are non-perturbative.

Significant departures with respect to the CMSSM values are found (with decreasing importance) for the following observables: left smuon mass, left selectron mass, mass of χ_1^0, m_{h^0} and χ_1^+. We have checked that all other observables have much milder dependences on m_{SS}, as expected. The smuon mass is more important than the selectron mass, despite the latter having a smaller predicted error, due to our choice of degenerate right-handed neutrinos in the fits. With this assumption the running of the smuon mass has contributions from Yukawas responsible for both, atmospheric and solar scale, while the selectron has contributions from the Yukawas of the solar scale only. The change in χ_1^0 and χ_1^+ masses are small in absolute scale, but it is expected that ILC will measure these masses with very high accuracy. Also m_{h^0} shows some mild dependence on m_{SS}, but on a scale of an expected experimental error of 50 MeV [142], i.e. much smaller than our current theoretical error, see below.

As the figure shows deviations from CMSSM expectations of the order of several standard deviations are reached for left smuon and selectron for values of m_{SS} above 10^{14} GeV. Comparing the results for P_1 (left) with those for P_5 (right) it is confirmed that P_5 shows much larger deviations from CMSSM. We have checked that results for the other points P_2-P_4 fall in between the extremes of P_1 and P_5. Lines for P_2 and P_3 are nearly indistinguishable in such a plot, apart from some

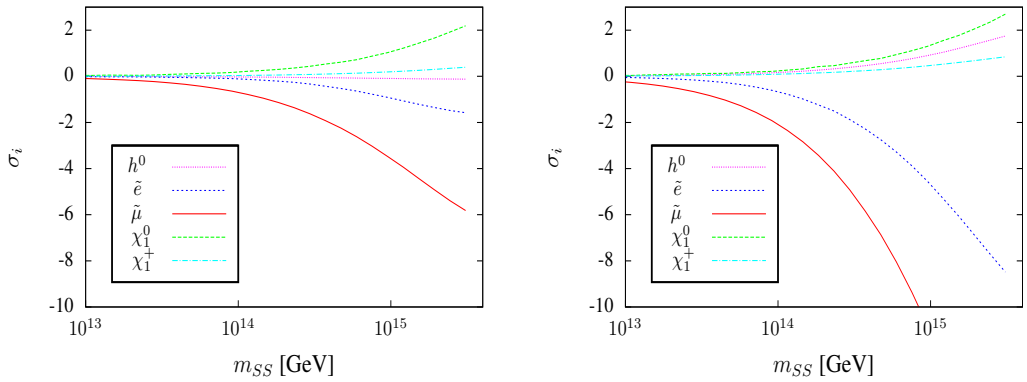

Figure 4.1: Calculated deviations of masses from their nominal cMSSM values as function of m_{SS} for the most important masses. To the left P_1, to the right P_5.

minor difference in the Higgs mass.

In fig. (4.2) we show the calculated χ^2 as a function of m_{SS} for 4 different CMSSM points. Here, χ^2 is calculated with respect to CMSSM expectations. To the left we show χ^2_T including all observables, to the right χ^2_T without the mass splitting in the (left) smuon-selectron sector. The figure demonstrates again that P_1 (P_5) has the smallest (largest) departures from CMSSM expectations. A non-zero value of A_0 can lead to significant departures from CMSSM expectations. Determination of A_0 from measurements involving 3rd generation sfermions and the lightest Higgs mass will therefore be important in fixing m_{SS}.

Fig. (4.2) also demonstrates that $\Delta(m_{\tilde{e}\tilde{\mu}})$ at its nominal error gives a significant contribution to the total χ^2. Thus, LHC measurements only might already give some hints for a type-I seesaw [147]. However, with the rather large error bars of mass measurements at the LHC it will not be possible to fix the CMSSM parameters with sufficient accuracy to get a reliable error on the value of m_{SS}. Unfortunately, also the accuracy with which $\Delta(m_{\tilde{e}\tilde{\mu}})$ can be measured at the LHC is quite uncertain. According to [148] such a splitting could be found for values as low as (few) 10^{-4} or as large as (several) percent, depending on the kinematical configuration realized in nature. Moreover, our points P_1-P_5 have heavier spectra than the ones studied in [148], so larger statistical errors are to be expected.

Fig. (4.3) shows the relative deviation of $\Delta(m_{\tilde{e}\tilde{\mu}})$ for P_1 (left) and P_5 (right) for

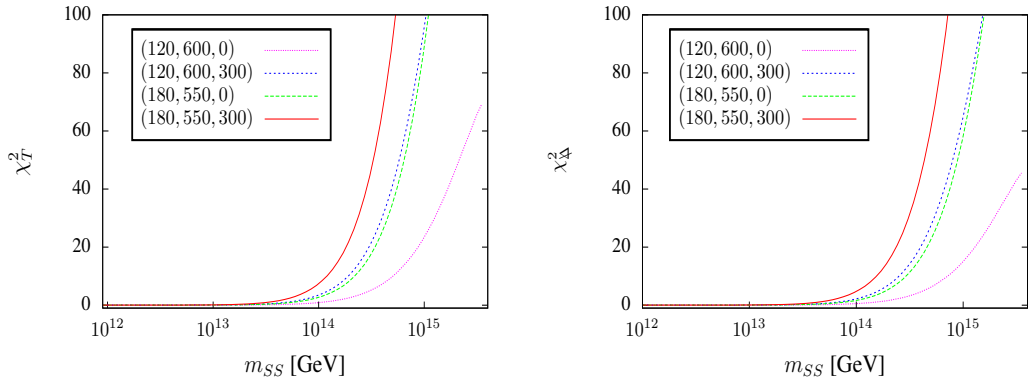

Figure 4.2: Calculated χ^2 as function of m_{SS} for 4 different CMSSM points. To the left: Total χ^2 including all observables, to the right total $\chi^2_{\not\Delta}$, i.e. χ_T without the mass splitting in the (left) smuon-selectron sector. Values quoted in the plots correspond to $(m_0, M_{1/2}, A_0)$. In all points shown we choose $\tan\beta = 10$ and $\mu > 0$.

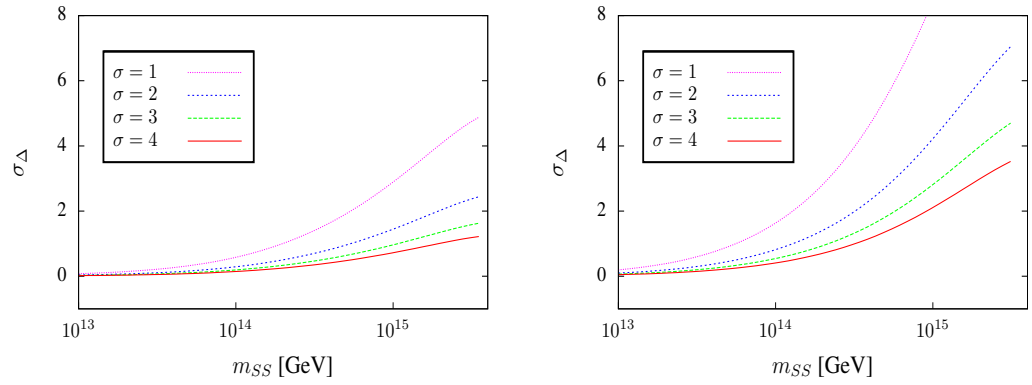

Figure 4.3: Calculated χ^2 for the observable $\Delta(m_{\tilde{e}\tilde{\mu}})$ as function of m_{SS} for different values of its error. To the left: P_1; to the right P_5.

different assumed values of the error in this observable, relative to cMSSM. Here, $\sigma = 1, 2, 3, 4$ means that we have multiplied the "error" quoted in [148] by factors $1, 2, 3, 4$. The deviation drops below one sigma for any value of m_{SS} shown for P_1 (P_5) when this error is larger than twice (six times) the nominal error. This implies that no hints for seesaw type-I can be found in LHC data if the error on $\Delta(m_{\tilde{e}\tilde{\mu}})$ is larger than 5 ‰ (1.6 %) in case of P_1 (P_5).

We should also mention that the actual value of $\Delta(m_{\tilde{e}\tilde{\mu}})$ is not only a function of m_{SS} and the CMSSM parameters, but also depends on the type of fit used to explain neutrino data. We have used degenerate right-handed neutrinos and $m_{\nu_1} \equiv 0$ in the plots shown above. Much smaller splittings are found for (a) nearly-degenerate light neutrinos, i.e. $m_{\nu_1} \geq 0.05$ eV; or (b) very hierarchical right-handed neutrinos. We have checked by an explicit calculation that, for example, for P_5 and $m_{\nu_1} \equiv 0$, $\Delta\chi^2 \geq 5.89$ [7] for values of m_{SS} larger than $m_{SS} \simeq 1.6 \times 10^{14}$ GeV from $\Delta(m_{\tilde{e}\tilde{\mu}})$ alone, whereas the same $\Delta\chi^2$ is reached for $m_{\nu_1} = 0.05$ eV only for $m_{SS} \gtrsim 7 \times 10^{14}$ GeV. Consequently, even though one expects that a finite mass difference between left smuon and selectron is found in CMSSM type-I seesaw, this is by no means guaranteed.

Similar comments apply to the errors for the selectron and smuon mass at the ILC. For P_1 (P_5) the departure of the left selectron mass from the cMSSM expectations is smaller than 1 σ even for $m_{SS} \sim 3 \times 10^{15}$ if the error on this mass is larger than 1.5‰ (1%). For the left smuon the corresponding numbers are for P_1 and P_5 approximately 1.5% and 5%, respectively.
Naively one expects LFV violation to be large, whenever the neutrino Yukawa couplings are large, i.e. for large values of m_{SS}. That is, the regions testable by SUSY mass measurements could already be excluded by upper bounds on LFV, especially the recent upper bound on $\mu \to e\gamma$ by MEG [166]. That this conjecture is incorrect is demonstrated by the example shown in fig. (4.4). In this figure we show the calculated $\mathrm{Br}(\mu \to e\gamma)$ to the left and the calculated χ^2 (total and only $\Delta(m_{\tilde{e}\tilde{\mu}})$) to the right for $\delta = \pi$ and two different values of the reactor angle, θ_{13} for the point P_1. For $\theta_{13} = 0$ all values of m_{SS} above approximately $m_{SS} \sim 10^{14}$ GeV are excluded by the upper bound $\mathrm{Br}(\mu \to e\gamma) \leq 2.4 \times 10^{-12}$ [166]. For $\theta_{13} = 6^\circ$ nearly all values of m_{SS} become allowed. At the same time, this "small" change

[7] $\Delta\chi^2 \geq 5.89$ corresponds to 1 σ c.l. for 5 free parameters.

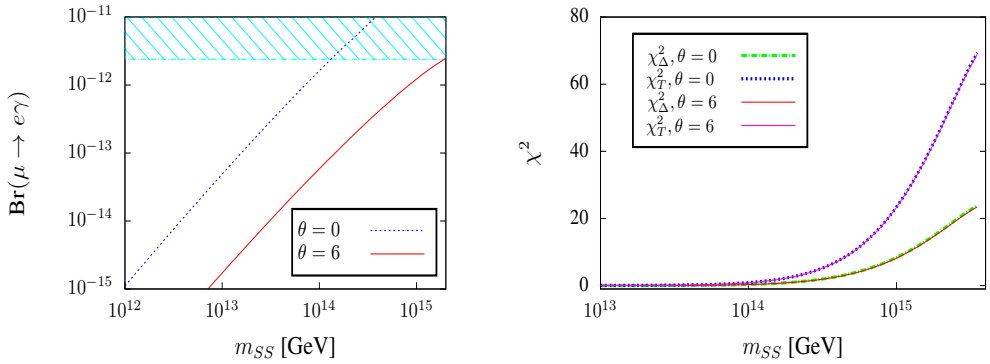

Figure 4.4: To the left $\mathrm{Br}(\mu \to e\gamma)$ and to right calculated χ^2 as function of m_{SS} for two different values of the reactor angle θ_R.

in the Yukawas has practically no visible effect on the calculated χ^2 from mass measurements as the plot on the right shows. This demonstrates that SUSY mass measurements and LFV probe different portions of seesaw type-I parameter space, contrary to what is sometimes claimed in the literature. That one can fit LFV and SUSY masses independently even for such a simple model as type-I seesaw is already obvious from eq. (4.1): Even after fixing all low energy neutrino observables we still have nine unknown parameters to choose from to fit any entry of the left slepton masses *independently*.

Fig. (4.4) also shows that non-zero values of θ_{13}, as preferred by the most recent experimental data [154, 155], should have very little effect on our parameter scans. In our numerical scans, discussed next, we therefore keep $\theta_{13} = 0$ unless mentioned otherwise. We will, however, also briefly comment on changes of our results, when θ_{13} is allowed to float within its current error.

Numerical scans

For the determination of errors on the CMSSM parameters and m_{SS} we have used two independent programmes, one based on MINUIT while the other uses a simple MonteCarlo procedure to scan over the free parameters. For a more detailed discussion see [143]. Plots shown below are obtained by the MonteCarlo procedure, but we have checked that results from MINUIT and our simplistic approach

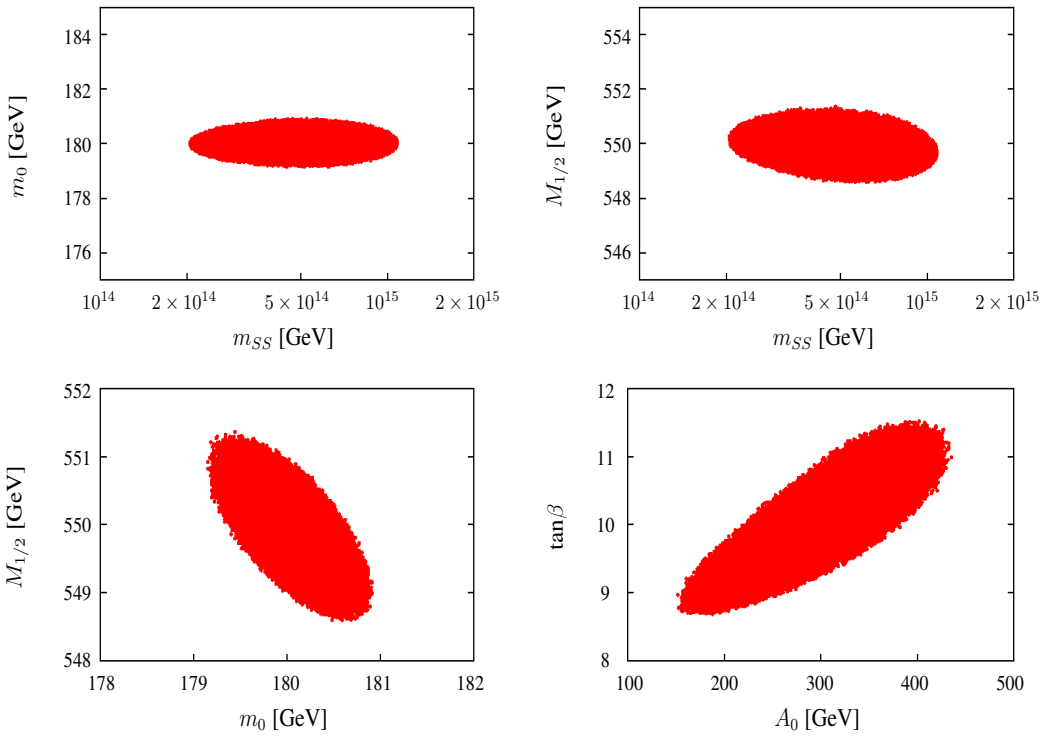

Figure 4.5: Calculated allowed parameter space for m_0, $M_{1/2}$, $\tan\beta$, A_0 and m_{SS} for 7 free parameters, P_5 and $m_{SS} = 5 \times 10^{14}$ GeV. For discussion see text.

described above give very similar estimates for the χ^2, with MINUIT only slightly improving the quality of the fit. In this section we always use all observables in the fits and quote all errors at 1 σ c.l., unless noted otherwise. Since our "fake" experimental data sets are perfect sets, the minimum of χ^2 calculated equals zero and is thus not meaningful; only $\Delta\chi^2$ calculated with respect to the best fit points has any physical meaning in the plots shown below.

Fig. (4.5) shows the allowed parameter space obtained in a MonteCarlo run for m_0, $M_{1/2}$, $\tan\beta$, A_0 and m_{SS} for 7 free parameters, P_5 and $m_{SS} = 5 \times 10^{14}$ GeV. Shown are the allowed ranges of m_0 and $M_{1/2}$ versus m_{SS}, as well as m_0 versus $M_{1/2}$ and $\tan\beta$ versus A_0. On top of the 4 CMSSM parameters and m_{SS} in this calculation we allow the solar angle (θ_{12}) and the atmospheric angle (θ_{23}) to float freely within their allowed range. Errors on neutrino angles for this plot are taken

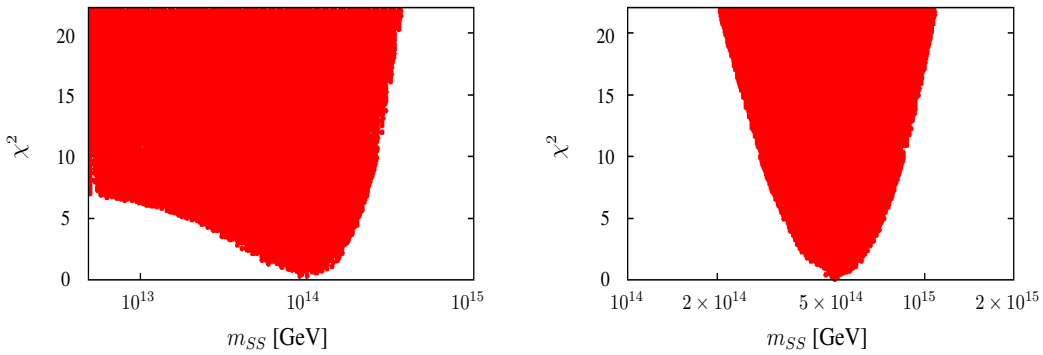

Figure 4.6: Calculated χ^2 distribution versus m_{SS} for 7 free parameters, P_5 and $m_{SS} = 10^{14}$ GeV (to the left) and $m_{SS} = 5 \times 10^{14}$ GeV (to the right).

from [167]. Plots for other points and/or different sets of free parameters look qualitatively very similar to the example shown in the figure. There is very little correlation among different parameters, contrary to the situation found in case of seesaw type-II and type-III [143]. Especially no correlations between m_0, $M_{1/2}$ and m_{SS} are found. However, there is some correlation between $\tan\beta$ and A_0, driven by the fact that $m_{h_1^0}$ alone can only fix a certain combination of these two parameters well. The correlation between $\tan\beta$ and A_0 is slightly stronger than in the cMSSM case, due to the contribution of A_0 in the running of slepton masses, see eq. (4.1).

For our assumed set of measurements, m_0 and $M_{1/2}$ are mainly determined by the highly accurate measurements of right slepton and gaugino masses of the ILC. A_0 and $\tan\beta$ are fixed by a combination of the lightest Higgs mass and the lighter stau mass. LHC measurements help to break degeneracies in parameter space, but are much less important. We stress that the highly accurate determination of cMSSM parameters shown in fig. (4.5) is a prerequisite for determining reliable errors on m_{SS}. [8]

Fig. (4.6) shows calculated χ^2 distributions versus m_{SS} for the same 7 free parameters as in fig. (4.5), P_5 and $m_{SS} = 10^{14}$ GeV (to the left) and $m_{SS} = 5 \times 10^{14}$

[8] We have checked this explicitly in a calculation using only LHC observables.

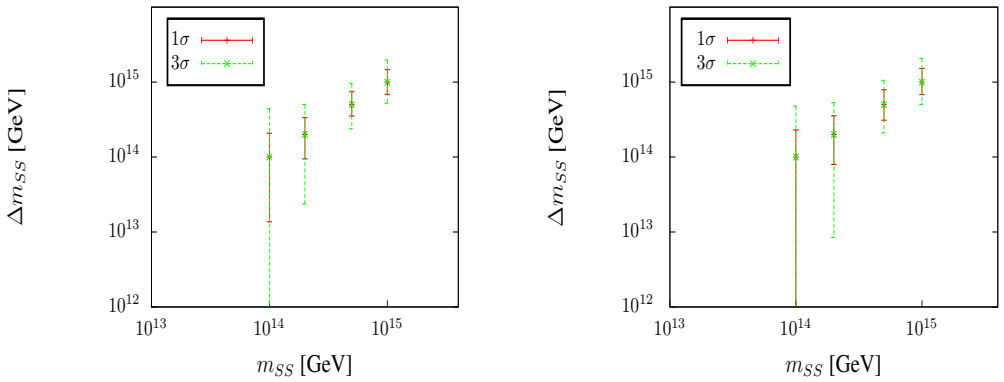

Figure 4.7: Calculated allowed range of m_{SS} versus m_{SS} for 5 (left) and 7 (right) free parameters and P_5. The two different error bars correspond to 1 and 3 σ c.l.

GeV (to the right). For the latter an upper (lower) limit of $m_{SS} \simeq 8 \times 10^{14}$ GeV ($m_{SS} \simeq 3 \times 10^{14}$ GeV) is found. For $m_{SS} = 10^{14}$ GeV a clear upper limit is found, but for low values of m_{SS} the χ^2 distribution flattens out at $\Delta\chi^2 \sim 6.5$. This different behaviour can be understood with the help of the results of the previous subsection, see fig. (4.2). For $m_{SS} = 5 \times 10^{14}$ GeV, there exists a notable difference in some observables with respect to the CMSSM expectation, especially left smuon and selectron mass can no longer be adequately fitted by varying m_0 and $M_{1/2}$ alone, without destroying the agreement with "data" for right sleptons and gauginos. Therefore both, a lower and an upper limit on m_{SS} exist for this point. The situation is different for $m_{SS} = 10^{14}$ GeV, for which the spectrum is much closer to CMSSM expectations. Larger values of m_{SS} are excluded, since they would require larger Yukawas, i.e. larger deviation from CMSSM than observed. Smaller values of m_{SS}, on the other hand, have ever smaller values of Y^ν, i.e. come closer and closer to CMSSM expectations. For an input value of m_{SS} just below $m_{SS} = 10^{14}$ GeV there is then no longer any lower limit on m_{SS}, i.e. the data becomes perfectly consistent with a pure CMSSM calculation. In this case one can only "exclude" a certain range of the seesaw, say values of m_{SS} above a few 10^{14} GeV.

One standard deviation is, of course, too little to claim an observation. We therefore show in fig. (4.7) $\Delta(m_{SS})$ versus m_{SS} for 5 (left) and 7 (right) free parameters and P_5 at 1 and 3 σ c.l. At $m_{SS} = 10^{14}$ formally a 1 sigma "evidence" could be

reached, but at 3 σ c.l. the spectrum is perfectly consistent with a pure CMSSM. For larger values of m_{SS}, however, several standard deviations can be reached. For the two largest values of m_{SS} calculated in this figure, a 5 σ "discovery" is possible.

Fig. (4.7) shows $\Delta(m_{SS})$ for 5 and 7 free parameters. We have repeated this exercise for different sets of free parameters and $m_{SS} = 5 \times 10^{14}$. Here, 5 free parameters correspond to the 4 CMSSM parameters plus m_{SS}, 7 free parameters are the original 5 plus θ_{12} and θ_{23}. We have also tried other combinations such as 6 parameters: original 5 plus θ_R and 8 parameters, where we let all 3 neutrino angles float freely. Sets with larger numbers of free parameters are no longer sufficiently sampled in our MonteCarlo runs, so we do not give numbers for these, although in principle the calculation could allow also to let the neutrinos mass squared differences to float freely. Error bars are slightly larger for larger number of free parameters, as expected. However, since there is little or no correlation among the parameters, the differences are so small as to be completely irrelevant.

4.4 Summary and conclusions

We have discussed the prospects for finding indirect hints for type-I seesaw in SUSY mass measurements. Since type-I seesaw adds only singlets to the SM particle content, only very few observables are affected and all changes in masses are small, even in the most favourable circumstances. Per-mille level accuracies will be needed, i.e. measurements at an ILC, before any quantitative attempt searching for type-I seesaw can hope for success, even assuming admittedly simplistic CMSSM boundary condtions.

Our calculation confirms *quantitatively* that slepton mass measurements can contain information about the type-I seesaw. Right sleptons are expected to be degenerate, while the left smuon and selectron show a potentially measurable splitting between their masses. If such a situation is indeed found, an estimate of m_{SS} might be derivable from ILC SUSY mass measurements.

Above we have commented only on experimental errors. However, given the per-mille requirements on accuracy, stressed several times, also theoretical errors in

the calculation of SUSY spectra are important. Various potential sources of errors come to mind. First of all, a 1-loop calculation of SUSY masses is almost certainly not accurate enough for our purposes. We have tried to estimate the importance of higher loop orders, varying the renormalization scale in the numerical calculation. Changes of smuon and selectron mass found are of the order of the ILC error or even larger, depending on SUSY point and variation of scale. For the mass of the lightest Higgs boson it has been shown that even different calculations at 2-loop still disagree at a level of few GeV [168]. Second, our calculation assumes a perfect knowledge of the GUT scale. Changes in the GUT scale do lead to sizeable changes in the calculated spectra for the same cMSSM parameters, which can be easily of the order of the required precision of the calculation and larger. In this sense, $\Delta(m_{\tilde{e}\tilde{\mu}})$ is an especially nice observable, since here the GUT scale uncertainty nearly cancels out in the calculation. In summary, if ILC accuracies on SUSY masses can indeed be reached experimentally, progress on the theoretical side will become necessary too.

In our calculations, we have considered only SUSY masses. We have not taken into account data from lepton flavour violation, mainly because currently only upper limits are available. If in the future finite values for $ł_i \to ł_j + \gamma$ become available, it would be very interesting to see, how much could be learned about the type-I seesaw parameters in a combined fit. Including LFV one could maybe also allow for non-degenerate right-handed neutrinos in the fits.

And, finally, despite all the limitations of our study, we find it very encouraging that hints for type-I seesaw might be found in SUSY mass measurements at all. We stress again, that LFV and SUSY mass measurements test different portions of seesaw parameter space. For a more complete "reconstruction" of seesaw parameters, than what we have attempted here, both kinds of measurements would be needed.

All fits were done in 2011, where points used were still allowed. However, ATLAS and CMS actual data exclude now all of them. If SUSY is found at LHC, this analysis could be repeated and then find realistic results.

Chapter 5

THE WITTEN MECHANISM IN FLIPPED $SU(5)$

5.1 Introduction

The apparent absence of supersymmetry in the sub-TeV domain indicated by the current LHC data reopens the question whether the unprecedented smallness of the absolute neutrino mass scale may be ascribed to a loop suppression with the underlying dynamics in the TeV ballpark rather than the traditional seesaw [14, 17, 134, 169, 170, 171] picture featuring a very high scale, typically far beyond our reach. Recently, there has been a lot of activity in this direction with, e.g., dedicated studies of the Zee [93], Zee-Babu [94, 172, 173, 174] and other models (cf. [175, 176] and references therein) focusing on their distinctive low-energy phenomenology and, in particular, their potential to be probed at the LHC and other facilities, see, e.g., [177, 178, 179, 180, 181].

With the upcoming generation of megaton-scale experiments [114, 182, 183] dedicated, besides precision neutrino physics, to the search of perturbative baryon number violating (BNV) processes such as proton decay, the same question can be readdressed from the high-energy perspective. In principle, there can be high-scale loop diagrams behind the right-handed (RH) neutrino masses underpinning the seesaw mechanism rather than a direct low-scale LL contraction, with possible imprints in the BNV physics.

Among such options, a prominent role is played by Witten's scheme [98] in the framework of the $SO(10)$ grand unification (GUT) where a pair of lepton-number violating vacuum expectation values (VEVs) is tied to the leptonic sector at two loops. Its main beauty consists in the observation that the RH neutrino masses are generated at the renormalizable level even in the simplest realization of $SO(10)$ with just the minimal scalar contents sufficient for the desired spontaneous symmetry breaking (i.e., $10 \oplus 16 \oplus 45$, cf. [184] and references therein); hence, there is in principle no need to invoke large scalar representations for that sake.

In practice, however, Witten's mechanism has never found a clearly natural realization as a basis for a potentially realistic model building. Among the possible reasons there is, namely, the dichotomy between the gauge unification constraints and the absolute size of Witten's loop governed by the position of the $B - L$ breaking scale M_{B-L} which is required to be around the GUT-scale (M_G), due to the $(\alpha/\pi)^2$ suppression factor, in order to yield the "correct" seesaw scale $M_R \sim (\alpha/\pi)^2 M_{B-L}^2/M_G$ in the 10^{13} GeV ballpark.
On one hand, this is exactly the situation encountered in supersymmetric GUTs where the one-step breaking picture characterized by a close proximity of M_{B-L} and M_G is essentially inevitable; at the same time, however, the low-scale supersymmetry makes the F-type loops at the GUT scale entirely academic due to the large cancellation involved. On the other hand, non-SUSY GUTs generally require $M_{B-L} \ll M_G$ in order to account for the gauge unification constraints for which Witten's mechanism yields contribution much below the desired $M_R \sim 10^{13}$ GeV.

In this respect, the beginning of the 1980s, when the low-energy SUSY was not yet mainstream and the lack of detailed information about the standard model (SM) gauge coupling evolution as well as the absolute light neutrino mass scale obscured the issue with the too low Witten's M_R in non-SUSY scenarios, was the only time when this business really flourished[1]. For a more recent attempt to implement such ideas in a simple, yet potentially realistic scenario the reader is deferred to, e.g., the works [185, 186] where the split supersymmetry scheme supports both $M_{B-L} \sim M_G$ and very heavy scalar superpartners for which, in turn, the GUT-scale F-type Witten's loop is not entirely canceled.

[1]This can be seen with the citation counts of the original study [98] as about 70% of its today's total dates back to before 1985.

In this chapter we approach this conundrum from a different perspective; in particular, we stick to the core of Witten's loop while relaxing, at the same time, the strict gauge unification constraints. For that sake, we depart from the canonical realization of Witten's mechanism in a full-fledged $SO(10)$ GUT to its "bare-bone" version which, as we point out, can be sensibly implemented within its simpler cousin, namely, the flipped $SU(5)$ [187, 188, 189]. Indeed, the strict full gauge unification constraints inherent to the $SO(10)$ GUTs are relaxed in such a scenario [owing to the nonsimple structure of its $SU(5) \otimes U(1)$ gauge group] which, in turn, makes it possible to have the rank-reducing vacuum expectation value (VEV) governing Witten's loop in the 10^{16} GeV ballpark even if the theory is nonsupersymmetric.

The reason we are focusing just on the flipped $SU(5)$ framework is twofold: First, the baryon-number violating observables such as the $d = 6$ proton decay [50] may still be used to constrain specific scenarios even if the underlying dynamics is as high as at 10^{16} GeV, as we will comment upon in the following. This virtue is obviously lost if one picks any of the "smaller" subgroups of $SO(10)$ such as Pati-Salam[2] [41], let alone the number of left-right symmetric (LR) settings based on the $SU(3) \otimes SU(2)_L \otimes SU(2)_R \otimes U(1)_{B-L}$ gauge symmetry. Second, the flipped variant of $SU(5) \otimes U(1) \subset SO(10)$ is the only one for which a radiative generation of the RH neutrino masses makes sense because in the standard $SU(5)$ the RH neutrinos are gauge singlets and as such they receive an explicit singlet mass term.

Besides this, the flipped scenario has got other virtues: the proton decay estimates[3] may be under better control than in the standard $SU(5)$ because the leading theoretical uncertainties in the GUT-scale calculation (namely, the few-percent ambiguities in the GUT-scale matching of the running gauge couplings due to the Planck-induced effects [103, 104, 105, 106]) are absent. Furthermore, the flipped scenario offers better perspectives for a solution of the doublet-triplet splitting problem (if desired; see, e.g., [102]) and, unlike in the "standard" $SU(5)$, there is no monopole problem in the flipped case either.

[2]Let us recall that proton decay in Pati-Salam requires a conspiracy in the Higgs sector as it does not run solely through the gauge interactions.

[3]For a nice discussion on how to use BNV observables to distinguish between the standard and the flipped $SU(5)$ see, e.g., [190].

On top of that, the proposed scenario is in a certain sense even simpler than the standard approach to the minimal[4] renormalizable flipped $SU(5)$ where the seesaw scale is associated to the VEV of an extra scalar representation transforming as a 50-dimensional four-index tensor under $SU(5)$ coupled to the fermionic $10 \otimes 10$ bilinear (see, e.g., [191]) ; indeed, such a large multiplet is not necessary in the flipped $SU(5)$ à la Witten; as we shall argue, the two models can even be distinguished from each other if rich-enough BNV physics is revealed at future facilities. In particular, we observe several features in the typical ranges predicted for the $\Gamma(p \to \pi^0 e^+)$ and $\Gamma(p \to \pi^0 \mu^+)$ partial widths [as well as for those related by the isospin symmetry such as $\Gamma(p \to \eta e^+)$ etc.] that are trivially absent in the model with 50_H in the scalar sector. Remarkably enough, this makes it even possible to obtain rather detailed information about all kinematically allowed $d = 6$ nucleon decay channels in large portions of the parameter space where the theory is stable and perturbative.

The chapter is organized as follows: In Sec. 5.2, after a short recapitulation of the salient features of the standard and flipped $SU(5)$ models and the generic predictions of the partial proton decay widths therein, we focus on the Witten's loop as a means to constrain the shape of the (single) unitary matrix governing the proton decay channels into neutral mesons in the flipped case. In Sec. 5.3 we perform a detailed analysis of the simplest scenario in which a set of interesting correlations among the different partial proton decay widths to neutral mesons are revealed with their strengths governed by the absolute size of Witten's diagram. In Sec. 5.4, we adopt this kind of analysis to the minimal potentially realistic scenario. Then we conclude.

5.2 $SU(5) \otimes U(1)$ à la Witten

Let us begin with a short account of the $d = 6$ proton decay in the $SU(5)$-based unifications focusing, namely, on the minimal versions of the standard and flipped scenarios and the potential to discriminate experimentally among them if proton

[4]Minimality here refers to models without extra matter fields; for an alternative approach including, for instance, extra singlet fermions see, e.g., [192].

decay would be seen in the future.

5.2.1 Proton decay in the standard and flipped $SU(5)$

Since the new dynamics associated to the rich extra gauge and scalar degrees of freedom of the flipped $SU(5)$ scenario takes place at a very high scale the most promising observables it can find its imprints in are those related to the perturbative baryon number violation, namely, proton decay. To this end, the flipped version of the $SU(5)$ unification is in a better shape than its "standard" cousin as it provides a relatively good grip [50, 188] on the partial proton decay widths to neutral mesons and *charged* leptons whereas there is usually very little one can say on general grounds about these in the standard $SU(5)$ where those are the charged meson plus antineutrino channels which are typically under better theoretical control. Needless to say, this is very welcome as the observability of the charged leptons in the large-volume liquid scintilator [114]/water-Cherenkow [182]/liquid Argon [183] experiments boosts the expected signal to background ratio and, hence, provides a way better sensitivity (by as much as an order-of-magnitude) in these channels than in those with the unobserved final-state antineutrino.

Let us just note that this has to do, namely, with the hypercharge of the heavy $d = 6$ proton-decay-generating gauge colored triplets which under the SM transform as $(3, 2, -\frac{5}{6})$ in the standard $SU(5)$ case and as $(3, 2, +\frac{1}{6})$ in the flipped $SU(5)$, respectively[5]. As for the former, the relevant $d = 6$ effective BNV operators are [50] of the $\mathcal{O}^I \propto \overline{u^c}Q\overline{e^c}Q$ and $\mathcal{O}^{II} \propto \overline{u^c}Q\overline{d^c}L$ type while for the latter these are $\mathcal{O}^{III} \propto \overline{d^c}Q\overline{u^c}L$ and $\mathcal{O}^{IV} \propto \overline{d^c}Q\overline{\nu^c}Q$ where "pairing" is always between the first two and the last two fields therein. Hence, the neutral meson+charged lepton decays in the standard $SU(5)$ receive contributions from both $\mathcal{O}^I$ and $\mathcal{O}^{II}$ while it is only $\mathcal{O}^{III}$ that drives it in the flipped scenario[6]. On the other hand, the situation is rather symmetric in the charged meson+neutrino channels which in both cases receive sizeable contributions from only one type of a contraction [$\mathcal{O}^{II}$ in $SU(5)$ and $\mathcal{O}^{III}$ in its flipped version]. Let us also note that the predictivity

[5]This is also reflected by the classical notation where the $SU(2)$ components of the former are called X and Y while for the latter these are usually denoted by X' and Y'.

[6]In fact, $\mathcal{O}^{IV}$ is almost always irrelevant as it yields a left-hand antineutrino in the final state with typically (in the classical seesaw picture) a very tiny projection on the light neutrino mass eigenstates.

for these channels is further boosted by the coherent summation over the (virtually unmeasurable) neutrino flavors; hence, the inclusive decay widths to specific charged mesons are typically driven by the elements of the Cabibbo-Kobayashi-Maskawa (CKM) matrix. For instance, in a wide class of simple $SU(5)$ GUTs (namely, those in which the up-type quark mass matrix is symmetric) the p-decay widths to π^+ and K^+ can be written as

$$\begin{aligned}\Gamma(p\to\pi^+\overline{\nu}) =& F_1|(V_{CKM})_{11}|^2 M\,, \\ \Gamma(p\to K^+\overline{\nu}) =& \left[F_2|(V_{CKM})_{11}|^2 + F_3|(V_{CKM})_{12}|^2\right] M\,,\end{aligned} \tag{5.1}$$

where $F_{1,2,3}$ are calculable numerical factors and M is a universal dimensionful quantity governed by the parameters of the underlying "microscopic" theory such as the GUT scale, the gauge couplings, etc. This feature is yet more pronounced in the simple flipped scenarios (namely, those in which the down-type quark mass matrix is symmetric[7]); there one even obtains a sharp prediction

$$\Gamma(p\to K^+\overline{\nu}) = 0, \tag{5.2}$$

which is a clear smoking gun of the flipped $SU(5)$ unification. For more details an interested reader is deferred to the dedicated analysis [190]. Coming back to the neutral meson channels in the simplest flipped $SU(5)$ scenarios (i.e., assuming symmetry of the down quark mass matrix), the partial widths of our main interest may be written in the form

$$\frac{\Gamma(p\to\pi^0 e^+_\alpha)}{\Gamma(p\to\pi^+\overline{\nu})} = \frac{1}{2}|(V_{CKM})_{11}|^2|(V_{PMNS}U_\nu)_{\alpha 1}|^2\,, \tag{5.3}$$

$$\frac{\Gamma(p\to\eta e^+_\alpha)}{\Gamma(p\to\pi^+\overline{\nu})} = \frac{C_2}{C_1}|(V_{CKM})_{11}|^2|(V_{PMNS}U_\nu)_{\alpha 1}|^2\,, \tag{5.4}$$

$$\frac{\Gamma(p\to K^0 e^+_\alpha)}{\Gamma(p\to\pi^+\overline{\nu})} = \frac{C_3}{C_1}|(V_{CKM})_{12}|^2|(V_{PMNS}U_\nu)_{\alpha 1}|^2\,, \tag{5.5}$$

where V_{PMNS} stands for the Pontecorvo-Maki-Nakagawa-Sakata leptonic mixing matrix and U_ν is the unitary matrix diagonalizing the light neutrino masses[8]. Note

[7] This, in fact, is the prominent case when the flipped-$SU(5)$ proton decay is robust, i.e., cannot be rotated away, cf. [50, 107, 190]; for a more recent account of the same in a flipped-$SU(5)$ scenario featuring extra matter fields see, e.g., [193].

[8] Let us anticipate that Eqs (5.3)-(5.5) are written in the basis in which the up-type quark mass matrix is diagonal and real; needless to say, the observables of our interest are all insensitive to such a choice. For more details see Appendix C.2.

that $V_{PMNS}U_\nu = U_e^L$ is the LHS diagonalization matrix in the charged lepton sector [see Eq. (C.9)]; we write it in such a "baroque" way because V_{PMNS} is measurable and, as will become clear, U_ν is constrained in the model under consideration. The absolute scale in Eqs. (5.3)-(5.5) is set by

$$\Gamma(p \to \pi^+ \overline{\nu}) = C_1 \left(\frac{g_G}{M_G}\right)^4 , \tag{5.6}$$

where g_G is the $SU(5)$ gauge coupling and the numerical factors

$$C_1 = \frac{m_p}{8\pi f_\pi^2} A_L^2 |\alpha|^2 (1 + D + F)^2, \tag{5.7}$$

$$C_2 = \frac{(m_p^2 - m_\eta^2)^2}{48\pi m_p^3 f_\pi^2} A_L^2 |\alpha|^2 (1 + D - 3F)^2, \tag{5.8}$$

$$C_3 = \frac{(m_p^2 - m_K^2)^2}{8\pi m_p^3 f_\pi^2} A_L^2 |\alpha|^2 \left[1 + \frac{m_p}{m_B}(D - F)\right]^2 , \tag{5.9}$$

are obtained by chiral Lagrangian techniques, see [50] (and references therein), [190] and Appendix C.1. From Eqs. (5.3)-(5.5), the theory's predictive power for the proton decay to neutral mesons (especially for the "golden" $p \to \pi^0 e^+$ channel), in particular, its tight correlation to neutrino physics, is obvious as the only unknown entry in Eqs. (5.2)-(5.5) is the unitary matrix U_ν.

In what follows we shall exploit the extra constraints on the lepton sector flavor structure emerging in the flipped $SU(5)$ model with Witten's loop in order to obtain constraints on the admissible shapes of the U_ν matrix and, hence, get a grip on the complete set of proton decay observables. Let us note that this is impossible in the models in which the RH neutrino masses are generated in the "standard" way (e.g., by means of an extra 50_H) where, due to the entirely new type of a contraction entering the lepton sector Lagrangian, U_ν typically remains unconstrained.

5.2.2 Witten's mechanism in flipped SU(5)

The main benefit of dealing with a unification which is not "grand" (i.e., not based on a simple gauge group) is the absence of the strict limits on the large-scale symmetry breaking VEVs from an overall gauge coupling convergence at around 10^{16} GeV. Indeed, unlike in the $SO(10)$ GUTs which typically require the rank-breaking VEV (e.g., that of 16- or 126-dimensional scalars) to be several orders

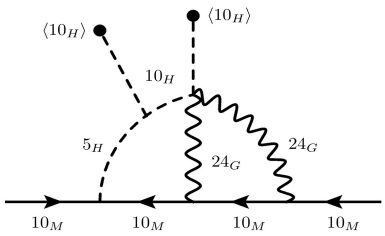

Figure 5.1: The gauge structure of Witten's loop in the flipped $SU(5)$ scenario under consideration. Note that we display just one representative out of several graphs that may be obtained from the one above by permutations.

of magnitude below M_G [194, 195, 196, 197] and, hence, too low for Witten's loop to account for the "natural" 10^{12-14} GeV RH neutrino masses domain, no such issue is encountered in the $SU(5) \otimes U(1)$ scenario due to its less restrictive partial unification pattern. In particular, only the non-Abelian SM gauge couplings are supposed to converge toward M_G which, in turn, should be compatible with the current proton lifetime limits; no other scale is needed. Furthermore, the $SU(5) \otimes U(1)$-breaking VEV $V_G \equiv \langle 10_H \rangle$ is perfectly fit from the point of view of the gauge structure of Witten's type of a diagram in this scenario.

Witten's loop structure

As in the original $SO(10)$ case the gauge and loop structure of the relevant graphs (cf., Fig. 5.1) conforms[9] several basic requirements: (i) there should be two V_G's sticking out of the diagram so that the correct "amount" of the $U(1)_X$ breaking is provided for the desired RH neutrino Majorana mass term; (ii) the interactions experienced by the fermionic current must mimic the $10_M 10_M 50_H$ coupling of the renormalizable models in which the RH neutrino mass is generated at the tree level; (iii) only the minimal set of scalars required for the spontaneous symmetry breaking should be employed. Given that, the structure depicted in Fig. 5.1 turns out to be the simplest option[10]; indeed, $5 \otimes 24 \otimes 24$ (where 24 stands for the gauge

[9]Note that the quantum numbers of the submultiplets under the $SU(5)$ subgroup of $SO(10)$ indicated in Witten's original work [98] are irrelevant here as the RH neutrinos in the flipped scenario reside in 10 of SU(5) rather than in a singlet.

[10]Note that minimality in this context depends on the specific construction of the perturbation expansion as, e.g., one diagram in the broken phase approach with massive propagators corresponds to a tower of graphs in the unbroken-phase theory when the VEVs are included in

fields) is the minimum way to devise the desired 50. Note also that the $U(1)_X$ charge of the gauge 24_G's is zero and, thus, the two units of X are delivered to the leptons via their Yukawa interaction with 5_H. We have checked by explicit calculation that, indeed, the gauge structure of the graph yields a nonzero contribution for, and only for, the RH neutrino.

The right-handed neutrino mass matrix

Following the standard Feynman procedure the RH neutrino mass matrix can be written in the form[11]

$$M_\nu^M = \left(\frac{1}{16\pi^2}\right)^2 g_G^4 Y_{10}\,\mu \frac{\langle 10_H\rangle^2}{M_G^2} \times \mathcal{O}(1)\,, \tag{5.10}$$

where g_G is the (unified) gauge coupling corresponding to that of the $SU(5)$ part of the gauge group, μ is the (dimensionful) trilinear scalar coupling among 10_H's and 5_H, cf. Eq. (5.12), Y_{10} is the Yukawa coupling of 5_H to the matter bilinear $10_M \otimes 10_M$, cf. Eq. (2.27), $\langle 10_H\rangle$ is the GUT-symmetry-breaking VEV, M_G denotes the GUT scale and, finally, the $\mathcal{O}(1)$ factor stands for the remainder of the relevant expression. Besides the double loop-momentum integration (up to the geometrical suppression factors that have already been taken out in Eq. (5.10)) this may contain other structures specific for a particular evaluation method[12] such as, e.g., unitary transformations among the defining and the mass bases in different sectors. Note also that the second power of M_G in the denominator is expected on dimensional grounds.

To proceed, we shall cluster g_G^2 with the two powers of V_G and formally cancel this against the M_G^2 factor (following the usual $M_G \sim g_G V_G$ rule of thumb)

$$M_\nu^M = \left(\frac{1}{16\pi^2}\right)^2 g_G^2 Y_{10}\,\mu\, K\,, \tag{5.11}$$

where the possible inaccuracy of this has been concealed into the definition of the (hitherto unknown) factor K. This, in fact, is the best one can do until all

the interaction Hamiltonian.

[11] Note that due to the symmetry of Y_{10} the algebraic structure of the "permuted" graphs is the same as the one in Fig. 5.1 and, hence, all contributions are covered by expression (5.10).

[12] Obviously, there are several equivalent approaches to the evaluation of the momentum integrals involved in the $\mathcal{O}(1)$ factor: one can either work in the mass basis in which the propagators are diagonal and the couplings contain the rotations from the defining to the mass basis or vice versa; in principle, one may even work in a massless theory with VEVs in the interaction part of the Lagrangian.

the scalar potential couplings are fixed; since, however, we do not embark on a detailed analysis of the effective potential and its spectrum underpinning any possible detailed account for the relevant gauge unification constraints, all our results will be eventually parametrized by the value of K. A qualified guess of the size of the loop integral [198] (assuming no random cancellations) puts this factor to the $\mathcal{O}(10)$ ballpark; hence, in what follows we shall consider K from about 5 to about 50.

In the rest of this section we shall elaborate on Eq. (5.11); although there are several undetermined factors there, namely, Y_{10}, μ and K, the former two are subject to perturbative consistency constraints following from the requirements of the SM vacuum stability and general perturbativity which, together with the above-mentioned bounds on K, impose rather strict limits on the absolute scale of the RH neutrino masses.

Constraints from the SM vacuum stability

Here we attempt to identify the parameter-space domains that may support a stable SM vacuum, i.e., those for which there are no tachyons (i.e., no negative-sign eigenvalues of the relevant scalar mass-squared matrix) in the spectrum.

Tree-level scalar potential. Let us parametrize the tree-level scalar potential as

$$\begin{aligned} V_0 &= \frac{1}{2}m_{10}^2\mathrm{Tr}(10_H^\dagger 10_H) + m_5^2 5_H^\dagger 5_H \\ &+ \frac{1}{8}(\mu\varepsilon_{ijklm}10_H^{ij}10_H^{kl}5_H^m + h.c.) + \\ &+ \frac{1}{4}\lambda_1[\mathrm{Tr}(10_H^\dagger 10_H)]^2 + \frac{1}{4}\lambda_2\mathrm{Tr}(10_H^\dagger 10_H 10_H^\dagger 10_H) \\ &+ \lambda_3(5_H^\dagger 5_H)^2 + \frac{1}{2}\lambda_4\mathrm{Tr}(10_H^\dagger 10_H)(5_H^\dagger 5_H) \\ &+ \lambda_5 5_H^\dagger 10_H 10_H^\dagger 5_H\,, \end{aligned} \tag{5.12}$$

where 10_H and 5_H are conveniently represented by a 5×5 complex antisymmetric matrix and a 5-component complex column vector, respectively, and the normalization factors in the interaction terms have been chosen such that they ensure simplicity of the resulting Feynman rules and, hence, of the results below. Note that we choose a basis in which the GUT-scale VEV V_G and the electroweak VEV

v are accommodated in the following components:

$$\left\langle 10^{45} \right\rangle = -\left\langle 10^{54} \right\rangle = V_G\,, \quad \left\langle 5^4 \right\rangle = v\,. \tag{5.13}$$

The SM vacuum. The SM vacuum stationarity conditions read

$$\begin{aligned} V_G\left[m_{10}^2 + V_G^2(2\lambda_1+\lambda_2) + v^2(\lambda_4+\lambda_5)\right] &= 0\,, \\ v\left[m_5^2 + 2v^2\lambda_3 + V_G^2(\lambda_4+\lambda_5)\right] &= 0\,. \end{aligned} \tag{5.14}$$

There are in general four solutions to this system, namely,

$$\begin{aligned} V_G = v = 0 &\;:\; SU(5)\otimes U(1)\,, \\ V_G \neq 0, v = 0 &\;:\; SU(3)\otimes SU(2)\otimes U(1)\,, \\ V_G \neq 0, v \neq 0 &\;:\; SU(3)\otimes U(1)\,, \\ V_G = 0, v \neq 0 &\;:\; SU(4)\otimes U(1)\,, \end{aligned}$$

with the preserved symmetry indicated on the right; the first three then correspond to consecutive steps in the physically relevant symmetry breaking chain.

The scalar masses. As long as only the signs of the scalar mass-squares are at stakes one can work in any basis. Using the "real field" one, i.e., $\Psi = \{10^*_{ij}, 10^{ij}, 5^*_i, 5^i\}$ the mass matrix $\mathcal{M}^2 \equiv \langle \partial^2 V/\partial\Psi^*\partial\Psi\rangle$ evaluated in the SM vacuum has the following system of eigenvalues (neglecting all subleading terms):

$$m^2_{G_{1,\ldots,16}} = 0 \tag{5.15}$$

$$m_H^2 = \left[4\lambda_3 - \frac{2(\lambda_4+\lambda_5)^2}{2\lambda_1+\lambda_2}\right]v^2\,, \tag{5.16}$$

$$m_S^2 = 2(2\lambda_1+\lambda_2)V_G^2\,, \tag{5.17}$$

$$\begin{aligned} m^2_{\Delta_1} &= -\tfrac{1}{2}(\lambda_2+\lambda_5)V_G^2 - \tfrac{1}{2}V_G\sqrt{(\lambda_2-\lambda_5)^2V_G^2+4\mu^2}, \\ m^2_{\Delta_2} &= -\tfrac{1}{2}(\lambda_2+\lambda_5)V_G^2 + \tfrac{1}{2}V_G\sqrt{(\lambda_2-\lambda_5)^2V_G^2+4\mu^2}. \end{aligned} \tag{5.18}$$

A few comments are worth making here:

- The 16 zeroes in Eq. (5.15) correspond to the Goldstone bosons associated to the spontaneous breakdown of the $SU(5)\otimes U(1)$ symmetry to the $SU(3)_c\otimes U(1)_Q$ of the low-energy QCD⊗QED,

- m_H is the mass of the SM Higgs boson. Let us note that the recent ATLAS [199] and CMS [200] measurements of m_H indicate that the running effective quartic Higgs coupling at around M_G, i.e., the parenthesis in Eq. (5.16) should be close to vanishing, see, e.g., [201] and references therein,
- m_S is the mass of the heavy singlet in 10_H,
- The remaining eigenvalues correspond to the leftover mixture of the colored triplets with the SM quantum numbers $(3, 1, -\frac{1}{3})$ from $5_H \oplus 10_H$ (6 real fields corresponding to each eigenvalue).

Absence of tachyons. Clearly, there are no tachyons in the scalar spectrum as long as

$$2\lambda_1 + \lambda_2 > 0\,, \tag{5.19}$$
$$2\lambda_3(2\lambda_1 + \lambda_2) > (\lambda_4 + \lambda_5)^2\,, \tag{5.20}$$
$$\lambda_2 + \lambda_5 < 0\,, \tag{5.21}$$

and, in particular,

$$|\lambda_2 + \lambda_5| V_G > \sqrt{(\lambda_2 - \lambda_5)^2 V_G^2 + 4\mu^2}\,, \tag{5.22}$$

which may be further simplified to $\mu^2 < \lambda_2\lambda_5 V_G^2$. Combining this with (5.21) one further concludes that both λ_2 and λ_5 must be negative. This also means that λ_1 must be positive and obey $2\lambda_1 > |\lambda_2|$ and, at the same time λ_3 must be positive. To conclude, the μ factor in formula (5.11) is subject to the constraint

$$|\mu| \leq \sqrt{\lambda_2\lambda_5} V_G. \tag{5.23}$$

in all parts of the parameter space that can, at the tree level, support a (locally) stable SM vacuum.

Perturbativity constraints

Let us briefly discuss the extra constraints on the RHS of Eq. (5.11) implied by the requirement of perturbativity of the couplings therein. Since the graph in Fig. 5.1 emerges at the GUT scale it is appropriate to interpret these couplings as the running parameters evaluated at M_G. Note that the effective theory below this

threshold is the pure SM and, thus, one may use the known qualitative features of the renormalization group evolution of the SM couplings to assess their behavior over the whole domain from v to V_G.

In general, one should assume that for all couplings perturbativity is not violated at M_G and below M_G the same holds for the "leftover" parameters of the effective theory. To that end, one should consider several terms in the perturbative expansion of all amplitudes in the relevant framework and make sure the (asymptotic) series thus obtained does not exhibit pathological growth of higher-order contributions (to a certain limit). This, in full generality, is clearly a horrendous task so we shall as usual adopt a very simplified approach. In particular, we shall make use of the fact that the running of all dimensionless couplings in the SM is rather mild so, in the first approximation, it is justified to consider their values at only one scale and assume the running effects will not parametrically change them. Hence, in what follows we shall assume that

$$|\lambda_i| \leq 4\pi \quad \forall i \tag{5.24}$$

for all the couplings in the scalar potential.

Resulting bounds on the U_ν matrix

With this at hand one can finally derive the desired constraints on the U_ν matrix governing the proton decay channels to neutral mesons (5.3)-(5.5). Indeed, using the seesaw formula, one can trade M_ν^M in Eq. (5.11) for the physical light neutrino mass matrix m_{LL} and the Dirac part of the full 6×6 seesaw matrix[13] $M_\nu^M = -M_\nu^D \left(m_{LL}\right)^{-1} \left(M_\nu^D\right)^T$ which, due to the tight link between M_ν^D and the up-type quark mass matrix in the simplest scenarios, $M_\nu^D = M_u^T$, yields $M_\nu^M = -M_u^T \left(m_{LL}\right)^{-1} M_u$. Furthermore, the basis in the quark sector can always be chosen such that the up-quark mass matrix is real and diagonal (see Appendix C.2); at the same time, one can diagonalize $m_{LL} = U_\nu^T D_\nu U_\nu$ and obtain:

$$M_\nu^M = -D_u U_\nu^\dagger D_\nu^{-1} U_\nu^* D_u \, . \tag{5.25}$$

[13] Needless to say, there are always at least three RH neutrinos in the flipped $SU(5)$ models.

Combining this with formula (5.11) and implementing the vacuum stability constraint (5.23) one obtains

$$|D_u U_\nu^\dagger D_\nu^{-1} U_\nu^* D_u| \leq \frac{\alpha_G}{64\pi^3}\sqrt{\lambda_2\lambda_5}|Y_{10}|V_G K\,, \tag{5.26}$$

where we denoted $\alpha_G \equiv g_G^2/4\pi$. Finally, assuming $\max_{i,j\in\{1,2,3\}}|(Y_{10})_{ij}| = 1$ and saturating the perturbativity constraints (5.24) we have

$$\max_{i,j\in\{1,2,3\}}|(D_u U_\nu^\dagger D_\nu^{-1} U_\nu^* D_u)_{ij}| \leq \frac{\alpha_G}{16\pi^2}V_G K\,, \tag{5.27}$$

which provides a very conservative global limit on the allowed form of U_ν and, hence, on the proton decay partial widths (5.3)-(5.5).

Unification constraints

Let us finish this preparatory section by discussing in brief the constraints from the requirement of the convergence of the running $SU(3)_c$ and $SU(2)_L$ gauge couplings at high energy which shall provide basic information about the scales involved, in particular, the approximate value of the V_G parameter. Given (5.13), the $SU(2)_L$ doublet of the proton-decay-mediating colored triplet gauge fields (X', Y') has mass $M_G = \frac{1}{2}g_G V_G$ while the mass of the heavy $U(1)_{T_{24}} \otimes U(1)_X$ gauge boson (i.e., the one orthogonal to the surviving massless SM B-field associated to hypercharge) reads $M_{B'} = 2\sqrt{\frac{3}{5}g_G^2 + g_X^2}V_G$ in the units in which the $U(1)_X$ generator is normalized as in Eqs. (2.25).

Let us note again that in the flipped scenario of our interest the M_G parameter corresponds to the scale at which the (X', Y') are integrated into the theory in order to obey the $SU(3)_c$ and $SU(2)_L$ unification constraints. The specific location of this point and, thus, the absolute size of the proton decay width, however, depends also on the position of the other thresholds due to the extra scalars to be integrated in at around M_G, in particular, the $SU(5)\otimes U(1)_X/SU(3)_c \otimes SU(2)_L \otimes U(1)_Y$ Goldstone bosons (5.15), the heavy singlet (5.17) and the heavy colored triplets (5.18). Rather than going into further details here we defer a dedicated analysis of the situation in Appendix C.3 and, in what follows, we shall stick to just a single reference scale of $M_G = 10^{16.5}$ GeV which corresponds to the lower limit obtained therein. This, in turn, yields $\Gamma^{-1}(p \to \pi^+\overline{\nu})$ of the order of $10^{38.5}$ years, cf. Fig. C.1. Remarkably enough, there is also an upper limit of the order of 10^{42}

years which, however, is attained only in a "fine-tuned" region where the inequality (5.23) is saturated.

5.3 A sample model analysis

In order to exploit formula (5.27), it is convenient to begin with its thorough inspection which, as we shall see, will provide a simple analytic information on the potentially interesting regions of the parameter space which will, subsequently, feed into the analysis of the BNV observables. Later on, we shall compare the analytics with results of a dedicated numerical analysis.

5.3.1 Parameter space

1. CP conserving setup. For the sake of simplicity, we shall start with U_ν real orthogonal which shall be parametrized by three CKM-like angles ω_{12}, ω_{23} and ω_{13}:

$$U_\nu = U_{2\text{-}3}(\omega_{23})U_{1\text{-}3}(\omega_{13})U_{1\text{-}2}(\omega_{12})$$

where $U_{i\text{-}j}(\omega_{ij})$ stands for a rotation in the i-j plane by an angle ω_{ij}, e.g.

$$U_{2\text{-}3}(\omega_{23}) = \begin{pmatrix} 1 & 0 & 0 \\ 0 & \cos\omega_{23} & \sin\omega_{23} \\ 0 & -\sin\omega_{23} & \cos\omega_{23} \end{pmatrix}. \tag{5.28}$$

Assuming normal neutrino hierarchy we parametrize the (diagonal) neutrino mass matrix $D_\nu = \mathrm{diag}(m_1, m_2, m_3)$ by the (smallest) mass m_1 of the mostly electronlike eigenstate. The other two masses are then computed from the oscillation parameters ($\Delta m^2_A = 2.43 \times 10^{-3}\,\mathrm{eV}^2$, $\Delta m^2_\odot = 7.54 \times 10^{-5}\,\mathrm{eV}^2$ [202, 203]) and, for the sake of this study, we mostly ignore the uncertainties in these observables. Let us note that for the inverted hierarchy the analysis is technically similar but physically less interesting, see below. As long as the ratios of m_i^{-1}'s are all below m_t/m_c, i.e., for $m_1 \gtrsim 10^{-4}\,\mathrm{eV}$ (which we shall assume in the simple analysis below), the LHS of Eq. (5.27) is maximized for $\left(D_u U_\nu^\dagger D_\nu^{-1} U_\nu^* D_u\right)_{33} = m_t^2 \left(U_\nu^\dagger D_\nu^{-1} U_\nu^*\right)_{33}$. Hence, Eq. (5.27) gets reduced to (using $V_G = 2M_G/g_G$)

$$\left(U_\nu^\dagger D_\nu^{-1} U_\nu^*\right)_{33} \leq K \frac{g_G}{32\pi^3 m_t^2} \times 10^{16.5}\mathrm{GeV} \approx K \times 3\,\mathrm{eV}^{-1}, \tag{5.29}$$

where we have taken[14] $g_G = 0.5$. Besides that, one gets

$$\left(U_\nu^\dagger D_\nu^{-1} U_\nu^*\right)_{33} = \frac{\sin^2\omega_{13}}{m_1} + \cos^2\omega_{13}\left(\frac{\sin^2\omega_{23}}{m_2} + \frac{\cos^2\omega_{23}}{m_3}\right), \tag{5.30}$$

which shows that the CKM-like parametrization of U_ν is very convenient because ω_{12} drops entirely from Eq. (5.30).

For further insight, let us consider the extreme cases first. For $\omega_{13} = \omega_{23} = 0$ (and for arbitrary ω_{12}) one has $\left(U_\nu^\dagger D_\nu^{-1} U_\nu^*\right)_{33} = m_3^{-1}$, whereas for $\omega_{13} = \omega_{23} = \frac{\pi}{2}$ the same equals to m_1^{-1}. While m_3^{-1} ranges from $11\,\mathrm{eV}^{-1}$ to $20\,\mathrm{eV}^{-1}$ for all m_1's lower than the current Planck and large-scale-structure limit of about[15] 0.08 eV [204], m_1^{-1} may range in principle from $12\,\mathrm{eV}^{-1}$ to infinity. This explains why the latter setting may not be allowed by (5.29) if m_1 and K are small enough. For the general case it is convenient to notice that the RHS of Eq. (5.30) is a convex combination of the inverse neutrino masses. Thus, for $m_1^{-1} \leq K \times 3\,\mathrm{eV}^{-1}$ the inequality (5.29) is satisfied trivially. This can be clearly seen in Fig. 5.2 where the allowed parameter space is depicted: for $m_1 \geq (3K)^{-1}\,\mathrm{eV}$, i.e, in the lower part of the plot, all ω_{23} and ω_{13} are are allowed. On the other hand, if $(m_3^{-1})_{\min} \approx 11\,\mathrm{eV}^{-1} > K \times 3\,\mathrm{eV}^{-1}$, i.e, if $K \lesssim 4$, (5.29) is never fulfilled.

There are two different regimes in the nontrivial region $m_1^{-1} \geq K \times 3\,\mathrm{eV}^{-1} \geq m_3^{-1}$: if $m_1^{-1} \geq K \times 3\,\mathrm{eV}^{-1} \geq m_2^{-1}$ then for small enough ω_{13} any ω_{23} is allowed. More interestingly, for $m_2^{-1} \geq K \times 3\,\mathrm{eV}^{-1} \geq m_3^{-1}$, the allowed domain is confined to bounded regions around[16] $\omega_{13} = \omega_{23} = 0$. This fully justifies the "chimneylike" shape in Fig. 5.2 for $m_1^{-1} \geq K \times 3\,\mathrm{eV}^{-1}$. It also follows that the allowed region becomes wider in the ω_{23} direction as K grows, see again Fig. 5.2. For K above a certain critical value, the chimney would be wide open in the ω_{23} direction.
This is also why the results are less interesting for the inverted hierarchy – there the two heavier neutrino masses are much closer to each other and, hence, the interesting region where ω_{13} and ω_{23} are constrained turns out to be too narrow.

[14] For further details see Appendix C.3.

[15] Note that this value corresponds to the Planck+BAO limit [56] quoted in [204], i.e., $\sum m_\nu < 0.23$ eV at 95% C.L.

[16] Note that the RHS of Eq. (5.30) is π-periodic.

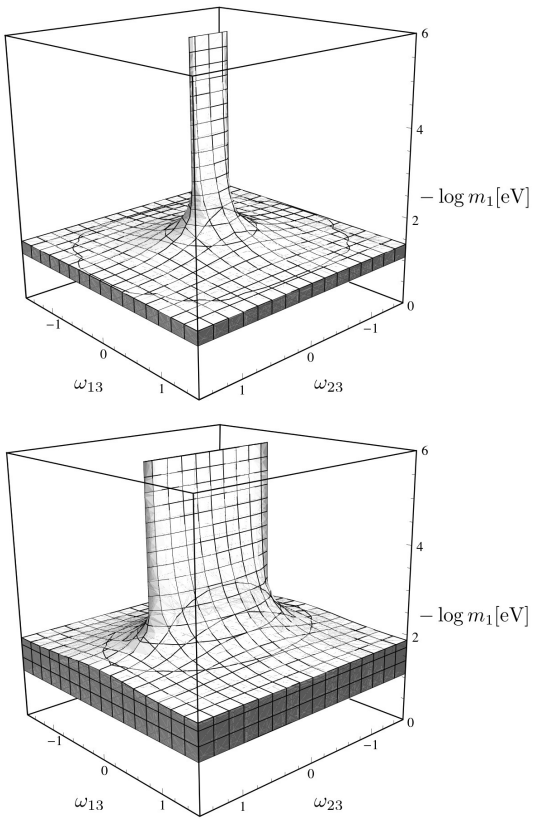

Figure 5.2: The shape of the allowed parameter space (ω_{23} and ω_{13} governing U_ν on the horizontal axes and the minus log of the lightest neutrino mass m_1 on the vertical; note that m_1 decreases from bottom to top) in the CP conserving setting discussed in Sec. 5.3.1 for $K = 10$ in the upper and $K = 30$ in the lower panel, respectively. The allowed points are all those in the interior of the depicted structure. The straight cut in the lower part corresponds to the current cosmology limit on the lightest neutrino mass $m_1 \lesssim 8 \times 10^{-2}$ eV [204], see the discussion in the text.

2. CP violation. Second, let us discuss the case when U_ν is an arbitrary unitary matrix. In the CKM-like parametrization

$$U_\nu = P_L U_{2\text{-}3}(\omega_{23}) U'_{1\text{-}3}(\omega_{13}, \sigma) U_{1\text{-}2}(\omega_{12}) P_R \,, \tag{5.31}$$

where, as usual, $P_L = \mathrm{diag}\,(e^{i\rho_1}, e^{i\rho_2}, e^{i\rho_3})$ and $P_R = \mathrm{diag}\,(1, e^{i\rho_4}, e^{i\rho_5})$ are pure phase matrices, $U_{2\text{-}3}(\omega_{23})$ and $U_{1\text{-}2}(\omega_{12})$ are as above, cf. Eq. (5.28), and $U'_{1\text{-}3}(\omega_{13}, \sigma)$ contains an extra Dirac-like phase σ analogous to the CP phase in the CKM matrix:

$$U'_{1\text{-}3}(\omega_{13}, \sigma) = \begin{pmatrix} \cos\omega_{13} & 0 & \sin\omega_{13} e^{-i\sigma} \\ 0 & 1 & 0 \\ -\sin\omega_{13} e^{i\sigma} & 0 & \cos\omega_{13} \end{pmatrix}.$$

It is clear that ρ_4 and ρ_5 drop from the $|(V_{PMNS} U_\nu)_{\alpha 1}|$ combination in the decay rates (5.3)-(5.5) and, hence, they do not need to be considered. Since the analytics gets too complicated here let us just note that ρ_1, ρ_2 and ρ_3 play a very minor role in shaping the allowed parameter space and, thus, the only important phase in the game is σ; for σ close to maximal the strict bounds on ω_{23} can be lost for much lighter m_1 than in the CP conserving case. As one can see in Fig. 5.3, for significant σ's the ω_{23} parameter is typically out of control unless m_1 is taken to be very tiny [assuming again, for simplicity, the dominance of the 33 element of the RH neutrino mass matrix (5.25)].

5.3.2 Observables

Since there is no U_ν in the partial proton decay widths to charged meson and the rates (5.4)-(5.5) differ from (5.3) only by calculable numerical factors let us focus here solely to $\Gamma(p \to \pi^0 \ell^+) \equiv \Gamma_\ell$ for $\ell = e,\ \mu$. It is not difficult to see that if ω_{23} can be arbitrary (such as in the lower parts of the allowed regions in Figs. 5.2 and 5.3) there is no control over Γ_ℓ. However, if both ω_{13} and ω_{23} are restricted, there may be an upper bound on $|(V_{PMNS} U_\nu)_{21}|$ and, hence, on Γ_μ, while there is no such feature observed in Γ_e. On the other hand, there is a strong correlation among Γ_e and Γ_μ which is clearly visible in the sum of the two decay rates; indeed, there is instead a lower bound on $\Gamma_e + \Gamma_\mu$. Hence, in what follows we shall stick to these two independent observables and note that very similar features can be seen in the decay rates to K^0 and η related to these by the isospin symmetry.

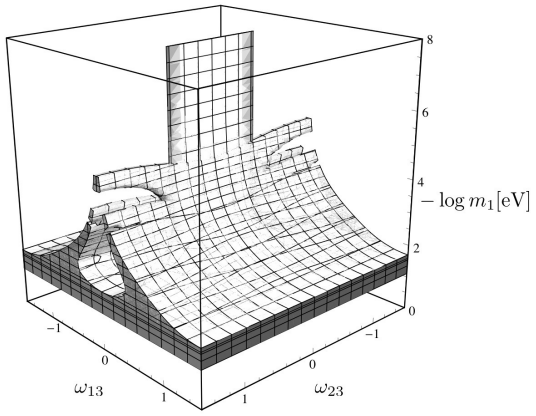

Figure 5.3: The same as in Fig. 5.2 for the CP violating setting with the "Dirac" phase in U_ν set to $\sigma = \pi/2$ and $K = 20$. The net effect of a nonzero σ is that ω_{23} remains unconstrained unless m_1 is really tiny [for which case the dominance of the 33 element in the RH neutrino mass formula (5.25) is assumed]. The effects of the "outer" phases of U_ν in the observables discussed in Sec. 5.3.1 are small so we conveniently fixed all of them to zero.

To proceed, one also has to take into account that both Γ_μ and $\Gamma_e + \Gamma_\mu$ in general depend on ω_{12}. Since, however, these relations are linear one can derive analytic expressions for "optimal" ω_{12}'s in each case such that Γ_μ is maximized and $\Gamma_e + \Gamma_\mu$ is minimized for any given values of ω_{13} and ω_{23}. Focusing, for simplicity, on the CP conserving case one has (V stands for the PMNS matrix)

$$\tan\omega_{12}^{\rm opt} = \frac{V_{23}\sin\omega_{23} - V_{22}\cos\omega_{23}}{V_{21}\cos\omega_{13} - \sin\omega_{13}\left(V_{23}\cos\omega_{23} + V_{22}\sin\omega_{23}\right)}$$

for the maximal value of Γ_μ (given ω_{13} and ω_{23}) , whereas $\Gamma_e + \Gamma_\mu$ is (for given ω_{13} and ω_{23}) minimized for

$$\tan\omega_{12}^{\rm opt} = \frac{V_{33}\sin\omega_{23} - V_{32}\cos\omega_{23}}{V_{31}\cos\omega_{13} - \sin\omega_{13}\left(V_{33}\cos\omega_{23} + V_{32}\sin\omega_{23}\right)}\,.$$

In Fig. 5.4, the solid contours in the upper two panels denote Γ_μ in units of $0.8 \times \frac{1}{2}\Gamma(p \to \pi^+\overline{\nu})|(V_{CKM})_{11}|^2 \sim (10^{38}y)^{-1}$ (see Appendix C.3) evaluated at the point $\{\omega_{12}^{\rm opt}(\omega_{23},\omega_{13}),\omega_{23},\omega_{13}\}$, i.e., at its upper limits for each ω_{23} and ω_{13}; similarly, the lower limits on $\Gamma_e + \Gamma_\mu$ are displayed in the lower panels (the color code is such that the decay rates decrease in darker regions). At the same time, the

dashed lines are boundaries of the regions allowed by (5.29) for different K's, i.e., the "horizontal cuts" through different "chimneys" such as those in Fig. 5.2 at a constant m_1.

Remarkably enough, if K is not overly large, there is a global upper limit on Γ_μ, and a global lower limit on $\Gamma_e + \Gamma_\mu$ on the boundaries of the relevant allowed regions. Sticking to the $(-\pi/2, +\pi/2)$ interval for both ω_{13} and ω_{23}, which is fully justified by the symmetry properties of the relevant formulas, the precise position of such a maximum (minimum) could be found numerically or well approximated by taking $\omega_{13} = 0$ and the relevant ω_{23} on the boundary:

$$\cos^2 \omega_{23} = \frac{m_2^{-1} - 3K\,\mathrm{eV}^{-1}}{m_2^{-1} - m_3^{-1}}\,. \tag{5.32}$$

This formula holds for both observables, i.e., for the maximum of Γ_μ as well as for the minimum of $\Gamma_e + \Gamma_\mu$; one just has to choose $\omega_{23} \in (0, \pi/2)$ for the former and $\omega_{23} \in (-\pi/2, 0)$ for the latter, respectively.

5.3.3 Results

In what follows, we shall focus on a pair of observables X_μ and $X_{e+\mu}$ defined conveniently as

$$X_\mu \equiv \frac{\Gamma(p \to \pi^0 \mu^+)}{\frac{1}{2}\Gamma(p \to \pi^+ \overline{\nu})|(V_{CKM})_{11}|^2}\,, \tag{5.33}$$

$$X_{e+\mu} \equiv \frac{\Gamma(p \to \pi^0 e^+) + \Gamma(p \to \pi^0 \mu^+)}{\frac{1}{2}\Gamma(p \to \pi^+ \overline{\nu})|(V_{CKM})_{11}|^2}\,; \tag{5.34}$$

their normalization (besides the trivial $|(V_{CKM})_{11}|^2$ piece) is fully governed by the size of the $\Gamma(p \to \pi^+ \overline{\nu})$ factor studied in detail in Appendix C.3.

1. CP conserving case. If U_ν is real and orthogonal, both analytic and numerical analyses are tractable so it is interesting to see how these compare. In the upper plot in Fig. 5.5, the solid lines indicate the analytic upper bounds on X_μ for a set of different K's whereas the lower plots depict the corresponding lower bounds on $X_{e+\mu}$, respectively. The points superimposed on both plots represent the results of a numerical analysis. For that sake, m_1 and the three CKM-like angles ω_{12}, ω_{23} and ω_{13} were chosen randomly and we fixed $K = 7$; only those

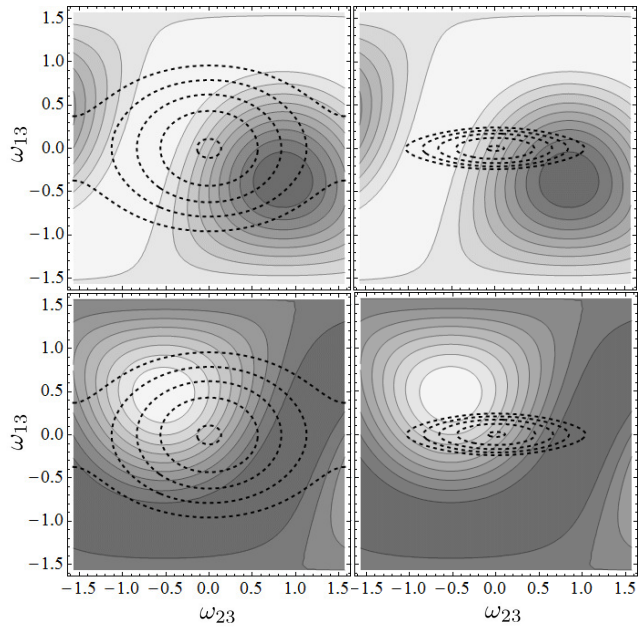

Figure 5.4: Contour plots of the ω_{12}-extremes (cf. Sec. 5.3.2) of the partial widths $\Gamma(p \to \pi^0 \mu^+)$ (upper panels, decreasing with darkening color) and $\Gamma(p \to \pi^0 e^+) + \Gamma(p \to \pi^0 \mu^+)$ (lower panels) superimposed with the (dashed) boundaries of the regions allowed by Eq. (5.29) evaluated for $m_1 = 0.8 \times 10^{-2}\,\text{eV}$ (left), and $m_1 = 0.8 \times 10^{-3}\,\text{eV}$ (right), respectively. In all the plots the innermost and outermost dashed contours correspond to $K = 7$ and $K = 30$ respectively.

points satisfying the inequality (5.27) are allowed in the plot. We can see that, in spite of the simple $\omega_{13} = 0$ assumption on the extremes of X's, the analytic curves fit fairly well with the numerics. The agreement is slightly worse for larger m_1 which, however, is the case when the $\omega_{13} = 0$ approximation becomes rather rough.[17]

Concerning the physical interpretation of the results there are several options of how to read figure Fig. 5.5 and similar plots given in the next section. For instance, for a fixed K (assuming, e.g., one can learn more about the high-scale structure of the theory from a detailed renormalization group analysis) a measurement of X_μ imposes a lower limit on mass of the lightest neutrino (e.g., $K = 7$ and $X_\mu \sim 0.8$ is possible if and only if $m_1 \gtrsim 10^{-2}$ eV etc.) Alternatively, for a given K and a measured value of m_1 one gets a prediction for X_μ (for example, if $K = 7$ and $m_1 \sim 10^{-2}$ eV then X_μ is required to be below about 0.8). Obviously, a similar reasoning can be applied to $X_{e+\mu}$.

2. CP violation. The numerical analysis for a complex U_ν is far more involved and, besides that, there is no simple analytics that it can be easily compared to. We allowed the three CKM-like angles and all the CP phases to vary arbitrarily within their domains and also m_1 was scanned randomly on the logarithmic scale. For σ close to zero one obtains similar features in X_μ and $X_{e+\mu}$ as in the CP conserving case regardless of the other three phases ρ_1, ρ_2, ρ_3, see Fig. 5.6. If, however, also σ is varied randomly, then both of these effects can be seen only for tiny $m_1 \lesssim 10^{-6}$ eV, cf. Fig. 5.7. This, at least for the case of a dominant 33 element of the RH neutrino mass formula (5.25), can be easily understood from the shape of the allowed parameter space depicted on Fig. 5.3—there is no restriction on ω_{23} for moderate m_1 while for m_1 very tiny ω_{13} and ω_{23} are again restricted to a bounded area.

[17] It is clear from Fig. 5.4 that the approximation of reaching the minimum at $\omega_{13} = 0$ is more accurate for smaller m_1 (plots on the right-hand side) where the allowed regions are very narrow in the ω_{13} direction.

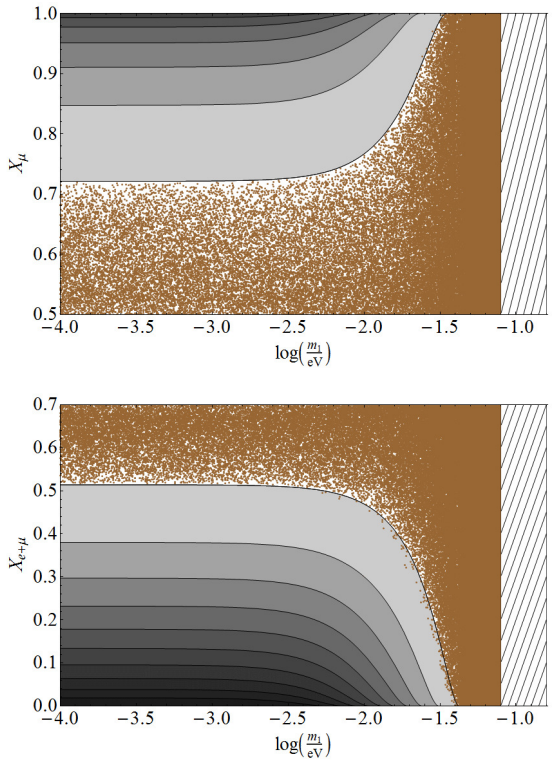

Figure 5.5: The global upper limits on X_μ (upper plot) and the global lower limits on $X_{e+\mu}$ (lower plot), cf. Eqs. (5.33) and (5.34), as functions of the lightest neutrino mass (in the normal hierarchy case). The lowermost line on the upper plot, and the uppermost line on the lower plot correspond to $K = 7$, with every consecutive contour for K increased by 2. The dots represent an independent numerical calculation of the same decay rates for $K = 7$ with randomly chosen real U_ν's; only those points satisfying (5.27) are permitted. The hatched area corresponds to $m_1 > 0.08\,\text{eV}$ which is disfavored by cosmology [204].

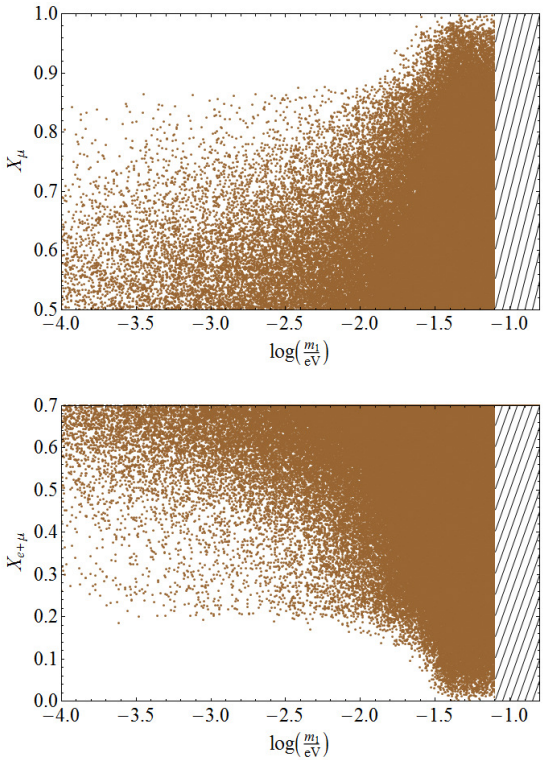

Figure 5.6: The same as in Fig. 5.5 but for a complex U_ν and $K = 8$. The "outer" phases ρ_1, ρ_2 and ρ_3 (cf. Eq. 5.31) are varied randomly while the "Dirac" phase σ of U_ν was fixed to zero. It is clear that the effect of ρ_i's is very mild as the desired features in the partial widths remain essentially intact.

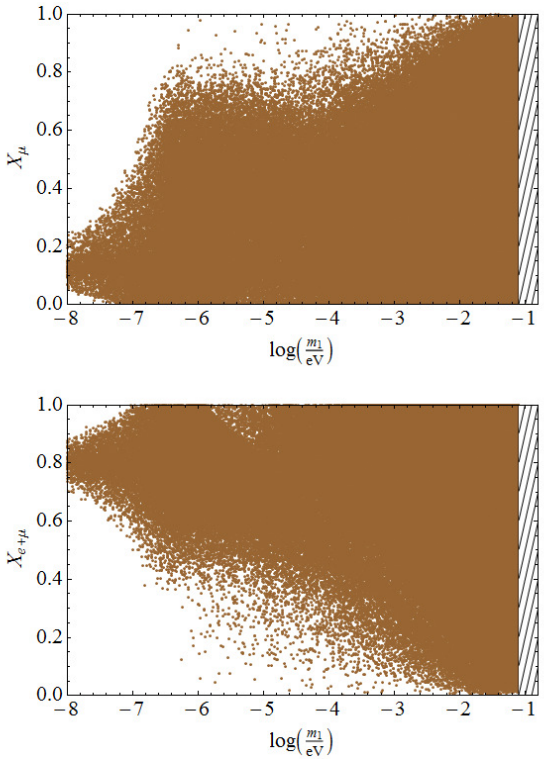

Figure 5.7: The same as in Fig. 5.6 but this time for entirely random phases in U_ν including σ. The effects in the partial widths are smeared until $m_1 \lesssim 10^{-6}\,\text{eV}$ because, for larger m_1, the important constraints on ω_{23} from perturbativity and SM vacuum stability are lost, see Fig. 5.3.

5.4 Potentially realistic scenarios

A careful reader certainly noticed that, up to now, we have left aside the fact that in the most minimal model with only a single 5_H in the scalar sector the size of the Yukawa matrix entering Witten's loop is further constrained by the need to reproduce the down-quark masses. Indeed, in such a case

$$Y_{10} \sim \tfrac{1}{\sqrt{2}} M_d/v\,, \tag{5.35}$$

which, barring renormalization group running, is at most of the order of $m_b/v \sim 2\%$. Hence, in the very minimal model Witten's loop is further suppressed and the inequality (5.27) cannot be satisfied unless K is extremely large. In this respect, the perturbativity limits implemented in the discussion above are, strictly speaking, academic.

Another issue is the $M_\nu^M \propto M_d$ correlation which, regardless of the size of the proportionality factor, renders the light neutrino spectrum too hierarchical. Indeed, for $m_{LL} \propto M_u^T (M_d)^{-1} M_u$ which in the M_d-diagonal basis reads

$$m_{LL} \propto W_R D_u V'_{CKM} (D_d)^{-1} V'^T_{CKM} D_u W_R^T, \tag{5.36}$$

(provided V'_{CKM} is the "raw" form of the CKM matrix including the five extra phases usually rotated away in the SM context and W_R is an unknown unitary matrix) one typically gets $m_2 : m_3 \sim 0.001$ while the data suggest this ratio to be close to $\sqrt{\Delta m^2_\odot / \Delta m^2_A} \sim 0.1$. Hence, a potentially realistic generalization of the minimal scenario is necessary together with a careful analysis of the possible impacts of the extra multiplets it may contain on the results obtained in the previous sections.

There are clearly many options on how to avoid the unwanted suppression of Y_{10} and get a realistic RH neutrino spectrum in more complicated models. One may, for example, add extra[18] vectorlike fermions that may allow large Y_{10} by breaking the correlation (5.35), heavy extra singlets etc. However, in many cases the structure of such a generalized scheme changes so much that some of the vital

[18] There does not seem to be any loop-induced effect in the quark and/or charged lepton sectors of the original model that may provide the desired departure from the $M_\nu^M \propto M_D$ degeneracy; thus, extra degrees of freedom are necessary.

ingredients of the previous analysis are lost. In order to deal with this, let us first recapitulate the main assumptions behind the central formula (5.27) underpinning the emergence of all the features in the proton decay channels into neutral mesons seen in Sec. 5.3: First, the down-type quark mass matrix M_d was required to be symmetric. This is not only crucial for the sharp prediction (5.2) but, on more general grounds, also to avoid the option of "rotating away" the $d = 6$ gauge-driven proton decay from the flipped $SU(5)$ altogether, cf. [50, 107, 190]. Second, in getting a grip on the LHS of Eq. (5.10) we made use of the tight $M_\nu^D = M_u^T$ correlation. Obviously, both these assumptions are endangered in case one embarks on indiscriminate model building.

5.4.1 The model with a pair of scalar 5's

Remarkably enough, the simplest concievable generalization of all, i.e., the model with an extra 5-dimensional scalar (which resembles the two-Higgs-doublet extension of the SM), renders the scheme perfectly realistic and, at the same time, it leaves all the key prerequisites of the analysis in Sec. 5.3 intact.

The Yukawa sector and flavor structure

Assuming both doublets in $5_H \oplus 5'_H$ do have nonzero projections onto the light SM Higgs the extended Yukawa Lagrangian

$$\begin{aligned} \mathcal{L} \ \ni \ & Y_{10} 10_M 10_M 5_H + Y'_{10} 10_M 10_M 5'_H + \\ + \ & Y_{\overline{5}} 10_M \overline{5}_M 5^*_H + Y'_{\overline{5}} 10_M \overline{5}_M {5'_H}^* \\ + \ & Y_1 \overline{5}_M 1_M 5_H + Y'_1 \overline{5}_M 1_M 5'_H + h.c. \end{aligned} \tag{5.37}$$

gives rise to the following set of sum rules for the effective quark and lepton mass matrices

$$M_\nu^D = M_u^T \propto Y_{\overline{5}} v_5^* + Y'_{\overline{5}} v_{5'}^*, \tag{5.38}$$

$$M_d = M_d^T = Y_{10} v_5 + Y'_{10} v_{5'} \tag{5.39}$$

$$M_e = Y_1 v_5 + Y'_1 v_{5'} \quad \text{arbitrary.} \tag{5.40}$$

Naïvely, one would say that adding three extra 3×3 Yukawa matrices (symmetric Y'_{10}, arbitrary $Y'_{\overline{5}}$ and Y'_1) the predictive power of the theory would be totally ruined. However, from the perspective of the analysis in Secs. 5.2 and 5.3 the

only really important change is the presence of Y'_{10}; adding $Y'_{\bar{5}}$ and Y'_1 does not worsen the predictive power of the minimal setting at all because, for the former, $M_\nu^D = M_u^T$ is still maintained and, for the latter, M_e remains as theoretically unconstrained as before.

Indeed, the net effect of Y'_{10} is just the breakdown of the unwanted $M_\nu^M \propto M_d$ correlation due to an extra term in the generalized version of formula (5.10):

$$M_\nu^M = \left(\frac{1}{16\pi^2}\right)^2 g_G^4 (Y_{10}\,\mu + Y'_{10}\,\mu') \frac{\langle 10_H \rangle^2}{M_G^2} \times \mathcal{O}(1)\,. \tag{5.41}$$

Here μ' is the trilinear coupling of $5'_H$ to the pair of 10_H's analogous to the third term in formula (5.12); as long as μ'/μ is different enough from v'/v one can fit all the down-quark masses without any need for a suppression in Y_{10} and Y'_{10}.
Given this, the whole analysis in Sec. 5.3 can be repeated with the only difference that Eq. (5.23) becomes more technically involved (but, conceptually, it remains the same) and, with that, there is essentially just an extra factor of 2 popping up on the RHS of the generalized formula (5.27):

$$\max_{i,j\in\{1,2,3\}} |(D_u U_\nu^\dagger D_\nu^{-1} U_\nu^* D_u)_{ij}| \leq \frac{\alpha_G}{8\pi^2} V_G K. \tag{5.42}$$

Hence, all results of Sec. 5.3 can be, in first approximation, adopted to the fully realistic case by a mere rescaling of the K factor. For example, the allowed points depicted in Fig. 5.6 for $K = 8$ in the basic model are allowed in the generalized setting with $K = 4$ and so on.

5.5 Summary and conclusions

In this work we point out that the radiative mechanism for the RH neutrino mass generation, identified by E. Witten in the early 1980s in the framework of the simplest $SO(10)$ grand unified models, can find its natural and potentially realistic incarnation in the realm of the flipped $SU(5)$ theory. This, among other things, makes it possible to resolve the long-lasting dichotomy between the gauge unification constraints and the position of the $B - L$ breaking scale governing Witten's graph: on one side, the current limits on the absolute light neutrino mass require M_{B-L} to be close to the GUT scale which, on the other hand, is problematic to devise in the nonsupersymmetric unifications and even useless in the SUSY case

where Witten's loop is typically canceled. In this respect, the relaxed unification constraints inherent to the flipped $SU(5)$ scheme allow not only for a natural and a very simple implementation of this old idea but, at the same time, for a rich enough GUT-scale phenomenology (such as perturbative baryon number violation, i.e., proton decay) so that the minimal model might be even testable at the near future facilities.

In particular, we have studied the minimal renormalizable flipped $SU(5)$ model focusing on the partial proton decay widths to neutral mesons that, in this framework, are all governed by a single unitary matrix U_ν to which one gets a grip through Witten's loop. Needless to say, this is impossible in the usual case when the tree-level RH neutrino masses are generated by means of an extra 50-dimensional scalar and/or extra matter fields due to the general lack of constraints on the new couplings in such models. Hence, there are two benefits to this approach: the scalar sector of the theory does not require any multiplet larger than the 10-dimensional two-index antisymmetric tensor of $SU(5)$ and, at the same time, one obtains a rather detailed information about *all* $d = 6$ proton decay channels in terms of a single and possibly calculable parameter.

To this end, we performed a detailed analysis of the correlations among the partial proton decay widths to π^0 and either e^+ or μ^+ in the final state and we observed strong effects in the $\Gamma(p \to \pi^0\mu^+)$ partial width (an upper bound) and in $\Gamma(p \to \pi^0 e^+) + \Gamma(p \to \pi^0\mu^+)$ (a lower bound) across a significant portion of the parameter space allowed by the perturbative consistency of the model, as long as normal neutrino hierarchy is assumed and the Dirac-type CP violation in the lepton sector is small. In other cases, such effects are observable only if the lightest neutrino mass is really tiny.

Concerning the strictness of the perturbativity and/or the SM vacuum stability constraints governing the size of these effects, there are several extra inputs that may, in principle, make these features yet more robust and even decisive for the future tests of the simplest models. If, for instance, proton decay would be found in the near future (at LBNE and/or Hyper-K) the implied upper limit on the unification scale (which, obviously, requires a dedicated higher-loop renormalization group analysis based on a detailed effective potential study) would further

constrain the high-scale spectrum of the theory which, in turn, feeds into the computation of Witten's loop and, thus, the K factor; this, in reality, may be subject to stronger constraints than those discussed in Sec. 5.2 with clear implications for the relevant partial widths. To this end, there are also other high-energy signals that may be at least partially useful for this sake such as the baryon asymmetry of the Universe; although the U_ν matrix drops from the "canonical" leading order contribution to the CP asymmetry of the RH neutrino decays in leptogenesis, the size of the effective Yukawa couplings may still be constrained and, thus, also the K factor. This, however, is beyond the scope of the current study and will be elaborated on elsewhere.

Chapter 6

SUSY AND NON-SUSY GUTS WITH LR SYMMETRY

6.1 $SO(10)$ INSPIRED MODELS WITH SLIDING SCALES

6.1.1 Introduction

In the MSSM ("Minimal Supersymmetric extension of the Standard Model") gauge couplings unify at an energy scale of about $m_G \simeq 2 \times 10^{16}$ GeV. Adding particles arbitrarily to the MSSM easily destroys this attractive feature. Thus, relatively few SUSY models have been discussed in the literature which have a larger than MSSM particle content at experimentally accessible energies. Neutrino oscillation experiments [7, 9, 10], however, have shown that at least one neutrino must have a mass $m_{\rm Atm} \geq 0.05$ eV. [1] A (Majorana) neutrino mass of this order indicates the existence of a new energy scale below m_G. For models with renormalizable interactions and perturbative couplings, as for example in the classical seesaw models [14, 95, 170, 205], this new scale should lie below approximately $\Lambda_{\rm LNV} \lesssim 10^{15}$ GeV.

From the theoretical point of view GUT models based on the group $SO(10)$ [99] offer a number of advantages compared to the simpler models based on $SU(5)$. For example, several of the chains through which $SO(10)$ can be broken to the SM gauge group contain the left-right (LR) symmetric group $SU(3)_c \times SU(2)_L \times$

[1] For the latest fits of oscillation data, see for example [8].

$SU(2)_R \times U(1)_{B-L}$ as an intermediate step [206], thus potentially explaining the observed left-handedness of the weak interactions. However, probably the most interesting aspect of $SO(10)$ is that it automatically contains the necessary ingredients to generate a seesaw mechanism [170]: (i) the right-handed neutrino is included in the **16** which forms a fermion family; and (ii) $(B-L)$ is one of the generators of $SO(10)$.

$SO(10)$ based models with an intermediate LR symmetry usually break the LR symmetry at a rather large energy scale, m_R. For example, [207, 208] use **210** and a pair of **126** and $\overline{\mathbf{126}}$ to break $SO(10)$ and conclude that, under certain assumptions about the supersymmetry breaking scale, m_R has to be larger than roughly 10^{10} GeV. Similar conclusions were reached in [209, 210], where **45**, **54** and a pair of **126** and $\overline{\mathbf{126}}$ where used to break $SO(10)$. Also in SUSY LR models inspired by these $SO(10)$ constructions usually m_R is assumed to be quite large. For example, if LR is broken in the SUSY LR model by the vev of $(B-L)=2$ triplets [211, 212] or by a combination of $(B-L)=2$ and $(B-L)=0$ triplets [213, 214], $m_R \simeq 10^{15}$ GeV is the typical scale consistent with gauge coupling unification (GCU). The authors of [215] find a lower limit of $m_R \gtrsim 10^9$ GeV from GCU for models where the LR symmetry is broken by triplets, even if one allows additional non-renormalizable operators or sizeable GUT-scale thresholds to be present. On the other hand, in models with an extended gauge group it is possible to formulate sets of conditions on the β-coefficients for the gauge couplings, which allow to enforce GCU independent of the energy scale at which the extended gauge group is broken. This was called the "sliding mechanism" in [33]. [2] However, [33] was not the first to present examples of "sliding scale" models in the literature. In [32] it was shown that, if the left-right group is broken to $SU(2)_L \times U(1)_R \times U(1)_{B-L}$ by the vacuum expectation value of a scalar field $\Phi_{1,1,3,0}$ then [3] the resulting $U(1)_R \times U(1)_{B-L}$ can be broken to $U(1)_Y$ of the SM in agreement with experimental data at any energy scale. In [215] the authors demonstrated that in fact a complete LR group can be lowered to the TeV-scale, if certain carefully chosen fields are added and the LR-symmetry is broken by right doublets. A particularly simple model of this kind was discussed in [217]. Finally,

[2] A different (but related) approach to enforcing GCU is taken by the authors of [216] with what they call "magic fields".

[3] The indices are the transformation properties under the LR group, see next section and appendix for notation.

the authors of [33] discussed also an alternative way of constructing a sliding LR scale by relating it to an intermediate Pati-Salam stage. We note in passing that these papers are not in contradiction with the earlier work [211, 212, 213, 214], which all have to have large m_R. As discussed briefly in the next section it is not possible to construct a sliding scale variant for an LR model including pairs of $\Phi_{1,1,3,-2}$ and $\Phi_{1,3,1,-2}$.

Three different constructions, based on different $SO(10)$ breaking chains, were considered in [33]. In chain-I SO(10) is broken in exactly one intermediate (LR symmetric) step to the standard model group:

$$SO(10) \to SU(3)_c \times SU(2)_L \times SU(2)_R \times U(1)_{B-L} \to \text{ MSSM.} \tag{6.1}$$

In chain-II SO(10) is broken first to the Pati-Salam group: [41]

$$\begin{aligned} SO(10) &\to SU(4) \times SU(2)_L \times SU(2)_R \\ &\to SU(3)_c \times SU(2)_L \times SU(2)_R \times U(1)_{B-L} \to \text{ MSSM.} \end{aligned} \tag{6.2}$$

And finally, in chain-III:

$$\begin{aligned} SO(10) &\to SU(3)_c \times SU(2)_L \times SU(2)_R \times U(1)_{B-L} \\ &\to SU(3)_c \times SU(2)_L \times U(1)_R \times U(1)_{B-L} \to \text{ MSSM.} \end{aligned} \tag{6.3}$$

In all cases the last symmetry breaking scale before reaching the SM group can be as low as $\mathcal{O}(1)$ TeV maintaining nevertheless GCU. [4] The papers discussed above [32, 33, 215, 217] give at most one or two example models for each chain, i.e. they present a "proof of principle" that models with the stipulated conditions indeed can be constructed in agreement with experimental constraints. It is then perhaps natural to ask: How unique are the models discussed in these papers? The answer we find for this question is, perhaps unsurprisingly, that a huge number of variants exist in each class. Even in the simplest class (chain-I) we have found a total of 53 variants (up to 5324 "configurations", see next section) which can have perturbative GCU and a LR scale below 10 TeV, consistent with experimental data. For the two other classes, chain-II and chain-III, we have found literally thousands of variants.

[4] In fact, the sliding mechanism would work also at even lower energy scales. This possibility is, however, excluded phenomenologically.

With such a huge number of variants of essentially "equivalent" constructions one immediate concern is, whether there is any way of distinguishing among all of these constructions experimentally. Tests could be either direct or indirect. Direct tests are possible, because of the sliding scale feature of the classes of models we discuss, see section 6.1.2. Different variants predict different additional (s)particles, some of which (being colored) could give rise to spectacular resonances at the LHC. However, even if the new gauge symmetry and all additional fields are outside the reach of the LHC, all variants have different β coefficients and thus different running of MSSM parameters, both gauge couplings and SUSY soft masses. Thus, if one assumes the validity of a certain SUSY breaking scheme, such as for example mSugra, indirect traces of the different variants remain in the SUSY spectrum, potentially measurable at the LHC and a future ILC/CLIC. This was discussed earlier in the context of indirect tests for the SUSY seesaw mechanism in [139, 218, 219] and for extended gauge models in [33]. We generalize the discussion of [33] and show how the "invariants", i.e. certain combinations of SUSY soft breaking parameters, can themselves be organized into a few classes, which in principle allow to distinguish class-II models from class-I or class-III and, if sufficient precision could be reached experimentally, even select specific variants within a class and give indirect information about the new energy scale(s).

6.1.2 Models

6.1.3 Supersymmetric SO(10) models: General considerations

Before entering into the details of the different model classes, we will first list some general requirements which we use in all constructions. These requirements are the basic conditions any model has to fulfill to guarantee at least in principle that a phenomenologically realistic model will result.

We use the following conditions:

- Perturbative SO(10) unification. That is, gauge couplings unify (at least) as well as in the MSSM and the value of α_G is in the perturbative regime.
- The GUT scale should lie above (roughly) 10^{16} GeV. This bound is motivated by the limit on the proton decay half-live.

- Sliding mechanism. This requirement is a set of conditions (different conditions for different classes of models) on the allowed β coefficients of the gauge couplings, which ensure the additional gauge group structure can be broken at any energy scale consistent with GCU.

- Renormalizable symmetry breaking. This implies that at each intermediate step we assume there are (at least) the minimal number of Higgs fields, which the corresponding symmetry breaking scheme requires.

- Fermion masses and in particular neutrino masses. This condition implies that the field content of the extended gauge groups is rich enough to fit experimental data, although we will not attempt detailed fits of all data. In particular, we require the fields to generate Majorana neutrino masses through seesaw, either ordinary seesaw or inverse/linear seesaw, to be present. [5]

- Anomaly cancellation. We accept as valid "models" only field configurations which are anomaly free.

- $SO(10)$ completable. All fields used in a lower energy stage must be parts of a multiplet present at the next higher symmetry stage. In particular, all fields should come from the decomposition of one of the $SO(10)$ multiplets we consider (multiplets up to **126**).

- Correct MSSM limit. All models must be rich enough in particle content that at low energies the MSSM can emerge.

A few more words on our naming convention and notations might be necessary. We consider the three different $SO(10)$ breaking chains, eq. (6.1)-(6.3), and will call these model "classes". In each class there are fixed sets of β-coefficients, which all lead to GCU but with different values of α_G and different values of α_R and α_{B-L} at low energies. These different sets are called "variants" in the following. And finally, (nearly) all of the variants can be created by more than one possible set of superfields. We will call such a set of superfields a "configuration". Configurations are what usually is called "model" by model builders, although we prefer to think of these as "proto-models", i.e. constructions fulfilling all our basic requirements. These are only proto-models (and not full-fledged models), since we do not check

[5] For $SO(10)$ based models including fit to fermion masses (also neutrinos) see, for example [220, 221].

for each configuration in a detailed calculation that all the fields required in that configuration can remain light. We believe that for many, but probably not all, of the configurations one can find conditions for the required field combinations being "light", following similar conditions as discussed in the prototype class-I model of [217].

All superfields are named as $\Phi_{3_c,2_L,2_R,1_{B-L}}$ (in the left-right symmetric stage), $\Psi_{4,2_L,2_R}$ (in the Pati-Salam regime) and $\Phi'_{3_c,2_L,1_R,1_{B-L}}$ (in the $U(1)_R \times U(1)_{B-L}$ regime), with the indices giving the transformation properties under the group. A conjugate of a field is denoted by, for example, $\bar{\Phi}_{3_c,2_L,2_R,1_{B-L}}$, however, without putting a corresponding "bar" (or minus sign) in the index. We list all fields we use, together with their transformation properties and their origin from $SO(10)$ multiplets, complete up to the **126** of $SO(10)$ in the appendix.

6.1.4 Model class-I: One intermediate (left-right) scale

We start our discussion with the simplest class of models with only one new intermediate scale (LR):

$$SO(10) \to SU(3)_c \times SU(2)_L \times SU(2)_R \times U(1)_{B-L} \to \text{MSSM} \ . \tag{6.4}$$

We do not discuss the first symmetry breaking step in detail, since it is not relevant for the following discussion and only mention that $SO(10)$ can be broken to the LR group either via the interplay of vevs from a **45** and a **54**, as done for example in [217], or via a **45** and a **210**, an approach followed in [32]. In the left-right symmetric stage we consider all irreducible representations, which can be constructed from $SO(10)$ multiplets up to dimension **126**. This allows for a total of 24 different representations (plus conjugates), their transformation properties under the LR group and their $SO(10)$ origin are summarized in table B.1 (and table B.2) of the appendix.

Consider gauge coupling unification first. If we take the MSSM particle content

as a starting point, the β-coefficients in the different regimes are given as: [6]

$$\begin{aligned}\left(b_3^{SM}, b_2^{SM}, b_1^{SM}\right) &= (-7, -3, 21/5)\,, \\ \left(b_3^{MSSM}, b_2^{MSSM}, b_1^{MSSM}\right) &= (-3, 1, 33/5)\,, \\ \left(b_3^{LR}, b_2^{LR}, b_R^{LR}, b_{B-L}^{LR}\right) &= (-3, 1, 1, 6) + \left(\Delta b_3^{LR}, \Delta b_2^{LR}, \Delta b_R^{LR}, \Delta b_{B-L}^{LR}\right) \end{aligned} \quad (6.5)$$

where we have used the canonical normalization for $(B-L)$ related to the physical one by $(B-L)^c = \sqrt{\frac{3}{8}}(B-L)^p$. Here, Δb_i^{LR} stands for the contributions from additional superfields, not accounted for in the MSSM.

As is well known, while the MSSM unifies, putting an additional LR scale below the GUT scale with $\forall \Delta b_i^{LR} = 0$ destroys unification. Nevertheless GCU can be maintained, if some simple conditions on the Δb_i^{LR} are fulfilled. First, since in the MSSM $\alpha_3 = \alpha_2$ at roughly 2×10^{16} GeV one has that $\Delta b_2^{LR} = \Delta b_3^{LR} \equiv \Delta b$ in order to preserve this situation for an arbitrary LR scale (sliding condition). Next, recall the matching condition

$$\alpha_1^{-1}(m_R) = \frac{3}{5}\alpha_R^{-1}(m_R) + \frac{2}{5}\alpha_{B-L}^{-1}(m_R), \quad (6.6)$$

which, by substitution of the LR scale by an arbitrary one above m_R, allows us to define an artificial continuation of the hypercharge coupling constant α_1 into the LR stage. The β-coefficient of this dummy coupling constant for $E > m_R$ is $\frac{3}{5}b_R^{LR} + \frac{2}{5}b_{B-L}^{LR}$ and it should be compared with b_1^{MSSM} $(E < m_R)$; the difference is $\frac{3}{5}\Delta b_R^{LR} + \frac{2}{5}\Delta b_{B-L}^{LR} - \frac{18}{5}$ and it must be equal to Δb in order for the difference between this α_1 coupling and $\alpha_3 = \alpha_2$ at the GUT to be independent of the scale m_R. These are the two conditions imposed by the sliding requirement of the LR scale on the β-coefficients [see eq. (6.7)]. Note, however, that we did not require (approximate) unification of α_R and α_{B-L} with α_3 and α_2; it was sufficient to require that $\alpha_2^{-1} = \alpha_3^{-1} \approx \frac{3}{5}\alpha_R^{-1} + \frac{2}{5}\alpha_{B-L}^{-1}$. In any case, we can always achieve the desired unification because the splitting between α_R and α_{B-L} at the m_R scale is a free parameter, so it can be used to force $\alpha_R = \alpha_{B-L}$ at the scale where α_3 and α_2 unify, which leads to an almost perfect unification of the four couplings. Also, we require that unification is perturbative, i.e. the value of the common coupling constant at the GUT scale is $\alpha_G^{-1} \geq 0$. From the experimental value of $\alpha_S(m_Z)$ [100] one can easily calculate the maximal allowed value of Δb as a function of the

[6] For b_1^{SM} and b_2^{SM} we use the SM particle content plus one additional Higgs doublet.

scale, where the LR group is broken to the SM group. This is shown in fig. 6.1 for three different values of α_G^{-1}. The smallest Max(Δb) is obtained for the smallest value of m_R (and the largest value of α_G^{-1}). For α_G^{-1} in the interval $[0, 3]$ one obtains Max(Δb) in the range $[4.7, 5.7]$, i.e. we will study cases up to a Max(Δb) = 5 (see, however, the discussion below).

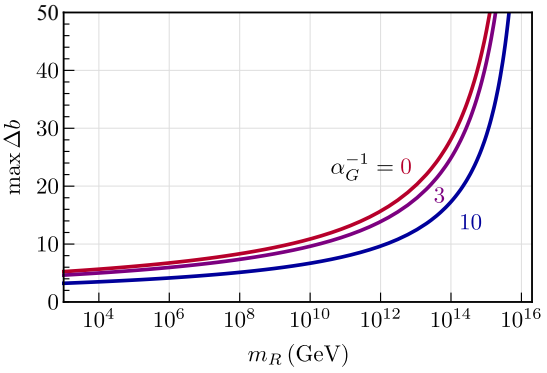

Figure 6.1: Maximum value of Δb allowed by perturbativity as function of the scale m_R in GeV. The three different lines have been calculated for three different values for the unified coupling α_G^{-1}, namely $\alpha_G^{-1} = 0, 3, 10$. An LR scale below 10 TeV (1 TeV) requires Max(Δb_3) $\lesssim$ 5.7 (5.2) if the extreme value of $\alpha_G^{-1} = 0$ is chosen and Max(Δb_3) $\lesssim$ 5.1 (4.7) for $\alpha_G^{-1} = 3$.

All together these considerations result in the following constraints on the allowed values for the Δb_i^{LR}:

$$\begin{aligned} \Delta b_2^{LR} = \Delta b_3^{LR} = \Delta b &\leq 5, \\ \Delta b_{B-L}^{LR} + \frac{3}{2}\Delta b_R^{LR} - 9 = \frac{5}{2}\Delta b &\leq \frac{25}{2}. \end{aligned} \tag{6.7}$$

Given eq. (6.7) one can calculate all allowed variants of sets of Δb_i^{LR}, guaranteed to give GCU. Two examples are shown in fig. 6.2. The figure shows the running of the inverse gauge couplings as a function of the energy scale, for an assumed value of $m_R = 10$ TeV and a SUSY scale of 1 TeV, for $(\Delta b_3^{LR}, \Delta b_2^{LR}, \Delta b_R^{LR}, \Delta b_{B-L}^{LR})$ $= (0, 0, 1, 15/2)$ (left) and $= (4, 4, 10, 4)$ (right). The example on the left has $\alpha_G^{-1} \simeq 25$ as in the MSSM, while the example on the right has $\alpha_G^{-1} \simeq 6$. Note that while both examples lead by construction to the same value of $\alpha_1(m_Z)$, they have very different values for $\alpha_R(m_R)$ and $\alpha_{B-L}(m_R)$ and thus predict different couplings for the gauge bosons W_R and Z' of the extended gauge group.

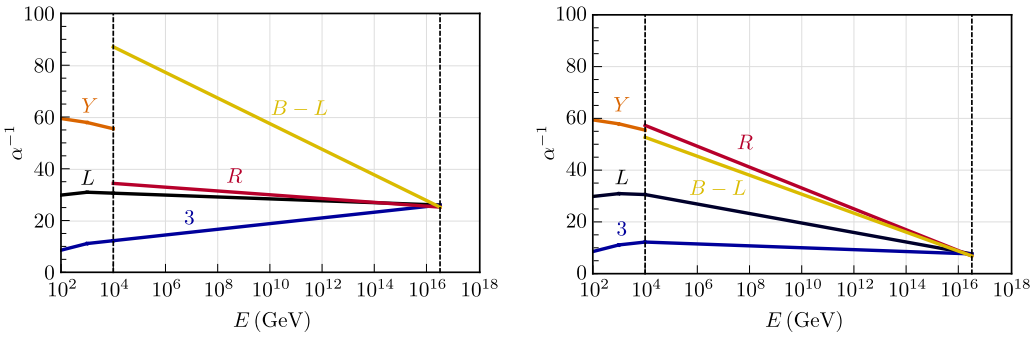

Figure 6.2: Gauge coupling unification in LR models for $m_R = 10^4$ GeV. Left panel is for $(\Delta b_3^{LR}, \Delta b_2^{LR}, \Delta b_R^{LR}, \Delta b_{B-L}^{LR}) = (0, 0, 1, 15/2)$ and right panel for $(4, 4, 10, 4)$.

With the constraints from eq. (6.7), we find that a total of 65 different variants can be constructed. However, after imposing that at least one of the fields that breaks correctly the $SU(2)_R \times U(1)_{B-L}$ symmetry to $U(1)_Y$ is present, either a $\Phi_{1,1,3,-2}$ or a $\Phi_{1,1,2,-1}$ (and/or their conjugates), the number of variants is reduced to 53. We list them in tables 6.1 and 6.2, together with one example of field configurations which give the corresponding Δb_i^{LR}.
We give only one example for each configuration in tables 6.1 and 6.2, although we went through the exercise of finding all possible configurations for the 53 variants with the field content of table B.5. In total there are 5324 anomaly-free configurations [222]. Only the variants (0,1), (0,2), (0,4) and (0,5) have only one configuration, while larger numbers of configurations are usually found for larger values of Δb_3^{LR}.

Not all the fields in table B.1 can lead to valid configurations. The fields which never give an anomaly-free configuration are: $\Phi_{8,2,2,0}$, $\Phi_{3,2,2,\frac{4}{3}}$, $\Phi_{3,3,1,-\frac{2}{3}}$, $\Phi_{3,1,3,-\frac{2}{3}}$, $\Phi_{6,3,1,\frac{2}{3}}$, $\Phi_{6,1,3,\frac{2}{3}}$ and $\Phi_{1,3,3,0}$. Also the field $\Phi_{3,2,2,-\frac{2}{3}}$ appears only exactly once in the variant (5,5) in the configuration $4\Phi_{1,2,1,1} + \Phi_{3,1,1,-\frac{2}{3}} + \Phi_{3,2,2,-\frac{2}{3}} + 4\Phi_{1,1,2,1} + 2\Phi_{1,1,1,2} + 5\Phi_{3,1,1,-\frac{2}{3}}$. Note that, the example configurations we give for the variants (1,3) and (1,4) are not the model-II and model-I discussed in [33].

Many of the 53 variants have only configurations with $\Phi_{1,1,2,-1}$ (and conjugate) for the breaking of the LR-symmetry. These variants need either the presence of $\Phi_{1,3,1,0}$ [as for example in the configuration shown for variant (2,1)] or $\Phi_{1,1,3,0}$ [see, for example (1,4)] or an additional singlet $\Phi_{1,1,1,0}$ (not shown, since no contribution

$(\Delta b, \Delta b_R)$	Sample field combination
(0, 1)	$\bar{\Phi}_{1,1,2,-1} + 2\bar{\Phi}_{1,1,1,2} + \Phi_{1,1,2,-1} + 2\Phi_{1,1,1,2}$
(0, 2)	$2\bar{\Phi}_{1,1,2,-1} + \bar{\Phi}_{1,1,1,2} + 2\Phi_{1,1,2,-1} + \Phi_{1,1,1,2}$
(0, 3)	$\bar{\Phi}_{1,1,2,-1} + \bar{\Phi}_{1,1,1,2} + \Phi_{1,1,2,-1} + \Phi_{1,1,3,0} + \Phi_{1,1,1,2}$
(0, 4)	$2\bar{\Phi}_{1,1,2,-1} + 2\Phi_{1,1,2,-1} + \Phi_{1,1,3,0}$
(0, 5)	$\bar{\Phi}_{1,1,2,-1} + \Phi_{1,1,2,-1} + 2\Phi_{1,1,3,0}$
(1, 1)	$\bar{\Phi}_{1,2,1,1} + \bar{\Phi}_{1,1,2,-1} + 2\bar{\Phi}_{1,1,1,2} + \bar{\Phi}_{3,1,1,-\frac{2}{3}} + \Phi_{1,2,1,1} + \Phi_{1,1,2,-1} + 2\Phi_{1,1,1,2} + \Phi_{3,1,1,-\frac{2}{3}}$
(1, 2)	$\bar{\Phi}_{1,1,2,-1} + 2\bar{\Phi}_{1,1,1,2} + \bar{\Phi}_{3,1,1,-\frac{2}{3}} + \Phi_{1,1,2,-1} + \Phi_{1,2,2,0} + 2\Phi_{1,1,1,2} + \Phi_{3,1,1,-\frac{2}{3}}$
(1, 3)	$2\bar{\Phi}_{1,1,2,-1} + \bar{\Phi}_{1,1,1,2} + \bar{\Phi}_{3,1,1,-\frac{2}{3}} + 2\Phi_{1,1,2,-1} + \Phi_{1,2,2,0} + \Phi_{1,1,1,2} + \Phi_{3,1,1,-\frac{2}{3}}$
(1, 4)	$\bar{\Phi}_{1,1,2,-1} + \bar{\Phi}_{1,1,1,2} + \bar{\Phi}_{3,1,1,-\frac{2}{3}} + \Phi_{1,1,2,-1} + \Phi_{1,1,3,0} + \Phi_{1,2,2,0} + \Phi_{1,1,1,2} + \Phi_{3,1,1,-\frac{2}{3}}$
(1, 5)	$2\bar{\Phi}_{1,1,2,-1} + \bar{\Phi}_{3,1,1,-\frac{2}{3}} + 2\Phi_{1,1,2,-1} + \Phi_{1,1,3,0} + \Phi_{1,2,2,0} + \Phi_{3,1,1,-\frac{2}{3}}$
(1, 6)	$\bar{\Phi}_{1,1,2,-1} + \bar{\Phi}_{3,1,1,-\frac{2}{3}} + \Phi_{1,1,2,-1} + 2\Phi_{1,1,3,0} + \Phi_{1,2,2,0} + \Phi_{3,1,1,-\frac{2}{3}}$
(2, 1)	$\bar{\Phi}_{1,1,2,-1} + 3\bar{\Phi}_{1,1,1,2} + 2\bar{\Phi}_{3,1,1,-\frac{2}{3}} + \Phi_{1,1,2,-1} + \Phi_{1,3,1,0} + 3\Phi_{1,1,1,2} + 2\Phi_{3,1,1,-\frac{2}{3}}$
(2, 2)	$2\bar{\Phi}_{1,1,2,-1} + 2\bar{\Phi}_{1,1,1,2} + 2\bar{\Phi}_{3,1,1,-\frac{2}{3}} + 2\Phi_{1,1,2,-1} + \Phi_{1,3,1,0} + 2\Phi_{1,1,1,2} + 2\Phi_{3,1,1,-\frac{2}{3}}$
(2, 3)	$\bar{\Phi}_{1,1,2,-1} + 2\bar{\Phi}_{1,1,1,2} + 2\bar{\Phi}_{3,1,1,-\frac{2}{3}} + \Phi_{1,1,2,-1} + 2\Phi_{1,2,2,0} + 2\Phi_{1,1,1,2} + 2\Phi_{3,1,1,-\frac{2}{3}}$
(2, 4)	$2\bar{\Phi}_{1,1,2,-1} + \bar{\Phi}_{1,1,1,2} + 2\bar{\Phi}_{3,1,1,-\frac{2}{3}} + 2\Phi_{1,1,2,-1} + 2\Phi_{1,2,2,0} + \Phi_{1,1,1,2} + 2\Phi_{3,1,1,-\frac{2}{3}}$
(2, 5)	$\bar{\Phi}_{1,1,2,-1} + \bar{\Phi}_{1,1,1-2} + 2\bar{\Phi}_{3,1,1,-\frac{2}{3}} + \Phi_{1,1,2,-1} + \Phi_{1,1,3,0} + 2\Phi_{1,2,2,0} + \Phi_{1,1,1,2} + 2\Phi_{3,1,1,-\frac{2}{3}}$
(2, 6)	$2\bar{\Phi}_{1,1,2,-1} + 2\bar{\Phi}_{3,1,1,-\frac{2}{3}} + 2\Phi_{1,1,2,-1} + \Phi_{1,1,3,0} + 2\Phi_{1,2,2,0} + 2\Phi_{3,1,1,-\frac{2}{3}}$
(2, 7)	$\bar{\Phi}_{1,1,2,-1} + 2\bar{\Phi}_{3,1,1,-\frac{2}{3}} + \Phi_{1,1,2,-1} + 2\Phi_{1,1,3,0} + 2\Phi_{1,2,2,0} + 2\Phi_{3,1,1,-\frac{2}{3}}$
(2, 8)	$\bar{\Phi}_{1,1,2,-1} + \bar{\Phi}_{3,1,2,\frac{1}{3}} + \Phi_{1,1,2,-1} + \Phi_{1,1,3,0} + 2\Phi_{1,2,2,0} + \Phi_{3,1,2,\frac{1}{3}}$
(3, 1)	$\bar{\Phi}_{1,2,1,1} + \bar{\Phi}_{1,1,2,-1} + 4\bar{\Phi}_{1,1,1,2} + \Phi_{1,2,1,1} + \Phi_{1,1,2,-1} + \Phi_{1,3,1,0} + \Phi_{8,1,1,0} + 4\Phi_{1,1,1,2}$
(3, 2)	$\bar{\Phi}_{1,1,2,-1} + 4\bar{\Phi}_{1,1,1,2} + \Phi_{1,1,2,-1} + \Phi_{1,3,1,0} + \Phi_{1,2,2,0} + \Phi_{8,1,1,0} + 4\Phi_{1,1,1,2}$
(3, 3)	$2\bar{\Phi}_{1,1,2,-1} + 3\bar{\Phi}_{1,1,1,2} + 2\Phi_{1,1,2,-1} + \Phi_{1,3,1,0} + \Phi_{1,2,2,0} + \Phi_{8,1,1,0} + 3\Phi_{1,1,1,2}$
(3, 4)	$\bar{\Phi}_{1,2,1,1} + \bar{\Phi}_{1,1,3,-2} + \Phi_{1,2,1,1} + \Phi_{1,3,1,0} + \Phi_{8,1,1,0} + \Phi_{1,1,3,-2}$
(3, 5)	$\bar{\Phi}_{1,1,3,-2} + \Phi_{1,3,1,0} + \Phi_{1,2,2,0} + \Phi_{8,1,1,0} + \Phi_{1,1,3,-2}$
(3, 6)	$\bar{\Phi}_{1,1,2,-1} + 2\bar{\Phi}_{1,1,1,2} + \Phi_{1,1,2,-1} + \Phi_{1,1,3,0} + 3\Phi_{1,2,2,0} + \Phi_{8,1,1,0} + 2\Phi_{1,1,1,2}$
(3, 7)	$2\bar{\Phi}_{1,1,2,-1} + \bar{\Phi}_{1,1,1-2} + 2\Phi_{1,1,2,-1} + \Phi_{1,1,3,0} + 3\Phi_{1,2,2,0} + \Phi_{8,1,1,0} + \Phi_{1,1,1,2}$
(3, 8)	$\bar{\Phi}_{1,1,2,-1} + \bar{\Phi}_{1,1,1,2} + \Phi_{1,1,2,-1} + 2\Phi_{1,1,3,0} + 3\Phi_{1,2,2,0} + \Phi_{8,1,1,0} + \Phi_{1,1,1,2}$
(3, 9)	$2\bar{\Phi}_{1,1,2,-1} + 2\Phi_{1,1,2,-1} + 2\Phi_{1,1,3,0} + 3\Phi_{1,2,2,0} + \Phi_{8,1,1,0}$
(3, 10)	$\bar{\Phi}_{1,1,2,-1} + \Phi_{1,1,2,-1} + 3\Phi_{1,1,3,0} + 3\Phi_{1,2,2,0} + \Phi_{8,1,1,0}$

Table 6.1: List of the 53 variants with a single LR scale. Shown are the 29 variants with $\Delta b_3 < 4$. In each case, the fields shown are the extra ones which are needed besides the ones contained in the MSSM representations (the 2 Higgs doublets are assumed to come from one bi-doublet $\Phi_{1,2,2,0}$). The $\Delta b_3, \Delta b_2, \Delta b_R, \Delta b_{B-L}$ values can be obtained from the first column through eqs (6.7).

$(\Delta b, \Delta b_R)$	Sample field combination
(4, 1)	$\bar{\Phi}_{1,1,2,-1} + 5\bar{\Phi}_{1,1,1,2} + \bar{\Phi}_{3,1,1,-\frac{2}{3}} + \Phi_{1,1,2,-1} + 2\Phi_{1,3,1,0} + \Phi_{8,1,1,0} + 5\Phi_{1,1,1,2} + \Phi_{3,1,1,-\frac{2}{3}}$
(4, 2)	$2\bar{\Phi}_{1,1,2,-1} + 4\bar{\Phi}_{1,1,1,2} + \bar{\Phi}_{3,1,1,-\frac{2}{3}} + 2\Phi_{1,1,2,-1} + 2\Phi_{1,3,1,0} + \Phi_{8,1,1,0} + 4\Phi_{1,1,1,2} + \Phi_{3,1,1,-\frac{2}{3}}$
(4, 3)	$\bar{\Phi}_{1,1,2,-1} + 4\bar{\Phi}_{1,1,1,2} + \bar{\Phi}_{3,1,1,-\frac{2}{3}} + \Phi_{1,1,2,-1} + \Phi_{1,3,1,0} + 2\Phi_{1,2,2,0} + \Phi_{8,1,1,0} + 4\Phi_{1,1,1,2} + \Phi_{3,1,1,-\frac{2}{3}}$
(4, 4)	$\bar{\Phi}_{1,1,1,2} + \bar{\Phi}_{3,1,1,-\frac{2}{3}} + \bar{\Phi}_{1,1,3,-2} + 2\Phi_{1,3,1,0} + \Phi_{8,1,1,0} + \Phi_{1,1,1,2} + \Phi_{3,1,1,-\frac{2}{3}} + \Phi_{1,1,3,-2}$
(4, 5)	$\bar{\Phi}_{1,1,2,-1} + \bar{\Phi}_{3,1,1,-\frac{2}{3}} + \bar{\Phi}_{1,1,3,-2} + \Phi_{1,1,2,-1} + 2\Phi_{1,3,1,0} + \Phi_{8,1,1,0} + \Phi_{3,1,1,-\frac{2}{3}} + \Phi_{1,1,3,-2}$
(4, 6)	$\bar{\Phi}_{3,1,1,-\frac{2}{3}} + \bar{\Phi}_{1,1,3,-2} + \Phi_{1,3,1,0} + 2\Phi_{1,2,2,0} + \Phi_{8,1,1,0} + \Phi_{3,1,1,-\frac{2}{3}} + \Phi_{1,1,3,-2}$
(4, 7)	$\bar{\Phi}_{1,1,2,-1} + 2\bar{\Phi}_{1,1,1,2} + \bar{\Phi}_{3,1,1,-\frac{2}{3}} + \Phi_{1,1,2,-1} + \Phi_{1,1,3,0} + 4\Phi_{1,2,2,0} + \Phi_{8,1,1,0} + 2\Phi_{1,1,1,2} + \Phi_{3,1,1,-\frac{2}{3}}$
(4, 8)	$2\bar{\Phi}_{1,1,2,-1} + \bar{\Phi}_{1,1,1,2} + \bar{\Phi}_{3,1,1,-\frac{2}{3}} + 2\Phi_{1,1,2,-1} + \Phi_{1,1,3,0} + 4\Phi_{1,2,2,0} + \Phi_{8,1,1,0} + \Phi_{1,1,1,2} + \Phi_{3,1,1,-\frac{2}{3}}$
(4, 9)	$\bar{\Phi}_{1,1,2,-1} + \bar{\Phi}_{1,1,1,2} + \bar{\Phi}_{3,1,1,-\frac{2}{3}} + \Phi_{1,1,2,-1} + 2\Phi_{1,1,3,0} + 4\Phi_{1,2,2,0} + \Phi_{8,1,1,0} + \Phi_{1,1,1,2} + \Phi_{3,1,1,-\frac{2}{3}}$
(4, 10)	$2\bar{\Phi}_{1,1,2,-1} + \bar{\Phi}_{3,1,1,-\frac{2}{3}} + 2\Phi_{1,1,2,-1} + 2\Phi_{1,1,3,0} + 4\Phi_{1,2,2,0} + \Phi_{8,1,1,0} + \Phi_{3,1,1,-\frac{2}{3}}$
(4, 11)	$\bar{\Phi}_{1,1,2,-1} + \bar{\Phi}_{3,1,1,-\frac{2}{3}} + \Phi_{1,1,2,-1} + 3\Phi_{1,1,3,0} + 4\Phi_{1,2,2,0} + \Phi_{8,1,1,0} + \Phi_{3,1,1,-\frac{2}{3}}$
(5, 1)	$\bar{\Phi}_{1,2,1,1} + \bar{\Phi}_{1,1,2,-1} + 5\bar{\Phi}_{1,1,1,2} + 2\bar{\Phi}_{3,1,1,-\frac{2}{3}} + \Phi_{1,2,1,1} + \Phi_{1,1,2,-1} + 2\Phi_{1,3,1,0} + \Phi_{8,1,1,0}$ $+5\Phi_{1,1,1,2} + 2\Phi_{3,1,1,-\frac{2}{3}}$
(5, 2)	$\bar{\Phi}_{1,1,2,-1} + 5\bar{\Phi}_{1,1,1,2} + 2\bar{\Phi}_{3,1,1,-\frac{2}{3}} + \Phi_{1,1,2,-1} + 2\Phi_{1,3,1,0} + \Phi_{1,2,2,0} + \Phi_{8,1,1,0} + 5\Phi_{1,1,1,2}$ $+2\Phi_{3,1,1,-\frac{2}{3}}$
(5, 3)	$2\bar{\Phi}_{1,1,2,-1} + 4\bar{\Phi}_{1,1,1,2} + 2\bar{\Phi}_{3,1,1,-\frac{2}{3}} + 2\Phi_{1,1,2,-1} + 2\Phi_{1,3,1,0} + \Phi_{1,2,2,0} + \Phi_{8,1,1,0} + 4\Phi_{1,1,1,2}$ $+2\Phi_{3,1,1,-\frac{2}{3}}$
(5, 4)	$\bar{\Phi}_{1,2,1,1} + \bar{\Phi}_{1,1,1,2} + 2\bar{\Phi}_{3,1,1,-\frac{2}{3}} + \bar{\Phi}_{1,1,3,-2} + \Phi_{1,2,1,1} + 2\Phi_{1,3,1,0} + \Phi_{8,1,1,0} + \Phi_{1,1,1,2} + 2\Phi_{3,1,1,-\frac{2}{3}}$ $+\Phi_{1,1,3,-2}$
(5, 5)	$\bar{\Phi}_{1,1,1,2} + 2\bar{\Phi}_{3,1,1,-\frac{2}{3}} + \bar{\Phi}_{1,1,3,-2} + 2\Phi_{1,3,1,0} + \Phi_{1,2,2,0} + \Phi_{8,1,1,0} + \Phi_{1,1,1,2} + 2\Phi_{3,1,1,-\frac{2}{3}}$ $+\Phi_{1,1,3,-2}$
(5, 6)	$\bar{\Phi}_{1,1,2,-1} + 2\bar{\Phi}_{3,1,1,-\frac{2}{3}} + \bar{\Phi}_{1,1,3,-2} + \Phi_{1,1,2,-1} + 2\Phi_{1,3,1,0} + \Phi_{1,2,2,0} + \Phi_{8,1,1,0} + 2\Phi_{3,1,1,-\frac{2}{3}}$ $+\Phi_{1,1,3,-2}$
(5, 7)	$2\bar{\Phi}_{3,1,1,-\frac{2}{3}} + \bar{\Phi}_{1,1,3,-2} + \Phi_{1,3,1,0} + 3\Phi_{1,2,2,0} + \Phi_{8,1,1,0} + 2\Phi_{3,1,1,-\frac{2}{3}} + \Phi_{1,1,3,-2}$
(5, 8)	$\bar{\Phi}_{3,1,2,\frac{1}{3}} + \bar{\Phi}_{1,1,3,-2} + 2\Phi_{1,3,1,0} + \Phi_{1,2,2,0} + \Phi_{8,1,1,0} + \Phi_{3,1,2,\frac{1}{3}} + \Phi_{1,1,3,-2}$
(5, 9)	$2\bar{\Phi}_{1,1,2,-1} + \bar{\Phi}_{1,1,1,2} + 2\bar{\Phi}_{3,1,1,-\frac{2}{3}} + 2\Phi_{1,1,2,-1} + \Phi_{1,1,3,0} + 5\Phi_{1,2,2,0} + \Phi_{8,1,1,0} + \Phi_{1,1,1,2}$ $+2\Phi_{3,1,1,-\frac{2}{3}}$
(5, 10)	$\bar{\Phi}_{1,1,2,-1} + \bar{\Phi}_{1,1,1,2} + 2\bar{\Phi}_{3,1,1,-\frac{2}{3}} + \Phi_{1,1,2,-1} + 2\Phi_{1,1,3,0} + 5\Phi_{1,2,2,0} + \Phi_{8,1,1,0} + \Phi_{1,1,1,2}$ $+2\Phi_{3,1,1,-\frac{2}{3}}$
(5, 11)	$2\bar{\Phi}_{1,1,2,-1} + 2\bar{\Phi}_{3,1,1,-\frac{2}{3}} + 2\Phi_{1,1,2,-1} + 2\Phi_{1,1,3,0} + 5\Phi_{1,2,2,0} + \Phi_{8,1,1,0} + 2\Phi_{3,1,1,-\frac{2}{3}}$
(5, 12)	$\bar{\Phi}_{1,1,2,-1} + 2\bar{\Phi}_{3,1,1,-\frac{2}{3}} + \Phi_{1,1,2,-1} + 3\Phi_{1,1,3,0} + 5\Phi_{1,2,2,0} + \Phi_{8,1,1,0} + 2\Phi_{3,1,1,-\frac{2}{3}}$
(5, 13)	$\bar{\Phi}_{1,1,2,-1} + \bar{\Phi}_{3,1,2,\frac{1}{3}} + \Phi_{1,1,2,-1} + 2\Phi_{1,1,3,0} + 5\Phi_{1,2,2,0} + \Phi_{8,1,1,0} + \Phi_{3,1,2,\frac{1}{3}}$

Table 6.2: List of the 53 variants with a single LR scale. Shown are the remaining 24 variants, with $\Delta b_3 \geq 4$.

to any Δb_i^{LR}), to generate seesaw neutrino masses. Using the $\Phi_{1,1,1,0}$ one could construct either an inverse [223] or a linear [119, 224] seesaw mechanism, while with $\Phi_{1,3,1,0}$ a seesaw type-III [134] is a possibility and, finally a $\Phi_{1,1,3,0}$ allows for an inverse seesaw type-III [33]. The first example where a valid configuration with $\Phi_{1,1,3,-2}$ appears is the variant (3,4). The simplest configuration is $\Phi_{1,2,1,1} + \Phi_{1,3,1,0} + \Phi_{8,1,1,0} + \Phi_{1,1,3,-2} + \bar{\Phi}_{1,2,1,1} + \bar{\Phi}_{1,1,3,-2}$ (not the example given in table 6.1). The vev of the $\Phi_{1,1,3,-2}$ does not only break the LR symmetry, it can also generate a Majorana mass term for the right-handed neutrino fields, i.e. configurations with $\Phi_{1,1,3,-2}$ can generate a seesaw type-I, in principle. Finally, the simplest possibility with a valid configuration including $\Phi_{1,3,1,-2}$ is found in variant (4,1) with $\Phi_{1,1,2,-1} + \Phi_{8,1,1,0} + \Phi_{1,1,1,2} + \Phi_{3,1,1,\frac{4}{3}} + \Phi_{1,3,1,-2} + \bar{\Phi}_{1,1,2,-1} + \bar{\Phi}_{1,1,1,2} + \bar{\Phi}_{3,1,1,\frac{4}{3}} + \bar{\Phi}_{1,3,1,-2}$. The presence of $\Phi_{1,3,1,-2}$ allows to generate a seesaw type-II for the neutrinos.

As mentioned in the introduction, it is not possible to construct a sliding scale model in which the LR symmetry is broken by two pairs of triplets: $\Phi_{1,3,1,-2} + \bar{\Phi}_{1,3,1,-2} + \Phi_{1,1,3,-2} + \bar{\Phi}_{1,1,3,-2}$. The sum of the Δb's for these fields adds up to $(\Delta b_3^{LR}, b_L^{LR}, \Delta b_R^{LR}, \Delta b_{B-L}^{LR}) = (0, 4, 4, 18)$. This leaves only the possibilities $(4, 4)$, $(5, 4)$, $(5, 5)$, etc. from table 6.2. However, the largest Δb_{B-L}^{LR} of these models is $(5, 4)$ which allows for $\Delta b_{B-L}^{LR} = 31/2$, smaller than the required 18. This observation is consistent with the analysis done in [215], where the authors have shown that a supersymmetric LR-symmetric model, where the LR symmetry is broken by two pairs of triplets, requires a minimal LR scale of at least 10^9 GeV (and, actually, a much larger scale in minimal renormalizable models, if GUT scale thresholds are small).

A few final comments on the variants with $\Delta b_2^{LR} = \Delta b_3^{LR} = 0$. Strictly speaking, none of these variants is guaranteed to give a valid model in the sense defined in sub-section 6.1.3, since they contain only one $\Phi_{1,2,2,0} \to (H_u, H_d)$ and no vector-like quarks (no $\Phi_{3,1,1,\frac{4}{3}}$ or $\Phi_{3,1,1,-\frac{2}{3}}$). With such a minimal configuration the CKM matrix is trivial at the energy scale where the LR symmetry is broken. We nevertheless list these variants, since in principle a CKM matrix for quarks consistent with experimental data could be generated at 1-loop level from flavor violating soft terms, as discussed in [225].

Before we end this section let us mention that variants with $\Delta b_3^{LR} = 5$ will not

be testable at LHC by measurements of soft SUSY breaking mass terms ("invariants"). This is discussed below in section 6.1.7.

6.1.5 Model class-II: Additional intermediate Pati-Salam scale

In the second class of supersymmetric $SO(10)$ inspired models we consider, $SO(10)$ is broken first to the Pati-Salam (PS) group. The complete breaking chain thus is:

$$\begin{aligned} SO(10) &\rightarrow SU(4) \times SU(2)_L \times SU(2)_R \\ &\rightarrow SU(3)_c \times SU(2)_L \times SU(2)_R \times U(1)_{B-L} \rightarrow \text{ MSSM.} \end{aligned} \tag{6.8}$$

The representations available from the decomposition of $SO(10)$ multiplets up to **126** are listed in table B.2 in the appendix, together with their possible $SO(10)$ origin. Breaking $SO(10)$ to the PS group requires that $\Psi_{1,1,1}$ from the **54** takes a vev. The subsequent breaking of the PS group to the LR group requires that the singlet in $\Psi_{15,1,1}$, originally from the **45** of $SO(10)$, acquires a vev. And, finally, as before in the LR-class, the breaking of LR to $SU(3)_c \times SU(2)_L \times U(1)_Y$ can be either done via $\Phi_{1,1,2,-1}$ or $\Phi_{1,1,3,-2}$ (and/or conjugates).

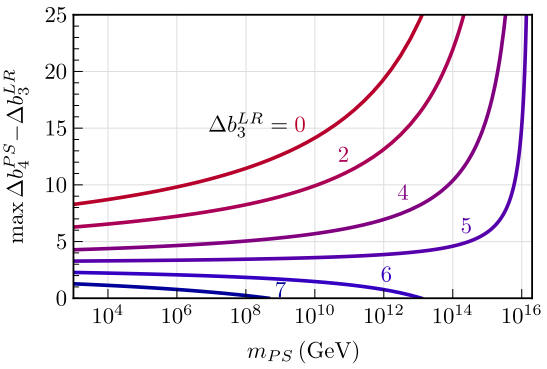

Figure 6.3: Maximum value of $\Delta b_4^{PS} - \Delta b_3^{LR}$ allowed by perturbativity as function of the scale m_{PS} in GeV. The different lines have been calculated for six different values of Δb_3^{LR}. The plot assumes that $m_R = 1$ TeV. The line near the bottom corresponds to $\Delta b_3^{LR} = 7$.

The additional b_i coefficients for the regime $[m_{PS}, m_{GUT}]$ are given by:

$$(b_4^{PS}, b_2^{PS}, b_R^{PS}) = (-6, 1, 1) + (\Delta b_4^{PS}, \Delta b_2^{PS}, \Delta b_R^{PS}), \tag{6.9}$$

where, as before, the Δb_i^{PS} include contributions from superfields not part of the MSSM field content.

In this class of models, the unification scale is independent of the LR one if the following condition is satisfied:

$$0 = \left(\Delta b_3^{LR} - \Delta b_2^{LR},\quad \tfrac{3}{5}\Delta b_R^{LR} + \tfrac{2}{5}\Delta b_{B-L}^{LR} - \Delta b_2^{LR} - \tfrac{18}{5}\right) \cdot \begin{pmatrix} 2 & 3 \\ -5 & 0 \end{pmatrix} \cdot \begin{pmatrix} \Delta b_4^{PS} - \Delta b_2^{PS} - 3 \\ \Delta b_R^{PS} - \Delta b_2^{PS} - 12 \end{pmatrix}. \tag{6.10}$$

It is worth noting that requiring also that m_{PS} is independent of the LR scale would lead to the conditions in eq. (6.7), which are the sliding conditions for LR models. We can see that this must be so in the following way: for some starting values at m_{PS} of the three gauge couplings, the scales m_{PS} and m_G can be adjusted such that the two splittings between the three gauge couplings are reduced to zero at m_G. This fixes these scales, which must not change even if m_R is varied. As such $\alpha_3^{-1}(m_{PS}) - \alpha_2^{-1}(m_{PS})$ and $\alpha_3^{-1}(m_{PS}) - \alpha_R^{-1}(m_{PS})$ are also fixed and they can be determined by running the MSSM up to m_{PS}. The situation is therefore equal to the one that lead to the equalities in eq. (6.7), namely the splittings between the gauge couplings at some fixed scale must be independent of m_R.

Since there are now two unknown scales involved in the problem, the maximum Δb_i^X allowed by perturbativity in one regime do not only depend on the new scale X, but also on the Δb_i^Y in the other regime as well. As an example, in fig. 6.3 we show the $\mathrm{Max}(\Delta b_4^{PS})$ allowed by $\alpha_G^{-1} \geq 0$ for different values of Δb_3^{LR} and for the choice $m_R = 1$ TeV and and $m_G = 10^{16}$ GeV. The dependence of $\mathrm{Max}(\Delta b_4^{PS})$ on m_R is rather weak, as long as m_R does not approach the GUT scale.
If we impose the limits $m_R = 10^3$ GeV, $m_{PS} \leq 10^6$ GeV and take $m_G = 10^{16}$ GeV,

the bounds for the different $\Delta b's$ can be written as: [7]

$$\Delta b_2^{PS} + \frac{3}{10}\Delta b_2^{LR} < 7.2, \tag{6.11}$$

$$\Delta b_4^{PS} + \frac{3}{10}\Delta b_3^{LR} < 10, \tag{6.12}$$

$$\frac{2}{5}\Delta b_4^{PS} + \frac{3}{5}\Delta b_R^{PS} + \frac{3}{10}\left(\frac{2}{5}\Delta b_{B-L}^{LR} + \frac{3}{5}\Delta b_R^{LR}\right) < 17. \tag{6.13}$$

However, as fig. (6.3) shows, $\mathrm{Max}(\Delta b_4^{PS})$ is a rather strong function of the choice of Δb_3^{LR}. Note, that if m_{PS} is low, say below 10^{10} GeV, larger Δb_3^{LR} are possible, up to $\Delta b_3^{LR} = 7$, see fig. (6.3). The large values of $\mathrm{Max}(\Delta b^{LR})$ and $\mathrm{Max}(\Delta b^{PS})$ allow, in principle, a huge number of variants to be constructed in class-II. This is demonstrated in fig. (6.4), where we show the number of variants for an assumed $m_R \sim 1$ TeV as a function of the scale m_{PS}. Up to $m_{PS} = 10^{15}$ GeV the list is exhaustive. For larger values of m_{PS} we have only scanned a finite (though large) set of possible variants. Note, that these are variants, not configurations. As in the case of class-I practically any variant can be made by several possible anomaly-free configurations. The exhaustive list of variants ($m_{PS} = 10^{15}$ GeV) contains a total of 105909 possibilities and can be found in [222].

With such a huge number of possible variants, we can discuss only some general features here. First of all, within the exhaustive set up to $m_{PS} = 10^{15}$ GeV, there are a total of 1570 different sets of Δb_i^{LR}, each of which can be completed by more than one set of Δb_i^{PS}. Variants with the same set of Δb_i^{LR} but different completion of Δb_i^{PS} have, of course, the same configuration in the LR-regime, but come with a different value for m_{PS} for fixed m_R. Thus, they have in general different values for α_{B-L} and α_R at the LR scale and, see next section, different values of the invariants. For example, for the smallest values of Δb_i^{LR}, that are possible in principle $[\Delta b_i^{LR} = (0, 0, 1, 3/2)]$, there are 342 different completing sets of Δb_i^{PS}.

The very simplest set of Δb_i^{LR} possible, $\Delta b_i^{LR} = (0, 0, 1, 3/2)$, corresponds to the configuration $\Phi_{1,1,2,-1} + \bar{\Phi}_{1,1,2,-1}$. These fields are necessary to break $SU(2)_R \times$

[7] In fact, the bounds shown here exclude a few variants with $m_{PS} < 10^6$ GeV. This is because of the following: while in most cases the most conservative assumption is to assume that m_{PS} is as large as possible ($= 10^6$ GeV; this leads to a smaller running in the PS regime) in deriving these bounds, there are some cases where this is not true. This is a minor complication which nonetheless was taken into account in our computations.

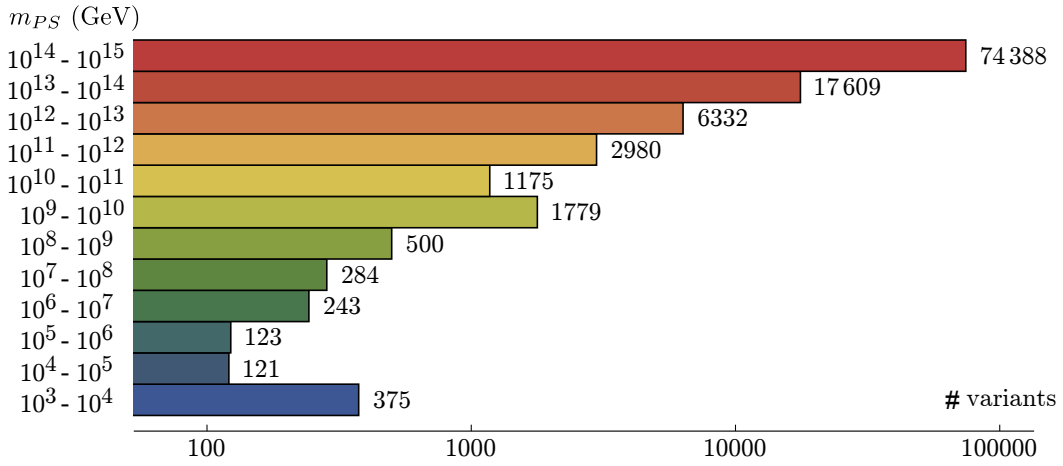

Figure 6.4: The number of possible variants in model class-II, assuming m_R is of order $m_R \simeq 1$ TeV as a function of m_{PS}. Up to $m_{PS} = 10^{15}$ GeV the list is exhaustive. For larger values of m_{PS} we have only scanned a finite (though large) set of possible variants.

$U(1)_{B-L} \to U(1)_Y$. Their presence in the LR regime requires that in the PS-regime we have at least one set of copies of $\Psi_{4,1,2} + \bar{\Psi}_{4,1,2}$. In addition, for breaking the PS group to the LR group, we need at least one copy of $\Psi_{15,1,1}$. However, the set of $\Psi_{4,1,2} + \bar{\Psi}_{4,1,2} + \Psi_{15,1,1}$ is not sufficient to generate a sliding scale mechanism and the simplest configuration that can do so, consistent with $\Delta b_i^{LR} = (0, 0, 1, 3/2)$, is $3\Psi_{1,2,2} + 4\Psi_{1,1,3} + \Psi_{4,1,2} + \bar{\Psi}_{4,1,2} + \Psi_{15,1,1}$, leading to $\Delta b_i^{PS} = (6, 3, 15)$ and a very low possible value of m_{PS} of $m_{PS} = 8.2$ TeV for $m_R = 1$ TeV (see, however, the discussion on leptoquarks below). The next possible completion for $\Phi_{1,1,2,-1} + \bar{\Phi}_{1,1,2,-1}$ is $3\Psi_{1,2,2} + 5\Psi_{1,1,3} + \Psi_{4,1,2} + \bar{\Psi}_{4,1,2} + \Psi_{15,1,1}$, with $\Delta b_i^{PS} = (6, 3, 17)$ and $m_{PS} = 1.3 \times 10^8$ GeV (for $m_R = 1$ TeV), etc.

As noted already in section 6.1.4, one copy of $\Phi_{1,2,2,0}$ is not sufficient to produce a realistic CKM matrix at tree-level. Thus, the minimal configuration of $\Phi_{1,1,2,-1} + \bar{\Phi}_{1,1,2,-1}$ relies on the possibility of generating all of the departure of the CKM matrix from unity by flavor violating soft masses [225]. There are at least two possibilities to generate a non-trivial CKM at tree-level, either by adding (a) another $\Phi_{1,2,2,0}$ plus (at least) one copy of $\Phi_{1,1,3,0}$ or via (b) one copy of "vector-like quarks" $\Phi_{3,1,1,\frac{4}{3}}$ or $\Phi_{3,1,1,-\frac{2}{3}}$. Consider the configuration $\Phi_{1,1,2,-1} + \bar{\Phi}_{1,1,2,-1} + \Phi_{1,2,2,0} + \Phi_{1,1,3,0}$ first. It leads to $\Delta b_i^{LR} = (0, 1, 4, 3/2)$. Since $\Phi_{1,2,2,0}$ and $\Phi_{1,1,3,0}$ must come from

$\Psi_{1,2,2}$ (or $\Psi_{15,2,2}$) and $\Psi_{1,1,3}$, respectively, the simplest completion for this set of Δb_i^{LR} is again $3\Psi_{1,2,2}+4\Psi_{1,1,3}+\Psi_{4,1,2}+\bar{\Psi}_{4,1,2}+\Psi_{15,1,1}$, leading to $\Delta b_i^{PS}=(6,3,15)$ and value of m_{PS} of, in this case, $m_{PS}=5.4$ TeV for $m_R=1$ TeV. Again, many completions with different Δb_i^{PS} exist for this set of Δb_i^{LR}.

The other possibility for generating CKM at tree-level, adding for example a pair of $\Phi_{3,1,1,-\frac{2}{3}}+\bar{\Phi}_{3,1,1,-\frac{2}{3}}$, has $\Delta b_i^{LR}=(1,0,1,5/2)$ and its simplest PS-completion is $4\Psi_{1,2,2}+4\Psi_{1,1,3}+\Psi_{4,1,2}+\bar{\Psi}_{4,1,2}+\Psi_{6,1,1}+\Psi_{15,1,1}$, with $\Delta b_i^{PS}=(7,4,16)$ and a $m_{PS}=4.6\times10^6$ TeV for $m_R=1$ TeV. Also in this case one can find sets with very low values of m_{PS}. For example, adding a $\Phi_{1,2,2,0}$ to this LR-configuration (for a $\Delta b_i^{LR}=(1,1,2,5/2)$), one finds that with the same Δb_i^{PS} now a value of m_{PS} as low as $m_{PS}=8.3$ TeV for $m_R=1$ TeV is possible.

We note in passing that the original PS-class model of [33] in our notation corresponds to $\Delta b_i^{LR}=(1,2,10,4)$ and $\Phi_{1,1,2,-1}+\bar{\Phi}_{1,1,2,-1}+\Phi_{1,2,1,1}+\bar{\Phi}_{1,2,1,1}+\Phi_{1,2,2,0}+4\Phi_{1,1,3,0}+\Phi_{3,1,1,-\frac{2}{3}}+\bar{\Phi}_{3,1,1,-\frac{2}{3}}$, completed by $\Delta b_i^{PS}=(9,5,13)$ with $\Psi_{4,1,2}+\bar{\Psi}_{4,1,2}+\Psi_{4,2,1}+\Psi_{4,2,1}+\Psi_{1,2,2}+4\Psi_{1,1,3}+\Psi_{6,1,1}+\Psi_{15,1,1}$. The lowest possible m_{PS} for a $m_R=1$ TeV is $m_{PS}=2.4\times10^8$ GeV. Obviously this example is not the simplest construction in class-II. We also mention that while for the β-coefficients it does not make any difference, the superfield $\Phi_{1,1,3,0}$ can be either interpreted as "Higgs" or as "matter". In the original construction [33] this "arbitrariness" was used to assign the 4 copies of $\Phi_{1,1,3,0}$ to one copy of $\Omega^c=\Phi_{1,1,3,0}$, [8] i.e."Higgs" and three copies of $\Sigma^c=\Phi_{1,1,3,0}$, i.e. "matter". In this way Ω^c can be used to generate the CKM matrix at tree-level (together with the extra bi-doublet $\Phi_{1,2,2,0}$), while the Σ^c can be used to generate an inverse seesaw type-III for neutrino masses.

As fig. (6.4) shows, there are more than 600 variant in which m_{PS} can, in principle, be lower than $m_{PS}=10^3$ TeV. Such low PS scales, however, are already constrained by searches for rare decays, such as $B_s\to\mu^+\mu^-$. This is because the $\Psi_{15,1,1}$, which must be present in all our constructions for the breaking of the PS group, contains two leptoquark states. We will not study in detail leptoquark phenomenology [226] here, but mention that in the recent paper [227] absolute lower bounds on leptoquarks within PS models of the order of $m_{PS}\simeq40$ TeV have been

[8] The original paper [33] called this field Ω. However, in our notation it would be natural to call $\Omega=\Phi_{1,3,1,0}$.

derived. There are 426 variants for which we find m_{PS} lower than this bound, if we put m_R to 1 TeV. Due to the sliding scale nature of our construction this, of course, does not mean that these models are ruled out by the lower limit found in [227]. Instead, for these models one can calculate a lower limit on m_R from the requirement that $m_{PS} = 40$ TeV. Depending on the model, lower limits on m_R between $m_R = [1.3, 27.7]$ TeV are found for the 426 variants from this requirement.

Two example solutions can be seen in fig. 6.5. We have chosen one example with a very low m_{PS} (left) and one with an intermediate m_{PS} (right). Note, that different from the class-I models, in the class-II models the GUT scale is no longer fixed to the MSSM value $m_G \approx 2 \times 10^{16}$ GeV. Our samples are restricted to variants which have m_G in the interval $[10^{16}, 10^{18}]$ GeV.

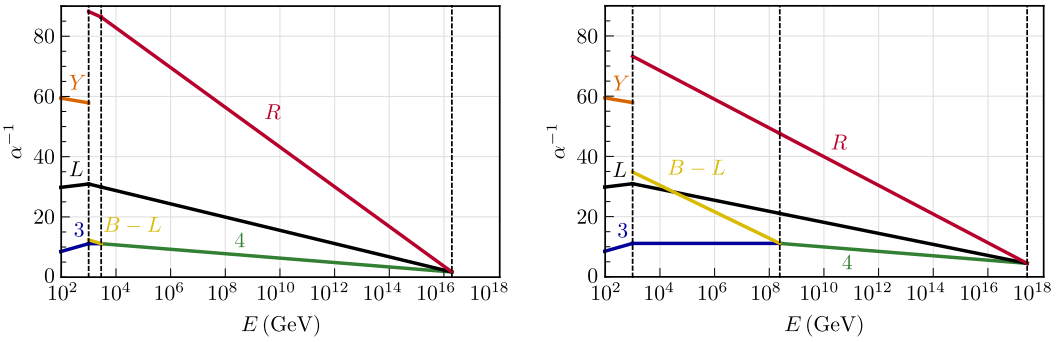

Figure 6.5: Gauge coupling unification for PS models with $m_R = 10^3$ GeV. In the plot to the left $(\Delta b_3^{LR}, \Delta b_L^{LR}, \Delta b_R^{LR}, \Delta b_{B-L}^{LR}, \Delta b_4^{PS}, \Delta b_L^{PS}, \Delta b_R^{PS}) = (3, 5, 10, 3/2, 8, 5, 17)$, while the plot to the right corresponds to $\Delta b's = (3, 4, 12, 6, 8, 4, 12)$.

6.1.6 Models with an $U(1)_R \times U(1)_{B-L}$ intermediate scale

Finally, we consider models where there is an additional intermediate symmetry $U(1)_R \times U(1)_{B-L}$ that follows the stage $SU(2)_R \times U(1)_{B-L}$. The field content relevant to this model is specified in table B.3 of the appendix. In this case the original $SO(10)$ is broken down to the MSSM in three steps,

$$\begin{aligned} SO(10) &\rightarrow SU(3)_c \times SU(2)_L \times SU(2)_R \times U(1)_{B-L} \\ &\rightarrow SU(3)_c \times SU(2)_L \times U(1)_R \times U(1)_{B-L} \rightarrow \text{MSSM}. \end{aligned} \tag{6.14}$$

The first step is achieved in the same way as in class-I models. The subsequent breaking $SU(2)_R \times U(1)_{B-L} \to U(1)_R \times U(1)_{B-L}$ is triggered by $\Phi_5 = \Phi_{1,1,3,0}$ and the last one requires $\Phi_4^{'} = \Phi'_{1,1,\frac{1}{2},-1}$, $\Phi_{20}^{'} = \Phi'_{1,1,1,-2}$ or their conjugates.

In theories with more that one $U(1)$ gauge factor, the one loop evolution of the gauge couplings and soft-SUSY-breaking terms are affected by the extra kinetic mixing terms. The couplings are defined by the matrix

$$G = \begin{pmatrix} g_{RR} & g_{RX} \\ g_{XR} & g_{XX} \end{pmatrix} \tag{6.15}$$

and $A(t) = (GG^T)/(4\pi) = (A^{-1}(t_0) - \gamma(t - t_0))^{-1}$, where $t = \frac{1}{2\pi}\log(\frac{\mu}{\mu_0})$ [33]. Here, μ and μ_0 stand for the energy scale and its normalization point and A is the generalization of α to matrix form. The matrix of anomalous dimension, γ, is defined by the charges of each chiral superfield f under $U(1)_R$ and $U(1)_{B-L}$:

$$\gamma = \sum_f Q_f Q_f^T, \tag{6.16}$$

where Q_f denotes a column vector of those charges. Taking the MSSM's field content we find

$$\gamma = \begin{pmatrix} 7 & 0 \\ 0 & 6 \end{pmatrix}. \tag{6.17}$$

To ensure the canonical normalization of the $B - L$ charge within the $SO(10)$ framework, γ should be normalized as $\gamma^{can} = N\gamma^{phys}N$, where $N = \mathrm{diag}(1, \sqrt{3/8})$.

Then, the additional β coefficients for the running step $[m_{B-L}, m_R]$ are given by,

$$\begin{aligned}(b_3^{B-L}, b_2^{B-L}, \gamma_{RR}^{B-L}, \gamma_{XR}^{B-L}, \gamma_{XX}^{B-L}) = (-3, 1, 6, 0, 7) + \\ (\Delta b_3^{B-L}, \Delta b_2^{B-L}, \Delta\gamma_{RR}, \Delta\gamma_{XR}, \Delta\gamma_{XX}).\end{aligned} \tag{6.18}$$

As in the previous PS case, we consider $m_{B-L} = 10^3$ GeV, $m_G \geq 10^{16}$ GeV and $m_R \leq 10^6$ GeV. Taking into account the matching condition:

$$p_Y^T \cdot A^{-1}(m_{B-L}) \cdot p_Y = \alpha_1^{-1}(m_{B-L}) \tag{6.19}$$

and $p_Y^T = (\sqrt{\frac{3}{5}}, \sqrt{\frac{2}{5}})$, the bounds on the Δb are,

$$\begin{aligned} \Delta b_2^{LR} + \frac{3}{10}\Delta b_2^{B-L} &< 7.1, \\ \Delta b_3^{LR} + \frac{3}{10}\Delta b_3^{B-L} &< 6.9, \\ \frac{3}{5}\Delta b_R^{LR} + \frac{2}{5}\Delta b_{B-L}^{LR} + \frac{3}{10} p_Y^T \cdot \Delta\gamma \cdot p_Y &< 10.8. \end{aligned} \tag{6.20}$$

Even with this restriction in the scales we found 15610 solutions, more than in the PS case, due to the fact that there are more $\Delta b^{'}s$ that can be varied to obtain solutions. The qualitative features of the running of the gauge couplings are shown for two examples in fig. (6.6). In those two examples the $(\Delta b_3^{LR}, \Delta b_L^{LR}, \Delta b_R^{LR}, \Delta b_{B-L}^{LR},$ $, \Delta b_3^{B-L}, \Delta b_L^{B-L}, \Delta\gamma_{RR}, \Delta\gamma_{XR}, \Delta\gamma_{XX})$ have been chosen as $(0, 1, 3, 3, 0, 0, 1/2,$ $, -\sqrt{3/8}, 3/4)$ (left) and $(2, 2, 4, 8, 2, 2, 1/2, -\sqrt{3/8}, 11/4)$ (right). The former corresponds to the minimal configuration $\Phi'_{1,1,1/2,-1} + \bar{\Phi}'_{1,1,1/2,-1}$ in the lower regime and $\Phi_{1,1,2,-1} + \bar{\Phi}_{1,1,2,-1} + \Phi_{1,1,3,0} + \Phi_{1,2,1,1} + \bar{\Phi}_{1,2,1,1}$ in the higher (LR-symmetric regime). The latter corresponds to $\Phi'_{1,1,1/2,-1} + \bar{\Phi}'_{1,1,1/2,-1} + \Phi'_{1,3,0,0} + 2\Phi'_{3,1,1,-2/3} + 2\bar{\Phi}'_{3,1,1,-2/3}$ and $2(\Phi_{1,1,2,-1} + \bar{\Phi}_{1,1,2,-1}) + \Phi_{1,1,3,0} + \Phi_{1,3,1,0} + \Phi_{1,1,1,2} + \bar{\Phi}_{1,1,1,2} + 2(\Phi_{3,1,1,-2/3} + \bar{\Phi}_{3,1,1,-2/3})$, respectively.

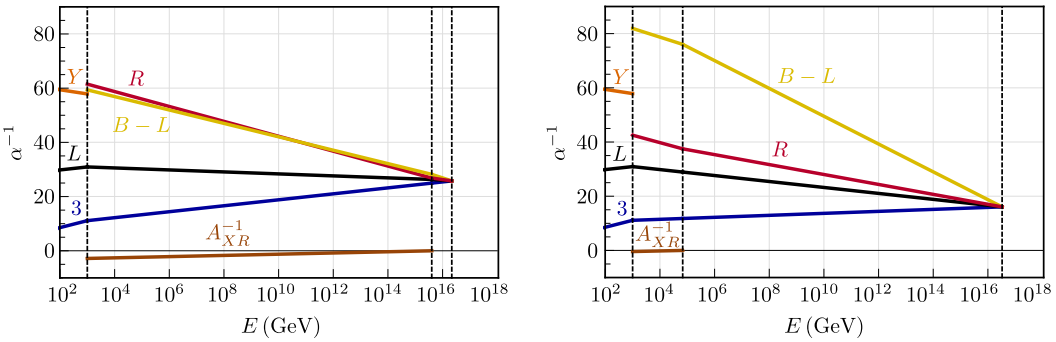

Figure 6.6: Gauge coupling unification in models with an $U(1)_R \times U(1)_{B-L}$ intermediate scale, for $m_R = 10^3$ GeV. Left: $(\Delta b_3^{LR}, \Delta b_L^{LR}, \Delta b_R^{LR}, \Delta b_{B-L}^{LR}, \Delta b_3^{B-L}, \Delta b_L^{B-L}, \Delta\gamma_{RR}, \Delta\gamma_{XR}, \Delta\gamma_{XX}) = (0, 1, 3, 3, 0, 0, 1/2, -\sqrt{3/8}, 3/4)$. Right: $(2, 2, 4, 8, 2, 2, 1/2, -\sqrt{3/8}, 11/4)$. The line, which appears close to zero in the $U(1)_R \times U(1)_{B-L}$ regime is the running of the off-diagonal element of the matrix A^{-1}, i.e. measures the size of the $U(1)$-mixing in the model.

For models in this class, the sliding condition requires that the unification scale is

independent of m_{B-L} and this happens when

$$0 = \left(\Delta b_3^{B-L} - \Delta b_2^{B-L}, \quad p_Y^T \cdot \Delta\gamma \cdot p_Y - \Delta b_2^{B-L}\right) \cdot \begin{pmatrix} 0 & 1 \\ -1 & 0 \end{pmatrix} \cdot \begin{pmatrix} \Delta b_3^{LR} - \Delta b_2^{LR} \\ \frac{3}{5}\Delta b_R^{LR} + \frac{2}{5}\Delta b_{B-L}^{LR} - \Delta b_2^{LR} - \frac{18}{5} \end{pmatrix}. \tag{6.21}$$

Similarly to PS models, in this class of models the higher intermediate scale (m_R) depends, in general, on the lower one (m_{B-L}). However, there is also here a special condition which makes both m_R and m_G simultaneously independent of m_{B-L}, which is

$$\Delta b_3^{LR} = \Delta b_2^{LR} = p_Y^T \cdot \Delta\gamma \cdot p_Y. \tag{6.22}$$

Models of this kind are, for example, those with $\Delta b_3 = 0$ and m_R large, namely $m_R \geq 10^{13}$ GeV. One case is given by the model in [33], where $m_R \simeq 4 \times 10^{15}$ GeV.

6.1.7 Leading-Log RGE Invariants

In this section we briefly recall the basic definitions [33] for the calculation of the "invariants" [139, 218, 219]. In mSugra there are four continuous and one discrete parameter: The common gaugino mass $M_{1/2}$, the common scalar mass m_0, the trilinear coupling A_0 and the choice of the sign of the μ-parameter, $\mathrm{sgn}(\mu)$. In addition, the ratio of vacuum expectation values of H_d and H_u, $\tan\beta = \frac{v_u}{v_d}$ is a free parameter. The latter is the only one defined at the weak scale, while all the others are assigned a value at the GUT scale.

Gaugino masses scale as gauge couplings do and so the requirement of GCU fixes the gaugino masses at the low scale

$$M_i(m_{SUSY}) = \frac{\alpha_i(m_{SUSY})}{\alpha_G} M_{1/2}. \tag{6.23}$$

Neglecting the Yukawa and soft trilinear couplings for the soft mass parameters of the first two generations of sfermions one can write

$$m_{\tilde{f}}^2 - m_0^2 = \frac{M_{1/2}^2}{2\pi\alpha_G^2} \sum_{R_j} \sum_{i=1}^{N} c_i^{f,R_j} \alpha_{i-}^{R_j} \alpha_{i+}^{R_j} \left(\alpha_{i-}^{R_j} + \alpha_{i+}^{R_j}\right) \log \frac{m_+^{R_j}}{m_-^{R_j}}. \tag{6.24}$$

Here, the sum over "R_j" runs over the different regimes in the models under consideration, while the sum over i runs over all gauge groups in a given regime. $m_+^{R_j}$ and $m_-^{R_j}$ are the upper and lower boundaries of the R_j regime and $\alpha_{i+}^{R_j}$, $\alpha_{i-}^{R_j}$ are the values of the gauge coupling of group i, α_i, at these scales. As for the coefficients c_i, they can be calculated from the quadratic Casimir of representations of each field under each gauge group i and are given for example in [33]. In the presence of multiple U(1) gauge groups the RGEs are different (see for instance [150] and references contained therein) and this leads to a generalization of equation (6.24) for the U(1) mixing phase [33]. Here we just quote the end result (with a minor correction to the one shown in this last reference) ignoring the non-U(1) groups:

$$\tilde{m}_{\tilde{f}-}^2 - \tilde{m}_{\tilde{f}+}^2 = \frac{M_{1/2}^2}{\pi\alpha_G^2} Q_f^T A_- \left(A_- + A_+\right) A_+ Q_f \log\frac{m_+}{m_-}, \tag{6.25}$$

where m_+ and m_- are the boundary scales of the U(1) mixing regime and A_+, A_- are the A matrix defined in the previous section (which generalizes α) evaluated in these two limits. Likewise, $\tilde{m}_{\tilde{f}+}^2$ and $\tilde{m}_{\tilde{f}-}^2$ are the values of the soft mass parameter of the sfermion $\tilde{f}$ at these two energy scales. The equation above is a good approximation to the result obtained by integration of the following 1-loop RGE for the soft masses which assumes unification of gaugino masses and gauge coupling constants:

$$\frac{d}{dt}\tilde{m}_f^2 = -\frac{4M_{1/2}^2}{\alpha_G^2} Q_f^T A^3 Q_f. \tag{6.26}$$

Note that in the limit where the U(1) mixing phase extends all the way up to m_G, the A matrix measured at different energy scales will always commute and therefore equation (6.25) presented here matches the one in [33] and in fact both are exact integrations of (6.26). However, if this is not the case, it is expected that there will be a small discrepancy between the two approximations, which nevertheless is numerically small and therefore negligible.

From the five soft sfermion mass parameters of the MSSM and one of the gaugino masses it is possible to form four different combinations that, at 1-loop level in the leading-log approximation, do not depend on the values of m_0 and $M_{1/2}$ and are

therefore called invariants:

$$\begin{aligned} LE &= (m^2_{\widetilde{L}} - m^2_{\widetilde{E}})/M_1^2, \\ QE &= (m^2_{\widetilde{Q}} - m^2_{\widetilde{E}})/M_1^2, \\ DL &= (m^2_{\widetilde{D}} - m^2_{\widetilde{L}})/M_1^2, \\ QU &= (m^2_{\widetilde{Q}} - m^2_{\widetilde{U}})/M_1^2. \end{aligned} \tag{6.27}$$

While being pure numbers in the MSSM, invariants depend on the particle content and gauge group in the intermediate stages, as shown by eq. (6.24).
We will not discuss errors in the calculation of the invariants in detail, we refer the interested reader to [33] and for classical $SU(5)$ based SUSY seesaw models to [218, 219].

We close this subsection by discussing that not all model variants which we presented in section 6.1.2 will be testable by measurements involving invariants at the LHC. According to [228] the LHC at $\sqrt{s} = 14$ TeV will be able to explore SUSY masses up to $m_{\tilde{g}} \sim 3.2$ TeV (3.6 TeV) for $m_{\tilde{q}} \simeq m_{\tilde{g}}$ and of $m_{\tilde{g}} \sim 1.8$ TeV (2.3 TeV) for $m_{\tilde{q}} \gg m_{\tilde{g}}$ with 300 fb^{-1} (3000 fb^{-1}). The LEP limit on the chargino, $m_\chi > 105$ GeV [100], translates into a lower bound for $M_{1/2}$, with the value depending on the Δb. For the class-I models with $\Delta b = 5$ this leads to $M_{1/2} \gtrsim 1.06$ TeV. One can assume conservatively $m_0 = 0$ GeV and calculate from this lower bound on $M_{1/2}$ a lower limit on the expected squark masses in the different variants. All variants with squark masses above the expected reach of the LHC-14 will then not be testable via measurements of the invariants. This discards all models with $\Delta b = 5$ as untestable unfortunately.

For completeness we mention that if we take the present LHC limit on the gluino, $m_{\tilde{g}} \gtrsim 1.1$ TeV [229], this will translate into a lower limit $M_{1/2} \gtrsim 4.31$ TeV for $\Delta b = 5$. We have also checked that models with $\Delta b = 4$, can still have squarks with masses testable at LHC, even for the more recent LHC bound on the gluino mass.

6.1.8 Classification for invariants

For a given model, the invariants defined in eq. (6.27) differ from the mSugra values, and the deviations can be either positive or negative once new superfields

(and/or gauge groups) are added to the MSSM. The mSugra limit is reached in our models when the intermediate scales are equal to m_G, but it should be noted that, in general, when there are two intermediate scales, the smallest one (henceforth called m_-) cannot be pushed all the way up to the unification scale. Therefore, in those cases, the invariants measured at the highest possible m_- are slightly different from the mSugra invariants.

With this in mind, for each variant of our models, we considered whether the invariants for min $m_-(=m_{SUSY})$ are larger or smaller than for max m_-, which tends to be within one or two orders of magnitude of m_G. With four invariants there are a priori $2^4 = 16$ possibilities, and in table 6.3 each of them is assigned a number.

Set #	1	2	3	4	5	6	7	8	9	10	11	12	13	14	15	16
ΔLE	+	+	+	+	+	+	+	+	−	−	−	−	−	−	−	−
ΔQE	+	+	+	−	+	−	−	−	+	+	+	−	+	−	−	−
ΔDL	+	+	−	+	−	+	−	−	+	+	−	+	−	+	−	−
ΔQU	+	−	+	+	−	−	+	−	+	−	+	+	−	−	+	−
Class-I?	✓	✓								✓				✓		
Class-II?	✓	✓	✓			✓	✓	✓		✓				✓		✓
Class-III?	✓	✓	✓			✓	✓	✓		✓				✓		

Table 6.3: The 16 different combinations of signs for 4 invariants. We assign a "+" if the corresponding invariant, when the lowest intermediate scale is set to m_{SUSY}, is larger than its value when this scale is maximized, and "−" otherwise. As discussed in the text, only 9 of the 16 different sign combinations can be realized in the models we consider. Moreover, for class-I only the sets 1,2, 10 and 14 can be realized, see discussion. For class-III we also have found only sets 1, 2, 3, 6, 7, 8, 10 and 14, but here our search was not exhaustive.

However, it is easy to demonstrate that not all of the 16 sets can be realized in the three classes of models we consider. This can be understood as follows. If all sfermions have a common m_0 at the GUT scale, then one can show that

$$m^2_{\widetilde{E}} - m^2_{\widetilde{L}} + m^2_{\widetilde{D}} - 2m^2_{\widetilde{U}} + m^2_{\widetilde{Q}} = 0 \tag{6.28}$$

holds independent of the energy scale, at which soft masses are evaluated. This relation is general, regardless of the combination of intermediate scales that we may consider and for all gauge groups we consider. It is a straightforward consequence of the charge assignments of the standard model fermions and can be easily checked by calculating the Dynkin coefficients of the E,L,D,U and Q representation in the different regimes. In terms of the invariants, this relation becomes:

$$QE = DL + 2QU, \tag{6.29}$$

i.e. only three of the four invariants are independent. From eq. (6.29) it is clear that if ΔDL and ΔQU are both positive (negative), then ΔQE must be also positive (negative). This immediately excludes the sets 4, 5, 12 and 13.

Within the MSSM group eq. (6.28) allows one relation among the invariants. However, one can calculate the relations among the Dynkin indices of the MSSM sfermions within the extended gauge groups we are considering and in these there is one additional relation:

$$QU = LE. \tag{6.30}$$

Since eq. (6.30) is valid only in the regime(s) with extended gauge group(s), it is not exact, once the running within the MSSM regime is included. However, taking into account the running within the MSSM group one can write:

$$QU = LE + f(m_R), \tag{6.31}$$

with

$$f\left(m_R\right) = \frac{2}{33}\left\{\left[\frac{33}{10\pi}\alpha_1^{MSSM}\log\left(\frac{m_R}{m_{SUSY}}\right) - 1\right]^{-2} - 1\right\}. \tag{6.32}$$

Here, α_1^{MSSM} is the value of α_1 at m_{SUSY}. It is easy to see that $f(m_R)$ is always small (< 0.3) and positive and, vanishes if m_R approaches m_{SUSY}. Note, that here m_R stands for the scale where the MSSM group is extended, in the class-III models it is therefore m_{B-L}.

Eq. (6.31) allows to eliminate three more cases from table 6.3. Since $f(m_R)$ is positive, $\Delta QU \leq \Delta LE$ always, so, it is not possible to have $\Delta LE = -$ and $\Delta QU = +$.

This excludes three additional sets from table 6.3: 9, 11 and 15, leaving a total of 9 possible sets.

Finally, in class-I models it is possible to eliminate four more sets, namely all of those with $\Delta DL < 0$. It is easy to see, with the help of eq.(6.24) that this is the case. It follows from the fact that in the LR case, the c_i^L are non-zero for $U(1)_{B-L}$ and $SU(2)_L$ with the values 3/4 and 3/2, respectively. Since also the sum is smaller than the c_3^D (and α_3 is larger than the other couplings, D must run faster than L in the LR-regime.
By the above reasoning set 6 seems to be, in principle, possible in class-I, but is not realized in our complete scan. We found a few examples in class-II, see below. Due to the (approximate) relation QU=LE it seems a particularly fine-tuned situation. We also note in passing, that in the high-scale seesaw models of type-II [218] and seesaw type-III [219] with running only within the MSSM group, all invariants run always towards larger values, i.e. only set 1 is realized in this case.

The above discussion serves only as a general classification of the types of sets of invariants that can be realized in the different model classes. The numerical values of the invariants, however, depend on both, the variant of the model class and the scale of the symmetry breaking. We will discuss one example for each possible set next.

Invariants in model class-I

Fig. (6.7) shows examples of the m_R dependence of the invariants corresponding to the four cases: sets 1, 2, 10 and 14 of table 6.3. Note that we have scaled down the invariants QE and DL for practical reasons. Note also the different scales in the different plots.
In all cases QU $\simeq$ LE, if the LR scale extends to very low energies. As explained above, this is a general feature of the extended gauge groups we consider and thus, measuring a non-zero QU-LE allows in our setups, in principle, to derive a lower limit on the scale at which the extended gauge group is broken.

Sets 1 and 2 show a quite similar overall behavior in these examples. Set 1, however, can also be found in variants of class-I with larger β coefficients, i.e. larger quantitative changes with respect to the mSugra values. It is possible to find vari-

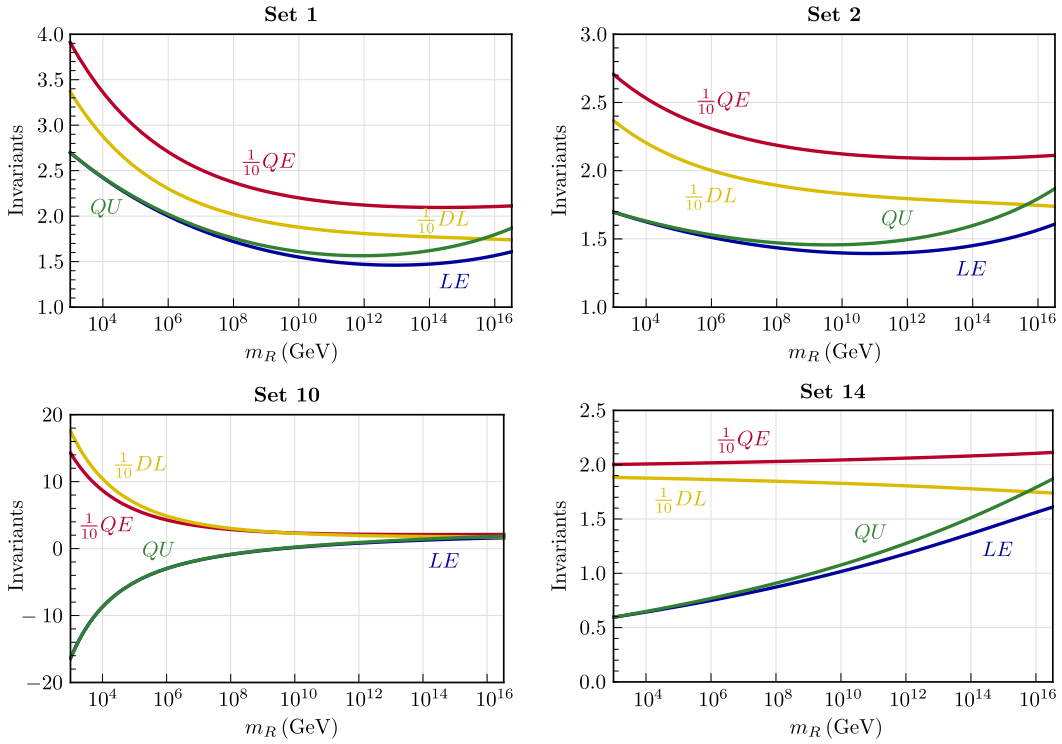

Figure 6.7: m_R dependence of the invariants in model class-I. The examples of $\Delta b_i^{LR} = (\Delta b_3^{LR}, b_L^{LR}, \Delta b_R^{LR}, \Delta b_{BL}^{LR})$ for these sets are as follows. Set 1: $(2, 2, 9, 1/2)$, Set 2: $(1, 1, 7, 1)$, Set 10: $(4, 4, 3, 29/2)$, Set 14: $(0, 0, 2, 6)$. For a discussion see text.

ants within class-I which fall into set 2, but again due to the required similarity of QU and LE, this set can be realized only if both QU and LE are numerically very close to their mSugra values. Set 14 in class-I, finally, is possible only with QE and DL close to their mSugra values, as can be understood from eq. (6.29).

In general, for variants with large Δb_3^{LR} changes in the invariants can be huge, see for example the plot shown for set 10. The large change is mainly due to the rapid running of the gaugino masses in these variants, but also the sfermion spectrum is very "deformed" with respect to mSugra expectations. For example, a negative LE means of course that left sleptons are lighter than right sleptons, a feature that can never be found in the "pure" mSugra model. Recall that for solutions with $\Delta b_3^{LR} = 5$, the value of the squark masses lies beyond the reach of the LHC.

6.1.9 Model class-II

Fig. (B.2) shows examples of the invariants for class-II models for those cases of sets, which can not be covered in class-I. Again, QU and DL are scaled and different plots show differently scaled axes.

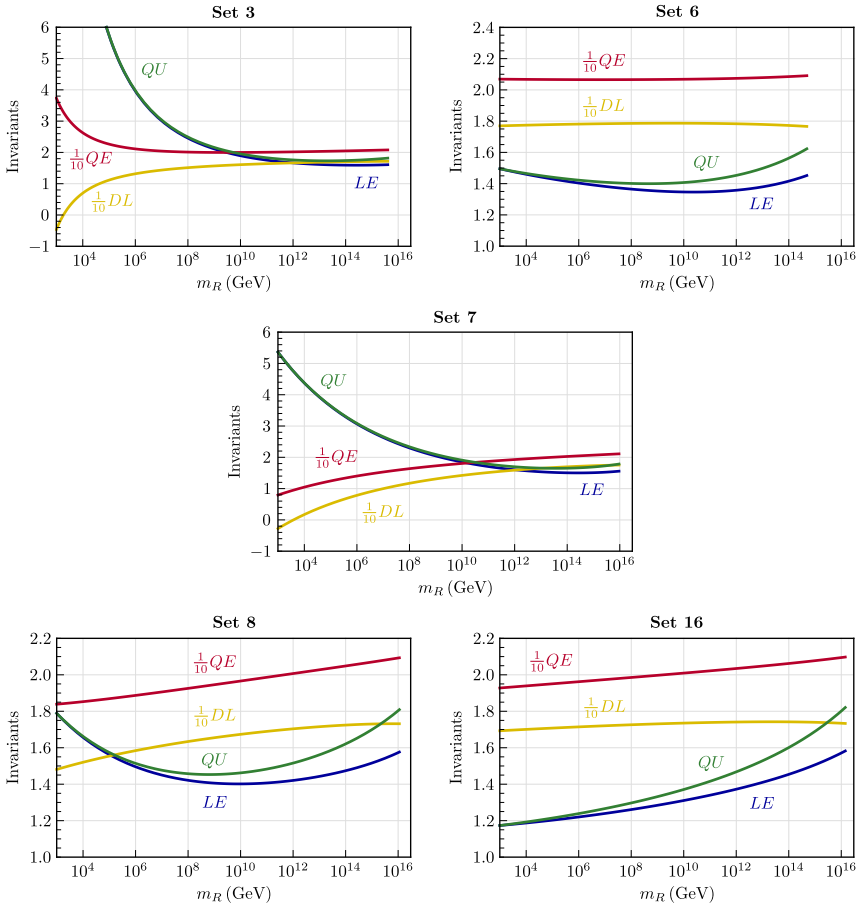

Figure 6.8: The m_R dependence of the invariants in model class-II. The examples shown correspond to the choices of $\Delta b = (\Delta b_3^{LR}, \Delta b_L^{LR}, \Delta b_R^{LR}, \Delta b_{BL}^{LR}, \Delta b_4^{PS}, \Delta b_L^{PS}, \Delta b_R^{PS})$: Set 3: $(0, 1, 10, 3/2, 14, 9, 13)$, Set 6: $(0, 0, 1, 9/2, 63, 60, 114)$, Set 7: $(0, 3, 12, 3/2, 6, 3, 15)$, Set 8: $(0, 0, 9, 3/2, 11, 8, 12)$, Set 16: $(0, 0, 7, 3/2, 11, 8, 10)$.

The example for set 3 shown in fig. (B.2) is similar to the one of the original prototype model constructed in [33]. For set 6 we have found only a few examples, all of them show invariants which hardly change with respect to the mSugra values of the invariants. The example for set 7 shows that also QE can decrease considerably in some variants with respect to its mSugra value. Set 8 is quantitatively

similar to set 2 and set 16 quite similar numerically to set 14. To distinguish these, highly accurate SUSY mass measurements would be necessary.
Again we note that larger values of Δb^{LR}, especially large Δb_3^{LR}, usually lead to numerically larger changes in the invariants, making these models in principle easier to test.

6.1.10 Model class-III

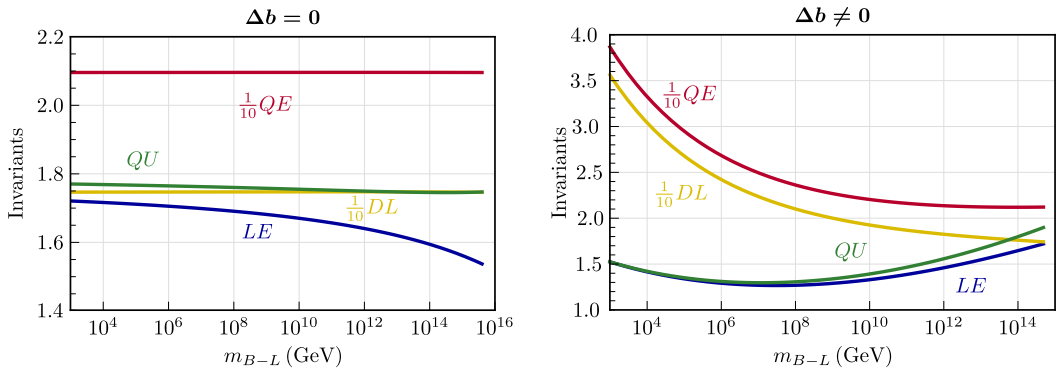

Figure 6.9: The m_{B-L} dependence of the invariants in class-III. To the left the example chooses: $(\Delta b_3^{LR}, \Delta b_L^{LR}, \Delta b_R^{LR}, \Delta b_{BL}^{LR}, \Delta b_3^{BL}, \Delta b_L^{BL}, \Delta\gamma_{RR}, \Delta\gamma_{XR}, \Delta\gamma_{XX}) = (0, 1, 3, 3, 0, 0, 1/2, -\sqrt{3/8}, 3/4)$. To the right: $(2, 2, 4, 8, 2, 2, 1/2, -\sqrt{3/8}, 11/4)$.

Here, the invariants depend on m_{B-L} with a milder or stronger dependence, depending on the value of Δb_3. For almost all the solutions with $\Delta b_3 = 0$, the values QU, DL, QE are constants and only in LE a mild variation with m_{B-L} is found. This fact was already pointed out in [33]. However, we have found that class-III models can be made with $\Delta b_3 > 0$ and these, in general, lead to invariants which are qualitatively similar to the case of class-I discussed above. In fig. (6.9) we show two examples of invariants for class-III, one with $\Delta b_3 = 0$ and one with $\Delta b_3 = 2$. The solutions with $\Delta b_3 \neq 0$ fall in two kinds: The minimum value of m_R is very large. Then, the invariants have the same behavior than those in which $\Delta b_3 = 0$. The minimum value of m_R is low. The invariants are not constants and look similar to the ones in the class-I models. The generally mild dependence on m_{B-L} can be understood, since it enters into the soft masses only through the changes in the abelian gauge couplings. Class-III models are therefore the hardest to "test" using invariants.

6.1.11 Comparison of model classes

The classification of variants that we have discussed in section 6.1.8 only takes into account what happens when the lowest intermediate scale is very low, $\mathcal{O}(m_{SUSY})$. When one varies continuously the lowest intermediate scale (m_R in the LR and PS-class models or m_{B-L} in the BL-class of models), each variant draws a line in the 4-dimensional space (LE, QU, DL, QE). The dimensionality of such a plot can be lowered if we use the (approximate) relations between the invariants shown above, namely $QU \approx LE$ and $QE = DL + 2QU$. We can then choose two independent ones, for example LE and QE, so that the only non-trivial information between the 4 invariants is encoded in a (LE, QE) plot. In this way, it is possible to simultaneously display the predictions of different variants. This was done in fig. (6.10), where LR-, PS- and BL-variants are drawn together. The plot is exhaustive in the sense that it includes all LR-variants, as well as all PS- and BL-variants which can have the highest intermediate scale below 10^6 GeV. In all cases, we required that α^{-1} at unification is larger than $1/2$ when the lowest intermediate scale is equal to m_{SUSY}.

There is a dot in the middle of the figure - the mSugra point - which corresponds to the prediction of mSugra models, in the approximation used. It is expected that every model will draw a line with one end close to this point. This end-point corresponds to the limit where the intermediate scales are close to the GUT scale and therefore the running in the LR, PS and BL phases is small so the invariants should be similar to those in mSugra models. So the general picture is that lines tend to start (when the lowest intermediate scale is of the order of 10^3 GeV) outside or at the periphery of the plot, away from the mSugra point and, as the intermediate scales increase, they converge towards the region of the mSugra point, in the middle of the plot. In fact, note that all the blue lines of LR-class models do touch this point, because we can slide the LR scale all the way to m_G. But in PS- and BL- models there are two intermediate scales and often the lowest one cannot be increased all the way up to m_G, either because that would make the highest intermediate scale bigger than m_G or because it would invert the natural ordering of the two intermediate scales.

It is interesting to note that the BL-class with low m_R can produce the same imprint in the sparticle masses as LR-models. This is to be expected because

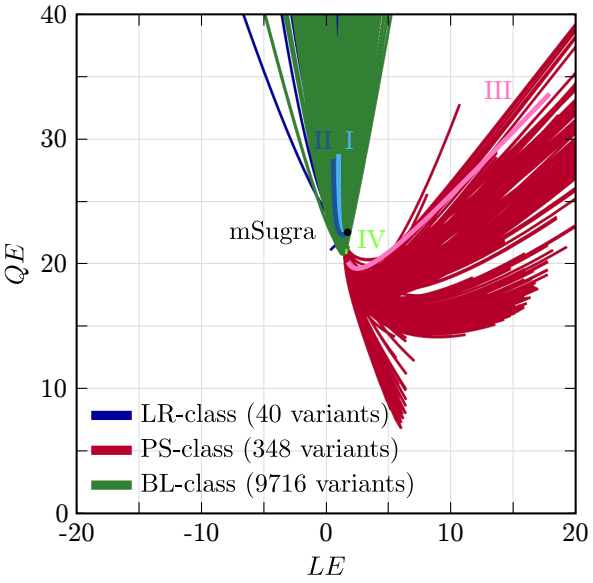

Figure 6.10: Parametric (LE, QE) plot for the different variants (see text). The thicker lines labeled with I, II, III and IV indicate the result for the four prototype models presented in [33].

with m_R close to m_{B-L} the running in the U(1)-mixing phase is small, leading to predictions similar to LR-models. The equivalent limit for PS-class models is reached for very high m_{PS}, close to the GUT scale (see below). On the other hand, from fig. (6.10) we can see that a low m_{PS} actually leads to a very different signal on the soft sparticle masses. For example, a measurement of $LE \approx 10$ and $QE \approx 15$, together with compatible values for the other two invariants ($QU \approx 10$ and $DL \approx -5$) would immediately exclude *all classes of models except PS-models*, and in addition it would strongly suggest low PS and LR scales.

Fig. (6.11) illustrates the general behavior of PS-models as we increase the separation between the m_{LR} and m_{PS} scales. The red region in the (LE, QE) plot tends to rotate anti-clockwise until it reaches, for very high m_{PS}, the same region of points which is predicted by LR-models. Curiously, we also see in fig. (6.11) that some of these models actually predict different invariant values from the ones of LR models. What happens in these cases is that since the PS phase is very short, it is possible to have many active fields in it which decouple at lower energies. So even though the running is short, the values of the different gauge couplings

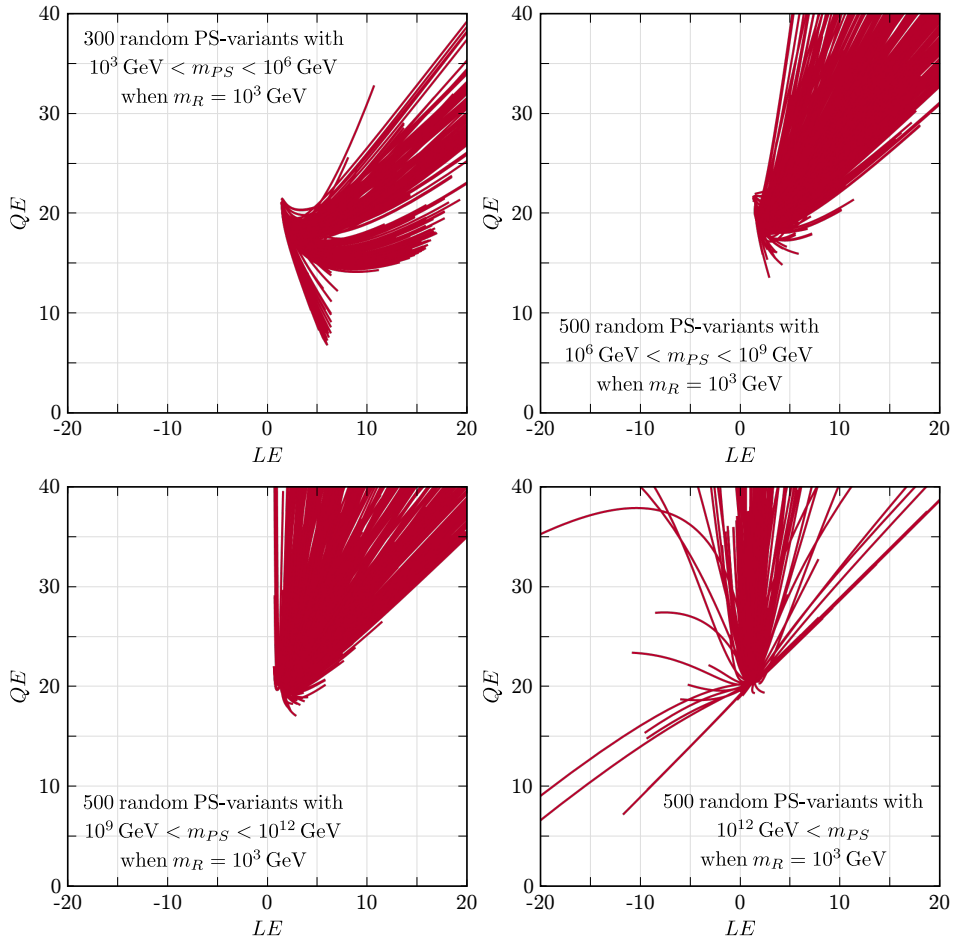

Figure 6.11: Parametric (LE, QE) plots for different PS-variants showing the effect of the PS scale.

actually get very large corrections in this regime and these are uncommon in other settings. For example, it is possible in this special subclass of PS-models for α_R to get bigger than α_3/α_4 before unifying!. One can see from fig. (6.11) that many, although not all PS-models can lead to large values of LE. This can happen for both low and high values of m_{PS} and is a rather particular feature of the class-II, which can not be found in the other classes.

6.1.12 Summary and conclusions

We have discussed $SO(10)$ inspired supersymmetric models with extended gauge group near the electro-weak scale, consistent with gauge coupling unification thanks

to a "sliding scale" mechanism. We have discussed three different setups, which we call classes of models. The first and simplest chain we use breaks $SO(10)$ through a left-right symmetric stage to the SM group, class-II uses an additional intermediate Pati-Salam stage, while in class-III we discuss models which break the LR-symmetric group first into a $U(1)_R \times U(1)_{B-L}$ group before reaching the SM group. We have shown that in each case many different variants and many configurations (or "proto-models") for each variant can be constructed.

We have discussed that one can not only construct sliding models in which an inverse or linear seesaw is consistent with GCU, as done in earlier work [32, 33, 217], but also all other known types of seesaws can, in principle, be found. We found example configurations for seesaw type-I, type-II and type-III and even inverse type-III (for which one example limited to class-II was previously discussed in [33]).

Due to the sliding scale property the different configurations predict potentially rich phenomenology at the LHC, although by the same reasoning the discovery of any of the additional particles the models predict is of course not guaranteed. However, even if all the new particles - including the gauge bosons of the extended gauge group - lie outside of the reach of the LHC, indirect tests of the models are possible from measurements of SUSY particle masses. We have discussed certain combinations of soft parameters, called "invariants", and shown that the invariants themselves can be classified into a few sets. Just determining to which set the experimental data belongs would allow to distinguish, at least in some cases, class-I from class-II models and also in all but one case our classes of models are different from the ordinary high-scale seesaw (type-II and type-III) models. Depending on the accuracy with which supersymmetric masses can be measured in the future, the invariants could be used to gain indirect information not only on the class of model and its variant realized in nature, but also give hints on the scale of beyond-MSSM physics, i.e. the energy scale at which the extended gauge group is broken.

We add a few words of caution. First of all, our analysis is done completely at the 1-loop level. It is known from numerical calculations for seesaw type-II [218] and seesaw type-III [219] that the invariants receive numerically important shifts

at 2-loop level. In addition, there are also uncertainties in the calculation from GUT-scale thresholds and from uncertainties in the input parameters. For the latter the most important is most likely the error on α_S [33]. With the huge number of models we have considered, taking into account all of these effects is impractical and, thus, our numerical results should be taken as approximate. However, should any signs of supersymmetry be found in the future, improvements in the calculations along these lines could be easily made, should it become necessary. More important for the calculation of the invariants is, of course, the assumption that SUSY breaking indeed is mSugra-like. Tests of the validity of this assumption can be made also only indirectly. Many of the spectra we find, especially in the class-II models, are actually quite different from standard mSugra expectations and thus a pure MSSM-mSugra would give a bad fit to experimental data, if one of these models is realized in nature. However, all of our variants still fulfill (by construction) a certain sum rule, see the discussion in section 6.1.8.

Of course, so far no signs of supersymmetry have been seen at the LHC, but with the planned increase of $\sqrt{s}$ for the next run of the accelerator there is still quite a lot of parameter space to be explored. We note in this respect that we are not overly concerned about the Higgs mass, $m_h \sim (125 - 126)$ GeV, if the new resonance found by the ATLAS [5] and CMS [6] collaborations turns out to be indeed the lightest Higgs boson. While for a pure MSSM with mSugra boundary conditions it is well-known [230, 231, 232, 233] that such a hefty Higgs requires multi-TeV scalars, [9] all our models have an extended gauge symmetry. Thus, there are new D-terms contributing to the Higgs mass [235, 236], alleviating the need for large soft SUSY breaking terms, as has been explicitly shown in [237, 238] for one particular realization of a class-III model [32, 33].

Finally, many of the configuration (or proto-models) which we have discussed contain exotic superfields, which might show up in the LHC. It might therefore be interesting to do a more detailed study of the phenomenology of at least some particular examples of the models we have constructed.

[9] Multi-TeV scalars are also required, if the MSSM with mSugra boundary conditions is extended to include a high-scale seesaw mechanism [234].

6.2 LHC-SCALE LEFT RIGHT SYMMETRY AND UNIFICATION

6.2.1 Introduction

It is well-known that with only the standard model (SM) field content the gauge couplings do not unify at a single energy scale, while the minimal supersymmetric standard model (MSSM) leads to quantitatively precise gauge coupling unification (GCU), if the scale of supersymmetry is "close" to the electro-weak (EW) scale [26]. [10] However, there are many extensions of the SM that lead to GCU without supersymmetry (SUSY). In particular, it is much less known that already in [30] GCU was studied in a number of non-SUSY extensions of the SM. We also mention one particular example with vector-like quarks (VLQ) that was discussed recently in [31], where the Higgs mass and stability bounds and the GCU were considered in an SM extension with two different VLQs.

On the other hand, there are rather few publications which discuss GCU within left-right symmetric extensions of the SM. The main reason for this is probably the fact that for minimal left-right (LR) symmetric extensions of the SM the couplings do not unify unless the LR scale is rather high, say $(10^9 - 10^{11})$ GeV, as has been shown already in [240].

While for the SM the term "minimal" is unambiguously defined, for LR symmetric extensions of the SM the term "minimal-LR" model has been used for quite different models in the literature. Usually in "minimal LR" models a second SM Higgs doublet is added to the SM field content at the LR scale to complete a bi-doublet, $\Phi_{1,2,2,0}$, [11] as required by the LR group. To break the LR group to the SM group one then (usually) adds a pair of triplets $\Phi_{1,3,1,-2} + \Phi_{1,1,3,-2}$ [45, 170, 241]. Here the presence of the left-triplet $\Phi_{1,3,1,-2}$ allows to maintain parity in the LR phase, i.e. $g_L = g_R$, sometimes also called "manifest LR" symmetry. This construction

[10] Actually, within supersymmetric models it is only required that the new fermions (higgsinos, wino and gluino) have masses near the EW scale, as in the so-called "split SUSY" scenario [29, 239].

[11] Throughout this thesis we will use the notation Φ for scalars and Ψ for fermions with the subscript denoting the quantum numbers with respect to either the left-right $(SU(3)_c \times SU(2)_L \times SU(2)_R \times U(1)_{B-L})$ or the SM group $(SU(3)_c \times SU(2)_L \times U(1)_Y)$.

automatically also creates a seesaw mass for the right-handed neutrinos from the vacuum expectation value of the $\Phi_{1,1,3,-2}$ [45]. We will call this setup the "minimal LR" (mLR) model in the following. Alternatively, also a pair of doublets, $\Phi_{1,2,1,-1}$ + $\Phi_{1,1,2,-1}$, could break the LR group for an equally simple setup. However, in this case one would need to rely on an inverse [223] (or linear [119, 224]) seesaw for generating neutrino masses.

In [242] it has been argued that a "truly minimal LR model" has only two doublets $\Phi_{1,2,1,-1}$ + $\Phi_{1,1,2,-1}$ but no bi-doublet. In this case, all fermion masses are generated from non-renormalizable operators (NROs). While this setup has indeed one field less than the above "minimal-LR" models, it needs some additional unspecified new physics to generate the NROs and, thus, can not be considered a complete model. Unification in this "truly minimal" setup is achieved for an LR scale around roughly 10^8 GeV (and a grand unified theory (GUT) scale of roughly 10^{15} GeV [243].

A LR model with only bi-doublets can not generate the observed Cabibbo-Kobayashi-Maskawa (CKM) mixing angles at tree-level, see the discussion in the next section. This can be solved by adding a second $\Phi_{1,2,2,0}$ plus a pair of $(B-L)$ neutral triplets, $\Phi_{1,3,1,0}$ + $\Phi_{1,1,3,0}$. A supersymmetric version of this setup has been discussed in [213, 214], see also [244]. We will call this model the "minimal ΩLR" (mΩLR) model. Fig. 6.12 shows the running of the gauge couplings for the minimal setup ("mLR"), including 2-loop beta coefficients, in the left plot and for the mΩLR model in the right plot. Note, that the best fit point (b.f.p.) for $m_{LR} = 3 \times 10^{10}$ GeV and $m_G = 2 \times 10^{15}$ GeV in the mLR model, while the b.f.p. for $m_{LR} = 3 \times 10^{11}$ GeV and $m_G = 6 \times 10^{14}$ GeV in the mΩLR model.[12]
Obviously, such a large scale for the LR-symmetry will never be probed experimentally and this explains, perhaps, why LR models have not been studied very much in the literature in the context of GCU. It is, however, quite straightforward to construct LR symmetric models, where the LR is close to the EW scale. Just to give an indication, the running of the inverse gauge couplings for two example models, which we will discuss later in this paper and which lead to correct GCU with a very low LR scale, are shown in fig. 6.13. As discussed in section 6.2.5,

[12]The authors of [213, 214] called this the "minimal supersymmetric LR" model. In this original supersymmetric version the b.f.p. for the LR scale from GCU is equal to the GUT scale.

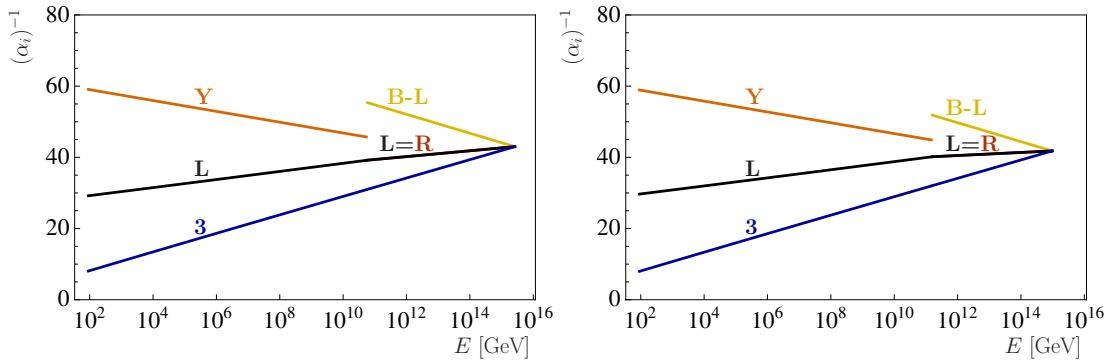

Figure 6.12: Gauge coupling unification, including the 2-loop β-coefficients, for two "minimal" left-right models, to the left "mLR", to the right "mΩLR" model. For definition of the models and discussion see text.

many such examples can be constructed and moreover, many of these examples give perfect GCU at a price of only (a few copies of) one or a few additional types of fields.

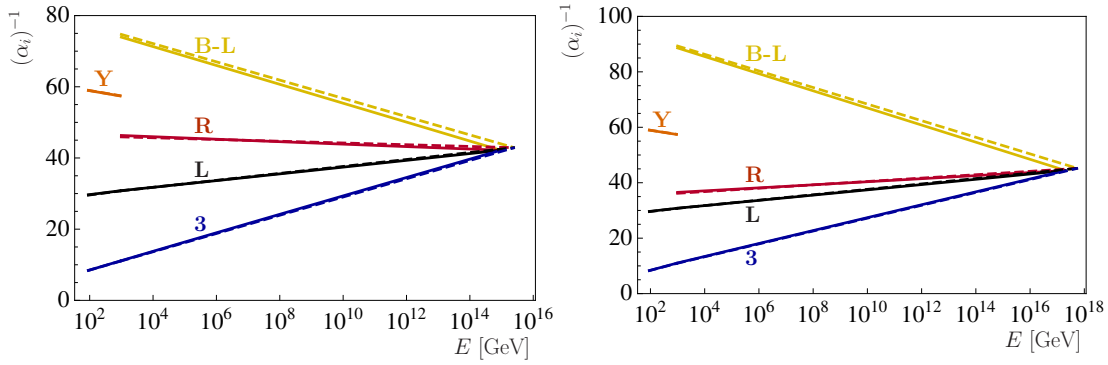

Figure 6.13: Gauge coupling unification at 2-loop level (full lines) and 1-loop level (dashed lines), for two LR models with a low scale of LR breaking. The figure to the left has the field content SM + $\Phi_{1,2,2,0} + 3\Phi_{1,1,3,0} + 2\Phi_{1,1,3,-2}$, while the model to the right is defined as SM + $2\Psi_{3,1,1,-2/3} + 2\Phi_{1,2,1,1} + 2\Phi_{1,1,3,-2}$. For discussion see text.

Our work is, of course, not the first paper in the literature to discuss GCU with a low LR scale. Especially supersymmetric models with an extended gauge group have attracted recently some attention. Different from the non-SUSY case, in SUSY LR models one needs to pay special attention not to destroy the unification

already achieved within the MSSM. This can be done in different ways. In the supersymmetric model of [32] the LR symmetry is broken at a large scale, but the subgroup $U(1)_R \times U(1)_{B-L}$ survives down to the EW scale. In this construction, the scale where $U(1)_R \times U(1)_{B-L}$ is broken to $U(1)_Y$ does not enter in the determination of the GUT scale, m_G. We call this a "sliding scale" mechanism, since $U(1)_R \times U(1)_{B-L}$ can slide down from (nearly) m_G to any arbitrary value, without destroying GCU. In [215] the authors demonstrated that in fact a complete LR group can be lowered to the TeV-scale, if certain carefully chosen fields are added and the LR-symmetry is broken by right doublets. A particularly simple model of this kind was discussed in [217]. Finally, the authors of [33] discussed also an alternative way of constructing a sliding LR model by relating it to an intermediate Pati-Salam stage. Many examples of such "sliding-scale" supersymmetric LR constructions have then be discussed in [2].

However, supersymmetry is not needed in low scale LR models to achieve GCU, as first discussed in the relatively unknown paper [245]. Our work is based on similar ideas as this earlier paper [245], but differs in the following aspects from it: (a) We do not insist on manifest LR symmetry. While parity maintaining LR models are, of course, a perfectly valid possibility, they only form a subclass of all LR models. (b) The study [245] concentrated exclusively on GCU. We also discuss constraints on model building due to the requirement of explaining correctly the CKM in LR symmetric models. We further take in account constraints coming from the requirement that we should have the necessary fields to have a successful seesaw mechanism for neutrino masses. (c) We add a discussion of "sliding models"; as discussed above a particular (but interesting) sub-class of LR models. And, (d) we pay special attention to uncertainties in the predictions of the LR and GUT scales (and the resulting uncertainty in the proton decay half-lives). As shown below, these uncertainties are entirely dominated by the current theory error, due to the (calculable but) unknown threshold errors.

The rest of this chapter is organized as follows. In the next section we discuss our minimal requirements for the construction of low-scale LR symmetric models. Special emphasis is put on the discussion of how to generate a realistic CKM matrix at tree-level. In section 6.2.5 we then discuss a number of possible LR models. We first consider "minimal" low-scale setups, i.e. models which fulfil all requirements

discussed in section 6.2.2 with a field content as small as possible. We then discuss also "sliding-scale LR models". By this term we understand models, which lead to the correct unification, but in which the scale, where LR symmetry is broken, is essentially a free parameter. This latter models are non-minimal, but reminiscent of the supersymmetric LR constructions discussed in [2]. In section 6.2.8 we then discuss uncertainties for the prediction of the LR scale and the proton decay half-life in the different models, before turning to a short summary and conclusion in section 6.2.9. A number of details and tables of possible models are given in the appendices.

6.2.2 Basic requirements

There are several basic conceptual and phenomenological requirements that we shall impose on the set of all possible LR-symmetric extensions of the Standard model. From the bottom-up perspective these are:

- Rich enough structure to account for the CKM mixing even after the SM Higgs doublet is promoted to the LR bi-doublet, and a rich enough structure to support some variant of the seesaw mechanism.
- Consistency of the assumed high-scale grand unified picture; here we shall be concerned, namely, with the perturbativity of the models up to at least the unification scale, the quality of the gauge coupling convergence (to be at least as good as in the minimal supersymmetric standard model) and compatibility with the current proton decay limits.

Technically, we shall also assume that the masses of the extra degrees of freedom are well clustered around at most two scales, i.e., the LR scale and the GUT scale; if this was not the case there would be no way to navigate through the plethora of possible scenarios. Implicitly, the LR scale will be located in the TeV ballpark otherwise decoupling would make the new physics escape all LHC tests.

6.2.3 Account for the SM flavour physics

The need to accommodate flavour physics is clearly the least speculative of the requirements above and, thus, the one we begin with.

Two bi-doublets plus one extra scalar

With just the SM fermions at hand, there must obviously be more than a single bi-doublet coupled to the quark and lepton bilinears in any renormalizable LR-symmetric theory; otherwise, the Yukawa lagrangian (in the "classical" LR notation with $Q \equiv \Psi_{3,2,1,1/3}$, $\Phi \equiv \Phi_{1,2,2,0}$ and so on, cf. table B.5)

$$\mathcal{L}_Y = Y_Q Q^T i\tau_2 \Phi Q^c + Y_L L^T i\tau_2 \Phi L^c + h.c.\,, \tag{6.33}$$

yields $M_u \propto M_d$ irrespective of the vacuum expectation value (VEV) structure of Φ and, hence, $V_{CKM} = \mathbb{1}$ at the $SU(2)_R$ breaking scale. With a second bi-doublet at play, one has instead

$$\mathcal{L}_Y = Y_Q^1 Q^T i\tau_2 \Phi^1 Q^c + Y_Q^2 Q^T i\tau_2 \Phi^2 Q^c + Y_L^1 L^T i\tau_2 \Phi^1 L^c + Y_L^2 L^T i\tau_2 \Phi^2 L^c + h.c.\,, \tag{6.34}$$

which admits M_u non-proportional to M_d (and, therefore, a potentially realistic CKM provided[13]

$$\frac{v_u^1}{v_u^2} \neq \frac{v_d^1}{v_d^2}\,, \quad \text{where} \quad \langle \Phi^i \rangle \equiv \begin{pmatrix} v_d^i & 0 \\ 0 & v_u^i \end{pmatrix}\,. \tag{6.35}$$

Note that we conveniently chose the $SU(2)_R$ index to label columns (i.e., they change in the vertical direction) while the $SU(2)_L$ indices label the rows. Needless to say, the VEV structure of such a theory is driven by the relevant scalar potential. With just the two bi-doublets at play it can be written in a very compact form

$$V \ni -\frac{1}{2}\mu_{ij}^2 \mathrm{Tr}(\tau_2 \Phi^{iT} \tau_2 \Phi^j)\,, \tag{6.36}$$

where the mass matrix μ can be, without loss of generality, taken symmetric, cf. eq. (6) in [213]. In such a simple case, however, it is almost obvious that the condition (6.35) can not be satisfied because of the $\Phi^1 \leftrightarrow \Phi^2$ interchange symmetry which yields $v_d^1/v_u^1 = v_d^2/v_u^2$ implying $v_d^1/v_d^2 = v_u^1/v_u^2$. Hence, either eq. (6.34) or eq. (6.36) require further ingredients.

Let us first try to devise (6.35) by adding some extra scalar fields so that the simple scalar potential (6.36) loses the $\Phi^1 \leftrightarrow \Phi^2$ symmetry.To this end, it is clear

[13] Note that in the opposite case one can go into a basis in which one of the two bi-doublets is entirely deprived of its VEVs and, hence, one is effectively back to the single-Φ case (6.33).

that the desired asymmetric term must contain at least a pair of Φ's and anything that can be coupled to such a bilinear, i.e., an $SU(2)_R$ singlet or a triplet, either elementary (with a super-renormalizable coupling) or as a compound of two doublets. Clearly, a singlet field (of any kind) behaves just like the explicit singlet mass term in (6.36) and, as such, it does not lift the undesired degeneracy.

Hence, only the triplet option is viable, either in the form of an elementary scalar[14] $\Phi_{1,1,3,0}$ (to be denoted Ω^c, see again table B.5) which couples to the bi-doublets via an *antisymmetric* coupling α

$$V \ni \alpha_{ij}\mathrm{Tr}[\Phi^{iT}\tau_2\vec{\tau}\Phi^j\tau_2].\vec{\Omega}^c\,, \tag{6.37}$$

or a non-elementary triplet made of a pair of $SU(2)_R$ doublets $\chi^c \equiv \Psi_{1,1,2,-1}$ (and $\chi^{c\dagger}$) replacing, effectively, $\vec{\Omega}^c \to \chi^{c\dagger}\vec{\tau}\chi^c$. Let us mention that the former option has been entertained heavily in the SUSY LR context [213, 214] where the requirement of renormalizability of the superpotential simply enforces this route; in the non-SUSY framework, however, the doublet solution is at least as good as the triplet one.

To conclude, we shall consider all settings with the SM matter content, a pair of LR bi-doublets and either and extra Ω^c-like $SU(2)_R$ triplet or an extra χ^c-like $SU(2)_R$ doublet consistent with the requirement of a realistic SM flavour.

Extra fermions

Relaxing the strictly SM-like-matter assumption, one may attempt to exploit the mixing of the chiral matter with possible vector-like fermions emerging in various extensions of the SM. Among these, one may, for instance, arrange the mixing of the SM left-handed quark doublet $Q = \Psi_{3,2,+1/6}$ with the Q' part of an extra Q-type vector-like pair

$$Q' \oplus Q'^* \quad \equiv \quad \Psi'_{3,2,+1/6} \oplus \Psi'_{\bar{3},\bar{2},-1/6}\,, \tag{6.38}$$

[14] We discard the "symmetric solution" with an elementary $\Omega \equiv \Phi_{1,3,1,0}$ because such a field can not get any significant VEV without ruining the SM ρ parameter.

or a mixing of the SM $u^c = \Psi_{\overline{3},1,-2/3}$ and/or $d^c = \Psi_{\overline{3},1,+1/3}$ (in the notation in which all matter fields are left-handed) with the extra u^c and/or d^c-like fields

$$u'^c \oplus u'^{c*} \equiv \Psi'_{\overline{3},1,-2/3} \oplus \Psi'_{3,1,+2/3}\,, \qquad d'^c \oplus d'^{c*} \equiv \Psi'_{\overline{3},1,+1/3} \oplus \Psi'_{3,1,-1/3}\,. \tag{6.39}$$

For the sake of simplicity, we shall consider all these possibilities at once and then focus on several special cases with either some of these fields missing or with extra correlations implied by the restoration of the LR symmetry at some scale. The relevant piece of the Yukawa-type + mass lagrangian in such a case reads (omitting all the gauge indices as well as the omnipresent transposition and C^{-1} Lorentz factors in all terms):

$$\begin{aligned}
\mathcal{L}^{matter}_{Y+mass} &= Y_u Q u^c H_u + Y_d Q d^c H_d + Y'_u Q' u^c H_u + Y'_d Q' d^c H_d + Y'^c_u Q u'^c H_u \\
&+ Y'^c_d Q d'^c H_d + Y''^c_u Q' u'^c H_u + Y''^c_d Q' d'^c H_d + M_{Q'Q'^*} Q' Q'^* \\
&+ M_{d'^c d'^{c*}} d'^c d'^{c*} + M_{u'^c u'^{c*}} u'^c u'^{c*} + M_{QQ'^*} Q Q'^* + M_{d^c d'^{c*}} d^c d'^{c*} \\
&+ M_{u^c u'^{c*}} u^c u'^{c*} + h.c.
\end{aligned} \tag{6.40}$$

where Y_u and Y_d are the standard 3×3 Yukawa matrices of the SM; the dimensionalities of the other matrix couplings (primed Y's) and/or direct mass terms (M's) should be obvious once the number of each type of the extra matter multiplets is specified.

In the QCD⊗QED phase, this structure gives rise to the following pair of the up- and down-type quark mass matrices (the last columns and rows indicate whether the relevant field comes from an $SU(2)_L$ doublet or a singlet and, hence, justify the qualitative structure of the mass matrix; note also that we display only one of the off-diagonal blocks of the full Dirac matrices written in the Weyl basis and we do not pay much attention to $\mathcal{O}(1)$ numerical factors such as Clebsches and/or normalisation):

M_u	u^c	u'^{c*}	u'^c	$SU(2)$
u	$Y_u v_u$	$M_{QQ'^*}$	$Y'^c_u v_u$	2
u'	$Y'_u v_u$	$M_{Q'Q'^*}$	$Y''^c_u v_u$	2
u'^{c*}	$M^T_{u^c u'^{c*}}$	$Y''^{cT}_u v_u$	$M^T_{u'^c u'^{c*}}$	1
$SU(2)$	1	2	1	

(6.41)

M_d	d^c	d'^{c*}	d'^c	$SU(2)$
d	$Y_d v_d$	$M_{QQ'^*}$	$Y'^c_d v_d$	2
d'	$Y'_d v_d$	$M_{Q'Q'^*}$	$Y''^c_d v_d$	2
d'^{c*}	$M^T_{d^c d'^{c*}}$	$Y''^{cT}_d v_d$	$M^T_{d'^c d'^{c*}}$	1
$SU(2)$	1	2	1	

Given this, there are several basic generic observations one can make:

- The spectrum of both these matrices always contains three "light" eigenvalues, i.e., those that are proportional to the $SU(2)_L$ breaking VEV. This, of course, provides a trivial consistency check of their structure.

- Removing the second row+column in both $M_{u,d}$ (that corresponds to integrating out $Q' \oplus Q'^*$) and/or the third row+column in M_u (and, thus, integrating out $u'^c \oplus u'^{c*}$) and/or the third row+column in M_d (and thus integrating out $d'^c \oplus d'^{c*}$) the game is reduced to all the different cases discussed in many previous studies in the SM context.

- There are several entries in M_u and M_d that are intercorrelated already at the SM level; yet stronger correlations can be expected if the effective lagrangian (6.40) descends from a LR-symmetric scenario. For example, grouping $u'^c \oplus u'^{c*}$ and $d'^c \oplus d'^{c*}$ into $SU(2)_R$ doublets $Q'^c \oplus Q'^{c*}$ the degeneracy among M_u and M_d would be exact up to (model-dependent) $SU(2)_R$-breaking terms; in such a case the (dis-)similarity of the up and down quark spectra and mixing matrices depends on the details of the specific $SU(2)_R$-breaking mechanism which, obviously, will be able to smear such degeneracies (and, thus, open room for a potentially realistic spectra and the CKM matrix) only if the relevant VEV is comparable to (or larger than) the singlet mass terms therein. Note that here we implicitly assume that there is no

other mechanism such as the one described in the previous section operating to our desire.

Hence, if one wants to make use of the extra vector-like fermions in order to account for a realistic SM quark masses and mixing in the LR setting, such extra matter fields should be included at (or below) the LR scale, otherwise they will effectively decouple. This is the second route to the realistic SM flavour that we shall entertain in what follows.

To conclude, without going into more details, we shall consider all scenarios including some of the combinations of the extra matter fields discussed above with masses at the LR scale eligible for the subsequent renormalization group (RG) analysis. In this respect, it is also worth stressing that there are many specific realisations of the structures above at the LR level that differ namely by the origin of the desired vector-like fermions therein and, thus, by the specific structure of the effective mass matrices above. An interested reader is deferred to section 6.2.5 where several examples are discussed in more detail.

Seesaw & neutrino masses

We also require there are fields in the model that may support some variant of the seesaw mechanism, either ordinary or inverse/linear, and, thus, provide Majorana masses for neutrinos. Technically, the requirements are identical to those given in the previous SUSY study [2] so we shall just recapitulate them here: i) in models where the LR symmetry is broken by $\Phi_{1,1,3,-2}$ one automatically has a right-handed neutrino mass and, thus, type-I seesaw; if $\Phi_{1,3,1,-2}$ is also present, type-II contribution to the seesaw formula is likely. ii) as for the models with the LR breaking driven by $\Phi_{1,1,2,-1}$ one may implement either an inverse [223] and/or linear [119, 224], seesaw if $\Psi_{1,1,1,0}$ is present, or a variant of type-III seesaw if $\Psi_{1,3,1,0}$ and/or $\Psi_{1,1,3,0}$ is available.

6.2.4 Consistency of the high-scale grand unification

Perturbativity

Since the analysis in the next sections relies heavily on perturbative techniques we should make sure these are under control in all cases of our interest. In particular,

one should assume that for all couplings perturbativity is not violated at m_G and below m_G the same holds for all the effective parameters of the low-energy theory. To this end we shall, as usual, adopt a very simplified approach assuming that none of the gauge couplings explodes throughout the whole "desert" and, at the same time, the unified coupling does not diverge right above the unification scale. On top of that, a perturbative description does not make much (of a quantitative) sense either even if the couplings are formally perturbative up to m_G (and the spectrum is compact) when some of them diverge very close above m_G: in fact, the results would be extremely sensitive to the matching scale selection because their rapid just-above-m_G growth is equivalent to large thresholds for not-so-well chosen matching scale.

Grand unification

Technically, m_G is best defined as the mass scale of the heavy vector bosons governing the perturbative baryon number violating (BNV) processes. At first approximation, this may be determined as the energy at which the running gauge couplings in the $\overline{\text{MS}}$ scheme converge to a point; from consistency, this is then assumed to be the scale where the heavy part of the scalar and vector spectrum is integrated in. Needless to say, if accuracy is at stakes, this picture is vastly oversimplified. The main issue of such an approach is the lack of a detailed information about the high-energy theory spectrum which, in reality, may be spread over several orders of magnitude[15]. The "threshold effects" thus generated can then significantly alter the naïve picture by as much as a typical two-loop β-function contribution.

This makes it particularly difficult to get a good grip on the GUT scale from a mere renormalization group equations (RGE) running - with the thresholds at play the running gauge couplings in the "usual" schemes such as $\overline{\text{MS}}$ do not intersect at a point and the only way m_G may be accurately determined is, indeed, a thorough inspection of the heavy spectrum, see, e.g., [247]. In this respect, perhaps the best that may be done in the bottom-up approach (in which, by definition, the shape

[15]Note that this, in fact, is rather typical for "simple" models which tend to suffer from the emergence of pseudo-Goldstone bosons associated to spontaneously broken accidental global symmetries, especially when there are several vastly different scales at play, cf. [184].

of the heavy spectrum is ignored) is to define m_G by means of a χ^2 optimisation based on an educated guess of the relevant theory error, cf. section 6.2.8.

Another issue which often hinders the determination of M_G is the proximity of the unification and Planck scales which usually makes it impossible to neglect entirely the Planck-suppressed effective operators, especially those that, in the broken phase, make the gauge kinetic terms depart from their canonical form. In the canonical basis, these then yield yet another source of out-of-control shifts in the GUT-scale matching conditions, i.e. smear the single-point gauge unification picture yet further, see for instance [105] and references therein. A simple back-of-the-envelope calculation reveals that in most cases such effects are again comparable to those of the two-loop contributions in the gauge beta functions. Furthermore, the real cut-off Λ associated to the quantum gravity effects may be further reduced below the Planck scale if the number of propagating degrees of freedom above is very large, cf. [246].

Since none of these issues may be addressed without a thorough analysis of the coupled system of the two-loop renormalization group equations augmented with a detailed information about the high-scale spectrum (and, possibly, even quantum gravity), in what follows we shall consider a unification pattern to be fine if the effective $\overline{\rm MS}$ running gauge couplings do converge to a small region characterised by a certain "radius" in the "$t-\alpha^{-1}$ plot" (with $2\pi t \equiv \log(\mu/M_Z)$ and μ denoting the $\overline{\rm MS}$ regularization scale). Note that, in practice, we shall perform a χ^2-analysis of the gauge coupling RG evolution pattern with three essentially free parameters at play, namely, m_{LR} (denoting the LR-scale where the part of the spectrum that restores the $SU(2)_R$ gauge symmetry is integrated in), m_G (the scale of the assumed intersection of the relevant effective gauge couplings of the intermediate-scale LR model) and α_G (the unified "fine structure" coupling); with these three degrees of freedom, however, an ideal fit of all three SM effective gauge couplings, i.e., α_s, α_L and α_Y, is (almost) always achievable. Hence, we shall push the χ^2-analysis further in attempt to assess the role of the theoretical uncertainties in the possible future determination of these three parameters that may be obtained in several different ways, cf. Sect. 6.2.8.

Proton lifetime

There are in general many ingredients entering the proton lifetime predictions in the grand unification context with very different impact on their quality and accuracy. Barring the transition from the hadronic matrix elements to the hard quark-level correlators (assumed to be reasonably well under control by the methods of the lattice QCD and/or chiral Lagrangian techniques), these are namely the masses of the mediators underpinning the effective BNV operators. At the $d = 6$ level, these are namely the notorious GUT-scale X and Y (and/or X' and Y') gauge bosons, and also the three types of potentially dangerous scalars $\Phi_{3,1,-1/3}$, $\Phi_{3,1,-4/3}$ and $\Phi_{3,3,-1/3}$ (descending from the fields nr. 9, 10, 14 and 19 in table B.5) with direct Yukawa couplings to matter. In both cases, the flavour structure of the relevant BNV currents is the central issue that can hardly be ignored in any dedicated proton lifetime analysis. From this point of view, the gauge-driven p-decay is usually regarded to as being under a better control because it depends only on the (unified) gauge coupling and a set of *unitary* matrices encoding transitions from the defining to the mass bases in the quark and lepton sectors (whose matrix elements, barring cancellations, are typically $\mathcal{O}(1)$) while the scalar BNV vertices are governed by the Yukawa couplings and, thus, are often (unduly) expected to be suppressed for the processes involving the first generation quarks and leptons. In either case, a detailed study of the flavour structure of the BNV currents is far beyond the scope of the current study; the best one can do then is to assume conservatively the gauge channels' dominance and suppose that the elements of the underlying unitary matrices are of order 1.

However, in theories with accidentally light (TeV-scale) states one should not finish at the $d = 6$ level but rather consider also $d > 6$ BNV transitions that may be induced by such "unusual" scalars. To this end, let us just note that the emergence of $d = 7$ baryon number violating operators has been recently discussed in some detail in [248] (see also [91, 249]) and a specific set of scalars (in particular, $\Phi_{3,2,1/6}$, $\Phi_{3,2,7/6}$ and $\Phi_{3,1,2/3}$) underpinning such transitions in $SO(10)$ GUTs has been identified. Nevertheless, in the relevant graphs these fields are often accompanied by the "usual" $d = 6$ scalars above and, thus, for acceptable $d = 6$ transitions the $d = 7$ BNV operators tend to be also suppressed so we shall not elaborate on them any further. Since neither these issues may be handled without a very detailed analysis of a specific scenario, for the sake of the simple classifica-

tion of potentially viable settings intended for the next section we shall stick to the leading order (i.e., $d = 6$) purely gauge transitions and implement the current SK constraint of $\tau_{p\to\pi^0 e^+} \gtrsim 10^{34}$ years [250]. This will be imposed through the simple phenomenological formula

$$\Gamma_p \approx \alpha_G^2 m_p^5/m_G^4\,, \tag{6.42}$$

which, technically, provides a further input to the χ^2 analysis in section 6.2.8. We shall also ignore all the effects related to pulling the effective $d = 6$ operators from m_G down to the electroweak scale, see, e.g., [251, 252, 253].

6.2.5 Low scale left-right models

We will start our discussion with the simplest class of models with only one new intermediate scale, which we will denote by m_{LR}. Later on we will also discuss the possibility to have a "sliding" LR scale "on top" of a SM-group stage with extended particle content. These latter models are slightly more complicated in their construction than the minimal ones, but interesting since they are reminiscent of the supersymmetric sliding models discussed in [2, 33].

We do not discuss the breaking of $SO(10)$ to the left-right group in detail and only mention that $SO(10)$ can be broken to the LR group either via the interplay of VEVs from a **45** and a **54**, as done for example in [217], or via a **45** and a **210**, an approach followed in [32]. In the left-right symmetric stage we consider all irreducible representations, which can be constructed from $SO(10)$ multiplets up to dimension **126**. The reason for considering multiplets up to the **126** is simply because the right triplet, $\Phi_{1,1,3,-2}$, which presents one of the two simplest possibilities to break the LR group correctly, comes from the **126** in the $SO(10)$ stage. Thus, we allow for a total of 24 different representations (plus conjugates), in our lists of models. Larger multiplets could be easily included, but lead of course to more elaborate models. The transformation properties of all our allowed multiplets under the LR group and their $SO(10)$ origin are summarized in table B.5 of the appendix.

In this section, we will keep the discussion mostly at the 1-loop level for simplicity. Two-loop β-coefficients can be easily included, but do not lead to any fundamental changes in the models constructed. Recall that at 1-loop order two copies of a complex scalar give the same shift in the β-coefficients $\Delta(b_i)$ as one copy of a

Weyl fermion. The coefficients for scalars and fermions differ at two-loop order, of course, but these differences are too small to be of any relevance in our model constructions considering current uncertainties, see section 6.2.8.

6.2.6 "Minimal" models

Consider gauge coupling unification first. At 1-loop level, the evolution of the inverse gauge couplings can be written as:

$$\alpha_i^{-1}(t) = \alpha_i^{-1}(t_0) + \frac{b_i}{2\pi}(t - t_0), \tag{6.43}$$

where $t_i = \log(m_i)$, as usual. Here, the β-coefficients in the different regimes are given as:

$$\begin{aligned} \left(b_3^{SM}, b_2^{SM}, b_1^{SM}\right) &= (-7, -19/6, 41/10)\,, \\ \left(b_3^{LR}, b_2^{LR}, b_R^{LR}, b_{B-L}^{LR}\right) &= (-7, -3, -3, 4) + \\ &\quad \left(\Delta b_3^{LR}, \Delta b_2^{LR}, \Delta b_R^{LR}, \Delta b_{B-L}^{LR}\right), \end{aligned} \tag{6.44}$$

where we have used the canonical normalization for $(B-L)$ related to the physical one by $(B-L)^c = \sqrt{\frac{3}{8}}(B-L)^p$. Here, Δb_i^{LR} stand for the contributions from additional fields, not accounted for in the SM, while the coefficients for the groups $SU(2)_L \times SU(2)_R$ include the contribution from one bi-doublet field, $\Phi_{1,2,2,0}$. We decided to include this field in the b_i^{LR} directly, since the SM Higgs $h = \Phi_{1,2,1/2} \in \Phi_{1,2,2,0}$ in all our constructions.

Next, recall the matching condition

$$\alpha_1^{-1}(m_{LR}) = \frac{3}{5}\alpha_R^{-1}(m_{LR}) + \frac{2}{5}\alpha_{B-L}^{-1}(m_{LR}). \tag{6.45}$$

Eq. (6.45) allows us to define an artificial continuation of the hypercharge coupling α_1^{eff} into the LR stage. The β-coefficient of this dummy coupling for $E > m_{LR}$ is $\frac{3}{5}b_R^{LR} + \frac{2}{5}b_{B-L}^{LR}$ and its definition allows us to find the GUT scale simply from the equality of three couplings, since the splitting between α_R and α_{B-L} at the m_{LR} scale is a free parameter.

Finding a model which unifies correctly, then simply amounts to calculating a set of consistency conditions on the $\Delta(b_i^{LR})$, which can be derived from eq. (6.43), by

equating $\alpha_1^{eff} = \alpha_2$ and $\alpha_2 = \alpha_3$. Two examples, for which a correct unification is found with a low value of m_{LR} are shown in fig. 6.14. Note that, the model to the left has a rather low unification scale (while the one to the right has a rather high one). The half-life for proton decay in the best fit point at 1-loop level (at 2-loop level) for the model on the left is estimated to be $T_{1/2} \simeq 10^{33}$ y ($T_{1/2} \simeq 10^{31}$ y), below the lower limit from Super-K [254, 250]. This will be important in the discussion on the error bar for proton decay in section 6.2.8 and is a particular feature of all model constructions without additional coloured fields, see below.

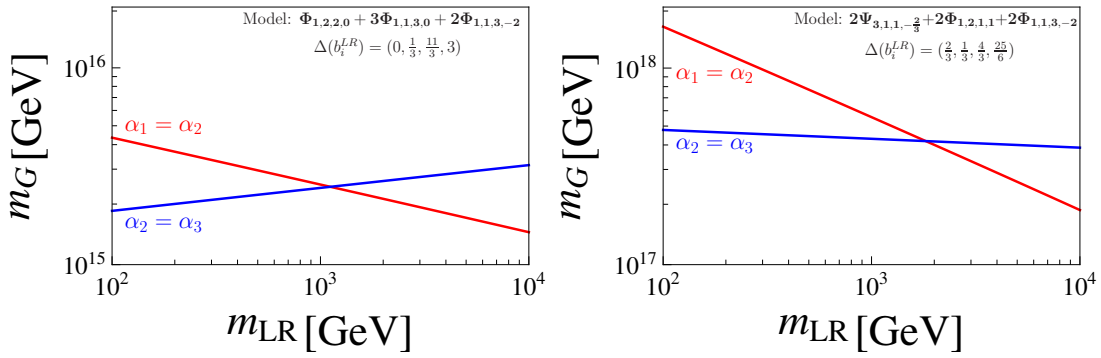

Figure 6.14: Two example models for which correct unification is found for a low value of the scale m_{LR}. The model to the left has a rather low unification scale, see text. Note that these are the same two models already shown in fig. 6.13 in the introduction.

As discussed in the previous section, we then require a number of additional conditions for a model to be both, realistic and phenomenologically interesting: (i) all models must have the agents to break the LR symmetry to the SM group; (ii) all models must contain (at least) one of the minimal ingredients to generate a realistic CKM and generate neutrino masses and angles; (iii) models must have perturbative gauge couplings all the way to m_G; (iv) m_G should be large enough to prevent too rapid proton decay, numerically we have used (somewhat arbitrarily) $m_G \geq 10^{15}$ GeV as the cut-off in our search; and, lastly (v) the predicted m_{LR} should be low enough such that at least some of the new fields have masses accessible at the LHC. As the cut-off in the search we used, again somewhat arbitrarily, $m_{LR} = 10$ TeV. [16]

[16]For both, m_G and m_{LR} the values quoted are only the limits used in the search for models.

Before discussing the different model classes, we first ask the question how involved our constructions are. Different criteria can be defined for comparing the complexity of different models, perhaps the two simplest ones are: (i) n_f: the number of additional different kinds of fields introduced and (ii) n_c: the total number of new fields introduced. Consider first the classical, "minimal" high-scale LR models, mentioned already in the introduction. As shown in table 6.4 the mLR [241, 170, 45] introduces only 2 kind of fields, each with only one copy for a total of 2 new fields, while the mΩLR already needs 5 different fields. However, a realistic model should not only try to minimize the number of new fields, it should also fulfil basic phenomenological constraints discussed previously. On this account, we would not consider the mLR a valid model, since it has a trivial CKM at tree-level, while the mΩLR is excluded (or at least at the boundary of being excluded [17]) by the constraints from the proton decay half-life. The model mmΩLR (more-minimal ΩLR), on the other hand, can pass the phenomenological tests, with only (n_f,n_c)=(3,3). However, this model does not have $g_L = g_R$ ("exact parity") at the scale where the LR symmetry is broken and exact parity symmetry was required in most constructions of LR models, that we have found in the literature. The question whether exact parity ("manifest") LR symmetry is a more important requirement for a "good" model than having the smallest possible number of new fields clearly is more a matter of taste than a scientific measure. We decided not to insist on exact parity and instead construct models with the fewest number of total fields possible. The models we construct then can be separated into two different classes: (a) models in which a realistic CKM is generated by the extension of the scalar sector and (b) models in which a realistic CKM is generated by the extension of the fermion sector.

Model class [a]: "Scalar" CKM models

Consider first models of class (a). The breaking the LR group can be either achieved via a right triplet, $\Phi_{1,1,3,-2}$ (case [a.1]), or by a (right) doublet, $\Phi_{1,1,2,-1}$ (case [a.2]), as discussed in the previous section. Several examples of simple models for both classes are given in table 6.4.

Consider the triplet case first. The minimal field content for the triplet case con-

Whether a particular model survives the constraints from proton decay searches depends not only on the values of m_G and α_G but also on their uncertainties, see section 6.2.8.

[17] See the discussion in section 6.2.8.

Name	Configuration	n_f	n_c	parity?	CKM?	m_{LR} [GeV]	$T_{1/2}$ [y]
mLR	$\Phi_{1,1,3,-2} + \Phi_{1,3,1,-2}$	2	2	✓	☹	$3 \cdot 10^{10}$	$10^{33\pm2.5}$
mΩLR	$\Phi_{1,2,2,0} + \Phi_{1,1,3,0} + \Phi_{1,3,1,0} + \Phi_{1,1,3,-2} + \Phi_{1,3,1,-2}$	5	5	✓	✓	$3 \cdot 10^{11}$	$10^{30.8\pm2.5}$
mmΩLR	$\Phi_{1,2,2,0} + \Phi_{1,1,3,0} + +\Phi_{1,1,3,-2}$	3	3	☹	✓	$3 \cdot 10^{9}$	$10^{34.3\pm2.5}$

Configuration	n_f	n_c	parity?	CKM?	m_{LR} [GeV]	$T_{1/2}$ [y]
$\Phi_{1,2,2,0} + \Phi_{1,1,3,0} + 3\Phi_{1,1,3,-2}$	3	5	☹	✓	$1 \cdot 10^{2}$	$10^{30.6\pm2.5}$
$\Phi_{1,2,2,0} + 3\Phi_{1,1,3,0} + 2\Phi_{1,1,3,-2}$	3	6	☹	✓	$2 \cdot 10^{3}$	$10^{31.3\pm2.5}$
$2\Phi_{1,2,2,0} + \Phi_{1,1,3,0} + \Phi_{8,1,1,0} + 2\Phi_{1,1,3,-2}$	4	6	☹	✓	$5 \cdot 10^{2}$	$10^{41.3\pm2.5}$
$3\Phi_{1,2,2,0} + \Phi_{1,1,3,0} + 3\Phi_{6,1,1,4/3} + 2\Phi_{1,3,1,-2} + \Phi_{3,1,2,-2}$	5	10	✓	✓	$4 \cdot 10^{2}$	$10^{36.3\pm2.5}$

Configuration	n_f	n_c	parity?	CKM?	m_{LR} [GeV]	$T_{1/2}$ [y]
$\Phi_{1,2,2,0} + 16\Phi_{1,1,2,-1}$	2	17	☹	✓	$1 \cdot 10^{4}$	$10^{31.6\pm2.5}$
$\Phi_{1,2,2,0} + \Phi_{1,1,2,-1} + 3\Phi_{1,1,3,-2}$	3	5	☹	✓	$2 \cdot 10^{3}$	$10^{31.3\pm2.5}$
$\Phi_{1,2,2,0} + \Phi_{1,1,2,-1} + \Phi_{1,1,3,-2} + \Phi_{3,1,3,-2/3}$	4	4	☹	✓	$2 \cdot 10^{3}$	???
$2\Phi_{1,2,2,0} + \Phi_{1,1,2,-1} + \Phi_{6,1,1,-4/3} + 2\Phi_{1,1,3,-2}$	4	6	☹	✓	$1 \cdot 10^{2}$	$10^{39.6\pm2.5}$
$\Phi_{1,2,2,0} + 2\Phi_{1,1,2,-1} + 2\Phi_{1,2,1,1} + \Phi_{8,1,1,0} + 10\Phi_{1,1,1,2}$	5	16	✓	✓	$3 \cdot 10^{3}$	$10^{41\pm2.5}$

Table 6.4: A comparison of some of the simplest possible LR models. Configuration gives the actual (extra) fields used in the model on top of the SM fields. n_f stands for #(fields) and counts how many different fields are used in the construction, while n_c is #(copies) and counts the total number of different copies of fields. "Parity?" gives whether a given model predicts $g_L = g_R$ and "CKM?" whether it has a non-trivial CKM matrix at tree-level, see the discussion in the previous section. m_{LR} gives the approximate best fit point (including 2-loop coefficients) for the scale of LR breaking, while $T_{1/2}$ [y] gives the estimated half-life for proton decay. The error bar quoted for $T_{1/2}$ is an estimation derived from the discussion in section 6.2.8. The first table gives "minimal" LR models for comparison: These models all have m_{LR} far above the EW scale. The second table gives models with low predicted m_{LR} and CKM generated by scalar triplets (model class [a.1]), while the 3rd gives model examples with CKM generated by right-doublets (model class [a.2]). For discussion see main text. The model containing the field $\Phi_{3,1,3,-2/3}$ does not give a proton decay half-life, since the scalar field $\Phi_{3,1,3,-2/3}$ can induce proton decay via an unknown Yukawa coupling.

sists in $n_{\Phi_{1,2,2,0}}\Phi_{1,2,2,0} + n_{\Phi_{1,1,3,0}}\Phi_{1,1,3,0} + n_{\Phi_{1,1,3,-2}}\Phi_{1,1,3,-2}$ and the simplest model we have found is given by $n_{\Phi_{1,2,2,0}} = 1$, $n_{\Phi_{1,1,3,0}} = 1$ and $n_{\Phi_{1,1,3,-2}} = 3$ for a total of $n_c = 5$ copies, followed by $n_{\Phi_{1,2,2,0}} = 1$, $n_{\Phi_{1,1,3,0}} = 3$ and $n_{\Phi_{1,1,3,-2}} = 2$ for a total of n_c=6. Both models have rather short proton decay half-lives, with the n_c=6 model doing slightly better than the n_c=5 model. For this reason we used the n_c=6 model in figs (6.13) and (6.14) and in section 6.2.8 for our discussion. Once additional new fields are allowed with non-zero coefficients, a plethora of models in this class can be found. Example models for each of the 24 fields are given in table B.6 in the appendix. Here, let us only briefly mention two more examples: $2\Phi_{1,2,2,0}+\Phi_{1,1,3,0}+\Phi_{8,1,1,0}+2\Phi_{1,1,3,-2}$ and $3\Phi_{1,2,2,0}+\Phi_{1,1,3,0}+3\Phi_{6,1,1,4/3}+2\Phi_{1,3,1,-2}+\Phi_{1,1,3,-2}$. The former shows (see discussion of fig. 6.15 below) that at the price of introducing one coloured field, the proton decay half-life constraint can be completely evaded, while the latter demonstrates that it is possible to obtain exact parity symmetry even with different number of copies of fields in the left and right sector of the model - at a price of a few additional copies of fields.

Consider now model class [a.2]: $n_{\Phi_{1,2,2,0}}\Phi_{1,2,2,0}+n_{\Phi_{1,1,2,-1}}\Phi_{1,1,2,-1}+\cdots$. In this case, in principle the simplest model possible consists in only two different fields, since $\Phi_{1,1,2,-1}$ can play the double role of breaking the LR symmetry and generating the non-trivial CKM, as explained in the previous section. However, as table 6.4 shows, our condition of having a low $m_{LR} \lesssim 10$ TeV enforces a large number of copies for this possibility: $n_{\Phi_{1,2,2,0}} = 1$, but $n_{\Phi_{1,1,2,-1}} = 16$, not a very minimal possibility. Table 6.4 also shows that with three different fields, much smaller multiplicities lead to consistent solutions. With 3 different fields a solution with n_c=5 exists, for four different fields n_c=4 is possible in one example. However, again, the example with n_c=5 has a rather short $T_{1/2}$, while the n_c=4 contains a copy of $\Phi_{3,1,3,-2/3}$. This field induces proton decay via a dimension-6 operator, see discussion in the previous section and thus does not lead to a realistic model, unless either the $\Delta(L) = 1$ or the $\Delta(B) = 1$ Yukawa coupling is eliminated by the imposition of some symmetry. The next simplest model then contains (n_f=4,n_c=5). This case, however, has a b.f.p. for the m_{LR} above our usual cutoff. Once we allow for (n_f=4,n_c=6) or larger, again many possibilities exist, one example is given in table 6.4. As for the case [a.1], models with exact parity are possible, but require a larger number of copies of fields.

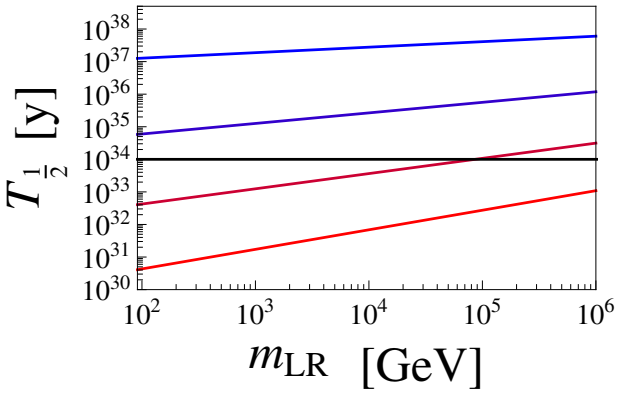

Figure 6.15: One-loop estimated proton lifetime for "colourless models" as a function of m_{LR}. The figure shows $T_{1/2}$ [y] estimated from m_G defined as the point where $\alpha_2 = \alpha_3$ with from top to bottom: $\Delta(b_2^{LR}) = 0$, $\frac{1}{6}$, $\frac{1}{3}$ and $\frac{1}{2}$ and $\Delta(b_3^{LR}) = 0$ ("colourless models"), see text. The horizontal line is the experimental limit from Super-K [250, 254].

Before closing this discussion on model class (a), we briefly comment on the comparatively low values for the proton lifetime for all cases in which *no coloured field* is added to the configuration. In the SM (with one Higgs and at 1-loop order) α_2 equals α_3 at a scale of roughly $m_{G_{23}} = 10^{17}$ GeV. Adding a second Higgs, as necessary to complete the bi-doublet in our LR models,[18] lowers this GUT scale to roughly $m_{G_{23}} = 2 \cdot 10^{16}$ GeV. Any addition of a field charged under $SU(2)_L$ increases b_2, leading to a further reduction in $m_{G_{23}}$, unless some coloured field is added at the same time. Thus, all models with a second $\Phi_{1,2,2,0}$ (or other fields charged under $SU(2)_L$) but no additional coloured particles will have a GUT scale below 10^{16} GeV. This is indeed quite an important constraint, as is shown in fig. 6.15. Recall, for a $\Phi_{1,2,1,1}$ the $\Delta(b_2^{LR}) = \frac{1}{6}$, while for $\Phi_{1,2,2,0}$ the $\Delta(b_2^{LR}) = \frac{1}{3}$. Thus, "colourless" models can have at most one additional $\Phi_{1,2,2,0}$, otherwise they are ruled out by proton decay constraints. We note, that the figure is based on a 1-loop calculation and that this conclusion is only strengthened, once 2-loop β coefficients are included, compare to the lifetimes quoted in table 6.4.

Configuration	n_f	n_c	parity?	CKM?	m_{LR} [GeV]	$T_{1/2}$ [y]
$2\Psi_{3,1,1,-2/3} + 2\Phi_{1,2,1,1} + 2\Phi_{1,1,3,-2}$	4	6	☹	✓	$3 \cdot 10^3$	$10^{40\pm5}$
$2\Psi_{3,1,1,-2/3} + 2\Phi_{1,1,2,-1} + \Phi_{1,2,2,0} + 4\Phi_{1,1,3,0}$	5	11	☹	✓	$1 \cdot 10^4$	$10^{39.9\pm2.5}$
$2\Psi_{3,1,1,-2/3} + 2\Phi_{1,1,2,-1} + 2\Phi_{1,2,1,1} + 4\Phi_{1,1,3,0}$	5	12	☹	✓	$9 \cdot 10^3$	$10^{39.9\pm2.5}$
$2\Psi_{3,1,1,-2/3} + \Phi_{1,2,1,1} + \Phi_{1,1,2,-1} + 9\Phi_{1,1,1,2}$	5	13	✓	✓	$1 \cdot 10^2$	$10^{43.4\pm2.5}$
$2\Psi_{3,1,1,4/3} + 3\Phi_{1,2,1,1} + \Phi_{1,1,3,-2} + \Phi_{3,1,1,4/3}$	5	7	☹	✓	$6 \cdot 10^3$	$10^{40\pm2.5}$
$2\Psi_{3,1,1,4/3} + 3\Phi_{1,2,1,1} + 5\Phi_{1,1,2,-1} + \Phi_{3,1,1,4/3}$	5	11	☹	✓	$1 \cdot 10^4$	$10^{40\pm2.5}$
$2\Psi_{3,2,1,1/3} + \Phi_{8,1,1,0} + 4\Phi_{1,1,3,-2}$	4	7	☹	✓	$1 \cdot 10^2$	$10^{43\pm2.5}$
$2\Psi_{3,2,1,1/3} + \Phi_{6,1,1,2/3} + 4\Phi_{1,1,3,-2}$	4	7	☹	✓	$1 \cdot 10^2$	$10^{39.3\pm2.5}$
$2\Psi_{3,2,1,1/3} + \Psi_{3,1,3,-2/3} + 6\Phi_{1,1,3,-2}$	4	9	☹	✓	$4 \cdot 10^3$	$10^{40.3\pm2.5}$

Table 6.5: A comparison of models with CKM generated by an extension in the fermion sector, "fermionic CKM" or "VLQ-CKM". In n_f we always count the two $\Psi_{3,i,j,k}$ as two separate fields, because both Ψ and $\bar{\Psi}$ are needed to generate the CKM.

Model class [b]: "Fermionic" CKM models

We now turn to a discussion of models with additional fermions, see table 6.5. As discussed in section 6.2.2, a non-trivial CKM can be generated in LR models with extensions in the fermion sector essentially by three kind of fields, corresponding to vector like copies of the SM fields u^c, d^c and Q. In the list of 24 different fields shown in table B.5 in the appendix, there are in fact several which contain states which can play the role of the VLQs after the breaking of the LR symmetry.

Consider, for example, the case of $u'^c = \Psi'_{\bar{3},1,-2/3}$. The $\Psi'_{\bar{3},1,-2/3}$ could be generated from $\Psi_{\bar{3},1,-2/3} \in \bar{\Psi}_{\bar{3},1,1,-4/3}$, $\bar{\Psi}_{\bar{3},1,2,-1/3}$ or $\bar{\Psi}_{\bar{3},1,3,2/3}$. Similarly, $d'^c = \Psi'_{\bar{3},1,1/3} \in \bar{\Psi}_{\bar{3},1,1,2/3}$, $\bar{\Psi}_{\bar{3},1,2,-1/3}$ or $\bar{\Psi}_{\bar{3},1,3,2/3}$, while $Q' = \Psi'_{3,2,1/6} \in \Psi_{3,2,1,1/3}$, $\Psi_{3,2,2,4/3}$, $\Psi_{3,3,1,-2/3}$ and $\Psi_{3,2,2,-2/3}$. In the SM regime, therefore, different terms from the LR regime can lead to the same effects. We will consider only the three simplest possibilities here, $\Psi'_{3,1,1,4/3}$, $\Psi'_{3,1,1,-2/3}$ and $\Psi'_{3,2,1,1/3}$, where we have marked the fields with a prime again to note that they have to be introduced in vector-like pairs. Other cases can be constructed in a similar manner. For these three fields the corresponding

[18] As in the MSSM, where a second Higgs doublet must be present.

Lagrangian terms in the LR-regime are:

$$\begin{aligned}\mathcal{L} &= m_{\Psi_{3,1,1,4/3}}\Psi'_{3,1,1,4/3}\bar{\Psi}'_{\bar{3},1,1,-4/3} + m_{\Psi_{3,1,1,-2/3}}\Psi'_{3,1,1,-2/3}\bar{\Psi}'_{\bar{3},1,1,2/3} \\ &+ m_{\Psi_{3,2,1,1/3}}\Psi'_{3,2,1,1/3}\bar{\Psi}'_{\bar{3},2,1,-1/3} + \bar{Y}_{\Psi_{3,1,1,4/3}}\bar{\Psi}'_{\bar{3},1,1,-4/3}\Phi_{1,2,1,1}\Psi_{3,2,1,1/3} \\ &+ Y_{\Psi_{3,1,1,4/3}}\Psi'_{3,1,1,4/3}\Phi_{1,1,2,-1}\Psi_{\bar{3},1,2,-1/3} + \bar{Y}_{\Psi_{3,1,1,-2/3}}\bar{\Psi}'_{\bar{3},1,1,2/3}\bar{\Phi}_{1,2,1,-1}\Psi_{3,2,1,1/3} \\ &+ Y_{\Psi_{3,1,1,-2/3}}\Psi'_{3,1,1,-2/3}\bar{\Phi}_{1,1,2,1}\Psi_{\bar{3},1,2,-1/3} + Y_{\Psi_{3,2,1,1/3}}\Psi'_{3,2,1,1/3}\Phi_{1,2,2,0}\Psi_{\bar{3},1,2,-1/3},\end{aligned} \tag{6.46}$$

where $\Psi_{3,2,1,1/3} = Q$ and $\Psi_{\bar{3},1,2,-1/3} = Q^c$ correspond to the SM left and right-handed quarks in the LR regime. Note, that $\Phi_{1,2,2,0}$ contains the SM-like VEV v_u, while for $\Psi_{3,1,1,4/3}$ and $\Psi_{3,1,1,-2/3}$ the corresponding mass terms are generated from the VEVs of $\Phi_{1,2,1,1}$ and $\Phi_{1,1,2,-1}$. Recall that, as discussed in section 6.2.2, not all terms are necessary and in principle two terms (one mass term and one Yukawa term) are sufficient in all cases to generate the desired structure.

In table 6.5 we give some simple example models for these cases: $\Psi'_{3,1,1,-2/3}$, $\Psi'_{3,1,1,4/3}$ and $\Psi'_{3,2,1,1/3}$. Here, we wrote 2Ψ for $\Psi + \bar{\Psi}$ simply to get a more compact table. Since we count these as two different kinds of fields and at least one $\Phi_{1,1,3,-2}$ or $\Phi_{1,1,2,-1}$ is needed to break the LR symmetry, the minimal n_f seems to be three in these constructions. However, once we impose $m_{LR} \lesssim 10$ TeV, no solution with n_f=3 survives, although there are many solutions with n_f=4 and 5. Perhaps the simplest case possible is the model in the first line, which fulfils all our conditions for the price of just two extra $\Phi_{1,1,2,1}$ and one extra $\Phi_{1,1,3,-2}$. In general, models which break the LR symmetry via $\Phi_{1,1,2,-1}$ need more copies of fields to get a consistent model with low m_{LR}, $n_c \geq 11$. Also, it is possible to conserve parity exactly, as the table shows. However, the model with the smallest n_c that we found still has n_c=13. We have not found any model with less than n_c=7 for the cases $\Psi'_{3,1,1,4/3} \to u^{c'}$ and $\Psi'_{3,2,1,1/3} \to Q'$.

In case of models with VLQs, the constraints from proton decay are relatively easy to fulfil, see table 6.5. This is simply due to the fact that VLQs add a non-zero $\Delta(b_3^{LR})$, by which m_G can be raised to essentially any number desired.

6.2.7 "Sliding" LR models

We now turn to the discussion of "sliding-LR" models. These are defined as models where the unification is independent of the intermediate scale m_{LR}. In (minimal)

supersymmetric extensions of the SM "sliding-LR" models are the only possibility to have a low m_{LR} [2, 32, 33]. However, as we show in this subsection, supersymmetry is *not* a necessary ingredient to construct sliding models.

We will discuss in the following just two examples of sliding LR models. The first one, based on the idea of "split" supersymmetry [29, 239], shows the relation of our non-supersymmetric sliding models, with the supersymmetric ones discussed in [2]. The second one is based on a SM extension with vector-like quarks, first mentioned in [30] and recently discussed in much more detail in [31]. This second example serves to show, how non-SUSY sliding models can be just as easily constructed as supersymmetric ones. The sliding conditions can be understood as a set of conditions on the allowed β coefficients of the gauge couplings in the LR regime [2], assuring that at 1-loop order $\Delta(\alpha_i)$ at the GUT scale are independent of the additional particle content in the LR regime. In order to achieve successful unification, therefore, it is necessary to first add to the standard model an additional field content at some scale m_{NP}. Although not necessary from a theoretical point of view, we require that m_{NP} is at a "low" scale, i.e. $m_{NP} \lesssim 10$ TeV, to ensure that the models predict some interesting collider phenomenology. We will call this additional field content "configuration-X" and "SM+X". A list of simple X-configurations, which when added to the SM at m_{NP} in the range m_{NP} (few) TeV lead to unification as precise or better than the one obtained in the MSSM, is given in table B.7 in the appendix. In this table (at least) one example for each one of our 24 fields is presented.

As the first example, we will discuss the "split SUSY-like" case, which corresponds to $X = 5\Phi_{1,2,1/2} + 2\Phi_{1,3,0} + 2\Phi_{8,1,0}$. As is well-known, in split SUSY the sparticle spectrum is "split" in two regimes: all scalars (squarks, sleptons and all Higgs fields except h^0) have masses at a rather high scale, typically 10^{10} GeV, while the fermions, gluino ($\Psi_{8,1,0}$), wino ($\Psi_{1,3,0}$), bino ($\Psi_{1,1,0}$) and the higgsinos ($\widetilde{H}_u = \Psi_{1,2,-1/2}$, and $\widetilde{H}_d = \Psi_{1,2,1/2}$) must have TeV-ish masses. This way GCU is maintained with a $\Delta(\alpha_i)$ at the GUT scale as small as is the case in the MSSM (but at a different value of α_G). However, while in split SUSY $\Phi_{1,2,1/2}$ is added at the high scale, for our LR constructions we will need this second Higgs at a low scale and, therefore, we call this scenario "split SUSY-like". Note that, while split SUSY uses fermions at the low scale, GCU can be maintained also with a

purely bosonic X, since only the 2-loop coefficients change (slightly), which can be compensated by a slight shift in m_{NP}. We note in passing that this particular X has, of course, all the interesting phenomenology of split SUSY, like a candidate for the dark matter, or a quasi-stable gluino at the LHC [29].

The quantum numbers of this particular particle content in the LR regime are then: $\Phi_{1,2,1/2} \in \Phi_{1,2,2,0}$, $\Phi_{1,3,0} \in \Phi_{1,3,1,0}$ and $\Phi_{8,1,0} \in \Phi_{8,1,1,0}$, with the Δb_i^{LR} coefficients corresponding to this particular X given by:

$$(\Delta b_3^{LR}, \Delta b_2^{LR}, \Delta b_R^{LR}, \Delta b_{B-L}^{LR}) = (2, 2, 2/3, 0). \tag{6.47}$$

Imposing now the requirement that m_G is independent of the intermediate scale m_{LR}, results in the set of conditions:

$$\Delta b_3^{LR} = \Delta b_2^{LR} \equiv \Delta b, \tag{6.48}$$

$$\Delta b_{B-L}^{LR} + \frac{3}{2}\Delta b_R^{LR} - 11 = \frac{5}{2}(\Delta b). \tag{6.49}$$

Obviously, many different sets of $\Delta b^{'}s$ can fulfil these conditions and also realize particle configurations that provide a realistic CKM. To provide just the simplest example, consider scalar CKM models, class [a.1]. These require at least one copy of $\Phi_{1,1,3,0}$ and $\Phi_{1,1,3,-2}$ each, as discussed in the previous subsection. The simplest sliding solution for this class is given by $\Phi_{1,1,3,0} + 4\Phi_{1,1,3,-2}$ with $\Delta b^{'}s = (0, 0, 10/3, 6)$ (and a $m_G = 2 \times 10^{16}$ GeV). In the LR regime we thus have SM (+ Higgs completed to one bi-doublet) particle content plus $\Psi_{1,2,2,0}+\Psi_{1,3,1,0}+\Psi_{8,1,1,0}+\Phi_{1,1,3,0} + 4\Phi_{1,1,3,-2}$. Fig. 6.16 shows the independence of the GCU from the value of m_{LR}. Note again, that GCU is lost, once m_{NP} is raised above a certain value, the b.f.p. for m_{NP}, including 2-loop coefficients, being $m_{NP} = 1.1$ TeV.

As in the case of the non-sliding solutions, of course it is also possible to construct sliding-LR models of class [a.2], the simplest 2-field solution is $2\Phi_{1,1,2,-1}+20\Phi_{1,1,1,2}$ with $\Delta b_i^{'} = (0, 0, 1/3, 21/2)$.

As mentioned above, unification in non-SUSY extensions of the SM have been studied already in [30]. A particular interesting example is the one studied in [31], which adds two kinds of VLQs to the SM particle content, namely $Q' = \Psi_{3,2,1/6}$ and $d'^c = \Psi_{\bar{3},1,1/3}$. This model could, potentially, explain the much discussed enhancement in $h \to \gamma\gamma$ [255, 256]. [19]

[19] The latest CMS data now gives much smaller $h \to \gamma\gamma$, see the web-page of CMS public results at: twiki.cern.ch/twiki/bin/view/CMSPublic/PhysicsResultsHIG.

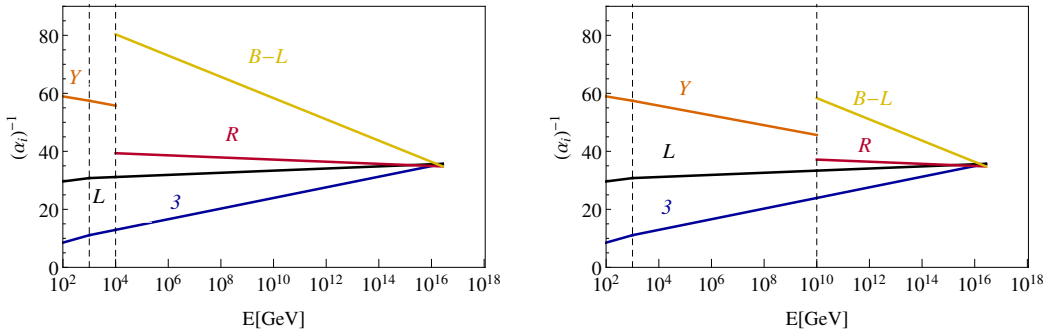

Figure 6.16: Evolution of the gauge couplings for the sliding-LR model example discussed in the text based on split SUSY. The plot to the left shows $m_{LR} = 10$ TeV, while the plot to the right has $m_{LR} = 10^{10}$ GeV.

As our second sliding-LR example, we thus choose $X = 2\Psi_{3,2,1/6} + 2\Psi_{3,1,1/3} + \Phi_{1,2,1/2}$, which in the LR regime corresponds to $X = 2\Psi_{3,2,1,1/3} + 2\Psi_{3,1,1,2/3}$, with the $\Phi_{1,2,1/2}$ used to complete the $\Phi_{1,2,2,0}$. The Δb_i^{LR} coefficients of this configuration are:

$$(\Delta b_3^{LR}, \Delta b_2^{LR}, \Delta b_R^{LR}, \Delta b_{B-L}^{LR}) = (2, 2, 0, 1). \tag{6.50}$$

The sliding conditions in this case are the same as above and the simplest solution following these conditions and allowing to break the LR symmetry correctly is: $2\Phi_{1,1,1,2} + 4\Phi_{1,1,3,-2}$, with $\Delta b_i' = (0, 0, 8/3, 7)$. The running of the inverse gauge couplings for this example is shown in fig. 6.17.

6.2.8 Uncertainties in new physics scale and proton half-life

One of the aspects of model building for new physics models, rarely discussed in the literature, are uncertainties. While ideally, of course, predictions such as the existence of new particles at the TeV scale should be testable over the whole range of the allowed parameter space, in reality most model builders content themselves with showing that for some particular choice of parameters consistent solutions for their favorite model exist. In this section we discuss uncertainties for the predictions of our LR models. In these models, once we have fixed the particle content of a particular version, there are essentially three free parameters: m_{LR}, m_G and

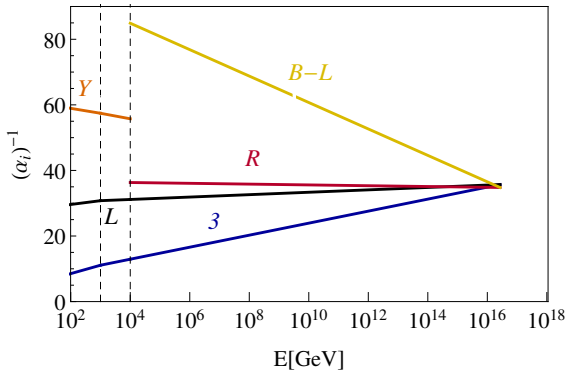

Figure 6.17: Evolution of the inverse gauge couplings in the second example of sliding-LR models: $2\Psi_{3,2,1,1/3} + 2\Psi_{3,1,1,2/3} + 2\Phi_{1,1,1,2} + 4\Phi_{1,1,3,-2}$. This example is non-SUSY and with a CKM explained by VLQs (class [b]).

α_G. However, since there are also three gauge couplings, with values fixed by experiment, for any given model m_{LR}, m_G and α_G are fixed up to some error by the requirement of gauge coupling unification. This results essentially in two predictions: First, the mass scale, where the gauge bosons of the extended gauge sector and (possibly) other particles of the model should show up. This scale coincides, of course, with the range of m_{LR}, as derived from the fit. And, second, derived from m_G and α_G, we obtain a range for the predicted half-life of proton decay.

The analysis of this section uses a χ^2 minimization, which fits the three measured SM gauge couplings as functions of the three unknowns. We start by discussing the error budget. The total error budget can be divided into a well defined experimental error plus a theory error. For the experimental input we use [100]:

$$\begin{aligned} \alpha_1^{-1} &= 58.99 \pm 0.020 \\ \alpha_2^{-1} &= 29.57 \pm 0.012 \\ \alpha_3^{-1} &= 8.45 \pm 0.050 \ . \end{aligned} \tag{6.51}$$

The experimental errors quoted are at the 1-σ confidence level (CL). Note especially the small value of $\Delta(\alpha_3^{-1})$, according to [100], compared to the older value of $\Delta(\alpha_3^{-1}) \simeq 0.14$ [257].

Much more difficult to estimate is the theory error. In our discussion presented in section (6.2.5) we have used 1-loop β-coefficients for simplicity. Two-loop β-coefficients for general non-supersymmetric theories, have been derived long ago [258, 259], see also [260], and can be easily included in a numerical analysis. However, a *consistent* 2-loop calculation requires the inclusion of the 1-loop thresholds from both, light states at the LR-scale and heavy states at the GUT scale. While we do fix in our constructions the particle content in the LR-symmetric phase, we have not specified the Higgs content for the breaking of $SO(10)$ to the LR group in detail. Thus, the calculation of the GUT scale thresholds is not possible for us, even in principle. The ignorance of the thresholds should therefore be included as (the dominant part of) the theoretical error, once two-loop β-coefficients are used in the calculation.

The 1-loop thresholds are formally of the order of a 2-loop effect and, thus, it seems a reasonable guess to estimate their size by a comparison of the results using 1-loop and 2-loop β coefficients in the RGE running. This, however, can be done using different assumptions. We have tried the following four different definitions for the theory error:

- (i) Perform a χ^2_{min} search at 1-loop and at 2-loop. Consider the difference $\Delta(\alpha_G^{-1})^{\rm th} \simeq |(\alpha_G^{-1})^{(1-{\rm loop})} - (\alpha_G^{-1})^{(2-{\rm loop})}|$ as the theoretical error, common to all α_i.

- (ii) Perform a χ^2_{min} search at 1-loop and at 2-loop. Calculate $\Delta(\alpha_i^{-1})^{\rm th} \simeq |(\alpha_i^{-1})^{\rm exp} - (\alpha_i^{-1})^{(2-{\rm loop})}|$ using $m_G^{1-{\rm loop}}$ as the starting point, but keeping the m_{LR} and α_G^{-1} from the 2-loop calculation. This generates $\Delta(\alpha_i^{-1})^{\rm th}$ which depend on the group i, but does not take into account the overall shift on α_G^{-1} caused by the change from 1-loop to 2-loop coefficients.

- (iii) Perform a χ^2_{min} search at 1-loop and at 2-loop. Calculate $\Delta(\alpha_i^{-1})^{\rm th} \simeq |(\alpha_i^{-1})^{\rm exp} - (\alpha_i^{-1})^{(2-{\rm loop})}|$ using $m_G^{1-{\rm loop}}$ *and* $(\alpha_G^{-1})^{1-{\rm loop}}$ as the starting point, but keeping the m_{LR} from the 2-loop calculation. This takes into account both, the shift of m_G and α_G^{-1} from 1-loop to 2-loop calculation.

- (iv) Perform a χ^2_{min} search at 1-loop. For the b.f.p. of m_G, α_G^{-1} and m_{LR} found, calculate the values of $(\alpha_i^{-1})^{(2-{\rm loop})}$. Use $\Delta(\alpha_i^{-1})^{\rm th} \simeq |(\alpha_i^{-1})^{\rm exp} - (\alpha_i^{-1})^{(2-{\rm loop})}|$ as the error. One should expect this definition to give, in

principle, the most pessimistic error estimate. See, however, the discussion below.

Def.:	$\Delta(\alpha_1^{-1})$	$\Delta(\alpha_2^{-1})$	$\Delta(\alpha_3^{-1})$	$\overline{\Delta}(\alpha^{-1})$
(i)	0.76	0.76	0.76	0.76
(ii)	0.57	0.41	1.18	0.72
(iii)	1.31	0.34	0.40	0.68
(iv)	1.21	0.41	0.40	0.67
Def.:	$\Delta(\alpha_1^{-1})$	$\Delta(\alpha_2^{-1})$	$\Delta(\alpha_3^{-1})$	$\overline{\Delta}(\alpha^{-1})$
(i)	0.86	0.86	0.86	0.86
(ii)	0.46	0.46	1.18	0.70
(iii)	1.30	0.39	0.30	0.66
(iv)	1.11	0.44	0.22	0.59

Table 6.6: Example shifts ("errors") in $\Delta(\alpha_i^{-1})$ for the particular models: SM + $\Phi_{1,2,2,0} + 3\Phi_{1,1,3,0} + 2\Phi_{1,1,3,-2}$ (left) and SM + $2\Psi_{3,1,1,-2/3} + 2\Phi_{1,2,1,1} + 2\Phi_{1,1,3,-2}$ (right), see also fig. 6.13, determined using the four different methods defined in the text. $\overline{\Delta}(\alpha^{-1})$ is the mean deviation.

Example shifts ("errors") in $\Delta(\alpha_i^{-1})$ determined by the four different methods defined above and for two particular models, discussed in previous sections, are given in table 6.6. The first and most important observation is that the theory errors estimated in this way are always much larger than the experimental errors on the gauge couplings. We would like to stress, however, that in absolute terms $\Delta(\alpha_G^{-1})^{\text{th}} \simeq 0.5$ corresponds only to a $1 \div 2$ % shift in the value of α_G^{-1}, depending on the model. It is found that all four methods lead to very similar $\overline{\Delta}(\alpha^{-1})$, but which of the couplings is assigned the smallest error depends on the method and on the model.

Perhaps more surprising is that method (iv) in the examples shown in the table *does not* automatically lead to the largest $\Delta(\alpha_i^{-1})$ nor to the largest average error, $\overline{\Delta}(\alpha^{-1})$, in these examples [20]. We can attribute this somewhat unexpected result

[20]For the MSSM method (iv) indeed leads to the largest $\Delta(\alpha_i^{-1})$, see below.

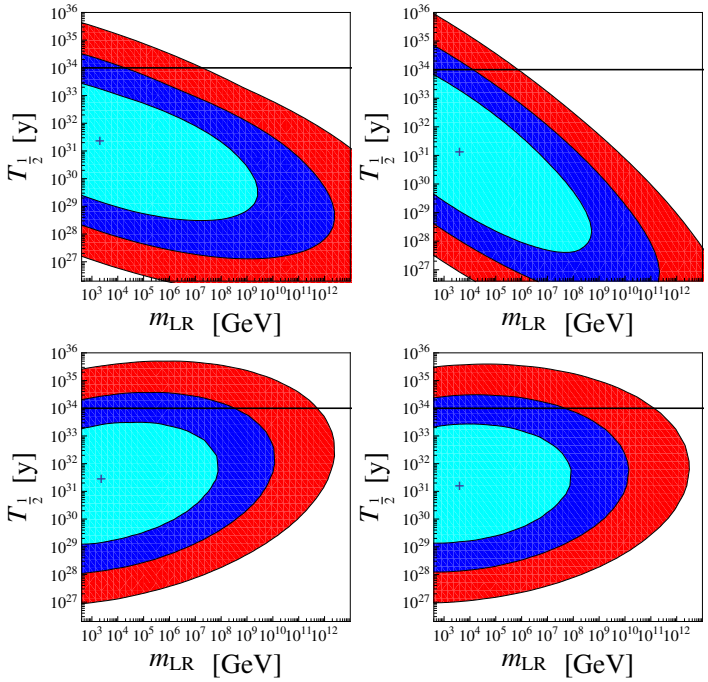

Figure 6.18: Contour plot of the χ^2 distribution in the plane $(m_{LR}, T_{1/2})$ for the model: SM + $\Phi_{1,2,2,0} + 3\Phi_{1,1,3,0} + 2\Phi_{1,1,3,-2}$, using the four different approaches to estimate the theoretical error, defined in the text: Top row: (i) left and (ii) right, bottom row (iii) left and (iv) right. The cyan (blue, red) region corresponds to the allowed region at 68 % (95 % and 3-σ) CL. In all four cases the model is ruled out by proton decay constraints at one sigma, but allowed at 2-σ CL. For further discussion see text.

to the correlated shifts induced by the simultaneous change in m_{LR} and m_G in method (iv), which can even conspire in some models to give an unrealistically small deviation in one particular coupling, see the value of $\Delta(\alpha_3^{-1})$ in the second model shown in table 6.6, for example.

In fig. 6.18 we then show the χ^2 distributions using the four different set of values of $\Delta(\alpha_i^{-1})$ for the model used in the left panel of table 6.6. Here, the $\chi^2_{\rm min}$ (denoted by the cross) and the corresponding 1, 2- and 3-σ CL contours are shown in the plane $(m_{LR}, T_{1/2})$, where $T_{1/2}$ is the proton decay half-life estimated via eq. (6.42). While at first glance, the different methods seem to produce somewhat different

results, a closer inspection reveals that the two main conclusions derived from this analysis are in fact independent of the method. First, in all four methods the model is excluded by the lower limit for the proton decay half-live from Super-K [254, 250] data at the one sigma level, but becomes (barely) allowed at 2-σ CL. And, second, while the model has a preferred value for the m_{LR} scale within the reach of the LHC, the upper limit on m_{LR} - even at only 1-σ CL! - is very large, between $[5\times10^7, 2\times10^9]$ GeV depending on the method. The model could therefore be excluded by (a) a slight improvement in the theoretical error bar or (b) from an improved limit on the proton decay, but not by direct accelerator searches. This latter conclusion is, of course, not completely unexpected, since the value of m_{LR} enters in the analysis only logarithmically as the difference between m_G and m_{LR}. As fig. 6.18 shows, in three of the four methods the error in the determination of the $T_{1/2}$ is around $2 \div 2.5$ orders of magnitude at one sigma, while in method (ii) - due to the correlation with m_{LR} - we find approximately $T_{1/2} = 10^{31+2.8-3.5}$ y. This is mainly due to a change in the GUT scale, when going from the 1-loop to the 2-loop β-coefficients. Note, that the value of m_G enters in the fourth power in the calculation of $T_{1/2}$; thus, an error of a factor of 100 corresponds only to a shift of a factor of $\Delta(m_G) \simeq 3$ in the GUT scale.

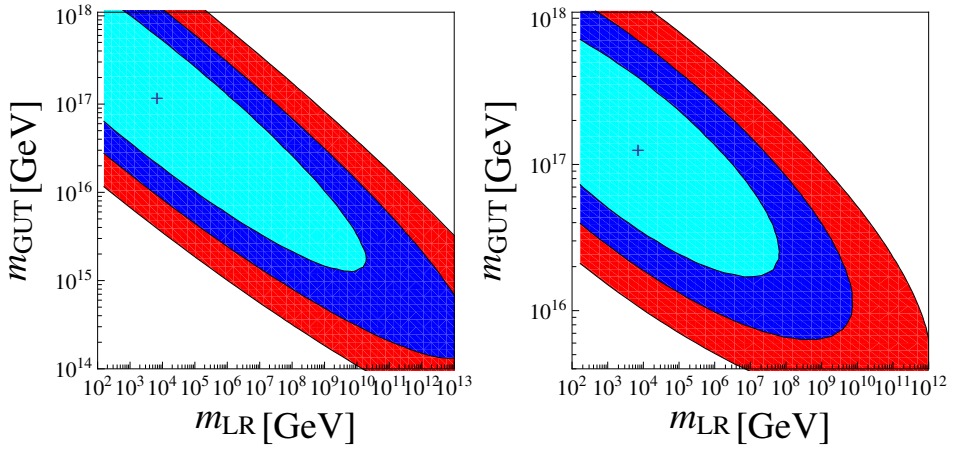

Figure 6.19: Contour plot of the χ^2 distribution in the plane (m_{LR}, m_G) for the model: SM + $2\Psi_{3,1,1,-2/3} + 2\Phi_{1,2,1,1} + 2\Phi_{1,1,3,-2}$, using the four different approaches to estimate the theoretical error, defined in the text: (i) left and (iv) right. Methods (ii) and (iii) lead to results similar to (i) and (iv), respectively, and are therefore not shown.

In fig. 6.19 we show the χ^2 distributions, for the model on the right panel of table 6.6, using two of the four methods for determining $\Delta(\alpha_i^{-1})$ of table 6.6. The plots for methods (ii) and (iii) lead to results similar to (i) and (iv), respectively, and are therefore not shown. Again, m_{LR} is only very weakly constrained in this analysis, but for this model, the b.f.p. of the GUT scale is much larger, around $m_G \simeq 10^{17}$ GeV, so proton decay provides hardly any constraints on this model. Note the strong correlation between m_{LR} and m_G in the plot on the left, which leads to a much larger "error" bar in the predicted range of the proton decay half-life for this model, roughly 5 orders of magnitude at one sigma CL.

We have repeated this exercise for a number of different LR models [21], see the appendix and discussion in the previous section and have always found numbers of similar magnitude. We have checked, however, that these "large" shifts in $\Delta(\alpha_i^{-1})$ *are not a particular feature of our LR models.* For this check we have calculated $\Delta(\alpha_G^{-1})^{\rm th}$ also for a number of models with only the SM group up to the GUT scale (see appendix). There, instead of m_{LR} we used the energy where the new particles appear, call it m_{NP}, as a free parameter. Very similar values and variations for $\Delta(\alpha_i^{-1})^{\rm th}$ are found in this study too. It may be interesting to note that the smallest $\Delta(\alpha_G^{-1})^{\rm th}$ we found corresponds to a model which is essentially like split supersymmetry [22] with a $\Delta(\alpha_G^{-1})^{\rm th}$ of only $\Delta(\alpha_G^{-1})^{\rm th} \simeq 0.25$. (In methods (ii)-(iv) the $\Delta(\alpha_G^{-1})^{\rm th}$ vary for this model between 0.05 and 0.78 with a mean of 0.55.) On the other hand, for the MSSM we find a $\Delta(\alpha_G^{-1})^{\rm th} \simeq 0.82$ and values of $\Delta(\alpha_i^{-1})^{\rm th}$ even up to $\Delta(\alpha_i^{-1})^{\rm th} \simeq 2$, depending on which of our four methods is used. Thus, the uncertainties discussed in this section should apply to practically all new physics models, which attempt to achieve GCU.

Reducing the theory error on α_i^{-1} will be possible only, if thresholds are calculated at *both new physics scales, m_{LR} and m_G.* Since this task is beyond the scope of the present work, in fig. 6.20 we show plots as a function of the unknown theory error $\Delta(\alpha^{-1})$. The model considered is excluded by the proton decay constraint at 2-σ CL up to an error of roughly $\Delta(\alpha^{-1}) \simeq 0.6$, indicating that even a minor improvement in the theory error can have important consequences for all models with a relatively low GUT scale, say $m_G \sim (1-3) \times 10^{15}$ GeV. On the other hand,

[21] Among them the two "minimal" LR models discussed in the introduction.

[22] This is the first example of SM+X configurations discussed in section 6.2.7.

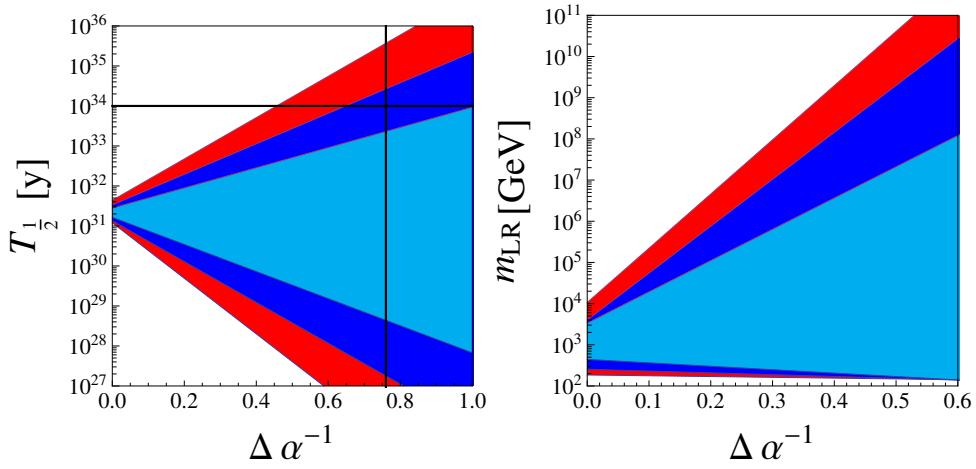

Figure 6.20: Allowed range cyan (blue, red) of $T_{1/2}$ (left) and m_{LR} (right) at 1-, 2- and 3-σ CL as a function of the error in $\Delta(\alpha^{-1})$. The plot is for the model SM + $\Phi_{1,2,2,0}+3\Phi_{1,1,3,0}+2\Phi_{1,1,3,-2}$. The horizontal line in the left plot is the experimental lower limit [254, 250], while the vertical line at $\Delta(\alpha^{-1}) = 0.76$ corresponds to the estimated uncertainty in this model using method (i).

in order to be able to fix the LR-scale to a value low enough such that accelerator tests are possible, requires a much smaller theory error. The exact value of this "minimal" error required depends on the model, but as can be seen from fig. 6.20 theory errors of the order of $\Delta(\alpha_i^{-1}) \lesssim 0.1$ will be necessary.

6.2.9 Summary and conclusions

In this work we attempted to construct a comprehensive list of non-SUSY models with LR-symmetric intermediate stage close to the TeV scale that may be obtained as simple low-energy effective theories within a class of renormalizable non-SUSY SO(10) grand unifications assuming some of the components of scalar representations with dimensions up to 126 to be accidentally light. In order to make our way through the myriads of options we assumed that all such light fields (besides those pushed down by the need to arrange for the low LR breaking scale) necessary to maintain the SO(10)-like gauge coupling unification are clustered around the same (TeV) scale.

Remarkably enough, the vast number of settings that pass all the phenomenological constraints (in particular, the compatibility with the quark and lepton masses and mixings, the current proton lifetime limits, perturbativity and gauge coupling unification) can be grouped into a relatively small number of types characterised, in our classification, by the extra fields underpinning the emergence of the SM flavour structure. Needless to say, the popular low-scale LR alternatives to the MSSM such as, e.g., split-SUSY, simple extensions of the mLR and/or mΩLR models, are all among these.

In the second part of the study we elaborate in detail on the theoretical uncertainties affecting the possible determination of (not only) the LR scale from the low-energy observables focusing namely on the impact of different definitions of the χ^2 reflecting the generic incapability of the simplistic bottom-up approach to account for most of the details of the full top-down analysis. To this end, we perform a numerical analysis of a small set of sample scenarios to demonstrate how difficult it is in general to extrapolate the low-energy information over the "desert" to draw any strong conclusion about the viability of the underlying unified theory without a detailed account for, e.g., the GUT-scale thresholds and other such high-scale effects. Nevertheless, within the bottom-up approach employed in this study the character of our results is inevitably just indicative and further improvements are necessary before drawing any far-fetched conclusions. To this end, the simple classification of the basic potentially realistic schemes given in Sect. 6.2.5 may be further improved in several directions, among which perhaps the most straightforward are, e.g., the viability of arranging the considered spectra in specific SO(10) GUTs, their perturbativity beyond the unification scale, etc.

6.3 $SO(10)$ and Dark Matter

Several astrophysical observations seem to indicate that the luminous matter in the Universe is just a tiny fraction of its total content. While the dark matter (DM) has not been directly detected, its gravitational effects have been observed, ranging from the inner kiloparsecs of galaxies out to some Mpc scales. The most relevant DM observations come from the rotational speed of galaxies (circular velocities of stars and gas as a function of their distance from their galactic centers), gravitational lensing, the cosmic microwave background and other extragalactic

measurements.

However, until now, the nature of the DM is still unknown. A widely studied candidate is the Weakly Interacting Massive Particle (WIMP) which interact weakly with ordinary matter and are electrically neutral. A plethora of *non-baryonic* DM candidates have been proposed, some of these are:
- *Neutralino:* If R-parity is conserved, the lightest supersymmetric particle (LSP) is stable and would provide a natural candidate for DM. The LSP neutralino (normally the lightest supersymmetric particle, a superposition of the superpartners of the gauge bosons and the Higgs bosons), is probably the best WIMP candidate.
- *Axions:* which can be efficiently produced through thermal and non-thermal processes in the early Universe under the form of cold, warm or even hot DM.
- *Gravitinos:* In models where the gravitino is the LSP, it is quite light (KeV) and thus, would be warm DM (WDM).

There are basically two ways to detect dark matter: direct and indirect detection. Direct searches detect DM particles by measuring nuclear recoils produced by DM elastic scattering [23]. Indirect DM searches try to detect the radiation produced in DM annihilations, i.e, the products of WIMP annihilations, such as gamma-rays, neutrinos, positrons, electrons and antiprotons. There are many experiments underway to attempt to detect WIMPs both directly and indirectly, whose sensitivity will be improved in the coming years. Direct detection experiments typically operate in deep under ground laboratories to reduce the background from cosmic rays. Experiment like XENON [261, 262] and LUX [263] will increase the sensitivity to Dark Matter Signals. Indirect detection experiments like PAMELA [264], EGRET [265] and the Fermi Gamma Ray Telescope search for the products (gamma rays) of WIMP annihilation or decay. Searches at LHC might provide some hints or even detect DM indirectly through missing energy searches.

Some other extended BSM scenarios can explain remarkably well DM too. Here, a discrete Z_2 symmetry must be added to stabilize the DM particle. On the other hand in GUT frameworks, for instance $SO(10)$, the Z_2 could be a remnant of the GUT group. In the next subsection we explain how these kind of scenarios are

[23] Another strategy for DM direct searches is the direct production of DM particles in laboratory experiments.

realized in $SO(10)$, discussing the possible DM candidates and configurations.

6.3.1 Dark Matter and GUTs

As is known, a discrete symmetry is needed to stabilize DM. It could be a remnant symmetry of the GUT group, in this case $SO(10)$. $SO(10)$ can be broken to the SM with an intermediate symmetry:

$$SO(10) \to SU(3)_c \times SU(2)_L \times SU(2)_R \times U(1)_{B-L}, \tag{6.52}$$

$U(1)_{B-L}$ can leave an Z_2 unbroken. This Z_2 is known as matter parity, denoted as M_p:

$$M_p = (-1)^{3(B-L)}. \tag{6.53}$$

A multiplet which belongs to the **16** and **144** $SO(10)$-reps is Z_2-odd and a multiplet which belong to the **45**, **54**, etc. $SO(10)$-reps is Z_2-even. Therefore for an extra field to be a possible candidate to dark matter must be either a or b:

a. An extra fermion charged even under $U(1)_{B-L}$.
b. An extra scalar charged odd under $U(1)_{B-L}$.

Table 2.2 shows the possible DM candidates contained in different $SO(10)$ representations up to the 126.
Some of the simple configurations which could be realistic to explain DM are:

$$\begin{gathered}\Phi_{1,2,2,0} + 2\Phi_{1,1,3,0} + 2\Phi_{1,1,2,-1} + 2\Phi_{1,1,3,-2}, \\ 2\Psi_{3,2,1,1/3} + \Phi_{8,1,1,0} + 4\Phi_{1,1,3,-2}, \\ \Phi_{1,1,2,0} + \Phi_{1,1,2,-1} + 3\Phi_{1,1,3,-2}.\end{gathered}$$

Note that, for the first configuration, the fields $\Phi_{1,2,2,0}$ and $\Phi_{1,1,3,0}$ realize the scalar CKM, $\Phi_{1,1,3,-2}$ breaks the LR symmetry and the neutral component of $\Phi_{1,1,2,-1}$ is the DM candidate.

For the first configuration: $\Phi_{1,1,2,0}+2\Phi_{1,1,3,0}+2\Phi_{1,1,2,-1}+\Phi_{1,1,3,-2}$, the most generic potential, compatible with the symmetries and also Z_2 invariant, is described by:

$SU(3)_c$	1	1	1
$SU(2)_L$	1	1	3
$SU(2)_R$	2	3	1
$U(1)_{B-L}$	-1	-2	-2
Q	0	0	0
$(B-L)$	odd	even	even
Rep	16	45	126
$Scalar$	✓		
$Fermion$		✓	✓

Table 6.7: Different dark matter candidates using $SO(10)$ representation up to 126.

$$
\begin{aligned}
W =& Y_Q Q\Phi Q^c + Y_L L\Phi L^c + \frac{\mu^2}{2}\Phi\Phi + m^2_{\Delta^c}\Delta^c\overline{\Delta^c} + m^2_{\Omega^c}\Omega^c\overline{\Omega^c} + m^2_{\chi^c}\chi^c\overline{\chi^c} + \\
&+ \alpha_1 L^c\overline{\Delta^c}L^c + \alpha_2\Phi\Omega^c\Phi + \alpha_3\chi^c\overline{\Delta^c}\chi^c + \alpha_4\overline{\chi^c\overline{\Delta^c}\chi^c} + \alpha_5\chi^c\Omega^c\overline{\chi^c} + \\
&\beta_1(\Delta^c\overline{\Delta^c})(\Delta^c\overline{\Delta^c}) + \beta_2(\Omega^c\overline{\Omega^c})(\Omega^c\overline{\Omega^c}) + \beta_3(\chi^c\overline{\chi^c})(\chi^c\overline{\chi^c}) + \\
&\beta_4(\Phi\Phi)(\chi^c\overline{\chi^c}) + \beta_5(\Phi\Phi)(\Omega^c\overline{\Omega^c}) + \beta_6(\Phi\Phi)(\Delta^c\overline{\Delta^c}).
\end{aligned} \tag{6.54}
$$

The couplings $\alpha_{2,....,5}$ have dimension of mass and α_1, $\beta_{1,....6}$ are dimensionless.

Chapter 7

CONCLUSIONS

The observation of neutrino masses in recent oscillation experiments is the main motivation for this thesis. The seesaw mechanism is, perhaps, the simplest way to explain neutrino masses and provides a rationale for their observed smallness. The seesaw type-I adds only singlets to the SM particle content, so all changes in the observables apart from neutrino masses are small. In addition, due to the large mass scales for the RH neutrinos involved, no direct experimental test will be possible. This motivates to study extensions of the SM which have testable observables. In this thesis four different BSM scenarios that explain neutrino masses were explored: i) a supersymmetric version of the seesaw type-I, ii) Witten's loop in a flipped $SU(5)$ model, iii) SUSY and iv) nonSUSY $SO(10)-$inspired GUT models with $U(1)_{B-L}$ intermediate symmetries where different seesaw mechanisms are realized. Below I present a summary and short conclusions of the different papers:

In [1] indirect hints of type-I seesaw that could be contained in SUSY mass measurements have been analyzed. Using published estimated errors on SUSY mass observables for a combined LHC+ILC analysis, we performed a theoretical χ^2 study to identify parameter regions where pure CMSSM and CMSSM plus seesaw type-I might be distinguishable with LHC+ILC data. This analysis was done before the recent LHC results. Now, negative searches for SUSY given by CMS [55] and ATLAS [56] define an excluded range in the CMSSM parameter space, ruling out all the SPS points studied in this work. However, future LHC data, if there are signals of supersymmetry, would reopen the window in the searches for signs of type-I seesaw in the SUSY spectra.

Although seesaw mechanism explains remarkably well the neutrino masses, the three RH neutrinos, which live at a high scale $m_R > 10^{14}$GeV, are added by hand. This motivates to study other methods to explain neutrino masses rather than the simple seesaw. For example, a *two loop suppression* for ν_R can arise in the Flipped $SU(5)$ model. Here interesting relations between the partial proton decay widths and the neutrino parameters can be found [4].

Neutrino masses are sucessfully explained in $SO(10)-$inspired GUT models with LR intermediate scales. In these scenarios, the $U(1)_{B-L}$ is a subgroup of $SO(10)$, so different realizations of the seesaw arise naturally. In SUSY $SO(10)$ models some conditions which enforce that the three gauge couplings unify independent of the intermediate scale m_{LR} where imposed. In this case, m_{LR} can be as low as 1 TeV, then phenomenologically testable models arise. In addition, assuming CMSSM boundary conditions some combinations of the soft terms, called "invariants" give information of the scale of beyond-MSSM physics. These aspects are studied in [2]. Considering that no signal of SUSY have been seen in the actual accelerators experiments, in [3] we also attempt to construct a comprehensive list of nonSUSY $SO(10)$ models with LR symmetric intermediate stages. These models unify equal or better than the MSSM even if the LR scale is in the LHC domain. The main aspects of a realistic model building conforming the basic constraints from the quark and lepton sector flavour structure, proton decay limits and neutrino mass are discussed. We put special attention on the theoretical uncertainties in particular, its role in the possible extraction of the LR-breaking scale.

Given the evidence of DM in the universe as well as the actual cosmological measurements hinting at inflation, we explored a possible connection between the nonSUSY $SO(10)$ models with DM. Very simple configurations which contain at least a DM candidate and respect some other phenomenological constraints were found. The relation between the DM and GUT parameters would be an interesting future topic to complete the work done in this thesis. Also, searches of perturbative baryon number violating (BNV) processes in the near future would constraint the high energy mass spectrum of the theory. A more precise computation using two-loop RGEs, as well as the inclusion of threshold effects could also be implemented to obtain more precise predictions.

In conclusion, supersymmetry and also grand unified theories are still considered to be among the most attractive candidates to address some of the shortcomings present in the SM. Neutrino masses and other interesting phenomenology like CKM mixing, proton decay limits and DM is successfully explained in these theories. It is expected that the next run of the LHC at 13-14 TeV center of mass energy, as well as new generation of low energy experiments help to address the models beyond the standard model. The future progress of experiments regarding the DM and baryon number violating (BNV) searches could give us interesting hints how to improve and complete the work here presented.

Appendix A

Some Algebra in Supersymmetry

A.1 Two component notation

In the Weyl representation, the gamma matrices are described by:

$$\gamma^{\mu} = \begin{pmatrix} 0 & \sigma^{\mu} \\ \overline{\sigma}^{\mu} & 0 \end{pmatrix}, \tag{A.1}$$

where $\mu = 0, 1, 2, 3$ and $\sigma^{\mu} = (I_2, \sigma)$, $\overline{\sigma}^{\mu} = (I_2, -\sigma) = \sigma_{\mu}$.

The Dirac spinor is written as:

$$\Psi_D = \Psi_R + \Psi_L. \tag{A.2}$$

In this basis, this spinor can be written in terms of two-component, complex and anticommuting objects: $\xi_{\alpha}, (\chi^{\dagger})^{\dot{\alpha}}$:

$$\begin{aligned} \Psi_D &= \begin{pmatrix} \xi_{\alpha} \\ \overline{\chi}^{\dot{\alpha}} \end{pmatrix} \\ \Psi_D^c &= \begin{pmatrix} \chi_{\alpha} \\ \overline{\xi}^{\dot{\alpha}} \end{pmatrix}, \end{aligned} \tag{A.3}$$

where: $\alpha, \dot{\alpha} : 1, 2$.

These latter definitions specify how to raise undotted indices and to lower dotted indices:

$$\begin{aligned} \chi^{\alpha} &= \epsilon^{\alpha\beta}\chi_{\beta} \\ \overline{\xi}_{\dot{\alpha}} &= \epsilon_{\dot{\alpha}\dot{\beta}}\xi^{\dot{\beta}}, \end{aligned} \tag{A.4}$$

where:

$$\begin{aligned} \epsilon^{\alpha\beta} &= \begin{pmatrix} 0 & -1 \\ 1 & 0 \end{pmatrix} \\ \epsilon_{\dot{\alpha}\dot{\beta}} &= \begin{pmatrix} 0 & 1 \\ -1 & 0 \end{pmatrix}. \end{aligned} \tag{A.5}$$

The left and right components of the Dirac spinor are written then:

$$\begin{aligned} \Psi_L &= \begin{pmatrix} \xi_{\alpha} \\ 0 \end{pmatrix} \\ \Psi_R &= \begin{pmatrix} 0 \\ \overline{\chi}^{\dot{\alpha}} \end{pmatrix}. \end{aligned} \tag{A.6}$$

With the properties of Majorana spinors:

$$\Psi_M^c = \Psi_M \tag{A.7}$$

and with the latter equations, it follows that, for Majorana spinors:

$$\xi_{\alpha} = \chi_{\alpha}, \tag{A.8}$$

which implies:

$$\overline{\chi}^{\dot{\alpha}} = \overline{\xi}^{\dot{\alpha}}. \tag{A.9}$$

It is sometimes useful to write a general Dirac spinor Ψ_D in terms of two Majorana spinors.

A.2 Supersymmetric Lagrangian

A supersymmetry transformation in a realistic supersymmetric model, turns a bosonic state Φ_i into its superpartner Weyl fermion Ψ_i state and vice versa. It also converts the gauge boson field A^α_μ into a two component Weyl fermion gaugino λ^a and vice versa [69]:

$$\begin{aligned}
\delta\phi_i &= \epsilon\Psi_i, \\
\delta(\Psi_i)_\alpha &= i(\sigma^\mu\epsilon^\dagger)_\alpha D_\mu\phi_i + \epsilon_\alpha F_i, \\
\delta F_i &= i\epsilon^\dagger\overline{\sigma}^\mu D_\mu\Psi_i + \sqrt{2}g(T^a\phi)_i\epsilon^\dagger\lambda^{\dagger a}, \\
\delta A^a_\mu &= -\frac{1}{\sqrt{2}}(\epsilon^\dagger\overline{\sigma}_\mu\lambda^a + \lambda^{\dagger a}\overline{\sigma}_\mu\epsilon), \\
\delta\lambda^a_\alpha &= -\frac{i}{2\sqrt{2}}(\sigma^\mu\overline{\sigma}^\nu\epsilon)_\alpha F^a_{\mu\nu} + \frac{1}{\sqrt{2}}\epsilon_a D^a, \\
\delta D^a &= \frac{1}{\sqrt{2}}(\epsilon^\dagger\overline{\sigma}^\mu D_\mu\lambda - D_\mu\lambda^\dagger\overline{\sigma}^\mu\epsilon).
\end{aligned} \tag{A.10}$$

The index i runs over the gauge and flavor indices of the fermions, ϵ^α is the infinitesimal, anti-commuting two-component Weyl fermion object which parameterizes the supersymmetry transformation, F_i and D_i are complex auxiliary fields which do not propagate and can be eliminated using their equations of motion. The index a runs over the adjoint representation of the gauge group under which all the chiral fields transform in a representation with hermitian matrices satisfying $[T_a, T_b] = if^{abc}T^c$.

The gauge transformations are described by:

$$\begin{aligned}
D_\mu\phi_i &= \partial_\mu\phi_i + igA^a_\mu(T^a\phi)_i, \\
D_\mu\Psi_i &= \partial_\mu\Psi_i + igA^a_\mu(T^a\phi)_i, \\
D_\mu\lambda^a &= \partial_\mu\lambda^a - igf^{abc}A^b_\mu\lambda^c, \\
F^a_{\mu\nu} &= \partial_\mu A^a_\mu - \partial_\nu A^a_\mu - gf^{abc}A^b_\mu A^c_\nu,
\end{aligned} \tag{A.11}$$

where g is the gauge coupling.

Under these transformations, the Lagrangian density can be written as:

$$L = L_K + L_{M\lambda} + L_Y + L_S, \tag{A.12}$$

where:

$$L_K = L_C + L_{MG} + L_{\lambda G} + L_{GG}, \tag{A.13}$$

$$L_{M\lambda} = ig\sqrt{2}(\phi_j^*(T_a)_{ik}\lambda^a\psi_k - \phi_i(T^a)_{ik}\overline{\lambda}^a\overline{\Psi}_k), \tag{A.14}$$

$$L_Y = -\frac{1}{2}[\sum_{lk}\frac{dW[\hat{\phi}]}{d\phi_l d\phi_k}\Psi_l\Psi_k + h.c], \tag{A.15}$$

$$L_S = -\frac{1}{2}|g\phi_i^*(T_a)_{ij}\phi_j|^2 - \sum_i|\frac{dW[\hat{\phi}]}{d\phi_i}|^2, \tag{A.16}$$

where $L_{M\lambda}$ includes the interactions between the SM fields, their supersymmetric partners and the gauginos (gauge field supersymmetric partners). L_Y includes all type of Yukawa interactions that appear in the superpotential. L_S includes the interactions between the scalar fields F and D (these fields are very important in the study of the symmetry breaking). L_K is defined by:

$$L_C = \sum_j|\partial_\mu\phi_j|^2 - i\overline{\Psi}_j\overline{\sigma}_\mu\partial^\mu\Psi_j - \frac{1}{4}V^a_{\nu\mu}V_a^{\mu\nu} - i\overline{\lambda}^a\overline{\sigma}_\mu\partial^\mu\lambda_a + h.c, \tag{A.17}$$

$$\begin{aligned} L_{MG} &= -g\overline{\Psi}_i\overline{\sigma}^\mu V^a_\mu(T_a)_{ij}\Psi_j - ig\phi_i^*V^a_\mu(T_a)_{ij}\overleftrightarrow{\partial^\mu}\phi_j \\ &+ g^2V^a_\mu V^{b\mu}\phi_i^*(T_aT_b)_{ij}\phi_j + h.c, \end{aligned} \tag{A.18}$$

$$L_{\lambda G} = igf_{abc}\lambda^a\sigma^\mu\overline{\lambda}^bV^c_\mu + h.c, \tag{A.19}$$

$$L_{GG} = -gF^a_{bc}V^b_\mu V^c_\nu \partial^\mu V^\nu_a - \frac{1}{4}g^2 F^a_{bc} f_{adc} V^b_\mu V^c_\nu V^{d\mu} V^{e\nu}, \quad \text{(A.20)}$$

where L_C are the kinetic terms, L_{MG} give the interactions between each particle with the gauge fields, $L_{\lambda G}$ the interactions between gauge fields and gauginos and L_{GG} describes the interactions between gauge fields.

The gauge fields are defined in the usual form:

$$V_{\mu\nu} = \partial_\mu V_\nu - \partial_\nu V_\mu, \quad \text{(A.21)}$$
$$F^a_{\mu\nu}(V) = \partial_\mu V^a_\nu - \partial_\nu V^a_\mu + g f^a_{bc} V^b_\mu V^c_\nu, \quad \text{(A.22)}$$
$$D^\mu = \partial^\mu - igV^a_\mu (T_a)_{ij}. \quad \text{(A.23)}$$

In a renormalizable supersymmetric field theory, the interactions and masses of all particles are determined by their gauge transformation properties and by the superpotential $W[\hat{\phi}_j]$. W is the most general supersymmetric term that contain the chiral matter fields and is renormalizable:

$$W[\hat{\phi}_j] = \sum_j k_i \phi_i + \frac{1}{2}\sum_{i,j} m_{ij}\hat{\phi}_i\hat{\phi}_j + \frac{1}{3}\sum_{i,j,k}\lambda_{ijk}\hat{\phi}_i\hat{\phi}_j\hat{\phi}_k. \quad \text{(A.24)}$$

W determines only part of the scalar interactions of the theory as well the fermion masses and the Yukawa couplings. Also the D-terms from the gauge part give contributions to the scalar potential.

A.3 Lie Group and Lie Algebras

As is known, the SM is the best descriptions of physics at low energies. However there are some theories beyond the SM which unify all the forces and particles and explain also successfully the interactions in the nature. The three best studied GUT models in literature are: Georgi and Glashow $SU(5)$ theories, models based in the Pati Salam PS group $SU(4) \times SU(2)_L \times SU(2)_R$, and $SO(10)$, all of which typically are studied with finite-dimensional gauge group representations. In this

chapter, group representations, algebras and particle content of these GUT models will be discussed.

GUT theories are described by simple Lie groups G that can not be decomposed as a product of other groups [266]. A gauge theory based on G requires an invariant inner product on its Lie algebra. When G is simple, this form is unique up to a scalar factor, called 'coupling constant'. When G is the product of simple factors, there is one coupling constant for each factor of G. Therefore, by using a simple Lie group, the number of coupling constants in the theory is minimized.

In order to understand how the SM can be extended to larger gauge symmetries, such that the matter content is agruped in a single representation (and then reduce the number of parameters in the theory), we need to explore some theoretical features of the Lie algebras [266, 267]:

A Lie Group is defined such that each of its elements depends smoothly on a set of continuous parameters:

$$g(\alpha). \tag{A.25}$$

The identity element e requires to choose the parametrization such that $\alpha = 0$ corresponds to e. Thus, in the neighbourhood of the identity, it is assumed the each element of the group can be described by N parameters such that:

$$g(\alpha)|_{\alpha=0} = e, \tag{A.26}$$

which is also followed by the representations of the group:

$$D(\alpha)|_{\alpha=0} = e. \tag{A.27}$$

In some neighbourhood of α a Taylor expansion of these representations can be done such that:

$$D(d\alpha) = 1 + i\frac{d}{d\alpha_\alpha}X_\alpha, \tag{A.28}$$

$$X_\alpha = -i\frac{d}{d\alpha_\alpha}D(\alpha)|_{\alpha=0}. \tag{A.29}$$

where X_α are the generators of the group. With the specific properties: $D(a)D(b) = D(ab)$ and $D(e) = 1$, the $D(\alpha)$ representation can be written like:

$$D(\alpha) = \lim_{k\to 0}(1 + id\alpha_\alpha X_\alpha/k)^k = e^{i\alpha_\alpha X_\alpha}, \tag{A.30}$$

in the limit when k is large, $(1 + id\alpha_\alpha X_\alpha/k)$ tends to (1.59). This defines a particular parametrization (exponential parametrization) which is widely used in the standard (U) representations of the Lie $SU(N)$ groups defined by:

$$U(\lambda) = e^{i\lambda}\alpha_\alpha X_\alpha, \tag{A.31}$$

and multiplied as:

$$U(\lambda_1)U(\lambda_2) = U(\lambda_1 + \lambda_2). \tag{A.32}$$

However, if we multiply two representations generated by diferent combinations of the generators, we have:

$$e^{i\alpha_\alpha X_\alpha}e^{i\beta_b X_b} \neq e^{i(\alpha_\alpha+\beta_\alpha)X_\alpha}. \tag{A.33}$$

A Lie algebra is described by the commutation relations between the generators of the group:

$$[X_a, X_b] = if_{abc}X_c. \tag{A.34}$$

This commutator relation is called the Lie Algebra of the group, which is determined by the structure constant which is fixed by the group multiplication laws.

If there is any unitary representation of the algebra, the f_{abc} coefficients are real, so:

$$[X_a, X_b]^\dagger = -if^*_{abc}X_c, \tag{A.35}$$

since we are interested in groups which have unitary representations, we will assume f_{abc} real.

Appendix B

Grand Unified Theories

B.1 Basics

B.1.1 $SU(5)$

$SU(5)$ is defined by its adjoint representation (the 5×5 complex unitary matrices with determinant 1). There are 25 independent real 5×5 matrices, i.e, 50 independent complex unitary matrices U. The unitary condition $UU^{\dagger} = 1$ and $detU = 1$, give $25 + 1$ constrains, leaving this 24 independent matrices (T_a). In the fundamental representation, $SU(5)$ is characterized by a generalization of the Gell-Mann matrices, denoted by M_a and $a = 1, ..., 24$, normalized as:

$$\begin{aligned} Tr(M_a M_b) &= 2\delta_{ab} \\ Tr(M_c) &= 0, \end{aligned} \tag{B.1}$$

and $T_a = \frac{M_a}{2}$, $a = 1, ..., 24$. The gauge bosons A_a^{μ}, belonging to the 24 adjoint representation, can be written as a 5×5 matrix:

$$A_{\mu} = \sum_{a=1}^{24} A_{\mu}^{a} \frac{M_a}{2}, \tag{B.2}$$

and taking into account the form of the 24 generators, we finally have:

$$A_\mu = \frac{1}{\sqrt{2}} \begin{pmatrix} & & & X_\mu^1 & Y_\mu^1 \\ & Gluones & & X_\mu^2 & Y_\mu^2 \\ & & & X_\mu^3 & Y_\mu^3 \\ \overline{X}_\mu^1 & \overline{X}_\mu^2 & \overline{X}_\mu^3 & W_\mu^3/\sqrt{2} & W_\mu^+ \\ \overline{Y}_\mu^1 & \overline{Y}_\mu^2 & \overline{Y}_\mu^3 & W_\mu^- & W_\mu^3/\sqrt{2} \end{pmatrix} + \frac{1}{\sqrt{30}} B_\mu \begin{pmatrix} -2 & 0 & 0 & 0 & 0 \\ 0 & -2 & 0 & 0 & 0 \\ 0 & 0 & -2 & 0 & 0 \\ 0 & 0 & 0 & 3 & 0 \\ 0 & 0 & 0 & 0 & 3 \end{pmatrix}. \tag{B.3}$$

The matrix contains the $SU(3)_c$ Gluons: $A_\mu^a = 1, ..., 8$, the $SU(2)_L$ gauge bosons: $W_\mu^3, W_\mu^+, W_\mu^-$ and the $U(1)_Y$ boson: B_μ. In addition there are twelve bosons, denoted as X, Y.

B.1.2 $SO(10)$

$SO(10)$ is described by the orthogonal $N \times N$ group transformation matrices which obey: $O^\dagger O = 1$ and $\det(O) = 1$. An infinitesimal transformation is defined by:

$$O^{ij} \to O^{ij} + w^{ij}. \tag{B.4}$$

We find, for example, the decomposition of the 45 dimensional representation of $SO(10)$ under $SU(3)_c \times SU(2)_L \times SU(2)_R \times U(1)_{B-L}$:

$$\begin{aligned} 45 \xrightarrow{G_{3221}} & (1,3,1,0) + (1,1,3,0) + (8,1,1,0) + (1,1,1,0) \\ & + (3,2,2,\frac{2}{3}) + (\overline{3},2,2,-\frac{2}{3}) + (3,1,1,\frac{1}{3}) + (\overline{3},1,1,-\frac{1}{3}). \end{aligned} \tag{B.5}$$

In order for a group G to break into a subgroup H, there must be a field transforming non-trivially under G which contains a singler of H that adquires a vacuum expectation value. We can see that, in this case the 45 contains a singlet of the

group $G_{3,2,2,1}$. Therefore, if the multiplet develops a vev in that direction, $G_{3,2,2,1}$ remains as an unbroken subgroup. On the other hand, some of the multiplets which can break $SO(10)$ to $G_{4,2,2}$ are contained in the representations: 54, 210, 16 and 126. In particular, for the 126 we have:

$$126 \xrightarrow{G_{422}} (6,1,1) + (15,2,2) + (10,3,1) + (\overline{10},1,3). \tag{B.6}$$

It is clear that the multiplet which breaks $G_{3,2,2,1}$ or $G_{4,2,2}$ down to the SM is contained in $(1,3,\overline{10})$. This 126 representation provides a large mass to the right handed neutrinos.

B.2 List of fields in the Left-Right models

We have considered $SO(10)$ inspired models which may contain any irreducible representation up to the dimension 126 (**1**, **10**, **16**, $\overline{\mathbf{16}}$, **45**, **54**, **120**, **126**, $\overline{\mathbf{126}}$). Once the gauge group is broken to $SU(4)\times SU(2)_L\times SU(2)_L$ or $SU(3)_c\times SU(2)_L\times SU(2)_R\times U(1)_{B-L}$ these $SO(10)$ fields break up into a multitude of different irreducible representation of these groups.

In addition, if $SU(2)_R$ is broken down further to $U(1)_R$ the following branching rules apply: $\mathbf{3}\to -1,0,+1$; $\mathbf{2}\to \pm\frac{1}{2}$; $\mathbf{1}\to 0$. The standard model hypercharge in the canonical normalization, is then equal to the combination $\sqrt{\frac{3}{5}}\,[U(1)_R \text{ hypercharge}] + \sqrt{\frac{2}{5}}\,[U(1)_{B-L} \text{ hypercharge}]$. In tables B.1, B.2 and B.3 we present the list of relevant fields respecting these conditions. Here we used ordered naming of the fields.

B.3 NonSUSY GUTs

Extending the SM with some particle content X particle added at the scale m_{NP} (new physics scale), it is possible to achieve a unification equal or better than in the MSSM. We find there is a large number of such solutions. However, all of these can be classified into a small number of series, that predict a specific value of m_G and $\Delta\alpha^{-1}(m_G)$. The Δb coefficients (shift with respect to the SM b's values) that

	Φ_1	Φ_2	Φ_3	Φ_4	Φ_5	Φ_6	Φ_7	Φ_8	Φ_9	Φ_{10}	Φ_{11}	Φ_{12}	Φ_{13}	Φ_{14}
		χ	χ^c	Ω	Ω^c	Φ			δ_d	δ_u				
$SU(3)_C$	**1**	**1**	**1**	**1**	**1**	**1**	**8**	**1**	**3**	**3**	**6**	**6**	**3**	**3**
$SU(2)_L$	**1**	**2**	**1**	**3**	**1**	**2**	**1**	**1**	**1**	**1**	**1**	**1**	**2**	**1**
$SU(2)_R$	**1**	**1**	**2**	**1**	**3**	**2**	**1**	**1**	**1**	**1**	**1**	**1**	**1**	**2**
$U(1)_{B-L}$	0	+1	-1	0	0	0	0	+2	$-\frac{2}{3}$	$+\frac{4}{3}$	$+\frac{2}{3}$	$-\frac{4}{3}$	$+\frac{1}{3}$	$+\frac{1}{3}$
PS	Ψ_1	$\overline{\Psi}_{12}$	Ψ_{13}	Ψ_3	Ψ_4	Ψ_2	Ψ_{10}	$\overline{\Psi}_9$	Ψ_8	Ψ_{10}	Ψ_9	Ψ_{11}	Ψ_{12}	Ψ_{13}
Origin	Ψ_{10}					Ψ_7	Ψ_{11}		Ψ_9					

	Φ_{15}	Φ_{16}	Φ_{17}	Φ_{18}	Φ_{19}	Φ_{20}	Φ_{21}	Φ_{22}	Φ_{23}	Φ_{24}
		Δ	Δ^c							
$SU(3)_C$	**8**	**1**	**1**	**3**	**3**	**3**	**6**	**6**	**1**	**3**
$SU(2)_L$	**2**	**3**	**1**	**2**	**3**	**1**	**3**	**1**	**3**	**2**
$SU(2)_R$	**2**	**1**	**3**	**2**	**1**	**3**	**1**	**3**	**3**	**2**
$U(1)_{B-L}$	0	-2	-2	$+\frac{4}{3}$	$-\frac{2}{3}$	$-\frac{2}{3}$	$+\frac{2}{3}$	$+\frac{2}{3}$	0	$-\frac{2}{3}$
PS	Ψ_7	Ψ_{16}	Ψ_{17}	Ψ_7	Ψ_{14}	Ψ_{15}	Ψ_{16}	Ψ_{17}	Ψ_5	Ψ_6
Origin					Ψ_{16}	Ψ_{17}				

Table B.1: Naming conventions and transformation properties of fields in the left-right symmetric regime (not considering conjugates). The charges under the $U(1)_{B-L}$ group shown here were multiplied by a factor $\sqrt{\frac{8}{3}}$.

	Ψ_1	Ψ_2	Ψ_3	Ψ_4	Ψ_5	Ψ_6	Ψ_7	Ψ_8	Ψ_9	Ψ_{10}	Ψ_{11}	Ψ_{12}	Ψ_{13}	Ψ_{14}	Ψ_{15}	Ψ_{16}	Ψ_{17}
$SU(4)$	**1**	**1**	**1**	**1**	**1**	**6**	**15**	**6**	**10**	**15**	**20'**	**4**	**4**	**6**	**6**	**10**	**10**
$SU(2)_L$	**1**	**2**	**3**	**1**	**3**	**2**	**2**	**1**	**1**	**1**	**1**	**2**	**1**	**3**	**1**	**3**	**1**
$SU(2)_R$	**1**	**2**	**1**	**3**	**3**	**2**	**2**	**1**	**1**	**1**	**1**	**1**	**2**	**1**	**3**	**1**	**3**
$SO(10)$	**1**	**10**	**45**	**45**	**54**	**45**	**120**	**10**	**120**	**45**	**54**	**16**	$\overline{\mathbf{16}}$	**120**	**120**	**126**	$\overline{\mathbf{126}}$
Origin	**54**	**120**				**54**	**126**	**126**									

Table B.2: Naming conventions and transformation properties of fields in the Pati-Salam regime (not considering conjugates)

	Φ'_1	Φ'_2	Φ'_3	Φ'_4	Φ'_5	Φ'_6	Φ'_7	Φ'_8	Φ'_9	Φ'_{10}	Φ'_{11}	Φ'_{12}	Φ'_{13}	Φ'_{14}	Φ'_{15}	Φ'_{16}
$SU(3)_C$	**1**	**1**	**1**	1	**1**	**1**	**1**	**8**	**1**	**3**	**3**	**6**	**6**	**3**	**3**	**3**
$SU(2)_L$	**1**	**2**	**1**	1	**3**	**1**	**2**	**1**	**1**	**1**	**1**	**1**	**1**	**2**	**1**	**1**
$U(1)_R$	0	0	$-\frac{1}{2}$	$+\frac{1}{2}$	0	+1	$+\frac{1}{2}$	0	0	0	0	0	0	0	$-\frac{1}{2}$	$+\frac{1}{2}$
$U(1)_{B-L}$	0	+1	-1	-1	0	0	0	0	+2	$-\frac{2}{3}$	$+\frac{4}{3}$	$+\frac{2}{3}$	$-\frac{4}{3}$	$+\frac{1}{3}$	$+\frac{1}{3}$	$+\frac{1}{3}$
LR	Φ_1	Φ_2	Φ_3	Φ_3	Φ_4	Φ_5	Φ_6	Φ_7	Φ_8	Φ_9	Φ_{10}	Φ_{11}	Φ_{12}	Φ_{13}	Φ_{14}	Φ_{14}
Origin	Φ_5				Φ_{23}				$\bar{\Phi}_{17}$	Φ_{20}		Φ_{22}				

	Φ'_{17}	Φ'_{18}	Φ'_{19}	Φ'_{20}	Φ'_{21}	Φ'_{22}	Φ'_{23}	Φ'_{24}	Φ'_{25}	Φ'_{26}	Φ'_{27}	Φ'_{28}	Φ'_{29}	Φ'_{30}	Φ'_{31}
$SU(3)_C$	**8**	**1**	**1**	**1**	**3**	**3**	**3**	**3**	**3**	**6**	**6**	**6**	**1**	**3**	**3**
$SU(2)_L$	**2**	**3**	**1**	**1**	**2**	**2**	**3**	**1**	**1**	**3**	**1**	**1**	**3**	**2**	**2**
$U(1)_R$	$+\frac{1}{2}$	0	-1	+1	$-\frac{1}{2}$	$+\frac{1}{2}$	0	-1	+1	0	-1	+1	+1	$-\frac{1}{2}$	$+\frac{1}{2}$
$U(1)_{B-L}$	0	-2	-2	-2	$+\frac{4}{3}$	$+\frac{4}{3}$	$-\frac{2}{3}$	$-\frac{2}{3}$	$-\frac{2}{3}$	$+\frac{2}{3}$	$+\frac{2}{3}$	$+\frac{2}{3}$	0	$-\frac{2}{3}$	$-\frac{2}{3}$
LR	Φ_{15}	Φ_{16}	Φ_{17}	Φ_{17}	Φ_{18}	Φ_{18}	Φ_{19}	Φ_{20}	Φ_{20}	Φ_{21}	Φ_{22}	Φ_{22}	Φ_{23}	Φ_{24}	Φ_{24}
Origin															

Table B.3: Naming conventions and transformation properties of fields in the U(1) mixing regime (not considering conjugates). The charges under the $U(1)_{B-L}$ group shown here were multiplied by a factor $\sqrt{\frac{8}{3}}$.

describe the elements of each series are related by:

$$(\Delta b_1, \Delta b_2, \Delta b_3) = (\Delta b_{1i} + (n/3), \Delta b_{2i} + (n/3) + \Delta b_{3i} + (n/3))$$

where the $\Delta b_i^{'} s$, for $n = 0$, describe the lowest variants that begin each series. There are 12 of these series, and again, each one with a specific value of m_G and $\Delta\alpha^{-1}(MG)$. The list of series is given in Table 7.4.

Series	m_G	$\Delta\alpha_G^{-1}$
$(0, 2, 2)$	1.03×10^{17}	0.391
$(1/10, 11/6, 3/2)$	7.79×10^{15}	0.516
$(2/15, 2, 11/6)$	2.68×10^{16}	0.082
$(1/6, 13/6, 13/6)$	1.03×10^{17}	0.387
$(1/6, 5/2, 8/3)$	4.46×10^{17}	0.172
$(4/15, 2, 5/3)$	7.79×10^{15}	0.516
$(3/10, 11/6, 3/2)$	7.79×10^{15}	0.428
$(3/10, 13/6, 2)$	2.68×10^{16}	0.082
$(3/10, 5/2, 5/2)$	1.03×10^{17}	0.639
$(1/3, 8/3, 17/6)$	4.46×10^{17}	0.172
$(7/15, 7/3, 13/6)$	2.68×10^{16}	0.082
$(7/15, 8/3, 8/3)$	1.03×10^{17}	0.639

Table B.4: List of the possible series of Δb leading to GCU. m_G is the GUT scale and $\Delta\alpha_G$ is the the difference of the couplings $\alpha_1^{-1} - \alpha_2^{-1}$ at m_G, for a fixed $m_{NP} = 1$TeV.

All the sets have $\Delta\alpha^{-1}(mG) < 0.8$. This means, we are finding solutions with a unification equal or better than for the MSSM.
Fig. 7.1 shows the behavior of $\Delta\alpha^{-1}(m_G)$ with m_{NP} for each one of the series. We can see that perfect unification ($\Delta\alpha^{-1}(m_G) = 0$) is reached at m_{NP}. We can see that some series, for example Series $12, 9, 6$ and 2 do not reach "perfect unification" if we consider values for m_{NP} into the interval $2 - 3$ TeV (realistic values for the

LHC). It is important to note that only 6 of these series predict different values for m_G and $\Delta\alpha^{-1}(m_G)$, as we can see also in the figure. This is expected because, for example: Serie4: Serie1 +(1/6), Serie6= Serie2 +(1/6)...and similar relation for other ones.

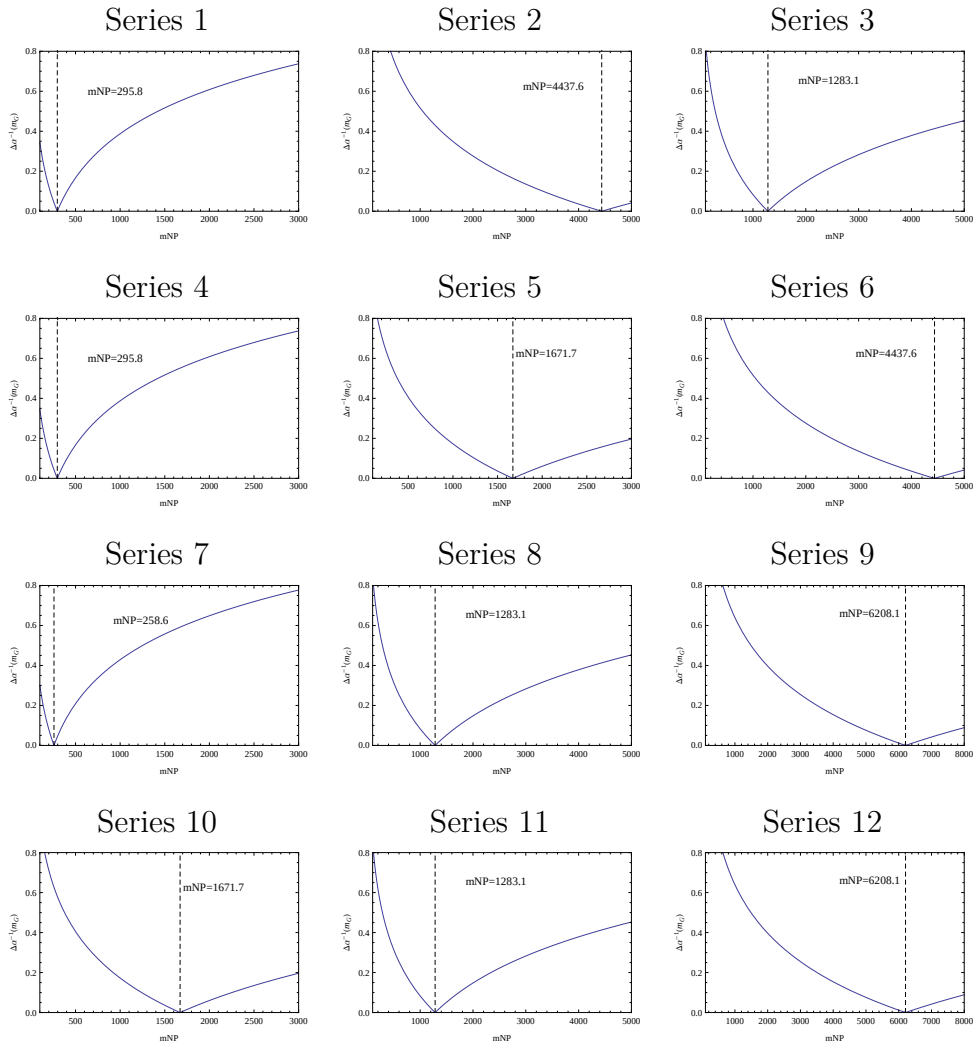

Figure B.1: α_G^{-1} as function of m_{NP} for the different series.

We analized the predicted value of $\alpha_S^{-1}(m_Z)$ for the models in each series in order to compare with the actual measured value, as in Fig. 7.2. Here, it is possible to find the interval m_{NP} in which the measured value of $\alpha_S^{-1}(m_Z)$ is reached in each

serie. For example, in Series 2 and 9 this value is reached for large values of m_{NP}. This can be also understood looking at Fig. 7.1.

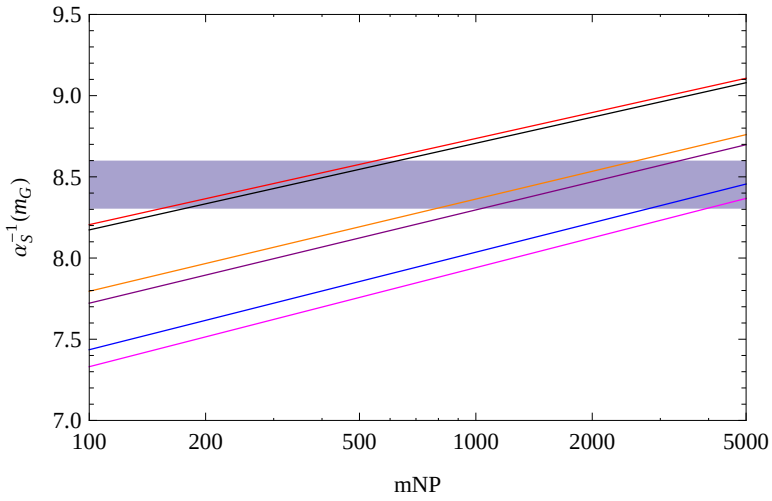

Figure B.2: Dependence of predicted $\alpha_S^{-1}(mZ)$ with the new physics scale m_{NP}. The colors correspond to: Black: (Serie1, Serie4), Blue: (Serie2, Serie6), Orange: (Serie3, Serie8, Serie11), Purple: (Serie5, Serie10), Red: (Serie7), Magenta: (Serie9, Serie12).

B.3.1 List of fields

We have considered $SO(10)$ based models which contain any irreducible representation up to dimension 126 $(1, 10, 16, \overline{16}, 45, 54, 120, 126, \overline{126})$. Once $SO(10)$ is broken, the fields divide into different irreducible representations and the quantum numbers under $SU(3)_c \times SU(2)_L \times SU(2)_R \times U(1)_{B-L}$ are presented in table B.5, where we used an ordered naming of the fields.

B.3.2 List of simple configurations-LR regime

The breaking of the LR symmetry to the SM: $LR \to SM$ requires the presence of one of the fields: $\Phi_{1,1,3,-2}$ or $\Phi_{1,1,2,-1}$. All configurations contain then at least one of these fields and also one bi-doublet $\Phi_{1,2,2,0}$ (to complete "$SM+$ bi-doublet" basic field content). Table B.6 shows the simplest LR configurations for $[a.1]$ scalar

CKM (where the necessary fields are: $\Phi_{1,1,3,0}$, $\Phi_{1,2,2,0}$, $\Phi_{1,1,3,-2}$ or $\Phi_{1,1,2,-1}$) for each one of the fields presented in table B.5.

B.3.3 SM-X extended unification: list of simple configurations

It is possible to achieve one-step unification of the SM coupling constants within non-SUSY models. This is performed adding to the SM a new particle content at scale m_{NP}. This particle content can be as simple as the configurations shown in table B.7, which added to the SM lead "$SM + X$" models that unify equal or even better than the MSSM. Therefore, for each one of the fields in table B.5 (in the SM version) one of the simplest X configurations is obtained as follows: $\alpha_2^{-1}(m_G) - \alpha_1^{-1}(m_G) < 0.9$ (unification equal or better that the MSSM) and $10^{15} < m_G < 10^{18}$ GeV in order to obtain proton life times allowed by the actual bounds.

	1	2	3	4	5	6	7	8	9	10	11	12	13	14
Scalar		χ	χ^c	Ω	Ω^c	Φ								
Fermion	$\widetilde{B}$	L	L^c	Σ	Σ^c		$\widetilde{G}$		δ_d	δ_u			Q	Q^c
$SU(3)_C$	**1**	**1**	**1**	**1**	**1**	**1**	**8**	**1**	**3**	**3**	**6**	**6**	**3**	**3**
$SU(2)_L$	**1**	**2**	**1**	**3**	**1**	**2**	**1**	**1**	**1**	**1**	**1**	**1**	**2**	**1**
$SU(2)_R$	**1**	**1**	**2**	**1**	**3**	**2**	**1**	**1**	**1**	**1**	**1**	**1**	**1**	**2**
$U(1)_{B-L}$	0	+1	-1	0	0	0	0	+2	$-\frac{2}{3}$	$+\frac{4}{3}$	$+\frac{2}{3}$	$-\frac{4}{3}$	$+\frac{1}{3}$	$+\frac{1}{3}$
SO(10) Origin	1 54 45	16	$\overline{16}$	45	45	10 120 126	45 54	120	10 126 120	45	120	54	16	$\overline{16}$

	15	16	17	18	19	20	21	22	23	24
Scalar		Δ	Δ^c							
Fermion										
$SU(3)_C$	**8**	**1**	**1**	**3**	**3**	**3**	**6**	**6**	**1**	**3**
$SU(2)_L$	**2**	**3**	**1**	**2**	**3**	**1**	**3**	**1**	**3**	**2**
$SU(2)_R$	**2**	**1**	**3**	**2**	**1**	**3**	**1**	**3**	**3**	**2**
$U(1)_{B-L}$	0	-2	-2	$+\frac{4}{3}$	$-\frac{2}{3}$	$-\frac{2}{3}$	$+\frac{2}{3}$	$+\frac{2}{3}$	0	$-\frac{2}{3}$
SO(10) Origin	120	126	$\overline{126}$	120 126	120 126	120 $\overline{126}$	126	$\overline{126}$	54	45 54

Table B.5: Naming conventions and transformation properties of fields in the left-right symmetric regime (not considering conjugates). The charges under the $U(1)_{B-L}$ group shown here were multiplied by a factor $\sqrt{\frac{8}{3}}$. The hypercharge is defined by: $Y = T_3^R + \frac{(B-L)}{2}$. $\widetilde{B}$ and $\widetilde{G}$ correspond to the bino and gluino respectively. Symbols in the lines called "Scalar" and "Fermion" quote names used for these fields in the literature.

Extra field	Configuration	$\Delta b's$	m_G	$T_{1/2}$
	$\Phi_{1,2,2,0} + 3\Phi_{1,1,3,0} + 2\Phi_{1,1,3,-2}$	$(0, \frac{1}{3}, \frac{11}{3}, 3)$	2×10^{15}	$10^{33\pm2.5}$
	$\Phi_{1,2,2,0} + \Phi_{1,1,3,0} + 3\Phi_{1,1,3,-2}$	$(0, \frac{1}{3}, 3, \frac{9}{2})$	2×10^{15}	$10^{33\pm2.5}$
$\Phi_{1,2,1,1}$	$2\Phi_{1,2,2,0} + 2\Phi_{1,1,3,0} + 4\Phi_{3,1,1,-2/3} + \Phi_{1,2,1,1} + 2\Phi_{1,1,3,-2}$	$(\frac{2}{3}, \frac{5}{6}, \frac{10}{3}, \frac{47}{12})$	8×10^{15}	$10^{35\pm2.5}$
$\Phi_{1,1,2,-1}$	$\Phi_{1,2,2,0} + 2\Phi_{1,1,3,0} + 2\Phi_{1,1,2,-1} + 2\Phi_{1,1,3,-2}$	$(0, \frac{1}{3}, \frac{10}{3}, \frac{7}{2})$	2×10^{15}	$10^{33\pm2.5}$
$\Phi_{1,3,1,0}$	$\Phi_{1,2,2,0} + \Phi_{1,1,3,0} + \Phi_{1,3,1,0} + 3\Phi_{1,1,3,-2}$	$(1, 1, 3, \frac{9}{2})$	3×10^{16}	$10^{37\pm2.5}$
$\Phi_{8,1,1,0}$	$2\Phi_{1,2,2,0} + \Phi_{1,1,3,0} + \Phi_{8,1,1,0} + 2\Phi_{1,1,3,-2}$	$(1, \frac{2}{3}, \frac{8}{3}, 3)$	4×10^{17}	$10^{42\pm2.5}$
$\Phi_{1,1,1,2}$	$\Phi_{1,2,2,0} + 2\Phi_{1,1,3,0} + 2\Phi_{1,1,1,2} + 2\Phi_{1,1,3,-2}$	$(0, \frac{1}{3}, 3, 4)$	2×10^{15}	$10^{33\pm2.5}$
$\Phi_{3,1,1,-2/3}$	$2\Phi_{1,2,2,0} + \Phi_{1,1,3,0} + 5\Phi_{3,1,1,-2/3} + 2\Phi_{1,1,3,-2}$	$(\frac{5}{6}, \frac{2}{3}, \frac{8}{3}, \frac{23}{6})$	1×10^{17}	$10^{39\pm2.5}$
$\Phi_{3,1,1,4/3}$	$3\Phi_{1,2,2,0} + \Phi_{1,1,3,0} + 4\Phi_{3,1,1,4/3} + 2\Phi_{1,1,3,-2}$	$(\frac{2}{3}, 1, 3, \frac{17}{3})$	2×10^{15}	$10^{33\pm2.5}$
$\Phi_{6,1,1,2/3}$	$2\Phi_{1,2,2,0} + \Phi_{1,1,3,0} + \Phi_{6,1,1,2/3} + 2\Phi_{1,1,3,-2}$	$(\frac{5}{6}, \frac{2}{3}, \frac{8}{3}, \frac{10}{3})$	1×10^{17}	$10^{39\pm2.5}$
$\Phi_{6,1,1,-4/3}$	$2\Phi_{1,2,2,0} + 3\Phi_{1,1,3,0} + \Phi_{6,1,1,-4/3} + \Phi_{1,1,3,-2}$	$(\frac{5}{6}, \frac{2}{3}, \frac{10}{3}, \frac{17}{6})$	1×10^{17}	$10^{39\pm2.5}$
$\Phi_{3,2,1,1/3}$	$\Phi_{1,2,2,0} + \Phi_{1,1,3,0} + 2\Phi_{3,1,1,-2/3} + \Phi_{3,2,1,1/3} + 3\Phi_{1,1,3,-2}$	$(\frac{2}{3}, \frac{5}{6}, 3, \frac{59}{12})$	8×10^{15}	$10^{35\pm2.5}$
$\Phi_{3,1,2,1/3}$	$\Phi_{1,2,2,0} + \Phi_{1,1,3,0} + \Phi_{3,1,2,/3} + 2\Phi_{1,1,3,-2}$	$(\frac{1}{3}, \frac{1}{3}, \frac{17}{6}, \frac{37}{12})$	3×10^{16}	$10^{37\pm2.5}$
$\Phi_{8,2,2,0}$	$4\Phi_{1,2,2,0} + 3\Phi_{1,1,3,0} + \Phi_{8,2,2,0} + 3\Phi_{1,1,3,-2}$	$(4, 4, 8, \frac{9}{2})$	3×10^{16}	$10^{37\pm2.5}$
$\Phi_{3,1,1,-2}$	$\Phi_{1,2,2,0} + \Phi_{1,1,3,0} + 2\Phi_{8,1,1,0} + 2\Phi_{1,3,1-2} + 2\Phi_{1,1,3,-2}$	$(2, \frac{5}{3}, \frac{7}{3}, 6)$	4×10^{17}	$10^{42\pm2.5}$
$\Phi_{3,2,2,4/3}$	$\Phi_{1,2,2,0} + \Phi_{1,1,3,0} + \Phi_{8,1,1,0} + 2\Phi_{3,2,2,4/3} + \Phi_{1,1,3-2}$	$(\frac{7}{3}, \frac{7}{3}, 4, \frac{11}{3}, \frac{41}{6})$	3×10^{16}	$10^{37\pm2.5}$
$\Phi_{3,3,1,-2/3}$	$\Phi_{1,2,2,0} + \Phi_{1,1,3,0} + 2\Phi_{8,1,1,0} + \Phi_{3,3,1,-2/3} + 4\Phi_{1,1,3-2}$	$(\frac{5}{2}, \frac{7}{3}, \frac{11}{3}, \frac{13}{2})$	1×10^{17}	$10^{37\pm2.5}$
$\Phi_{3,1,3,-2/3}$	$2\Phi_{1,2,2,0} + 2\Phi_{1,1,3,0} + \Phi_{3,1,3,-2/3} + \Phi_{1,1,3,-2}$	$(\frac{1}{2}, \frac{2}{3}, \frac{14}{3}, 2)$	8×10^{15}	$10^{35\pm2.5}$
$\Phi_{6,3,1,2/3}$	$\Phi_{1,2,2,0} + 3\Phi_{1,1,3,0} + 2\Phi_{8,1,1,0} + \Phi_{6,3,1,2/3} + 5\Phi_{1,1,3,-2}$	$(\frac{9}{2}, \frac{13}{3}, \frac{17}{3}, \frac{17}{2})$	1×10^{17}	$10^{39\pm2.5}$
$\Phi_{6,1,3,2/3}$	$2\Phi_{1,2,2,0} + \Phi_{1,1,3,0} + 3\Phi_{1,3,1,0} + \Phi_{6,1,3,2/3} + 2\Phi_{1,1,3,-2}$	$(\frac{5}{2}, \frac{8}{3}, \frac{20}{3}, 4)$	8×10^{15}	$10^{35\pm2.5}$
$\Phi_{1,3,3,0}$	$2\Phi_{1,2,2,0} + 3\Phi_{1,1,3,0} + 3\Phi_{8,1,1,0} + \Phi_{1,3,3,0} + 2\Phi_{1,1,3,-2}$	$(3, \frac{8}{3}, 6, 3)$	4×10^{17}	$10^{42\pm2.5}$
$\Phi_{3,2,2,-2/3}$	$\Phi_{1,2,2,0} + 1\Phi_{1,1,3,0} + 3\Phi_{3,1,2,1/3} + \Phi_{3,2,2,-2/3} + \Phi_{1,1,3,-2}$	$(\frac{5}{3}, \frac{4}{3}, \frac{25}{6}, \frac{29}{12})$	4×10^{17}	$10^{42\pm2.5}$

Table B.6: Simple LR configurations which can explain $[a.1]$ scalar CKM. One of the bi-doublets $\Phi_{1,2,2,0}$ is already considered in the basic field content (SM+bi-doublet). m_G and $T_{1/2}$ have been calculated at 1-loop. The first two configurations correspond to the minimal solutions, each one with the basic $[a.1]$ scalar CKM field content.

Extra field	Configuration	$\Delta b's$	m_G
$\Phi_{1,2,1/2}$	$\Phi_{1,2,1/2} + 4\Phi_{3,2,1/6} + 4\Phi_{3,1,1/3}$	$(\frac{1}{2}, \frac{13}{6}, 2)$	3×10^{16}
	$5\Phi_{1,2,1/2} + 2\Phi_{1,3,0} + 2\Phi_{8,1,0}$	$(\frac{1}{2}, \frac{13}{6}, 2)$	3×10^{16}
$\Phi_{3,2,1/6}$	$3\Phi_{3,2,1/6}$	$(\frac{1}{10}, \frac{3}{2}, 1)$	2×10^{15}
	$4\Phi_{3,2,1/6} + 2\Phi_{3,1,-1/3}$	$(\frac{4}{15}, 2, \frac{5}{3})$	8×10^{15}
$\Phi_{3,1,2/3}$	$4\Phi_{3,1,2/3} + 2\Phi_{1,2,1/2} + 5\Phi_{3,2,1/6}$	$(\frac{43}{30}, \frac{17}{6}, \frac{17}{3})$	2×10^{15}
	$4\Phi_{3,1,2/3} + \Phi_{1,2,1/2} + 5\Phi_{1,3,0} + 3\Phi_{8,1,0}$	$(\frac{7}{6}, \frac{7}{2}, \frac{11}{3})$	4×10^{17}
$\Phi_{3,1,-1/3}$	$4\Phi_{3,1,-1/3} + \Phi_{1,2,1/2} + 4\Phi_{3,2,1/6}$	$(\frac{1}{2}, \frac{13}{6}, 2)$	3×10^{16}
	$4\Phi_{3,1,-1/3} + 4\Phi_{1,2,1/2} + 3\Phi_{1,3,0} + 2\Phi_{8,1,0}$	$(\frac{2}{3}, \frac{8}{3}, \frac{8}{3})$	1×10^{17}
$\Phi_{1,1,-1}$	$3\Phi_{1,1,-1} + 3\Phi_{1,2,1/2} + 3\Phi_{1,3,0} + 2\Phi_{8,1,0}$	$(\frac{9}{10}, \frac{5}{2}, 2)$	2×10^{15}
	$\Phi_{1,1,-1} + 2\Phi_{1,3,0} + 2\Phi_{8,2,1/2}$	$(\frac{9}{5}, 4, 4)$	1×10^{17}
$\Phi_{3,1,0}$	$3\Phi_{1,3,0} + 2\Phi_{8,1,0}$	$(0, 2, 2)$	1×10^{17}
$\Phi_{8,1,0}$	$2\Phi_{8,1,0} + 3\Phi_{1,3,0}$	$(0, 2, 2)$	1×10^{17}
$\Phi_{6,1,1/3}$	$2\Phi_{6,1,1/3} + 3\Phi_{1,3,0}$	$(\frac{4}{15}, 2, \frac{5}{3})$	8×10^{15}
$\Phi_{6,1,-2/3}$	$2\Phi_{6,1,-2/3} + \Phi_{6,3,1/3} + \Phi_{3,2,-5/2}$	$(\frac{23}{10}, \frac{9}{2}, \frac{9}{2})$	1×10^{17}
$\Phi_{8,2,1/2}$	$\Phi_{8,2,1/2} + 3\Phi_{3,2,1/6} + \Phi_{1,2,1/2}$	$(1, 3, 3)$	1×10^{17}
$\Phi_{1,3,-1}$	$3\Phi_{1,3,-1} + 3\Phi_{1,3,0} + 4\Phi_{8,2,1/2}$	$(\frac{9}{5}, 4, 4)$	1×10^{17}
$\Phi_{1,1,-2}$	$2\Phi_{1,1,-2} + 2\Phi_{3,3,-1/3} + 3\Phi_{8,1,0}$	$(2, 4, 4)$	1×10^{17}
$\Phi_{3,2,7/6}$	$\Phi_{3,2,7/6} + 2\Phi_{1,3,0} + 3\Phi_{8,2,1/2} + 2\Phi_{1,3,-1}$	$(\frac{16}{3}, \frac{22}{3}, \frac{22}{3})$	1×10^{17}
$\Phi_{3,3,-1/3}$	$\Phi_{3,3,-1/3} + \Phi_{1,3,-1} + 2\Phi_{8,1,0}$	$(\frac{4}{5}, \frac{8}{3}, \frac{5}{2})$	3×10^{16}
$\Phi_{3,1,-4/3}$	$5\Phi_{3,1,-4/3} + 2\Phi_{6,3,1/3} + 2\Phi_{8,1,0}$	$(\frac{92}{15}, 8, \frac{47}{6})$	3×10^{16}
$\Phi_{6,3,1/3}$	$\Phi_{6,3,1/3} + \Phi_{6,1,4/3} + \Phi_{8,2,1/2}$	$(\frac{10}{3}, \frac{16}{3}, \frac{16}{3})$	1×10^{17}
$\Phi_{6,1,4/3}$	$\Phi_{6,1,4/3} + \Phi_{6,3,1/3} + \Phi_{8,2,1/2}$	$(\frac{10}{3}, \frac{16}{3}, \frac{16}{3})$	1×10^{17}
$\Phi_{3,2,-5/6}$	$\Phi_{3,2,-5/6} + 4\Phi_{1,3,0} + 3\Phi_{8,1,0}$	$(\frac{5}{6}, \frac{19}{6}, \frac{10}{3})$	4×10^{17}

Table B.7: Simple X configurations which lead "SM+X" unification at m_G: $[10^{15}, 10^{18}]$ GeV. The first two configurations correspond to the examples described in section 6.2.7. Note that fields $\Phi_{3,1,-1/3}$, $\Phi_{3,1,-4/3}$, and $\Phi_{3,3,-1/3}$ are potentially dangerous for d=6 proton decay, see section 6.2.2.

Appendix C

Proton decay and flipped $SU(5)$

C.1 The proton decay rates

In this appendix we rederive some of the results of paper [190] and rewrite them in our notation. The proton decay partial widths to neutral mesons in the flipped $SU(5)$ model read

$$\Gamma(p \to \pi^0 e_\beta^+) = \frac{C_1}{2} \left| c(e_\beta, d^C) \right|^2 , \tag{C.1}$$

$$\Gamma(p \to \eta e_\beta^+) = C_2 \left| c(e_\beta, d^C) \right|^2 , \tag{C.2}$$

$$\Gamma(p \to K^0 e_\beta^+) = C_3 \left| c(e_\beta, s^C) \right|^2 . \tag{C.3}$$

with the constants C_1, C_2, C_3 defined in (5.7)-(5.9). The p-decay widths to charged mesons obey

$$\Gamma(p \to \pi^+ \overline{\nu}) = C_1 \sum_{i=1}^{3} \left| c(\nu_i, d, d^C) \right|^2 , \tag{C.4}$$

$$\Gamma(p \to K^+ \overline{\nu}) = \sum_{i=1}^{3} \left| B_4 c(\nu_i, d, s^C) + B_5 c(\nu_i, s, d^C) \right|^2 , \tag{C.5}$$

where

$$B_4 = \frac{m_p^2 - m_K^2}{2 f_\pi \sqrt{2\pi m_p^3}} A_L |\alpha| \frac{2 m_p}{3 m_B} D \, ,$$

$$B_5 = \frac{m_p^2 - m_K^2}{2 f_\pi \sqrt{2\pi m_p^3}} A_L |\alpha| \left[1 + \frac{m_p}{3 m_B} (D + 3F) \right] ,$$

can be obtained from the chiral Lagrangian. A_L takes into account renormalization from M_Z to 1 GeV. The flavor structure of the basic contractions can be written as

$$c(e_\alpha, d_\beta^C) = k^2 \left(U_d (U_u^L)^\dagger\right)_{\beta 1} (U_u^R (U_e^L)^\dagger)_{1\alpha}, \tag{C.6}$$

$$c(\nu_l, d_\alpha, d_\beta^C) = k^2 (U_d U_d^\dagger)_{\beta\alpha} (U_u^R U_\nu^\dagger)_{1l}. \tag{C.7}$$

Here $k = g_G/M_G$ and the unitary matrices U_d, $U_u^{R,L}$, U_ν and $U_e^{R,L}$ provide the diagonalization of the quark and lepton mass matrices:

$$\begin{aligned} m_{LL} &= U_\nu^T D_\nu U_\nu \\ M_e &= (U_e^L)^T D_e U_e^R \\ M_d &= U_d^T D_d U_d \\ M_u &= (U_u^L)^T D_u U_u^R. \end{aligned}$$

Note that M_d and m_{LL} are symmetric, hence, instead of a biunitary, a single-unitary-matrix transformation can be used to diagonalize each of them. In this notation

$$V_{CKM} \propto U_u^L U_d^\dagger \tag{C.8}$$

$$V_{PMNS} \propto U_e^L U_\nu^\dagger \tag{C.9}$$

where the proportionality sign turns into equality once the extra phases (unphysical from the SM perspective) are stripped down. Hence, the flavor structure of the $d = 6$ proton decay widths to neutral mesons and charged leptons is governed by

$$\left|c(e_\alpha, d_\beta^C)\right|^2 = k^4 |(V_{CKM})_{1\beta}|^2 |(U_u^R (U_e^L)^\dagger)_{1\alpha}|^2. \tag{C.10}$$

For a symmetric M_d another important feature of the flipped $SU(5)$ scheme is recovered: $c(\nu_l, d_\alpha, d_\beta^C) \propto \delta_{\alpha\beta}$; this implies $\Gamma(p \to K^+\overline{\nu}) = 0$. Moreover, considering $\sum_{l=1}^3 |(U_u^R U_\nu^\dagger)_{1l}|^2 = 1$ one gets

$$\Gamma(p \to \pi^+\overline{\nu}) = \frac{m_p}{8\pi f_\pi^2} A_L^2 |\alpha|^2 (1 + D + F)^2. \tag{C.11}$$

C.2 The choice of M_u diagonal basis

It is convenient to choose the basis in which M_u is diagonal, i.e., $U_u^L = U_u^R = I$. To justify this choice, we have to prove that all the quantities of our interest are

independent of this choice. This concerns, in particular, the CKM and PMNS matrices and the proton decay widths (C.1)-(C.5), i.e., the coefficient (C.10).

First, obviously, a transformation $U_u^L \to U_u^L V$ where V is a unitary matrix must be compensated by a simultaneous change $U_d \to U_d V$ so that the CKM matrix (C.8) remains intact. Second, changing $U_u^R \to U_u^R W$ by a unitary W requires $U_e^L \to U_e^L W$ otherwise (C.10) is not preserved. On top of that, U_u^R is related to U_ν via see-saw $m_{LL} = U_\nu^T D_\nu U_\nu = M_u^T \left(M_\nu^M\right)^{-1} M_u = -(U_u^R)^T D_u U_u^L \left(M_\nu^M\right)^{-1} (U_u^L)^T D_u U_u^R$, hence also $U_\nu \to U_\nu W$ is induced. The transformations of U_e^L and U_ν then act against each other so that also the PMNS matrix (C.9) remains unchanged. Thus, it is possible to choose $U_u^L = U_u^R = I$ without affecting any of the quantities discussed in Secs 5.2 and 5.3. In the M_u-diagonal basis the coefficient (C.10) reads

$$\left|c(e_\alpha, d_\beta^C)\right|^2 = k_2^4 |(V_{CKM})_{1\beta}|^2 |(V_{PMNS} U_\nu)_{\alpha 1}|^2. \tag{C.12}$$

C.3 $SU(3)_c \otimes SU(2)_L$ gauge unification

In order to get any quantitative grip on the absolute scale of the proton lifetime in the model(s) of interest, in particular, on $\Gamma(p^+ \to \pi^+ \overline{\nu})$ providing the overall normalization of the results depicted in Figs [4.5, 4.6, 4.7] one has to inspect thoroughly the constraints emerging from the requirement of the (partial) gauge coupling unification. Since the model is not "grand" unified in the sense that only the non-Abelian part of the SM gauge group is embedded into a simple component of the high-energy gauge group, this concerns only the convergence of the g_3 and g couplings of the SM. Besides the "initial condition" defined by the values of α_s and $\alpha_2 \equiv g^2/4\pi = \alpha/\sin^2\theta_W$ at the M_Z scale and the relevant beta-functions the most important ingredient of such analysis is the heavy gauge and scalar spectrum shaping the evolution of α_s and α_2 in the vicinity of M_G [conveniently defined as the mass of the (X', Y') gauge bosons] and, ultimately, their coalescence above the last of the heavy thresholds.

As a reference setting let us start with the situation corresponding to the very simplest approximation in which all these heavy fields happen to live at a single scale (M_G); then, M_G turns out to be at $10^{16.8} - 10^{17}$ GeV at one loop where the uncertainty corresponds to the 3-σ band for $\alpha_s(M_Z)$ and it gets reduced to about $10^{16.6} - 10^{16.8}$ GeV at two loops.

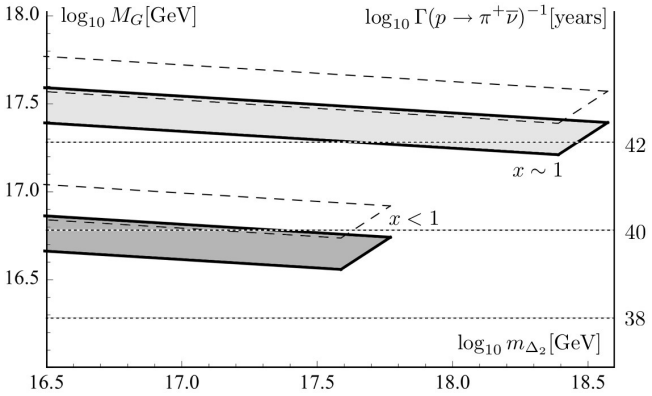

Figure C.1: The unification constraints on the mass of the (X', Y') gauge bosons (the left ordinate) and $\Gamma^{-1}(p^+ \to \pi^+ \overline{\nu})$ (the right ordinate) drawn for constant $x = \mu/\lambda V_G$ as functions of the masses of the scalar colored triplets Δ_1 and Δ_2, cf. (5.18) in the simplified case of $\lambda_2 = \lambda_5$. The upper part of the plot corresponds to the "fine-tuned" region with x very close to 1 with the mass of Δ_1 significantly lower than M_G, cf. Eq. (5.23), while the lower part corresponds to $x < 1$. The bands (one loop in dashed and two loops in solid) correspond to the 3-σ uncertainty in α_s and their boundary on the right depicts the "perturbativity" limit $|\lambda_i| < 4\pi$, cf. Sec. 5.2.2.

Needless to say, such a single-mass-scale assumption is oversimplified as, in fact, the masses of the heavy colored triplet scalars Δ_1 and Δ_2, cf. Eq. (5.18) and the masses of the (X', Y') gauge bosons [to quote only those states that are relevant here, i.e., $SU(3)_c \otimes SU(2)_L$ nonsinglets] depend on different sets of parameters and, hence, may differ considerably; this, in particular, applies for Δ_1 that may be almost arbitrarily light if the inequality (4.26) gets saturated. This, obviously, may lead to a significant change in the "naïve" estimate above.

In what follows, we shall focus on a simplified setting in which $\lambda_2 = \lambda_5 \equiv \lambda$ reflecting the symmetry of the relevant relations (5.18) and (5.23) under their exchange and fix $g_G = 0.5$. Hence, the masses of Δ_1, Δ_2 and (X', Y') are fully fixed given λ, μ and V_G. This also means that if one fixes m_{Δ_2}, λ and μ, then m_{Δ_1} and M_G are fully determined and the unification condition can be tested. In turn, it can be used to get a correlation among the unification-compatible values of, say, m_{Δ_2} and M_G; the resulting situation is depicted in Fig. C.1. The shape of the allowed

regions therein (in particular, the relatively shallow slope of the allowed bands for a fixed proportionality factor x between μ and λV_G) is easily understood: the effect of integrating in the (X', Y') gauge bosons (plus the relevant Goldstones in the Feynman gauge) is much stronger than that of the two colored scalars $\Delta_{1,2}$ (assuming $x < 1$, i.e., m_{Δ_1} not parametrically smaller than m_{Δ_2}) and, hence, a small shift in M_G is enough to compensate even for significant changes in $m_{\Delta_{1,2}}$.

To conclude, the (two-loop) unification constraints limit the allowed domain of M_G to the interval stretching from approximately $10^{16.5}$ GeV attained in the bulk of the parameter space up to about $10^{17.5}$ GeV if the fine-tuned configurations with $x \sim 1$ are considered.

Bibliography

[1] C. Arbelaez, M. Hirsch and L. Reichert, JHEP **1202**, 112 (2012) [arXiv:1112.4771 [hep-ph]].

[2] C. Arbelaez, R. M. Fonseca, M. Hirsch and J. C. Romao, Phys. Rev. D **87**, no. 7, 075010 (2013) [arXiv:1301.6085 [hep-ph]].

[3] C. Arbeláez, M. Hirsch, M. Malinský and J. C. Romão, Phys. Rev. D **89**, 035002 (2014) [arXiv:1311.3228 [hep-ph]].

[4] C. Arbeláez Rodríguez, H. Kolešová and M. Malinský, Phys. Rev. D **89**, 055003 (2014) [arXiv:1309.6743 [hep-ph]].

[5] ATLAS Collaboration, G. Aad *et al.*, Phys.Lett. **B716**, 1 (2012), arXiv:1207.7214.

[6] CMS Collaboration, S. Chatrchyan *et al.*, Phys.Lett. **B716**, 30 (2012), arXiv:1207.7235.

[7] Y. Fukuda *et al.* [Super-Kamiokande Collaboration], Phys. Rev. Lett. **81**, 1562 (1998)

[8] D. V. Forero, M. Tortola and J. W. F. Valle, arXiv:1405.7540 [hep-ph].

[9] SNO, Q. R. Ahmad *et al.*, Phys. Rev. Lett. **89**, 011301 (2002), [nucl-ex/0204008].

[10] KamLAND, K. Eguchi *et al.*, Phys. Rev. Lett. **90**, 021802 (2003), [hep-ex/0212021].

[11] S. Abe *et al.* [KamLAND Collaboration], Phys. Rev. Lett. **100**, 221803 (2008) [arXiv:0801.4589 [hep-ex]].

[12] For a recent review on the status of neutrino oscillation data, see: T. Schwetz, M. A. Tortola and J. W. F. Valle, New J. Phys. **10**, 113011 (2008) [arXiv:0808.2016 [hep-ph]]. Version 3 on the arXive is updated with data until Feb 2010

[13] K. Nakamura *et al.* [Particle Data Group], J. Phys. G **37** (2010) 075021.

[14] P. Minkowski, Phys. Lett. B **67** (1977) 421.

[15] T. Yanagida, in *KEK lectures*, ed. O. Sawada and A. Sugamoto, KEK, 1979; M Gell-Mann, P Ramond, R. Slansky, in *Supergravity*, ed. P. van Niewenhuizen and D. Freedman (North Holland, 1979);

[16] R.N. Mohapatra and G. Senjanovic, *Phys. Rev. Lett.* **44** 912 (1980).

[17] J. Schechter and J. W. F. Valle, Phys. Rev. D **22**, 2227 (1980).

[18] T. P. Cheng and L. F. Li, Phys. Rev. D **22**, 2860 (1980).

[19] G.A Nuijten, J.Phys.:Conf.Ser.308 012029.

[20] J. Alonso *et al.* [DAEdALUS Collaboration], arXiv:1008.4967 [hep-ex].

[21] E.Witten, Phys. Lett. B **91**, 81 (1980).

[22] S. Dimopoulos, S. Raby, and F. Wilczek, Phys.Rev. **D24**, 1681 (1981).

[23] L. E. Ibanez and G. G. Ross, Phys.Lett. **B105**, 439 (1981).

[24] W. J. Marciano and G. Senjanovic, Phys.Rev. **D25**, 3092 (1982).

[25] M. Einhorn and D. Jones, Nucl.Phys. **B196**, 475 (1982).

[26] U. Amaldi, W. de Boer, and H. Furstenau, Phys.Lett. **B260**, 447 (1991).

[27] P. Langacker and M.-x. Luo, Phys.Rev. **D44**, 817 (1991).

[28] J. R. Ellis, S. Kelley, and D. V. Nanopoulos, Phys.Lett. **B260**, 131 (1991).

[29] N. Arkani-Hamed and S. Dimopoulos, JHEP **0506**, 073 (2005), arXiv:hep-th/0405159.

[30] U. Amaldi, W. de Boer, P. H. Frampton, H. Furstenau, and J. T. Liu, Phys.Lett. **B281**, 374 (1992).

[31] I. Gogoladze, B. He, and Q. Shafi, Phys.Lett. **B690**, 495 (2010), arXiv:1004.4217.

[32] M. Malinsky, J. C. Romao and J. W. F. Valle, Phys. Rev. Lett. **95**, 161801 (2005) [hep-ph/0506296].

[33] V. De Romeri, M. Hirsch and M. Malinsky, Phys. Rev. D **84**, 053012 (2011) [arXiv:1107.3412 [hep-ph]].

[34] L. Basso, B. O'Leary, W. Porod and F. Staub, JHEP **1209** (2012) 054 [arXiv:1207.0507 [hep-ph]].

[35] M. Kadastik, K. Kannike and M. Raidal, Phys. Rev. D **80**, 085020 (2009) [Erratum-ibid. D **81**, 029903 (2010)] [arXiv:0907.1894 [hep-ph]].

[36] M. Frigerio and T. Hambye, Phys. Rev. D **81**, 075002 (2010) [arXiv:0912.1545 [hep-ph]].

[37] M. Baak, M. Goebel, J. Haller, A. Hoecker, D. Kennedy, R. Kogler, K. Moenig and M. Schott *et al.*, Eur. Phys. J. C **72**, 2205 (2012) [arXiv:1209.2716 [hep-ph]].

[38] M. Baak, M. Goebel, J. Haller, A. Hoecker, D. Ludwig, K. Moenig, M. Schott and J. Stelzer, Eur. Phys. J. C **72**, 2003 (2012) [arXiv:1107.0975 [hep-ph]].

[39] S.L. Glashow, Nucl. Phys **22**,579 (1961);

[40] S. Weinberg, Phys. Rev. Lett **19**,1264 (1967).

[41] J. C. Pati and A. Salam, Phys. Rev. **D 10**, 275 (1974).

[42] H. Georgi and S.L Glashow, Phys. Rev. Lett **32**, 438 (1974).

[43] A. Neveu and J. Schwarz, Nucl. Phys. **B 31**, 86 (1971).

[44] R.N. Mohapatra, " Unification and Supersymmetry. The frontiers of Quarks-Lepton Physics."

[45] Rabindra N. Mohapatra, Goran Senjanovic, Phys. Rev. **D23** (1981) 165.

[46] K. S. Babu, I. Gogoladze, S. Raza and Q. Shafi, arXiv:1406.6078 [hep-ph].

[47] S. Raby, arXiv:1309.3247 [hep-ph].

[48] K. S. Babu, PoS ICHEP **2010**, 379 (2010) [arXiv:1103.3491 [hep-ph]].

[49] G. Senjanovic, AIP Conf. Proc. **1200**, 131 (2010) [arXiv:0912.5375 [hep-ph]].

[50] P. Nath and P. Fileviez Perez, Phys. Rept. **441**, 191 (2007) [hep-ph/0601023].

[51] C. L. Bennett *et al.* [WMAP Collaboration], Astrophys. J. Suppl. **148**, 1 (2003) [astro-ph/0302207].

[52] A.D. Sakharov, JETP. Lett. 91B, 24 (1967)

[53] M. Fukugita and T. Yanagida, Phys. Lett. B **174**, 45 (1986).

[54] C. S. Fong, E. Nardi and A. Riotto, Adv. High Energy Phys. **2012**, 158303 (2012) [arXiv:1301.3062 [hep-ph]].

[55] S. Davidson, E. Nardi and Y. Nir, Phys. Rept. **466**, 105 (2008) [arXiv:0802.2962 [hep-ph]].

[56] P. A. R. Ade *et al.* [Planck Collaboration], arXiv:1303.5076 [astro-ph.CO].

[57] P. A. R. Ade *et al.* [BICEP2 Collaboration], arXiv:1403.3985 [astro-ph.CO].

[58] P. A. RAde *et al.* [BICEP2 Collaboration], arXiv:1403.4302 [astro-ph.CO].

[59] M. Hashimoto, S. Iso and Y. Orikasa, Phys. Rev. D **89**, 016019 (2014) [arXiv:1310.4304 [hep-ph]].

[60] M. Civiletti, C. Pallis and Q. Shafi, Phys. Lett. B **733**, 276 (2014) [arXiv:1402.6254 [hep-ph]].

[61] G. Panotopoulos, Phys. Rev. D **89**, 047301 (2014) [arXiv:1403.0931 [hep-ph]].

[62] M. Agostini *et al.* [GERDA Collaboration], Phys. Rev. Lett. **111**, no. 12, 122503 (2013) [arXiv:1307.4720 [nucl-ex]].

[63] M. Auger *et al.* [EXO Collaboration], Phys. Rev. Lett. **109**, 032505 (2012) [arXiv:1205.5608 [hep-ex]].

[64] A. Gando *et al.* [KamLAND-Zen Collaboration], Phys. Rev. Lett. **110**, no. 6, 062502 (2013) [arXiv:1211.3863 [hep-ex]].

[65] J. Lesgourgues and S. Pastor, Adv. High Energy Phys. **2012**, 608515 (2012) [arXiv:1212.6154 [hep-ph]].

[66] G. Bertone, D. Hooper and J. Silk, Phys. Rept. **405**, 279 (2005) [hep-ph/0404175].

[67] E. W. Kolb, D. J. H. Chung and A. Riotto, In *Heidelberg 1998, Dark matter in astrophysics and particle physics 1998* 592-614 [hep-ph/9810361].

[68] G. Steigman and M. S. Turner, Nucl. Phys. B **253**, 375 (1985).

[69] S. P. Martin, Adv. Ser. Direct. High Energy Phys. **21**, 1 (2010) [hep-ph/9709356].

[70] M. Drees, hep-ph/9611409.

[71] Y. .A. Golfand and E. P. Likhtman, JETP Lett. **13**, 323 (1971) [Pisma Zh. Eksp. Teor. Fiz. **13**, 452 (1971)].

[72] D. V. Volkov and V. P. Akulov, Phys. Lett. B **46**, 109 (1973).

[73] J. Wess and B. Zumino, Phys. Lett. B **49**, 52 (1974).

[74] A. Salam and J. A. Strathdee, Phys. Lett. B **51**, 353 (1974).

[75] M. Drees, R. Godbole, P. Roy, Hackensack, USA: World Scientific (2004) 555 p.

[76] G. Senjanovic, Int. J. Mod. Phys. Conf. Ser. **13**, 182 (2012) [arXiv:1205.5557 [hep-ph]].

[77] G. Jungman, M. Kamionkowski and K. Griest, Phys. Rept. **267**, 195 (1996) [hep-ph/9506380].

[78] V. De Romeri and M. Hirsch, JHEP **1212**, 106 (2012) [arXiv:1209.3891 [hep-ph]].

[79] D. Bailin, A. Love, Bristol, UK: IOP (1994) 322 p. (Graduate student series in physics).

[80] P. Binetruy, Oxford, UK: Oxford Univ. Pr. (2006) 520 p

[81] S. Kraml, In *Karlsruhe 2007, SUSY 2007* 132-139 [arXiv:0710.5117 [hep-ph]].

[82] Atlas collaboration, https://atlas.web.cern.ch

[83] P. Adamson *et al.* [MINOS Collaboration], Phys. Rev. Lett. **110**, no. 25, 251801 (2013) [arXiv:1304.6335 [hep-ex]].

[84] P. Adamson *et al.* [MINOS Collaboration], Phys. Rev. Lett. **110**, no. 17, 171801 (2013) [arXiv:1301.4581 [hep-ex]].

[85] F. Kaether, W. Hampel, G. Heusser, J. Kiko and T. Kirsten, Phys. Lett. B **685**, 47 (2010) [arXiv:1001.2731 [hep-ex]].

[86] G. Bellini, J. Benziger, D. Bick, S. Bonetti, G. Bonfini, M. Buizza Avanzini, B. Caccianiga and L. Cadonati *et al.*, Phys. Rev. Lett. **107**, 141302 (2011) [arXiv:1104.1816 [hep-ex]].

[87] F. P. An *et al.* [DAYA-BAY Collaboration], Phys. Rev. Lett. **108**, 171803 (2012) [arXiv:1203.1669 [hep-ex]].

[88] J. K. Ahn *et al.* [RENO Collaboration], Phys. Rev. Lett. **108**, 191802 (2012) [arXiv:1204.0626 [hep-ex]].

[89] K. Abe *et al.* [T2K Collaboration], Phys. Rev. Lett. **112**, 181801 (2014) [arXiv:1403.1532 [hep-ex]].

[90] A. Santamaria, Phys. Lett. B **305**, 90 (1993) [hep-ph/9302301].

[91] S. Weinberg, Phys. Rev. D **22**, 1694 (1980).

[92] E. Ma, Phys. Rev. Lett. **81**, 1171 (1998) [hep-ph/9805219].

[93] A. Zee, Phys. Lett. B **93**, 389 (1980) [Erratum-ibid. B **95**, 461 (1980)].

[94] K. S. Babu, Phys. Lett. B **203**, 132 (1988).

[95] M. Gell-Mann, P. Ramond and R. Slansky, Conf. Proc. C **790927**, 315 (1979) [arXiv:1306.4669 [hep-th]].

[96] E. Ma and D. P. Roy, Nucl. Phys. B **644**, 290 (2002) [hep-ph/0206150].

[97] J. A. Casas and A. Ibarra, Nucl. Phys. B **618**, 171 (2001) [hep-ph/0103065].

[98] E. Witten, Phys. Lett. **91B**, 81 (1980).

[99] H. Fritzsch and P. Minkowski, Annals Phys. **93**, 193 (1975).

[100] J. Beringer *et al.* [Particle Data Group Collaboration], Phys. Rev. D **86**, 010001 (2012).

[101] R.N. Mohapatra, Contemporary Physics (Spriinger, Berlin, Germany)(1986).

[102] I. Antoniadis, J. R. Ellis, J. S. Hagelin and D. V. Nanopoulos, Phys. Lett. B **194**, 231 (1987).

[103] C. T. Hill, Phys. Lett. B **135**, 47 (1984).

[104] Q. Shafi and C. Wetterich, Phys. Rev. Lett. **52**, 875 (1984).

[105] X. Calmet, S. D. H. Hsu and D. Reeb, Phys. Rev. Lett. **101**, 171802 (2008) [arXiv:0805.0145 [hep-ph]].

[106] J. Chakrabortty and A. Raychaudhuri, Phys. Lett. B **673**, 57 (2009) [arXiv:0812.2783 [hep-ph]].

[107] I. Dorsner and P. Fileviez Perez, Phys. Lett. B **606**, 367 (2005) [hep-ph/0409190].

[108] I. Dorsner and P. Fileviez Perez, Phys. Lett. B **642**, 248 (2006) [hep-ph/0606062].

[109]

[109] D. -G. Lee, R. N. Mohapatra, M. K. Parida and M. Rani, "Predictions for proton lifetime in minimal nonsupersymmetric SO(10) models: An update," Phys. Rev. D **51**, 229 (1995) [hep-ph/9404238].

[110] B. Dutta, Y. Mimura and R. N. Mohapatra, Phys. Rev. Lett. **94** (2005) 091804 [hep-ph/0412105].

[111] A. D. Sakharov, Pisma Zh. Eksp. Teor. Fiz. **5**, 32 (1967) [JETP Lett. **5**, 24 (1967)] [Sov. Phys. Usp. **34**, 392 (1991)] [Usp. Fiz. Nauk **161**, 61 (1991)].

[112] J. M. Cline, hep-ph/0609145.

[113] E. Kearns *et al.* [Hyper-Kamiokande Working Group Collaboration], arXiv:1309.0184 [hep-ex].

[114] D. Autiero, J. Aysto, A. Badertscher, L. B. Bezrukov, J. Bouchez, A. Bueno, J. Busto and J. -E. Campagne *et al.*, JCAP **0711**, 011 (2007) [arXiv:0705.0116 [hep-ph]].

[115] MEMPHYS experiment, http://www.apc.univ-paris7.fr/APC-CS/Experiences/MEMPHYS

[116] T. M. Undagoitia, F. von Feilitzsch, M. Goger-Neff, C. Grieb, K. A. Hochmuth, L. Oberauer, W. Potzel and M. Wurm, Phys. Rev. D **72**, 075014 (2005) [hep-ph/0511230].

[117] E. Kearns, ISOUPS, Asilomar, CA. Boston University, May 25, 2013.

[118] R. N. Mohapatra and J. W. F. Valle, Phys. Rev. **D34**, 1642 (1986).

[119] E. Akhmedov, M. Lindner, E. Schnapka and J. W. F. Valle, Phys. Rev. **D53**, 2752 (1996), [hep-ph/9509255];

[120] F. Borzumati and A. Masiero, Phys. Rev. Lett. **57**, 961 (1986).

[121] J. Hisano, T. Moroi, K. Tobe, M. Yamaguchi and T. Yanagida, Phys. Lett. B **357**, 579 (1995) [arXiv:hep-ph/9501407].

[122] J. Hisano, T. Moroi, K. Tobe and M. Yamaguchi, Phys. Rev. D **53**, 2442 (1996) [arXiv:hep-ph/9510309].

[123] J. R. Ellis, J. Hisano, M. Raidal and Y. Shimizu, Phys. Rev. D **66**, 115013 (2002) [arXiv:hep-ph/0206110].

[124] F. Deppisch, H. Pas, A. Redelbach, R. Ruckl and Y. Shimizu, Eur. Phys. J. C **28**, 365 (2003) [arXiv:hep-ph/0206122].

[125] E. Arganda and M. J. Herrero, Phys. Rev. D **73**, 055003 (2006) [arXiv:hep-ph/0510405].

[126] S. Antusch, E. Arganda, M. J. Herrero and A. M. Teixeira, JHEP **0611**, 090 (2006) [arXiv:hep-ph/0607263].

[127] E. Arganda, M. J. Herrero and A. M. Teixeira, JHEP **0710**, 104 (2007) [arXiv:0707.2955 [hep-ph]].

[128] J. Hisano, M. M. Nojiri, Y. Shimizu and M. Tanaka, Phys. Rev. D **60**, 055008 (1999) [arXiv:hep-ph/9808410].

[129] G. A. Blair, W. Porod and P. M. Zerwas, Eur. Phys. J. **C27**, 263 (2003), [hep-ph/0210058].

[130] A. Freitas, W. Porod and P. M. Zerwas, Phys. Rev. **D72**, 115002 (2005), [hep-ph/0509056].

[131] S. T. Petcov, S. Profumo, Y. Takanishi and C. E. Yaguna, Nucl. Phys. B **676** (2004) 453 [arXiv:hep-ph/0306195]; S. Pascoli, S. T. Petcov and C. E. Yaguna, Phys. Lett. B **564** (2003) 241 [arXiv:hep-ph/0301095]; S. T. Petcov, T. Shindou and Y. Takanishi, Nucl. Phys. B **738** (2006) 219 [arXiv:hep-ph/0508243]; S. T. Petcov and T. Shindou, Phys. Rev. D **74** (2006) 073006 [arXiv:hep-ph/0605151].

[132] M. Hirsch, J. W. F. Valle, W. Porod, J. C. Romao and A. Villanova del Moral, Phys. Rev. D **78**, 013006 (2008) [arXiv:0804.4072 [hep-ph]].

[133] M. Hirsch, Nucl. Phys. Proc. Suppl. **217**, 318 (2011).

[134] R. Foot, H. Lew, X. G. He and G. C. Joshi, Z. Phys. C **44**, 441 (1989).

[135] A. Rossi, Phys. Rev. D **66**, 075003 (2002) [arXiv:hep-ph/0207006].

[136] M. Hirsch, S. Kaneko and W. Porod, Phys. Rev. D **78**, 093004 (2008) [arXiv:0806.3361 [hep-ph]].

[137] J. N. Esteves, J. C. Romao, M. Hirsch, F. Staub and W. Porod, Phys. Rev. D **83**, 013003 (2011) [arXiv:1010.6000 [hep-ph]].

[138] C. Biggio and L. Calibbi, arXiv:1007.3750 [hep-ph].

[139] M. R. Buckley and H. Murayama, Phys. Rev. Lett. **97**, 231801 (2006) [arXiv:hep-ph/0606088].

[140] V. De Romeri, M. Hirsch and M. Malinsky, Phys. Rev. D **84**, 053012 (2011) [arXiv:1107.3412 [hep-ph]].

[141] G. Weiglein *et al.* [LHC/LC Study Group], Phys. Rept. **426** (2006) 47 [arXiv:hep-ph/0410364].

[142] J. A. Aguilar-Saavedra *et al.*, Eur. Phys. J. C **46**, 43 (2006) [arXiv:hep-ph/0511344].

[143] M. Hirsch, L. Reichert, W. Porod, JHEP **1105**, 086 (2011). [arXiv:1101.2140 [hep-ph]].

[144] J. A. Aguilar-Saavedra *et al.* [ECFA/DESY LC Physics Working Group], arXiv:hep-ph/0106315.

[145] F. Deppisch, A. Freitas, W. Porod and P. M. Zerwas, Phys. Rev. D **77** (2008) 075009 [arXiv:0712.0361 [hep-ph]].

[146] K. Kadota and J. Shao, Phys. Rev. D **80** (2009) 115004 [arXiv:0910.5517 [hep-ph]].

[147] A. Abada, A. J. R. Figueiredo, J. C. Romao and A. M. Teixeira, JHEP **1010**, 104 (2010) [arXiv:1007.4833 [hep-ph]].

[148] B. C. Allanach, J. P. Conlon and C. G. Lester, Phys. Rev. D **77**, 076006 (2008) [arXiv:0801.3666 [hep-ph]].

[149] S. P. Martin and M. T. Vaughn, Phys. Rev. D **50**, 2282 (1994) [Erratum-ibid. D **78**, 039903 (2008)] [arXiv:hep-ph/9311340].

[150] R. Fonseca, M. Malinsky, W. Porod and F. Staub, arXiv:1107.2670 [hep-ph].

[151] W. Porod, Comput. Phys. Commun. **153** (2003) 275 [arXiv:hep-ph/0301101].

[152] W. Porod and F. Staub, arXiv:1104.1573 [hep-ph].

[153] P. F. Harrison, D. H. Perkins and W. G. Scott, Phys. Lett. B **530**, 167 (2002) [hep-ph/0202074].

[154] M. Khabibullin and f. t. T. Collaboration, arXiv:1111.0183 [hep-ex].

[155] Double CHOOZ experiment, talk by H.De. Kerrect at LowNu2011, http://workshop.kias.re.kr/lownu11/

[156] H. Bachacou, I. Hinchliffe and F. E. Paige, Phys. Rev. D **62** (2000) 015009 [arXiv:hep-ph/9907518].

[157] B. C. Allanach, C. G. Lester, M. A. Parker and B. R. Webber, JHEP **0009** (2000) 004 [arXiv:hep-ph/0007009].

[158] C. G. Lester, "Model independent sparticle mass measurements at ATLAS"; CERN-THESIS-2004-003

[159] S. Chatrchyan *et al.* [CMS Collaboration], Phys. Rev. Lett. **107** (2011) 221804; arXiv:1109.2352 [hep-ex].

[160] G. Aad *et al.* [ATLAS Collaboration], arXiv:1109.6572 [hep-ex].

[161] B. C. Allanach *et al.*, in *Proc. of the APS/DPF/DPB Summer Study on the Future of Particle Physics (Snowmass 2001)* ed. N. Graf, Eur. Phys. J. C **25**, 113 (2002) [arXiv:hep-ph/0202233].

[162] G. Belanger, F. Boudjema, P. Brun, A. Pukhov, S. Rosier-Lees, P. Salati and A. Semenov, Comput. Phys. Commun. **182**, 842 (2011) [arXiv:1004.1092 [hep-ph]].

[163] G. Belanger, F. Boudjema, A. Pukhov and A. Semenov, Comput. Phys. Commun. **180**, 747 (2009) [arXiv:0803.2360 [hep-ph]].

[164] G. Belanger, F. Boudjema, A. Pukhov and A. Semenov, Comput. Phys. Commun. **176**, 367 (2007) [hep-ph/0607059].

[165] G. Belanger, F. Boudjema, A. Pukhov and A. Semenov, Comput. Phys. Commun. **174**, 577 (2006) [hep-ph/0405253].

[166] J. Adam *et al.* [MEG Collaboration], Phys. Rev. Lett. **107**, 171801 (2011) [arXiv:1107.5547 [hep-ex]].

[167] T. Schwetz, M. Tortola and J. W. F. Valle, New J. Phys. **13**, 063004 (2011) [arXiv:1103.0734 [hep-ph]].

[168] B. C. Allanach, A. Djouadi, J. L. Kneur, W. Porod and P. Slavich, JHEP **0409**, 044 (2004) [hep-ph/0406166].

[169] T. Yanagida, in *Proceedings of the Workshop on the Baryon Number of the Universe and Unified Theories*, edited by O. Sawada and A. Sugamoto (1979), p. 95.

[170] R. N. Mohapatra and G. Senjanovic, Phys. Rev. Lett. **44**, 912 (1980).

[171] G. Lazarides, Q. Shafi, and C. Wetterich, Nucl. Phys. **B181**, 287 (1981).

[172] A. Zee, Phys.Lett. **161B**, 141 (1985).

[173] A. Zee, Nucl.Phys. **B264**, 99 (1986).

[174] J. Herrero-Garcia, M. Nebot, N. Rius and A. Santamaria, arXiv:1402.4491 [hep-ph].

[175] F. Bonnet, M. Hirsch, T. Ota, and W. Winter, J.High Energy Phys. 07 (2012) 153.

[176] P. W. Angel, N. L. Rodd, and R. R. Volkas, Phys.Rev. **D 87**, 073007 (2013).

[177] S. Baek, P. Ko, and E. Senaha, arXiv:1209.1685.

[178] T. Ohlsson, T. Schwetz, and H. Zhang, Phys.Lett. **B 681**, 269 (2009).

[179] M. Nebot, J. F. Oliver, D. Palao, and A. Santamaria, Phys.Rev. **D 77**, 093013 (2008).

[180] D. Aristizabal Sierra and M. Hirsch, J. High Energy Phys. 12 (2006) 052.

[181] P. H. Frampton, M. C. Oh, and T. Yoshikawa, Phys.Rev. **D 65**, 073014 (2002).

[182] K. Abe *et al.*, arXiv:1109.3262.

[183] T. Akiri *et al.*, (LBNE Collaboration), arXiv:1110.6249.

[184] S. Bertolini, L. Di Luzio, and M. Malinsky, Phys. Rev. **D 81**, 035015 (2010).

[185] B. Bajc and G. Senjanovic, Phys. Lett. **B 610**, 80 (2005).

[186] B. Bajc and G. Senjanovic, Phys.Rev.Lett. **95**, 261804 (2005).

[187] A. De Rújula, H. Georgi, and S. L. Glashow, Phys. Rev. Lett. **45**, 413 (1980).

[188] S. M. Barr, Phys. Lett. **112B**, 219 (1982).

[189] J. Derendinger, J. E. Kim, and D. V. Nanopoulos, Phys.Lett. **139B**, 170 (1984).

[190] I. Dorsner and P. Fileviez Perez, Phys.Lett. **B 605**, 391 (2005).

[191] C. Das, C. Froggatt, L. Laperashvili, and H. Nielsen, Mod.Phys.Lett. **A 21**, 1151 (2006).

[192] S. Abel, Phys.Lett. **B 234**, 113 (1990).

[193] S. Barr, Phys. Rev. D 88, 057702 (2013).

[194] D. Chang, R. N. Mohapatra, J. Gipson, R. E. Marshak, and M. K. Parida, Phys. Rev. **D 31**, 1718 (1985).

[195] N. G. Deshpande, E. Keith, and P. B. Pal, Phys. Rev. **D 46**, 2261 (1993).

[196] N. G. Deshpande, E. Keith, and P. B. Pal, Phys. Rev. **D 47**, 2892 (1993).

[197] S. Bertolini, L. Di Luzio, and M. Malinsky, Phys. Rev. **D 80**, 015013 (2009).

[198] K.S. Babu (private communication).

[199] G. Aad *et al.*, (ATLAS Collaboration) Phys.Lett. **B 716**, 1 (2012).

[200] S. Chatrchyan *et al.* (CMS Collaboration) Eur.Phys.J. **C 73**, 2469 (2013).

[201] D. Buttazzo *et al.*, J. High Energy Phys. 12 (2013) 089.

[202] D. Forero, M. Tortola, and J. Valle, Phys.Rev. **D 86**, 073012 (2012).

[203] G. Fogli *et al.*, Phys.Rev. **D 86**, 013012 (2012).

[204] S. Riemer-Sørensen, D. Parkinson, and T. M. Davis, arXiv:1306.4153.

[205] T. Yanagida, KEK lectures, ed. O. Sawada and A. Sugamoto, Tsukuba, Japan (1979).

[206] R. N. Mohapatra, Contemporary Physics (Springer, Berlin, Germany) (1986).

[207] C. S. Aulakh and R. N. Mohapatra, Phys. Rev. D **28**, 217 (1983).

[208] T. E. Clark, T. -K. Kuo and N. Nakagawa, Phys. Lett. B **115**, 26 (1982).

[209] C. S. Aulakh, B. Bajc, A. Melfo, A. Rasin and G. Senjanovic, Nucl. Phys. B **597**, 89 (2001) [hep-ph/0004031].

[210] C. S. Aulakh, B. Bajc, A. Melfo, G. Senjanovic and F. Vissani, Phys. Lett. B **588**, 196 (2004) [hep-ph/0306242].

[211] M. Cvetic and J. C. Pati, Phys.Lett. **B135**, 57 (1984).

[212] R. Kuchimanchi and R. Mohapatra, Phys.Rev. **D48**, 4352 (1993), arXiv:hep-ph/9306290.

[213] C. S. Aulakh, K. Benakli, and G. Senjanovic, Phys.Rev.Lett. **79**, 2188 (1997), arXiv:hep-ph/9703434.

[214] C. S. Aulakh, A. Melfo, A. Rasin, and G. Senjanovic, Phys.Rev. **D58**, 115007 (1998), arXiv:hep-ph/9712551.

[215] S. K. Majee, M. K. Parida, A. Raychaudhuri, and U. Sarkar, Phys.Rev. **D75**, 075003 (2007), arXiv:hep-ph/0701109.

[216] L. Calibbi, L. Ferretti, A. Romanino, and R. Ziegler, Phys.Lett. **B672**, 152 (2009), arXiv:0812.0342.

[217] P. B. Dev and R. Mohapatra, Phys.Rev. **D81**, 013001 (2010), arXiv:0910.3924.

[218] M. Hirsch, S. Kaneko, and W. Porod, Phys.Rev. **D78**, 093004 (2008), arXiv:0806.3361.

[219] J. Esteves, J. Romao, M. Hirsch, F. Staub, and W. Porod, Phys.Rev. **D83**, 013003 (2011), arXiv:1010.6000.

[220] K. S. Babu and R. N. Mohapatra, Phys. Rev. Lett. **70**, 2845 (1993) [hep-ph/9209215].

[221] B. Bajc, G. Senjanovic and F. Vissani, Phys. Rev. Lett. **90**, 051802 (2003) [hep-ph/0210207].

[222] J. Romao *et al.*, http://porthos.ist.utl.pt/arXiv/AllSO10GUTs.

[223] R. N. Mohapatra and J. W. F. Valle, Phys. Rev. D **34**, 1642 (1986).

[224] E. K. Akhmedov, M. Lindner, E. Schnapka, and J.W.F. Valle, Phys.Lett. **B368**, 270 (1996), arXiv:hep-ph/9507275.

[225] K. Babu, B. Dutta, and R. Mohapatra, Phys.Rev. **D60**, 095004 (1999), arXiv:hep-ph/9812421.

[226] S. Davidson, D. C. Bailey, and B. A. Campbell, Z.Phys. **C61**, 613 (1994), arXiv:hep-ph/9309310.

[227] A. Kuznetsov, N. Mikheev, and A. Serghienko, (2012), arXiv:1210.3697.

[228] H. Baer, V. Barger, A. Lessa, and X. Tata, (2012), arXiv:1207.4846.

[229] ATLAS Collaboration, G. Aad *et al.*, ATLAS-CONF-2012-109 (2012).

[230] A. Arbey, M. Battaglia, A. Djouadi, F. Mahmoudi, and J. Quevillon, Phys.Lett. **B708**, 162 (2012), arXiv:1112.3028.

[231] H. Baer, V. Barger, and A. Mustafayev, Phys.Rev. **D85**, 075010 (2012), arXiv:1112.3017.

[232] O. Buchmueller *et al.*, Eur.Phys.J. **C72**, 2020 (2012), arXiv:1112.3564.

[233] J. Ellis and K. A. Olive, Eur.Phys.J. **C72**, 2005 (2012), arXiv:1202.3262.

[234] M. Hirsch, F. Joaquim, and A. Vicente, JHEP **1211**, 105 (2012), arXiv:1207.6635.

[235] H. E. Haber and M. Sher, Phys.Rev. **D35**, 2206 (1987).

[236] M. Drees, Phys.Rev. **D35**, 2910 (1987).

[237] M. Hirsch, W. Porod, L. Reichert, and F. Staub, Phys.Rev. **D86**, 093018 (2012), arXiv:1206.3516.

[238] M. Hirsch, M. Malinsky, W. Porod, L. Reichert, and F. Staub, JHEP **1202**, 084 (2012), arXiv:1110.3037.

[239] G. F. Giudice and A. Romanino, Nucl.Phys. **B699**, 65 (2004), arXiv:hep-ph/0406088.

[240] B. Brahmachari, U. Sarkar, and K. Sridhar, Phys.Lett. **B297**, 105 (1992).

[241] R. N. Mohapatra, F. E. Paige, and D. P. Sidhu, Phys.Rev. **D17**, 2462 (1978).

[242] B. Brahmachari, E. Ma, and U. Sarkar, Phys.Rev.Lett. **91**, 011801 (2003), arXiv:hep-ph/0301041.

[243] F. Siringo, Phys.Part.Nucl.Lett. **10**, 94 (2013), arXiv:1208.3599.

[244] J. N. Esteves *et al.*, JHEP **1201**, 095 (2012), arXiv:1109.6478.

[245] M. Lindner and M. Weiser, Phys.Lett. **B383**, 405 (1996), arXiv:hep-ph/9605353.

[246] G. Dvali, Fortsch. Phys. **58**, 528 (2010) [arXiv:0706.2050 [hep-th]].

[247] S. Bertolini, L. Di Luzio, and M. Malinsky, Phys.Rev. **D87**, 085020 (2013), arXiv:1302.3401 [hep-ph].

[248] K. S. Babu and R. N. Mohapatra, Phys.Rev. **D86**, 035018 (2012), arXiv:arXiv:1203.5544.

[249] H. A. Weldon and A. Zee, Nucl.Phys. **B173**, 269 (1980).

[250] Super-Kamiokande Collaboration, K. Abe *et al.*, (2013), arXiv:1305.4391.

[251] A. J. Buras, J. R. Ellis, M. K. Gaillard, and D. V. Nanopoulos, Nucl.Phys. **B135**, 66 (1978).

[252] J. R. Ellis, M. K. Gaillard, and D. V. Nanopoulos, Phys.Lett. **B88**, 320 (1979).

[253] F. Wilczek and A. Zee, Phys.Rev.Lett. **43**, 1571 (1979).

[254] Super-Kamiokande, H. Nishino *et al.*, Phys.Rev. **D85**, 112001 (2012), arXiv:1203.4030.

[255] ATLAS Collaboration, (2013).

[256] CMS Collaboration, S. Chatrchyan *et al.*, JHEP **1306**, 081 (2013), arXiv:1303.4571.

[257] Particle Data Group, C. Amsler *et al.*, Phys.Lett. **B667**, 1 (2008).

[258] D. R. T. Jones, Phys.Rev. **D25**, 581 (1982).

[259] M. E. Machacek and M. T. Vaughn, Nucl.Phys. **B222**, 83 (1983).

[260] M.-x. Luo, H.-w. Wang, and Y. Xiao, Phys.Rev. **D67**, 065019 (2003), arXiv:hep-ph/0211440.

[261] J. Angle *et al.* [XENON Collaboration], Phys. Rev. Lett. **100**, 021303 (2008) [arXiv:0706.0039 [astro-ph]].

[262] E. Aprile *et al.* [XENON Collaboration], Phys. Rev. Lett. **107**, 131302 (2011) [arXiv:0706.0039 [astro-ph]].

[263] C. Faham [for the LUX Collaboration], arXiv:1405.5906 [hep-ex].

[264] S. B. Ricciarini, O. Adriani, G. C. Barbarino, G. A. Bazilevskaya, R. Bellotti, M. Boezio, E. A. Bogomolov and M. Bongi *et al.*, EPJ Web Conf. **71**, 00115 (2014).

[265] F. Gargano, "Fermi view of the EGRET pulsars,"

[266] R. M. Sousa da Fonseca, arXiv:1310.1296 [hep-ph].

[267] J. C. Baez and J. Huerta, Bull. Am. Math. Soc. **47**, 483 (2010) [arXiv:0904.1556 [hep-th]].